

Laura Walther

Development of a Weather Routing System for Analysis and Optimization of Ship Voyages



Fraunhofer Center for
Maritime Logistics and Services CML

INNOVATIONS FOR MARITIME LOGISTICS VOLUME 5
INNOVATIONEN FÜR DIE MARITIME LOGISTIK

Editor: Prof. Dr.-Ing. Carlos Jahn

Development of a Weather Routing System for Analysis and Optimization of Ship Voyages

Laura Walther

FRAUNHOFER VERLAG

Contact:

Fraunhofer Center for Maritime Logistics and Services CML
Am Schwarzenberg-Campus 4, Building D
21073 Hamburg, Germany
Phone +49 40 42878-4450
Fax +49 40 42878-4452
E-Mail info@cml.fraunhofer.de
URL <http://www.cml.fraunhofer.de>

Bibliographic information of the German National Library

The German National Library lists this publication in the Deutsche Nationalbibliografie; detailed bibliographic data is available in the Internet at www.dnb.de.

ISBN 978-3-8396-1679-6

D 830

Zugl: Hamburg, TU, Diss., 2020

Cover: © Hapag-Lloyd AG

Print and finishing:
Fraunhofer Verlag, Mediendienstleistungen

This book was printed with chlorine- and acid-free paper.

© by Fraunhofer Verlag, 2021
Nobelstrasse 12
70569 Stuttgart
Germany
verlag@fraunhofer.de
www.verlag.fraunhofer.de

is a constituent entity of the Fraunhofer-Gesellschaft, and as such has no separate legal status.

Fraunhofer-Gesellschaft zur Förderung
der angewandten Forschung e.V.
Hansastraße 27c
80686 München
Germany
www.fraunhofer.de

All rights reserved; no part of this publication may be translated, reproduced, stored in a retrieval system, or transmitted in any form or by any means, electronic, mechanical, photocopying, recording or otherwise, without the written permission of the publisher.

Many of the designations used by manufacturers and sellers to distinguish their products are claimed as trademarks. The quotation of those designations in whatever way does not imply the conclusion that the use of those designations is legal without the consent of the owner of the trademark.

Development of a Weather Routing System for Analysis and Optimization of Ship Voyages

Vom Promotionsausschuss der
Technischen Universität Hamburg

zur Erlangung des akademischen Grades

Doktor-Ingenieurin (Dr.-Ing.)

genehmigte Dissertation

von
Laura Sophia Walther

aus
Hamburg

2020

Erstgutachter: Prof. Dr.-Ing. Carlos Jahn

Zweitgutachter: Prof. Dr.-Ing. Moustafa Abdel-Maksoud

Vorsitzende des Prüfungsausschusses: Prof. Dr. rer. pol. Kathrin Fischer

Tag der mündlichen Prüfung: 28. September 2020

Vorwort des Herausgebers

Der starke internationale Wettbewerb, geringe Margen und hoher Kostendruck zwingen Schiffahrtsunternehmen zunehmend, Effizienzpotenziale im Schiffsbetrieb zu identifizieren und auszuschöpfen. In diesem Zusammenhang stellt das Wetter-Routing eine der wesentlichen Maßnahmen der Schiffsführung dar, bei Einhaltung von Terminvorgaben Treibstoffeinsparungen zu erzielen und sicher zu navigieren. Damit können Kosten und Emissionen gesenkt werden. Am Markt haben sich verschiedene Software-Systeme für das Wetter-Routing etabliert.

Für das Errechnen von Routen gehen in die Wetter-Routing-Systeme neben Wetter-, Fahrtzeit- und Seekarteninformationen auch hydrodynamische und weitere Schiffseigenschaften als wesentliche Eingangsgrößen ein. Um einen möglichst großen Kundenkreis, d.h. verschiedene Schiffstypen und unterschiedliche Reiseprofile, anzusprechen, ist den meisten Systemen gemeinsam, dass sie mit vereinfachten Modellierungsansätzen diese Schiffscharakteristika abbilden.

Eine sowohl für die Wissenschaft als auch die Praxis interessante Fragestellung ist es, ob sich durch eine detailliertere Modellierung der Schiffscharakteristika bessere Routenempfehlungen für Schiffe ermitteln lassen. Zudem stellt sich die Frage, ob diese Verbesserungen hinsichtlich der Minimierung des Treibstoffverbrauchs durch Kurs- und Geschwindigkeitsoptimierungen die damit verbundenen höheren Modellierungsaufwände rechtfertigen. Diesen Fragen geht Frau Dr.-Ing. Walther in ihrer Dissertation nach.

Für die systematische und wissenschaftlich fundierte Beantwortung dieser Fragen verfolgt Frau Dr.-Ing. Walther drei Teilziele: Zum Ersten und als Grundlage ihrer Untersuchungen erstellt sie eine der bisher umfassendsten Übersichten über verwendete Optimierungsansätze und entwickelt ein algorithmisches Lösungsverfahren für das Wetter-Routing-Problem. Zum Zweiten entwirft und programmiert Frau Dr.-Ing. Walther ein eigenes graphentheoretisch basiertes Wetter-Routing-System, das eine detailliertere Modellierung von Schiffscharakteristika ermöglicht. Frau Dr.-Ing. Walther wählt dafür zwei Ansätze: die einfachere Berechnung des Zusatzwiderstands sowie die erweiterte Berechnung der Zusatzleistung. Der zweite Ansatz zeichnet sich durch die zusätzliche Modellierung der Manövriereigenschaften sowie die zusätzliche Modellierung der Hauptmaschinen- und Propellereigenschaften aus. Zum Dritten führt Frau Dr.-Ing. Walther Berechnungen für unterschiedliche Routen, Ankunftszeiten und Wetterbedingungen für ein 14.000-TEU-Containerschiff-Modell (Duisburg Test Case) durch. Die erzielten Ergebnisse werden mit Daten echter Schiffsreisen mit einem dem Duisburg Test Case sehr ähnlichen Containerschiff verglichen, analysiert und Erkenntnisse des Mehrwertes der zusätzlichen Modellierungsaufwände bewertet.

Als zentrale Erkenntnisgewinne kann Frau Dr.-Ing. Walther zeigen, dass die Steigerung des Modellierungsumfangs um die Manövriereigenschaften von Schiffen nur einen sehr geringen Einfluss auf die Ergebnisse hat. Der Mehraufwand für die Modellierung der Manövriereigenschaften und für die Berechnungen lohnt sich daher nicht. Die zusätzliche Modellierung von Maschinen- und Propellercharakteristika erweist sich dagegen als sinnvoll. Es lassen sich damit bessere Routen- und Geschwindigkeitsprofile für eine Schiffsreise und damit Treibstoffeinsparungen erzielen. Der Mehraufwand für diese zusätzliche Modellierung ist daher gerechtfertigt.

Frau Dr.-Ing. Walther liefert mit ihrer Dissertation positive Beiträge zur wissenschaftlichen Diskussion auf dem Gebiet des Wetter-Routings in der Schifffahrt und der dieser zugrundeliegenden Modellierung. Ich wünsche Ihnen viel Freude und interessante Einblicke beim Lesen dieser herausragenden Dissertationsschrift, die gleichzeitig Band 5 der Reihe „Innovationen für die Maritime Logistik“ ist.

Hamburg, Dezember 2020

Prof. Dr.-Ing. Carlos Jahn

Leiter des Instituts für Maritime Logistik der Technischen Universität Hamburg
Leiter des Fraunhofer-Centers für Maritime Logistik und Dienstleistungen CML

Acknowledgment

The present thesis was written in parallel to my work as a research associate at the Fraunhofer Center for Maritime Logistics and Services CML in Hamburg. It is the result of many late hours in office and sacrificed weekends. I am extremely grateful for all the support and encouragement I have received throughout this time. Without it, this research would not have been possible.

I would like to express my deep gratitude to my supervisor Prof. Dr.-Ing. Carlos Jahn for his professional guidance, which has been vital to the success of this research. I am especially thankful for the confidence he has shown in my work and his substantial assistance in finding the right course even in harsh weather conditions. My sincere appreciation also goes to Prof. Dr.-Ing. Moustafa Abdel-Maksoud for his review and valuable advice, which was instrumental in defining the path of my research. I would also like to thank Prof. Dr. rer. pol. Kathrin Fischer for chairing the examination board.

Very special thanks go to Jörn Springer and Martin Köpke from Hapag-Lloyd for their invaluable insights into shipping, to Bjørn Åge Hjøllo from Navtor for providing the software NavStation and to Martin Scharf from the Institute for Fluid Dynamics and Ship Theory at the Hamburg University of Technology for his assistance with the *ProWe* code.

I would like to extend my thanks to my colleagues at Fraunhofer CML and Hamburg University of Technology. I feel deeply grateful for the unwavering support provided by Srikanth Shetty. His positive nature, never-ending patience, and extensive programming skills have not only helped me to go bug hunting for hours, days or even weeks but also to smile in difficult phases and never give up. This accomplishment would not have been possible without him. I also owe my deepest gratitude to Dr.-Ing. Torsten Münsterberg. As an unparalleled role model who completed his own thesis, he has been an inspiration and extraordinarily supportive. His good humor and unceasing encouragement have been essential to finally reach the goal. Many thanks to Anisa Rizvanolli for the illuminating discussions on mathematical optimization as well as Ann-Kathrin Lange whose help with the administrative process cannot be overestimated. I wish to thank both of them for going most of the way together. I thank Hans-Christoph Burmeister for the opportunity to be part of various interesting projects influencing my research in one way or another. Also the valuable contributions of student research projects and assistance, particularly by Niclas Moorbrink, are highly appreciated.

Last but not least, from the bottom of my heart I thank my family, especially my parents, and my dearest friends for their infinite patience and indulgence, for their encouraging words and continuous support, as well as for moments of joy and relaxation.

Abstract

International maritime shipping faces stricter emission regulations and significant cost pressure due to strong competition. In this regard, weather routing systems are becoming increasingly popular to reduce fuel consumption and emissions. Numerous systems have been developed for commercial purposes and as a result of academic research. The comprehensive overview compiled as part of this thesis reveals a broad variety of applied approaches. To ensure applicability for various types of ships and to reduce data requirements, weather-dependent ship motions and fuel consumption are frequently considered in a simplified way. Since simplifications are often regarded as insufficiently accurate, the objective of this thesis is to analyze the impact of ship performance methods on weather routing. Therefore, a graph based ship weather routing system is developed in C++. It aims at minimum fuel consumption by route and/or speed optimization. When optimizing a voyage, either a rather simple ship performance method, referred to as added resistance method, or a more advanced, so called added power method can be selected. The latter includes a maneuvering model as well as propeller and engine characteristics. The validity of the results is demonstrated by comparing computed figures with data collected on board of container ships.

The influence of the two ship performance methods on weather routing is investigated by means of sensitivity analyses. The optimization problem, i.e. the number of decision variables, the arrival time, thus the ship's average speed, and the weather conditions are varied for two voyages. All calculation runs show that the added power method generally yields a lower total fuel consumption for a voyage than the added resistance method which is mainly caused by a higher propulsive efficiency. When varying the arrival time, it can be seen that the lower the average speed is, the smaller the difference becomes. Based on these assessments, it is suggested to consider the engine and propeller characteristics in a ship weather routing system, for example, by integrating an open-water diagram. In contrast, the integration of a maneuvering model is considered to be less important based on the evaluations. The minor impact of transverse drift and rudder forces on the resulting route, speed profile and consumption cannot compensate for the additional data requirements, development tasks and computational effort. These findings as well as the developed system with its various features contribute to advancing the research in the field of ship weather routing.

Contents

List of Figures	V
List of Tables	VII
Abbreviations	IX
Symbols	XI
1 Introduction	1
1.1 Initial Situation and Objectives	1
1.2 Scientific Relevance and Contribution	2
1.3 Methodology and Structure	3
2 Influence of Weather in Maritime Shipping	5
2.1 Principles of Voyage Planning and Weather Routing	5
2.2 Maritime Safety and Weather Risks	8
2.3 Maritime Emission and Efficiency Regulations	10
2.4 Weather Routing as Energy Efficiency Measure	12
2.5 Commercial Weather Routing Services	16
3 Meteorological and Oceanographic Data	25
3.1 Global Atmospheric Circulation and Winds	25
3.2 Global Oceanic Circulation and Currents	27
3.3 Ocean Surface Waves and Natural Seaway	29
3.4 Meteorological and Oceanographic Forecasting	32
4 Mathematical Modeling and Optimization Approaches	37
4.1 Optimization in Relation to Ship Weather Routing	37
4.2 Linear and Nonlinear Programming	41
4.2.1 Unconstrained Optimization Methods	42
4.2.2 Constrained Optimization Methods	44
4.3 Graph Theory and Network Optimization	44
4.4 Dynamic Programming	51
4.4.1 Continuous Dynamic Programming	52
4.4.2 Discrete Dynamic Programming	54
4.5 Metaheuristic Methods	60
4.5.1 Simulated Annealing	61
4.5.2 Evolutionary Methods	61

5	Aspects of Ship Performance	67
5.1	Reference Frames and Equations of Motion	67
5.1.1	Earth Related Reference Frames	67
5.1.2	Ship Related Reference Frame	68
5.1.3	Equations of Motion	71
5.2	Ship Resistance in Service Conditions	73
5.2.1	Calm Water Resistance	73
5.2.2	Added Resistance Components	75
5.2.3	Speed Reduction Approach	76
5.3	Influence of Oceanic Surface Currents	77
5.4	Influence of Wind and Ship Aerodynamics	78
5.5	Influence of Waves and Ship Seakeeping	79
5.5.1	Prediction of Ship Motions in Waves	79
5.5.2	Aspects of Ship Safety and Comfort	84
5.5.3	Ship Safety in Weather Routing	86
5.6	Principles of Ship Propulsion	88
5.6.1	Propeller Characteristics	88
5.6.2	Engine Load and Fuel Consumption	91
5.6.3	Added Power Prediction Method	94
5.6.4	Approaches in Weather Routing	96
6	Design and Implementation of the Weather Routing System	99
6.1	Description of the Weather Routing Problem	99
6.1.1	Generic Requirements	99
6.1.2	Scope and Assumptions	101
6.1.3	Classification of the Problem	103
6.2	Mathematical Model of the Problem	104
6.2.1	Objective Function	104
6.2.2	Decision Variables	105
6.2.3	Constraints	105
6.2.4	Parameters	107
6.3	Description of the Solution Procedure	107
6.3.1	Design of the Algorithm	108
6.3.2	Discretization and Graph Design	111
6.4	Development of the Weather Routing System	112
6.4.1	Graphical User Interface	113
6.4.2	Input and Output Data	113
6.4.3	Architecture of the System	117
6.4.4	Ship Performance Model	120
6.4.5	Handling of the Weather Data	122
7	Testing and Application of the Weather Routing System	127
7.1	Ship Related Input Data	127

7.2	Testing of the System	130
7.2.1	Verification	130
7.2.2	Validation	136
7.3	Evaluation of Scenarios	142
7.3.1	Definition of Scenarios	143
7.3.2	Influence of the Problem	144
7.3.3	Influence of Ship Speed	148
7.3.4	Influence of Weather Conditions	151
7.4	Discussion of the Results	157
7.5	Limits and Benefits of the System	158
8	Conclusion and Outlook	159
	Bibliography	163
A	Additional Analyses	191

List of Figures

1.1	Approach and Structure	4
2.1	Aspects of Ship Weather Routing	8
2.2	Top Five Causes of Total Shipping Losses from 2007 to 2016	9
2.3	Global and Regional Fuel Oil Sulfur Limits	11
2.4	Overview of Energy Efficiency Measures	13
2.5	Cost-effective Operational Measures and Implementation Rates	14
2.6	Potential Savings of Emissions and Fuel Costs through Weather Routing	15
2.7	Commercial Weather Routing Systems and Features	18
3.1	Schematic of Global Atmospheric Circulation	26
3.2	Schematic of Global Oceanic Surface Circulation	28
3.3	Parameters of a Regular Wave	30
4.1	Examples of Graph Designs	47
4.2	Graph with Intermediate Waypoint	49
4.3	Minimum Time Route derived by Calculus of Variations	54
4.4	Principle of the Modified Isochrone Method	56
4.5	Principle of the 3D Modified Isochrone Method	57
4.6	Principle of the 3D Dynamic Programming Method	58
4.7	Illustration of Isopones reachable with a Specified Amount of Fuel	60
4.8	Solution Space for the Objectives Min. Arrival Time and Consumption	63
5.1	North-East-Down and WGS 84 Coordinate Systems	68
5.2	Definition of 6 DOF Motions in Ship-fixed Reference System	69
5.3	Definition of Angles and Motion Components in the Horizontal Plane	70
5.4	Definition of Encounter Angle and Sailing Conditions	70
5.5	Model based on Longitudinal Ship Motion with or without Propeller	72
5.6	Calm Water Resistance Curve for Post-Panmax Container Ship	74
5.7	Concept of Speed Reduction Curves	76
5.8	Schematic of a Ship's Hull Subdivision in Strip Theory	82
5.9	Schematic of a Ship's Changing Water Plane Area in Waves	85
5.10	Open-Water Diagram for a Post-Panmax Container Ship	89
5.11	Engine Load Diagram of MAN B&W 9S90ME-C10.2	92
5.12	Specific Fuel Oil Consumption of MAN B&W 9S90ME-C10.2	93
5.13	Model including Transverse Drift Forces, Rudder and Propeller	94
6.1	Input and Output Model of the Weather Routing System	101

6.2	Map of the Landmasses based on an Electronic Nautical Chart	107
6.3	Definitions of Neighbors to Design the Graph	112
6.4	Graphical User Interface of the Weather Routing System	114
6.5	Generic Flowchart of Weather Routing System	117
6.6	Generic Flowchart of Optimization Function	118
6.7	Generic Flowchart of Exact Cost Function	119
6.8	Generic Flowchart of Heuristic Cost Function	120
6.9	Generic Flowchart of Added Resistance Function	120
6.10	Generic Flowchart of Added Power Function	121
6.11	Significant Height of Combined Waves Visualized in Weather Module	125
6.12	Global Combined Ocean and Tidal Current on 01 January 2016 00:00	126
6.13	Global Wind Speed on 01 January 2016 00:00	126
7.1	Side View of the Hull Geometry of the Post-Panmax Container Ship	127
7.2	Added Resistance Coefficients of the Post-Panmax Container Ship	130
7.3	Exemplary Visualization of the Shortest Route and Spatial Search Space	131
7.4	Comparison of Great Circle, Rhumb Line and Computed Shortest Route	131
7.5	Ocean Current, Wave and Wind Information at Sample Point	133
7.6	Ocean Current, Swell and Wind Information for Sample Route	134
7.7	Graphical Visualization of Routes used for Validation	137
7.8	Comparison of Operational Data of Sample Voyages	139
7.9	Time Series of Operational Data during Voyage 1	141
7.10	Analysis of Metocean Conditions during Sample Voyages	142
7.11	Impact of Optimization Problem on Consumption and Resistance	144
7.12	Graphical Visualization of Resulting Routes in NavStation	145
7.13	Time Series of Optimization Results for Voyage 1	147
7.14	Impact of Ship Speed on Consumption and Resistance	148
7.15	Time Series of Results for Voyage 1 with Varying Arrival Times	150
7.16	Weather Sensitivity of Total Fuel Consumption for Voyage 1 and 3	152
7.17	Weather Sensitivity of Voyage 1	154
7.18	Weather Sensitivity of Voyage 3	156
A.1	Time Series of Operational Data during Voyage 2	193
A.2	Time Series of Operational Data during Voyage 3	194
A.3	Time Series of Operational Data during Voyage 4	196
A.4	Time Series of Optimization Results for Voyage 3	197
A.5	Time Series of Results for Voyage 3 with Varying Arrival Times	199

List of Tables

5.1 Notation for Ship Motion Components	69
5.2 Guidance according to MSC.1/Circ. 1228	84
6.1 Optimization Problems solvable by the Ship Weather Routing System	102
6.2 Extract of Global Data provided by Tidetech	123
6.3 Relevant Parameters of provided Weather Data	124
7.1 Main Ship Characteristics of the Post-Panmax Container Ship	128
7.2 Additional Ship Data of the Post-Panmax Container Ship	129
7.3 Weather Data along Sample Route	132
7.4 Added Resistance Data along Sample Route	135
7.5 Added Power Data along Sample Route	136
7.6 Sample Voyages for Validation	137
7.7 Departure and Arrival Data of the Voyage Scenarios	143
7.8 Overview of Calculation Runs	143

Abbreviations

2DDP	2-dimensional Dynamic Programming
3DDP	3-dimensional Dynamic Programming
AMQP	Advanced Message Queuing Protocol
AWT	Applied Weather Technology Inc.
BVS	Bon Voyage System
CFD	Computational Fluid Dynamics
DIRPW	Primary Wave Direction
DMI	Danish Meteorological Institute
DOF	Degree of Freedom
DP	Dynamic Programming
DPGA	Distance-based Pareto Genetic Algorithm
ECA	Emission Control Area
ECC	Equatorial Counter Current
ECDIS	Electronic Chart Display and Information System
ECMWF	European Centre for Medium-Range Weather Forecasts
EEDI	Energy Efficiency Design Index
EEOI	Energy Efficiency Operational Indicator
ENC	Electronic Nautical Chart
EU	European Union
ETA	Estimated Time of Arrival
ETD	Estimated Time of Departure
GCR	Great Circle Route
GDAL	Geospatial Data Abstraction Library
GFM	Green Function Method
GFS	Global Forecast System
GRIB1	GRIB Edition 1 (Gridded binary)
GRIB2	GRIB Edition 2
	(General regularly distributed information in binary form)
GUI	Graphical User Interface
HTSGW	Significant Height of Combined Wind Waves and Swell Surface
IERS	International Earth Rotation Service
IMO	International Maritime Organization
IMS	Integrated Maritime Suite
ITCZ	Intertropical Convergence Zone
LP	Linear Programming
MARPOL	International Convention for the Prevention of Pollution from Ships

Metocean	Meteorological and Oceanographic
MEWRA	Multicriteria Evolutionary Weather Routing Algorithm
NCEP	National Centers for Environmental Prediction
NEC	Northern Equatorial Current
NMM	Nelder-Mead-Method
NOAA	National Oceanic and Atmospheric Administration
NSGA	Non-dominated Sorting Genetic Algorithm
NWP	Numerical Weather Prediction
OSR	Optimum Ship Routeing
PERPW	Primary Wave Mean Period
PM	Particulate Matters
RANS	Reynolds-Averaged Navier-Stokes
RAO	Response Amplitude Operator
RCGA	Real-Coded Genetic Algorithm
RPM	Revolutions per Minute
RSM	Rankine Singularity Method
SEC	Southern Equatorial Current
SEEMP	Ship Energy Efficiency Management Plan
SFOC	Specific Fuel Oil Consumption
SHOPERA	Energy Efficient Safe Ship Operation
SMCR	Specified Maximum Continuous Rating
SOG	Speed over Ground
SOLAS	International Convention for the Safety of Life at Sea
SPEA	Strength-Pareto Evolutionary Algorithm
SPOS	Ship Performance Optimisation System
STW	Speed through Water
SWDIR	Direction of Swell Waves Degree True
SWELL	Significant Height of Swell Waves
SWPER	Mean Period of Swell Waves
UGRD	u-Component of Wind
UKMO	UK Met Office
UOGRD	u-Component of Current
V-PER	Vessel Performance Management Toolbox
VGRD	v-Component of Wind
VOGRD	v-Component of Current
VVOS	Vessel and Voyage Optimization Solution
WAM	Wave Model
WGS 84	World Geodetic System 1984
WMO	World Meteorological Organization
WNI	Weathernews Inc.
WVDIR	Direction of Wind Waves Degree True
VVHGT	Significant Height of Wind Waves
VVPER	Mean Period of Wind Waves

Symbols

It is to be noted that the following non-exhaustive notation is used throughout the thesis, unless stated otherwise. Each additional notation is introduced and defined when required.

Latin Symbols

A_F	Ship frontal projected area above sea level
A_L	Ship lateral projected area above sea level
A_R	Wetted projected rudder area
B	Ship breadth
c	Wave phase velocity
c_g	Group velocity of waves
C_{AW}	Added resistance coefficient
C_{ij}	Exact costs between waypoint i and j
d_{ij}	Distance between waypoint i and j
D_p	Propeller diameter
$F(i, t_i)$	Actual cost of the optimal path at node i and time t_i
$\hat{F}(i, t_i)$	Estimate of actual cost of a path at node i and time t_i
Fn	Froude number
g	Gravitational acceleration
$G(i, t_i)$	Exact cost from start to node i at time t_i
$\hat{G}(i, t_i)$	Estimate of exact cost from start to node i at time t_i
GM	Metacentric height
$H(i, t_i)$	Heuristic cost from node i at time t_i to destination
$\hat{H}(i, t_i)$	Estimate of heuristic cost from node i at time t_i to destination
H_W	Wave height of a regular wave
H_S	Significant wave height
i	Radius of gyration
I_{xx}	Mass moment of inertia
J	Advance coefficient
k	Wave number
k_Q	Propeller torque coefficient
k_T	Propeller thrust coefficient
L_{CG}	Longitudinal center of gravity from aft perpendicular
L_{OA}	Ship length overall
L_{PP}	Ship length between perpendiculars

m_{Fuel}	Absolute fuel consumption (mass)
n	Propeller rate of revolutions
N	Hydrodynamic yaw moment (z)
P_B	Brake power
P_D	Delivered power
P_E	Effective power
P_{Fuel}	Fuel price
Q	Propeller torque
Q_0	Open-water propeller torque
R_0	Calm water ship resistance
R_{Rudder}	Added resistance due to rudder
R_T	Total ship resistance
R_{Wind}	Added resistance due to wind
R_{Wave}	Added resistance due to waves
$S_\zeta(\omega)$	One-dimensional wave spectrum
$S_\zeta(\omega, \mu)$	Two-dimensional wave spectrum
t_{ij}	Time between waypoint i and j
t	Thrust deduction fraction
T	Propeller thrust
T_E	Encounter period
T_P	Peak wave period
T_R	Natural roll period of the ship
T_W	Wave period
u	Ship speed component in longitudinal direction (x)
u_a	Inflow velocity to propeller
u_R	Inflow velocity to rudder
\mathbf{U}_A	Vector of apparent wind speed
\mathbf{U}_G	Vector of geographic wind speed
\mathbf{U}_T	Vector of true wind speed
v	Ship speed component in transverse direction (y)
\mathbf{V}_C	Vector of ocean current velocity
\mathbf{V}_G	Vector of ship speed over ground
\mathbf{V}_S	Vector of ship speed through water
w	Wake fraction
X	Hydrodynamic force in longitudinal direction (x)
Y	Hydrodynamic force in transverse direction (y)

Greek Symbols

α_C	Current direction, against North
α_G	Ship's ground course, against North
α_T	True wind direction, against North
α_W	Geographic wind direction, against North
β_A	Apparent wind angle of attack
β_D	Drift angle, against ship longitudinal axis
β_G	Ground drift angle, against ship longitudinal axis
γ_T	True wind angle against ship longitudinal axis
Δ	Ship's displacement
ϵ	Initial phase
$\zeta(x, t)$	Wave elevation
ζ_A	Wave amplitude
η_0	Open-water propeller efficiency
η_D	Propulsive efficiency
η_H	Hull efficiency
η_R	Relative rotative efficiency
η_S	Shaft efficiency
λ	Geographic longitude
λ_W	Wave length
μ	Wave propagation angle
μ_0	Main wave propagation angle
μ_e	Encounter angle
$\mu_{e,IMO}$	Encounter angle according to IMO definition ($\mu_{e,IMO} = \mu_e - 180^\circ$)
ρ	Density of water
ρ_{Air}	Density of air
Φ	Geographic latitude
Φ_W	Wave potential
χ	Course angle, against North
ψ	Heading angle, against North
ω	Wave frequency
ω_e	Encounter frequency
ω_P	Peak frequency

1 Introduction

1.1 Initial Situation and Objectives

International maritime shipping constantly faces significant cost pressure and tough competition. At the same time, the increasing regulatory stringency poses additional challenges. Important in this regard are the regulations aiming to reduce the environmental pollution caused by ships which are included in the International Convention for the Prevention of Pollution from Ships (MARPOL) (IMO 2017b). The commercial challenges and regulatory requirements are drivers of operational improvements as well as innovative technologies and designs, both, of ships and in shipping (Buhaug et al. 2009; Lloyd's Register 2016a). Technical levers range from ship hull optimization through alternative fuels and propulsion technologies, such as liquid natural gas, hybrid propulsion systems or exhaust gas treatment, to innovative ship designs. Also operational measures, such as slow steaming, trim and voyage optimization, are applied to improve a ship's fuel economy and comply with emission regulations. The development and realization of such next generation technologies and strategies is crucial to meet tomorrow's demands regarding sustainable sea transport.

One of the top operational measures to optimize ship voyages is weather routing (Rehmatulla 2014). By optimizing route and speed throughout a voyage, ship weather routing systems typically aim at minimum fuel costs or voyage time, maximum safety or comfort, or a combination of these objectives. To provide sound routing support, it is essential to take meteorological and oceanographic information, ship characteristics and voyage related restrictions into account. Various types of ships on numerous routes with significantly varying weather conditions can, however, pose challenges in this regard. This is one reason why simplified methods with a wide scope of application are popular to consider ship motions and fuel consumption in dependence of the weather conditions. At the same time, simplifications are often regarded as insufficiently accurate. In addition, it is frequently claimed that adequate consideration of a ship's propulsion and steering ability is required to ensure safe and efficient operation and navigation of ships. Particularly in adverse conditions, a ship's maneuverability critically depends on the main engine and propulsion system being modeled correctly under high load (IMO 2016a). In this way, misleadingly optimistic predictions and engine overload can be avoided. Specifically with regard to weather routing systems, Bertram and Couser (2014) and Shigunov (2017) emphasize that the integration of a simple maneuvering model and propulsion data influences the optimization results.

In general, a barrier to the implementation of efficiency measures is the lack of reliable information on cost and savings (Rehmatulla 2014). Also the actual improvements associated with integrating a maneuvering model and propulsion data into a weather routing system are often not quantifiable without prior implementation. Moreover, development expenditures, computational effort and data requirements are expected to be high. For this reason, more advanced complex methods are often not used, although their application is recommended. To overcome the lack of studies and reliable information on the benefits and drawbacks, the impact of different ship performance approaches on weather routing needs to be investigated. This leads to the formulation of the central research question of this thesis: To which extent can the integration of more extensive ship data and more complex models for ship dynamics and propulsion be justified by an improved quality of results? To answer this question, the thesis has the following three objectives:

- Determination of a suitable algorithmic solution procedure to solve the constructed weather routing problem
- Design and implementation of a weather routing system to allow voyage optimization considering two ship performance methods
- Analysis of optimization results to assess the impact of ship performance methods on weather routing

1.2 Scientific Relevance and Contribution

The field of ship weather routing is characterized by its interdisciplinary nature. Combining the disciplines of maritime logistics, naval architecture, mathematics, operations research, computer sciences, meteorology and economics, weather routing requires extensive and in-depth knowledge of the relevant subjects from each discipline. Thus, the origin of past and future research questions ranges from numerical models and forecasting in meteorology and oceanography through optimization approaches to solve the constructed ship weather routing problem to the ship's performance during a voyage in dependence of the service conditions.

A fundamental part of this thesis is related to the evaluation of mathematical modeling and optimization approaches applied in ship weather routing. Developing an adequate model and determining a suitable optimization algorithm is essential to solve the optimization problem at hand. Whether an approach, commercially or scientifically used, is suitable and produces sufficient results depends on the specific requirements regarding accuracy and computational effort as well as the problem including optimization objectives, decision variables and constraints (Walther et al. 2016). The evaluation reveals a broad variety of approaches and results in one of the most comprehensive overviews of approaches applied in ship weather routing to date.

An aspect that is inevitably linked to any weather routing approach refers to the modeling of the ship's performance during a voyage. Similar to the variation in optimization

approaches, the dynamics and propulsion of a ship are considered with varying level of detail. Frequently, simplified methods are favored to ensure a wide scope of application without the need for detailed ship data. In contrast, higher efforts associated with more advanced and complex methods often impede their application. This situation combined with a lack of detailed studies in this context suggests further investigations and points to the scientific relevance of the addressed topic. It motivates the development of a ship weather routing system to analyze the impact of ship performance methods on voyage optimization and to answer the research question.

The development of a weather routing system within this thesis allows to formulate the mathematical model and develop an algorithm in line with the specific requirements related to the research question as well as the available ship and weather data. In addition to a rather simple ship performance method, referred to as added resistance method, a so called added power method that includes a simple maneuvering model as well as propeller and engine characteristics can be selected in the system. Hence, it allows to assess the influence of the ship performance methods on weather routing. The robustness of the results can be evaluated by varying the optimization problem, the ship's average speed, and the weather conditions for different voyages.

In summary, the scientific contribution is related to three aspects. First, one of the most comprehensive overviews of optimization approaches applied in ship weather routing to date has been compiled. Second, a new ship weather routing system capable of solving three different optimization problems, of handling forecast and hindcast weather data, and of considering two different ship performance methods has been developed. Third, new findings concerning the impact of ship performance methods on weather routing contribute to the scientific discussion in this field.

1.3 Methodology and Structure

The aim of the thesis to develop a weather routing system and to analyze the impact of ship performance methods on voyage optimization is approached in line with Fig. 1.1. While Chpt. 1 deals with the introduction, Chpt. 2 provides an overview of weather related aspects in maritime shipping as a basis for the development and evaluations. It elaborates on the principles of voyage planning and weather routing as well as on relevant aspects of maritime safety, emission regulations and energy efficiency. Moreover, it gives a summary of implemented energy efficiency measures and of commercial weather routing services. The meteorological and oceanographic data itself including data formats, numerical models, forecasting ranges and types is subject to Chpt. 3. Special attention is paid to the global atmospheric circulation and winds, to the global oceanic circulation and currents as well as to surface waves and natural seaway.

In order to develop a ship weather routing system to optimize a voyage based on meteorological and oceanographic information, great importance is attached to the math-

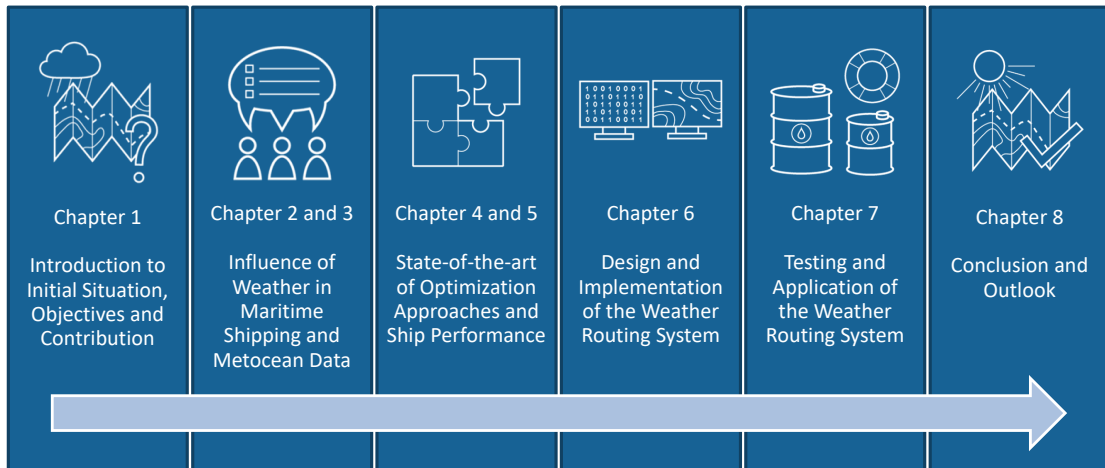


Figure 1.1: Approach and Structure

ematical model and algorithmic solution procedure as well as to the ship's performance during the voyage. While Chpt. 4 provides an overview of mathematical modeling and optimization approaches applied in ship weather routing so far, Chpt. 5 addresses relevant aspects of ship performance. This includes the impact of currents, wind and waves on the ship's motion as well as the principles of ship propulsion. In this context, both ship performance methods are explained. Moreover, approaches applied in ship weather routing so far are mentioned in the respective sections.

The design and implementation of the ship weather routing system is treated in Chpt. 6. This includes the descriptive and mathematical model as well as the algorithmic solution procedure, the ship performance model and the weather data handling. The algorithmic solution procedure is translated into an executable program using the object-oriented programming language C++. In order to ensure simplified application, it is executable via an user-friendly graphical interface. This is described in addition to the input and output data as well as the architecture of the system and its functions.

Chpt. 7 is dedicated to the testing and application of the weather routing system. The system is verified and validated by comparing computed results to figures derived manually and to actual data collected on board of container ships. Furthermore, sensitivity analyses are conducted to evaluate the influence of the two ship performance methods on weather routing and to demonstrate the robustness of the results. Therefore, the optimization problem, the arrival time, i.e. the ship's average speed, and the weather conditions are varied for two voyages. Final conclusions are drawn in Chpt. 8. Here, the findings and achievements of the research are summarized and an outlook dealing with potentials for further research is presented.

2 Influence of Weather in Maritime Shipping

The maritime shipping industry continuously aims to maximize efficiency and cost competitiveness particularly as a consequence of cost pressure and tough competition. Performance and cost efficiency improvements, though, must not impair the safety of ship, cargo and crew. To ensure safety of life at sea, safe and efficient navigation and environmental protection, voyage planning is considered to be essential. The principles of voyage planning and the classification of voyage optimization and weather routing are subject to Sec. 2.1. The topic of maritime safety particularly with regards to weather risks is addressed in Sec. 2.2. At the same time increasingly stricter maritime regulations concerning emissions and ship efficiency are introduced by the International Maritime Organization (IMO) and pose additional challenges described in Sec. 2.3. Sec. 2.4 provides an overview of energy efficiency measures and deals with potential gains in efficiency through weather routing. Weather routing is generally supported by commercial systems, summarized in Sec. 2.5, to effectively exploit the efficiency potentials.

2.1 Principles of Voyage Planning and Weather Routing

Voyage planning is considered critical for safe navigation and the avoidance of dangerous situations, which are addressed in Chapter V Regulation 34 of the International Convention for the Safety of Life at Sea (SOLAS) (IMO 2009c). To ensure safe but also efficient navigation of ships, every ship's voyage has to be planned based on appropriate nautical charts and publications as well as guidelines published by the IMO. Prior to proceeding to sea the ship's master has to approve the voyage plan. The master shall not be prevented from taking any decision based on professional judgment, which is beneficial for safety of life at sea and the marine environment (IMO 2009c). The importance of a well planned ship's voyage for safety of life at sea, safe and efficient navigation and environmental protection is also recognized by the IMO in resolution A.893(21) *Guidelines for Voyage Planning* (IMO 1999). As to the resolution, the need for developing a voyage plan and continuously comparing the plan with the actual progress of the ship applies to all ships. It further gives the following objective (IMO 1999, p. 2):

Voyage and passage planning includes appraisal, i.e. gathering all information relevant to the contemplated voyage or passage; detailed planning of the whole voyage or passage from berth to berth, including those areas necessitating the presence of a pilot; execution of the plan; and the monitoring of the progress of the vessel in the implementation of the plan.

According to SOLAS, the voyage plan is intended to identify a route considering relevant ships' routing systems, ensuring safe passage by sufficient sea-room, taking into account adverse weather conditions, known navigational hazards and applicable environmental protection measures as well as avoiding actions potentially endangering the environment. Ships' routing is subject to SOLAS Chapter V Regulation 10 (IMO 2009c) as well as to resolution A.572(14) *General Provisions on Ships' Routeing* (IMO 1985) and the publication *Ships' Routeing* (IMO 2015c). In the resolution the following objective is given (IMO 1985, p. 85):

The purpose of ships' routeing is to improve the safety of navigation in converging areas and in areas where the density of traffic is great or where freedom of movement of shipping is inhibited by restricted sea-room, the existence of obstructions to navigation, limited depths or unfavourable meteorological conditions.

Ships' routing systems contribute to achieving this specific objective in addition to safety, efficiency and environmental protection in general. These systems include, for instance, traffic separation schemes and traffic lanes but also precautionary areas and areas that shall be avoided due to exceptional dangers or for environmental reasons (IMO 2016c). Besides ships' routing systems, adverse weather conditions are crucial, as meteorological and oceanographic factors can directly or indirectly cause damages to or even total losses of ships. In this regard, resolution A.528(13) *Recommendation on Weather Routeing* acknowledges that weather routing is beneficial to ship operations and safety of the ship itself, its crew and cargo. Hence, the IMO (1983, p. 144) recognizes the following:

Weather routeing advice is available to shipping in the form of recommended 'optimum routes' for individual crossings of the oceans.

Among others, meteorological services listed by the World Meteorological Organization (WMO) provide this advice to the master, who makes the final decision on the ship's navigation (IMO 1983, 2016c). For safe navigation and efficient operation of a ship, weather routing is an important measure. It is often considered as one key aspect of voyage optimization. According to the Second IMO GHG Study (Buhaug et al. 2009, p. 47), voyage optimization is defined as follows:

Voyage optimization is the optimization of ship operation that the master can achieve within the constraints that are imposed by logistics, scheduling, contractual arrangements and other constraints.

Voyage optimization in this regard comprises, in addition to weather routing, ballast and trim optimization as well as just-in-time arrival, taking into account tides, queues, arrival windows and contractual arrangements such as penalties for late arrival. Weather routing is described by Buhaug et al. (2009, p. 48) in the following way:

Selection of optimal routes with respect to weather and currents in order to minimize energy consumption.

The description implies that the ship weather routing problem is an optimization problem with an objective function, decision variables and constraints. Typically, ship weather routing aims at minimum energy consumption or fuel costs, while considering meteorological and oceanographic forecasts and various constraints. Other objectives, though, can be maximum safety or comfort, minimum voyage time or distance, or combinations of these objectives. A more detailed description of weather routing considering different objectives is given by Bowditch (2002, p. 545):

Ship weather routing develops an optimum track for ocean voyages based on forecasts of weather, sea conditions, and a ship's individual characteristics for a particular transit. Within specified limits of weather and sea conditions, the term optimum is used to mean maximum safety and crew comfort, minimum fuel consumption, minimum time underway, or any desired combination of these factors.

Providing an optimal track for a ship's voyage as result indicates that the ship's heading is the only decision variable allowing route but no speed optimization. Thus, weather routing as seen by Bowditch (2002) corresponds to the traditional heading-only weather routing described by Chen (2013). Accordingly, traditional weather routing is said to neglect ship responses, engine overload and speed management and to rely on only one source for weather forecasts. Due to these limitations, advanced voyage optimization is to be favored. However, many traditional weather routing systems have been continuously improved to address the named limitations. This not only applies to commercial systems but also academic ones, which are often referred to as weather routing systems but may be much more advanced than the traditional heading-only weather routing. Consequently, differentiation is not made regarding the classification as weather routing or voyage optimization system in the following, particularly in Sec. 2.5 and Chpt. 4. Instead it is focused on differences with regards to the main aspects of weather data, modeling and optimization approaches and ship performance including the type and number of objectives, decision variables and constraints.

The main aspects of weather routing are illustrated in Fig. 2.1. Environmental factors affecting a ship's voyage and its operation are generally winds, seas, currents, fog and ice (Bowditch 2002, pp. 547f.). Weather data influencing the ship's energy consumption and fuel costs, though, mainly comprise meteorological and oceanographic information related to winds, waves and currents (see Chpt. 3). In addition, the energy consumption significantly depends on the ship itself, its calm water resistance, added resistance due to wind and waves as well as the propulsion unit (see Chpt. 5). Ship characteristics, such as a maximum speed, but also ship and voyage specific comfort or safety requirements, e.g. wave height limits, may be considered as constraints. Concerning navigational information, constraints can be given by geographic conditions including areas with restricted water depth, traffic separation schemes, emission control areas or ice. Moreover, restrictions can arise from the voyage schedule, for instance by an estimated time of departure ETD and arrival ETA.



Figure 2.1: Aspects of Ship Weather Routing

Considering all these impacts, the optimal voyage with an optimal combination of the decision variables, such as speed and heading of the ship, is generally determined by mathematically modeling the defined problem and applying an optimization algorithm (see Chpt. 4). Nowadays, finding the optimal route is supported by commercial weather routing services (see Sec. 2.5).

2.2 Maritime Safety and Weather Risks

Maritime safety is a key aspect to global economy as approximately 90 % of global trade is transported by international shipping (Dobie 2017, p. 2). Safety is critical to ship operation and the avoidance of situations that endanger not only crew and passengers but also the ship itself and its cargo. Encouragingly, shipping losses are on a long-term downward trend, decreasing by 50 % over the past decade and by 16 % from 101 in 2015 to 85 in 2016 (Dobie 2017, p. 4). However, significant pressure on operational costs may potentially lead to fewer investments in maintenance and safety (Dobie 2016, p. 20, 2017, pp. 7, 17). This is endorsed by the results of the research project *Energy Efficient Safe Ship Operation (SHOPERA)* provided by the IMO (2016a). The project addresses the concern that the requirements due to the Energy Efficiency Design Index (EEDI) (see Sec. 2.3) may be met by reduced installed power instead of innovative propulsion concepts. This can result in insufficient steering and propulsion abilities to ensure maneuverability in adverse weather conditions (IMO 2016a, p. 1).

The analysis of accident statistics in SHOPERA (IMO 2016a, p. 3) reveals that sufficient maneuverability-related safety of the existing fleet is provided, but that general cargo ships followed by Ro-Ro ferries, bulk carriers and tankers are most vulnerable regarding navigational accidents in adverse weather conditions. Wave heights and wind speeds recorded during accidents, though, are rather moderate, which agrees with inter-

view results showing that 50 % of the ship masters move away from the coast when significant wave heights reach 5 m and wind speeds Beaufort 8 (IMO 2016a, p. 3). Grounding accidents related to heavy weather are most frequently caused by waiting at anchor in adverse conditions and starting the ship's engine too late. Although applying full engine power the ships were not able to turn into seaways or leave the coastal areas. Also in the open sea, sufficient propulsive power and steering ability are required to escape the storm and sail into safe conditions (IMO 2016a, Annex p. 9).

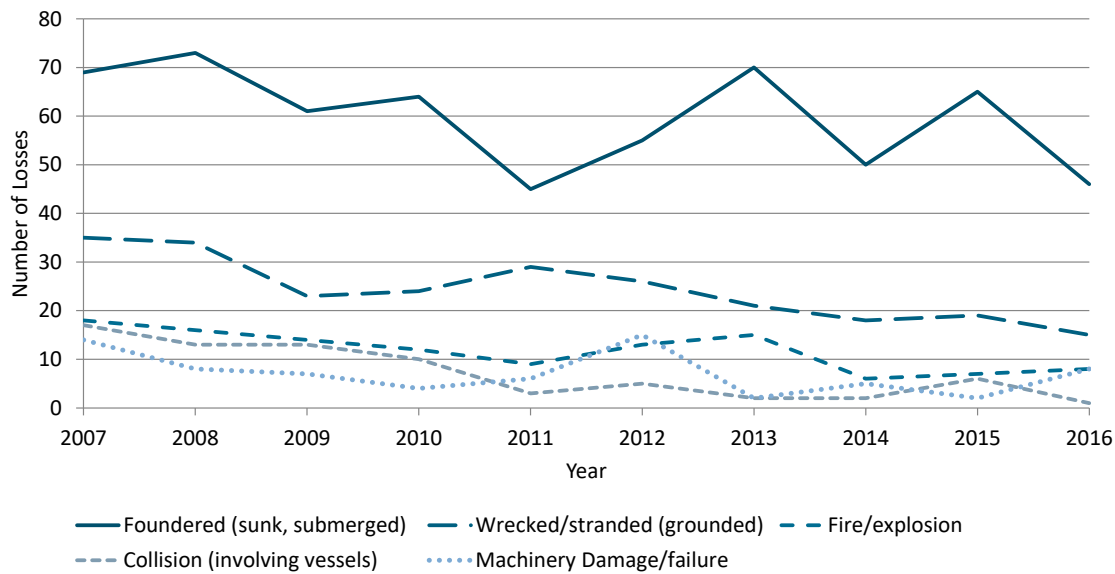


Figure 2.2: Top Five Causes of Total Shipping Losses from 2007 to 2016, adapted from *The Safety and Shipping Review 2017* by Dobie (2017, p. 10)

Foundering, hence sinking or submerging, is the most common cause of shipping losses, as shown in Fig. 2.2. Foundering is often driven by harsh weather including hurricanes (Dobie 2016, p. 7). It accounts for approximately 50 % (46) in 2016 and also for half (598) of all losses over the past decade (Dobie 2017, pp. 10f.). A negative impact on this number and further safety threats are expected due to more extreme weather conditions being anticipated by meteorological predictions. Also the DNV GL (2014, p. 37) states that not only more severe weather conditions but also increased wave heights and a shift in wave patterns are expected. This demands improved ship designs with sufficient propulsion and steering ability as well as improved operational safety standards.

In order to avoid dangerous situations in adverse weather and sea conditions the IMO has published a guidance to the master in MSC.1/Circ. 1228 applicable for all types of merchant ships (IMO 2007). Adverse weather and sea conditions refer to some combinations of wave height and wave length under specific operational conditions that may lead to heavy rolling or even capsizing of the ship (see Sec. 5.5.2). The probability that a ship encounters these dangerous phenomena in a certain sea state and its vul-

nerability, however, not only depend on ship size and speed, but also on hull geometry and actual stability parameters. This implies that the guidance may be too generous for ships with insufficient stability but too restrictive for certain other ships (IMO 2007).

Existing regulations were reviewed in SHOPERA, such as the *IMO Standards for Ship Manoeuvrability* (IMO 2002) and the *2013 Interim Guidelines for Determining Minimum Propulsion Power* (IMO 2013). Furthermore, accident statistics were analyzed and details investigated to identify scenarios as a basis for criteria and corresponding standards to assess propulsion and steering systems sufficient for maneuverability in adverse weather conditions. In correspondence with the scenarios, the three criteria of weather-vaning ability to change and maintain heading in head to bow-quartering waves, steering ability to perform any maneuver in any wave direction, and propulsion ability to maintain a certain speed (6 knots proposed) in any wave direction are suggested (IMO 2016a, p. 3). A ship's maneuverability in adverse weather conditions critically depends on the main engine and propulsion system being modeled correctly under high load in adverse conditions to avoid misleadingly optimistic predictions. The evaluation of the three criteria shows that marginal wave heights may differ significantly with respect to ship type and size (IMO 2016a, p. 6). This should be considered when defining and applying standard wave heights for maneuverability assessments in adverse conditions.

Due to the expectation of ever more extreme weather conditions, current and future emission and efficiency regulations and their implications for safe ship operation, not only improved ship design, but also advanced voyage optimization and weather routing are becoming increasingly important (Dobie 2016, p. 7). Weather routing needs to allow optimization of speed and heading to avoid hazardous situations or increased fuel consumption in severe weather conditions (Chen 2013; Jeffery 2015). Sound routing support can only be provided when accounting for involuntary weather induced speed reduction and voluntary speed reduction. The latter aims to avoid navigational hazards and excessive ship motions, slamming, propeller racing or engine overloading, which may result from efficiency regulations met by reduced installed power. Thus, considering speed and route optimization as well as adequate modeling of a ship's propulsion and steering ability are critical to ensure safe and efficient operation and navigation of ships.

2.3 Maritime Emission and Efficiency Regulations

The environmental pollution caused by ships' operation or accidents is covered by MARPOL (IMO 2017b). MARPOL Annex VI, the Prevention of Air Pollution from Ships, regulates airborne emissions mainly related to sulfur oxides (SO_x), nitrous oxides (NO_x) and Particulate Matters (PM) (IMO 2008). It aims at a progressive reduction of these emissions globally and introduces so called Emission Control Areas (ECAs) with even lower emission limits (IMO 2008, p. 4). Established ECAs are the Baltic Sea area, the North Sea, the North American area and the United States Caribbean Sea area (IMO 2018b). In these designated sea areas limits for SO_x and PM of 0.10% are applicable

since 01 January 2015 (IMO 2008, p. 21), as visualized in Fig. 2.3 (expressed in terms of % m/m – that is by mass). Globally, a sulfur limit of 3.50 % is reduced to 0.50 % from 01 January 2020. In the North American and United States Caribbean Sea ECAs, ships constructed on or after 01 January 2016 shall additionally comply with NO_x Tier III standards for diesel engines. In the North and Baltic Sea ECAs, this applies to ships constructed on or after 01 January 2021 (IMO 2017a). The different levels of control, Tier I to III, with NO_x limits depending on the engine’s rated speed apply according to the ship construction date (IMO 2018a).

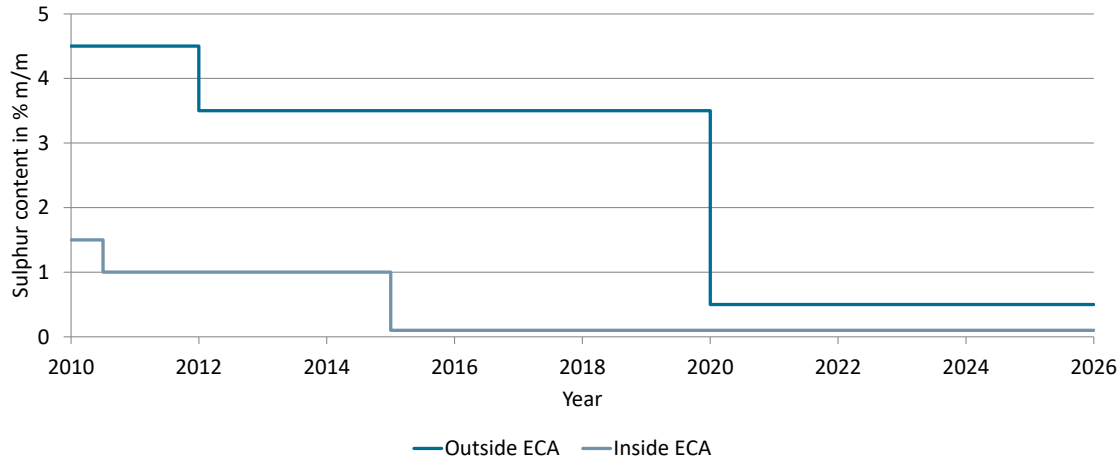


Figure 2.3: Global and Regional Fuel Oil Sulfur Limits, adapted from IMO (2018b)

In order to further control and reduce global greenhouse gas emissions from international shipping, the IMO introduced technical and operational energy efficiency measures with the adoption of amendments to MARPOL Annex VI (IMO 2016b). For new ships above 400 gross tonnage (GT), the Energy Efficiency Design Index (EEDI) is applicable since 01 January 2013. It aims to promote engines and equipment that are more energy efficient and less polluting. Depending on ship type and size, the EEDI requires a minimum energy efficiency level per capacity mile (e.g. tonne mile) (IMO 2016b). However, the introduction of the EEDI is highly controversial. Particularly concerning RoRo ships, investigations have revealed critical mathematical and physical inconsistencies. These result in a severe speed limit and the requirement of physically impossible negative wave resistances to fulfil the EEDI at the desired design speed (IMO 2009a, p. 15). The speed limit correlates to a lower design speed and hence limited power (Deltamarin Ltd 2009). As a consequence, the EEDI leads to propulsion systems often being optimized for calm weather trial conditions. This leads to engine overloading in bad weather with strong winds and high waves (Chen 2013; Jeffery 2015). Although alternative calculation methods for the EEDI have already been proposed (IMO 2009a, pp. 19ff.) and calculation methods in greater detail have been published (IMO 2014), it is essential that limits and effects like these are considered.

Operational measures mainly refer to the Ship Energy Efficiency Management Plan (SEEMP) and Energy Efficiency Operational Indicator (EEOI). The first is mandatory since 01 January 2013 (IMO 2016b). The latter provides voluntary guidance and can assist energy efficiency measurements over a time period during the ship's operation as a monitoring tool (IMO 2009b, p. 7). The SEEMP aims to establish a mechanism to support a shipping company or a ship with planning and improving the energy efficiency of a ship's operation (IMO 2012, p. 3). Furthermore, it provides guidance on best practices for fuel-efficient ship operation (IMO 2012, p. 7). Practices range from improved voyage planning, weather routing and speed optimization, through optimum trim, ballast and use of rudder to hull and propulsion system maintenance as well as waste heat recovery, improved fleet management and cargo handling.

Moreover, the SEEMP provides guidance on the methodology for collecting data on fuel oil consumption (IMO 2012). In 2016, the IMO agreed on a global data collection system for fuel oil consumption of ships as a measure to reduce carbon dioxide emissions (European Commission 2017). In the European Union (EU), since 2018 ships above 5 000 GT are required to monitor their carbon dioxide emissions under Regulation (EU) 2015/757 (European Union 2015). This corresponds to 55 % of the ships calling into EU ports causing 90 % of related emissions (Lloyd's Register 2016b, p. 7). From 2019, the data has to be reported to the ship's flag State for verification. At a later stage the pricing of those emissions has the aim to motivate further reductions (European Union 2015).

Considering the mandatory technical and operational emission reduction measures, the IMO projects that the energy efficiency improvement of all new build ships will be roughly 30 % in 2025 (IMO 2015a) and in average 50 % in 2050 relative to 2012 levels (Smith et al. 2015, p. 283). High gains in energy efficiency can consequently be expected from a new ship with a propulsion system based on marine fuel complying with the emission regulations at all times. Despite these positive prospects some energy efficiency measures may unexpectedly compromise a ship's safety (Dobie 2016, p. 16). Emission reduction measures, particularly the use of ultra-low sulfur fuel, have caused engine and power problems. Power losses and electrical blackouts have been reported, which are particularly critical during maneuvers in narrow coastal waters where low-sulfur fuels are used due to emission control areas. As more stringent emission regulations enter into force, the number of these incidents is likely to increase further. Nevertheless, the challenge that maritime safety and emission control seem to present slightly opposing objectives needs to be addressed by standard specifications for low sulfur fuels, by appropriate advice related to operation and maintenance and by the implementation of adequate energy efficiency measures, not by less stringent environmental provisions.

2.4 Weather Routing as Energy Efficiency Measure

Maritime emission reduction targets and the need for decarbonization require the implementation of adequate energy efficiency measures. Potential pathways and scenarios to

decarbonize maritime shipping and the influence on the global fleet’s technological and operational characteristics are presented by Lloyd’s Register (2016a). Different scenarios will result in a different use of alternative fuels and mix of technical and operational measures due to the impact of numerous uncertainties. These are among others related to future regulations and transport demand, future ship design and operations, potential reductions and costs of measures, as well as the great number of possible combinations of various technologies and operational measures (Lloyd’s Register 2016a, p. 15).

An overview of key areas for energy efficiency, shown in Fig. 2.4, can be found in the Second IMO GHG Study 2009 (Buhaug et al. 2009, p. 54). Slightly different categorizations are among others given by ABS (2013), Bännstrand et al. (2016), and Calleya (2014). In line with Buhaug et al. (2009, pp. 44f.), the category of technical measures targets ship design. It refers to concept, design speed and capability, e.g. geared or ice-class ships, to an optimized steel structure, an improved power and propulsion system as well as to exhaust gas treatment. In addition, it includes low-carbon fuels, such as liquefied natural gas, and renewable energy, such as onboard utilization of wind or solar energy and on-shore generated energy converted into hydrogen or any other energy carrier. While technical measures and design changes are primarily suitable for new ships, operational measures can generally be introduced on all ships. The first subcategory refers to fleet management, logistics and incentives for efficient operation, e.g. by contractual arrangements. The second one addresses energy management including monitoring and optimizing the onboard energy consumption. Lastly, voyage optimization as defined in Sec. 2.1 aims at optimal ship operation within given constraints.

In order to investigate an appropriate mix of technical and operational measures, a model to generate many ship design options with different arrangements of energy efficiency measures was developed by Smith et al. (2016, p. 11) and applied by Calleya et al.

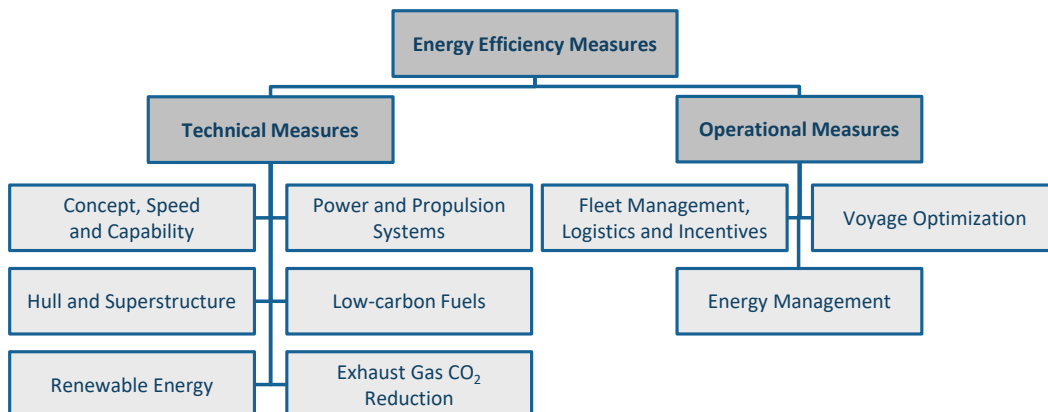


Figure 2.4: Overview of Energy Efficiency Measures, adapted from Buhaug et al. (2009, p. 54)

(2016). Those measures with the highest potential gain in energy efficiency should be introduced. But the sheer number of technical and operational energy efficiency measures is challenging. Which efficiency measures are considered most beneficial depends among others on the owner, the operator, the charter contract or the ship itself. The level of implementation of energy efficient operational measures and its barriers were analyzed empirically by Rehmatulla (2014) and Rehmatulla and Smith (2015). A survey was conducted among global shipping companies from the wetbulk, drybulk, container and mixed sector, of which 149 responded (Rehmatulla 2012). The results in Fig. 2.5 show that the top three measures selected by the respondents are fuel consumption monitoring, weather routing and general speed reduction. They have an implementation rate of only 50 % to 75 %, which is unexpectedly low considering their high cost-effectiveness and energy saving potential (Rehmatulla and Smith 2015, p. 55). Further measures in the order of implementation rate refer to voyage execution, crew awareness, trim draught optimization, autopilot adjustment, port efficiency and optimization of ballast voyages.

Although weather routing is one of the top three measures, perceived barriers to its implementation are a lack of reliable information on cost and savings, a lack of direct control over operations as well as difficult implementation under some types of charter. Generally, the implementation rate of companies having the majority of their fleet on time charter is higher than that of companies with most ships on voyage charter, which can be attributed to a time charterer's greater incentive to save fuel (Rehmatulla 2014). Also Maddox Consulting (2012, p. 77) name difficulties with some charter types in addition to minor technical barriers, which are addressed by constant improvements of weather routing systems (see Sec. 2.5), and administrative barriers, such as proper training of the crew. As knowledge, motivation and skilled application of these

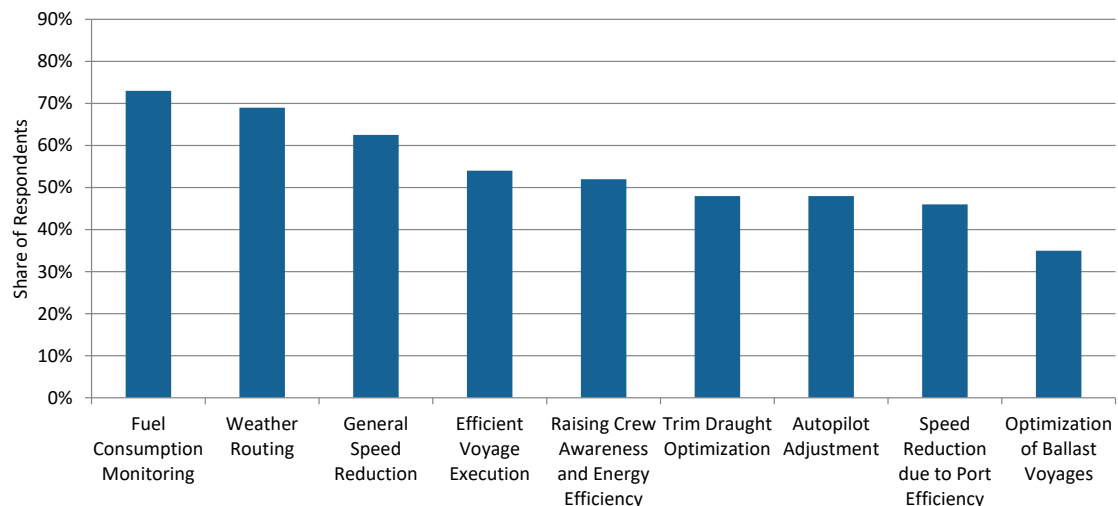


Figure 2.5: Cost-effective Operational Measures and their Average Implementation Rate, adapted from Rehmatulla (2014, p. 177)

systems are essential for efficient operation, measures such as incentive schemes aim to increase efficiency (Buhaug et al. 2009, p. 48). While many barriers can be addressed by certain actions, the main one remains the lack of reliable information on cost and savings.

The large scatter and lack of reliably quoted saving potentials of fuel efficiency measures are widely observed (ABS 2013; Bertram 2012; Buhaug et al. 2009; Höppner 2009). It is indicated in Fig. 2.6. As to Buhaug et al. (2009, pp. 48, 54), just-in-time arrival by weather routing may result in energy savings of 1% to 5%, while voyage optimization may yield savings of 1% to 10% of CO₂ per tonne-mile. Correspondingly, the IMO (2015b, p. 15) states that weather routing may reduce carbon dioxide and black carbon emissions by 2% in case of a low abatement potential and by 10% in case of a high abatement potential. In comparison, Maddox Consulting (2012, p. 29) consider a fuel saving potential by weather routing of 1% to be likely, while 4% are rather optimistic.

Figures given by weather routing service providers may be more optimistic, as manufacturers frequently quote best cases (Höppner 2009). In this regard, Napa vice president Esa Henttinen states that the service provided by ClassNK-NAPA GREEN can achieve a fuel cost reduction of more than 10% with 2% to 4% savings from trim optimization and 6% to 8% from speed and route optimization (Wingrove 2016a). Nevertheless, the impact of weather routing can be substantial in certain situations. In January 2014, a route from eastern England to the Gulf of Mexico was planned via the English Channel, where a storm with wave heights of up to 20 meters had its center. The recommended route north of Scotland resulted in a longer distance but a 15% lower fuel consumption by avoiding these high waves (McMillan et al. 2014). Similarly, 15.5% of the fuel costs were saved on a voyage from the Caribbean to the Baltic in March 2015. StormGeo’s weather routing recommended a route north of Scotland (Schlinkert 2015). In January 2012, three alternative Pacific routes for the same arrival time are compared as to distance, fuel consumption and ship motions by Jeffery (2015). While a 30% higher fuel

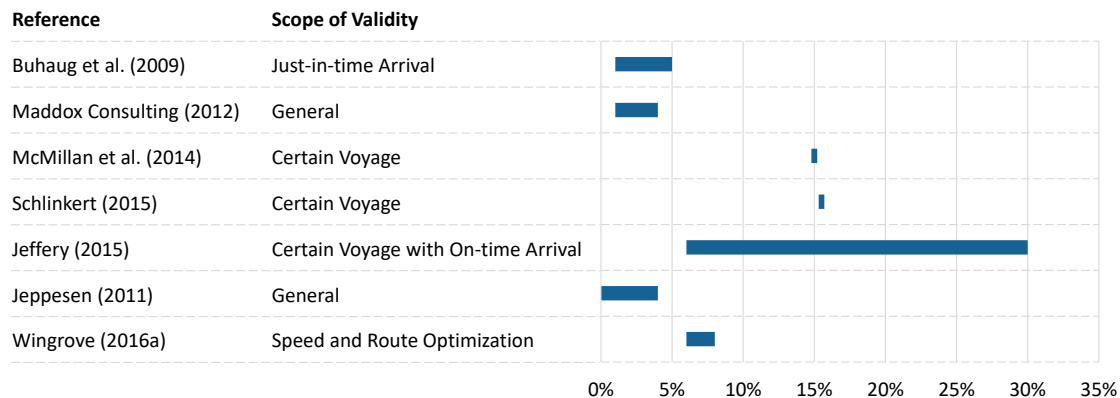


Figure 2.6: Potential Savings of Carbon Dioxide Emissions and Fuel Costs through Weather Routing

consumption is expected on a longer southern route compared to the optimum achieved by Jeppesen's Vessel and Voyage Optimization Solution (now C-MAP IMS, see Sec. 2.5), 6% can be saved when following the optimum instead of the actual route. Jeppesen (2011) further states that up to 4% fuel savings over a sample period, a 87% decrease in cargo damage claims, a 73% decline in structural damage claims and 29% in overall claims as well as a reduction of 80% in the actual number of hours delayed due to heavy weather are proven results from a long-time client. In general, a reduced fuel consumption by up to 4% over performance baseline, reduced ship motions by up to 25% and improved schedule integrity, reliability and operations planning by 7% may be expected.

Notable variations of quoted efficiency gains are mainly attributed to savings being strongly dependent on climate, route, voyage length and vessel performance (ABS 2013, pp. 56ff.). In principle, weather routing has the greatest benefit to the efficient operation of ships on longer, navigationally unrestricted voyages in harsh climates (Bowditch 2002, p. 556; ABS 2013, p. 58). The route should be longer than 1500 nautical miles and the weather should be a key factor to the vessel's performance causing a substantial slowdown in a seaway. As to the WMO (2001, p. 2-8), particularly in the northern hemisphere in the months of December, January and February and in the southern hemisphere in June, July and August potential gains may be greatest. In addition to severe weather conditions, the possibility of just-in-time arrival allowed by charter agreements may result in significant savings. On these voyages a great number of route options is available to avoid harsh weather conditions and hull damages, minimize speed and improve efficiency. Short-term benefits are mainly related to reduced costs, enhanced safety and avoided or at least minimized delays. In the long term, weather routing may be beneficial due to reduced ship damage and less repairs, fewer injured crew members and improved overall health as well as an extended ship's lifetime and lower insurance rates (Bowditch 2002, p. 556). Furthermore, optimizing ship voyages already during a ship's design process allows to determine ship design criteria and may further contribute to performance and safety improvements (Chen 2013, p. 27).

In conclusion, weather routing may particularly contribute to improved energy efficiency, reduced emissions and cost savings for certain routes. Due to significantly varying numbers and the dependence on present ship operation, it is difficult to identify a generally valid potential for improving efficiency by weather routing. Since provided information on fuel savings allows only rough estimates, detailed analyses and case by case evaluations based on computational methods are required for quantitative assessments.

2.5 Commercial Weather Routing Services

Meteorological ship routing as part of voyage planning has been supported by aid of computers for at least fifty years (ABS 2013, p. 56). Weather routing nowadays should not only aim to recommend a fast and safe route but also an optimal speed profile to minimize fuel consumption, while ensuring just-in time arrival and safety of the ship,

its crew, passengers and cargo. Often, weather routing is understood as a service rather than a product assisting ship operators. Different service providers have different meteorological experience and mathematical atmospheric and oceanic models, use different generic or exact ship performance, motion and structural computer models and offer different shipboard and/or shoreside applications (ABS 2013, p. 57). Moreover, different optimization approaches for finding the optimal route, different objectives as well as different constraints may be used. Due to the named differences combined with the considerable number of services offered, ABS (2013, p. 58) concludes that a ship operator is advised to keep these aspects in mind in order to select a suitable service provider meeting the operator's specific requirements.

An overview of four commercial weather routing systems and service providers for merchant shipping is given by Walther et al. (2014) and a brief updated summary by Walther (2015). This overview comprises the Bon Voyage System (BVS) by Applied Weather Technology Inc. (AWT) a StormGeo Company, Seaware EnRoute (not offered anymore) by StormGeo AS, the Ship Performance Optimisation System (SPOS) by MeteoGroup BV and the Vessel and Voyage Optimization Solution (VVOS) by Jeppesen. The same four systems as well as SeaPlanner by FORCE Technology are identified as market forerunners in terms of weather routing and are studied by interviews and questionnaires by Larsson and Simonsen (2014). In *Fleet Management Systems 2015 and 2018*, John and Werner (2015) and John (2018) provide an international market review of software applications for shipping companies. It is updated regularly due to continuous enhancements of the products and changes in the industry.

Mainly based on John (2018) but complemented by information from Walther et al. (2014), Larsson and Simonsen (2014) as well as the providers, a non-exhaustive overview of weather routing service providers for merchant shipping, their systems and features is given in Fig. 2.7. It is focused on the features related to weather data, ship resistance and propulsion, ship motions, route planning and optimization. The overview includes SPOS Onboard by MeteoGroup BV, V-PER by SkySails GmbH, BVS by StormGeo AS and Optimum Ship Routeing (OSR) by Weathernews Inc. (WNI), which are named by John (2018). As SPOS Onboard is MeteoGroup's main system addressing weather routing, further systems from the review are not discussed here. Marorka Voyages by Marorka is excluded due to a lack of route optimization. It aims to minimize voyage costs by identifying the most efficient speed profiles for given routes and ETAs (Marorka 2017). Instead, the overview additionally includes Integrated Maritime Suite (IMS) by C-MAP (formerly VVOS), SeaPlanner by FORCE Technology and CLASSNK-NAPA Green by NAPA Group.

The overview in Fig. 2.7, the following brief descriptions and the continuous improvements of weather routing systems indicate that importance is attached to weather data quality and ensemble forecasts, ship performance and motion models, advanced optimization algorithms and computational power as well as system integration.

2 INFLUENCE OF WEATHER IN MARITIME SHIPPING

Provider		C-MAP	FORCE	MeteoGroup	NAPA Group	SkySails	StormGeo	WNI
Product		IMS	SeaPlanner	SPOS Onboard	CLASSNK-NAPA Green	V-PER	BVS	OSR
Office Application		•			•	•	•	•
Onboard Application		•	•	•	•	•	•	•
Weather Data	Atmospheric Model / Forecast Provider	Several Sources	DMI	ECMWF, NCEP, MetOffice	ECMWF	ECMWF, MetOffice, US Navy	GFS, ECMWF	WNI GRAND-MASTER, WNI OWN2
	Ocean Model / Forecast Provider		DMI	ECMWF, NCEP, MetOffice	ECMWF	ECMWF	WWIII	WWIII
	Forecast Period [days]	15	10	9	14	10	16	15
	Update Period [per day]	No Info	2	4	2	No Info	4	4
	Hurricane Forecasts	•		•		•	•	•
	Ensemble Forecasts	•		•				•
	Considered Weather Effects	Wind, Wave, Surface and Tidal Currents	Wind, Wave, Surface and Tidal Currents, Pressure	Wind, Wave, Currents, Visibility, Temperature	Wind, Wave, Sea Current, Surface Pressure	No Info	Wind, Wave, Currents, Ice, Temperature	Wind, Wave, Currents, Ice, Fronts, SST, Pressure, Visibility, Temperature
Ship Resistance & Propulsion	Ship's Particulars	Ship Model	No Info	Length, Breadth, Deadweight	3D Ship Model	No Info	Length, Breadth	Length, Breadth
	Loading Condition	Trim, Draft, GM	Trim, Draft, GM	Trim	Trim and Draft	Trim and Draft	Draft, GM	Trim, Draft, Hydrostatic Tables, GM
	Loading Comp. Interface	No Info	No Info		•			•
	Ship Propulsion Data	Detailed Ship-specific Engine, Propeller and Hydrodynamic Model	Advanced and Flexible Propulsion Model	Speed Reduction and Fuel Consumption Curves, Max. Engine Power	Propulsion and Engine Model incl. Engine Configuration	Speed Reduction and Fuel Consumption Curves, Max. Engine Power	Speed Reduction and Fuel Consumption Curves, Max. Engine Power	Speed Reduction and Fuel Con. Curves, Max. Engine Power, Open-Water Diagram
	Cost Aspects	Fuel Costs Inside/Outside ECA, Hire	Fuel Costs Engine Configuration	Fuel Costs Main and Aux. Engine, Boiler, Crewing	Fuel Costs Engine Configuration	Fuel Costs Main Engine	Fuel Costs Main Engine	Fuel Costs Main Engine, Hire Rates
Ship Motions	Resonance Module	•	No Info	•	Optional		•	•
	Response Amplitude Operators (RAOs)	•	•		No Info			
	CFD-Calculations		•		No Info			•
	Motion Sensors			SPOS Seakeeping	•	•	•	•
	Real-Time Assessment	•			•	•		
	Safety Restrictions	Roll and Pitch Angle, Parametric Roll, Bow Slam, Deck Submergence, Propeller Emergence, Lateral and Vertical Accelerations	No Info	Roll and Pitch Motions, Surge, Sway, Heave and Yaw	Max. Wave/Swell Height, Max. Wind Speed, Max. Roll Angle, Max. Accelerations at User-set Point	None	Roll Motions, Surf-riding and Broaching-to	Roll and Pitch Motions, Surf-riding and Broaching-to, Slamming
Route Planning	Route Alternatives	•	•	•	No Info	•	•	•
	ECDIS Interface	Import/Export to 30 Formats		•		•		•
	Route Restrictions	Safety Limits and Data from Electronic Navigational Charts incl. Piracy, ECAs, Ice Areas	Piracy, ECAs, Ice Areas	Piracy, ECAs, TSS, Shallow Waters, Ice Areas, Safety and Weather Limits, Marpol Areas	Safety and Geographical Limits	Weather and Navigational Limits	Piracy, ECAs, TSS, Shallow Waters, Ice Areas, Weather Limits, No go Areas	Piracy, ECAs, TSS, Shallow Waters, Ice Areas, Safety, Weather and Customer Specific Limits
Optimization	Objectives	Min. Fuel at Required ETA	Min. Fuel, Min. Time, Req. ETA at Const. RPM (Revolutions)/Power/Speed	Min. Costs, Min. Time, Min. Distance, Min. Safety Risks	Min. Costs, Min. Time, Opt. Route at Const. RPM/Full Load	No Info	Min. Costs, Min. Time, Min. Distance	Min. Costs, Min. Time, Min. Distance, Min. Safety Risks, Max. Comfort
	Variables	Route and Speed	Route and Speed	Route, Speed, ETA	Route and Speed	Route, Speed, Ship Specific Parameters	Route and Speed	Route and Speed
	Algorithm	3D Dynamic Programming	Simulated Annealing (Monte Carlo)	No Info	No Info	No Info	No Info	No Info
	Calculation Time	Few Minutes	Avg. 1 Minute	2 Minutes	No Info	No Info	No Info	3 Hours

Figure 2.7: Commercial Weather Routing Systems and Features (References see Text)

C-MAP - IMS The Vessel and Voyage Optimization Solution (VVOS), originally offered by Ocean Systems Inc., is based on a dynamic program for minimum cost ship routing under uncertainty by Chen (1978). The company was acquired by Jeppesen, a Boeing company, in 2008, of which the marine division was acquired by Digital Marine Solutions in 2016 (Golden 2016). As a separate entity but under the C-MAP brand the Jeppesen Marine and C-MAP portfolio continue to operate. Part of the C-MAP Integrated Maritime Suite (IMS) is VVOS (C-MAP 2016). Using official electronic navigational charts and 15-day high-resolution forecasts for wind, waves and ocean currents, route and speed are varied to achieve the navigationally safest and most efficient route. User-defined safety constraints and restrictions due to a charter party speed, a scheduled time of arrival, slow steaming or excessive ship motions and hull stresses are taken into account. Considered motion risks are related to roll and pitch angle, parametric roll, bow slam, deck submergence and propeller emergence as well as lateral and vertical accelerations (C-MAP 2017). Ship responses may be predicted using forecast wave spectra (see Sec. 3.3) and Response Amplitude Operators (RAOs) (see Sec. 5.5) (Chen 2011, p. 3). Thus, ship-specific motion, engine and propeller models allow to compute engine power and propeller revolutions in varying weather conditions (C-MAP 2016).

Weather forecasts from several sources, high-resolution data, ensemble forecasts and tropical cyclone forecasts are seen as key aspects for ship motion predictions and advanced voyage optimization (Chen 2011, 2013). Forecasts automatically updated by email allow daily continued refinements of the voyage plan and accurate arrival time predictions (C-MAP 2016; Wingrove 2016b). Considering a range of arrival times and operational safety constraints given by the ship's master, the optimization problem with the two variables speed and heading and the objective of minimum fuel consumption can be solved within a few minutes using 3D dynamic programming (see Sec. 4.4.2) on a user-defined grid (Chen 2013, p. 26). Total costs include bunker costs inside and outside ECAs as well as optionally daily hire rates. Optimal routes can be compared to traditional routes, such as those with constant speed, and may be exported to thirty different ECDIS formats (C-MAP 2017). An analysis view allows the ship's crew to graphically monitor weather effects, ship motions and real-time seakeeping, engine parameters and propulsion performance along the ship's route (C-MAP 2016). A polar diagram visualizes operating speeds and headings exceeding safety limits, while another diagram displays the effect of ship heading alterations on wave-induced shear forces and bending moments at critical frames (Chen 2011, p. 4). In addition, C-MAP provides 24/7 routing support by onshore experts (C-MAP 2017).

FORCE Technology - SeaPlanner SeaPlanner has been developed by FORCE Technology in cooperation with the Danish Meteorological Institute (DMI). Originally, it was designed for DFDS ferries operating in the Baltic and North Sea with rapidly changing weather conditions, in particular sea currents, and shallow water effects (IHS Fairplay 2010). SeaPlanner enables operators to plan a voyage by optimizing a ship's route and speed on board the ship while avoiding unfavorable weather conditions and ship motions

(FORCE Technology 2016). Routes can be calculated as combinations of rhumb lines and great circles or as optimized great circle route or rhumb line when considering high-resolution forecasts for wind, wave and currents. Global weather forecasts comprising pressure, wind, wave, surface current and freak wave index data are provided by DMI twice a day with a forecast period of ten days (Larsson and Simonsen 2014). Options concerning optimization objectives and constraints include minimum fuel consumption, minimum voyage time, given ETA at constant engine power, at constant revolutions per minute (RPM) or at optimized speed as well as fixed calm water speed.

An advanced and flexible propulsion model allows e.g. to select the number of engines in operation. The model considers the ship's loading condition based on trim and draught, its resistance in calm water and due to shallow water, waves and wind as well as propeller characteristics, engine configuration, hull and propeller fouling and poor maintenance. Data sources include semi-empirical models, model tests, sea trial data, seakeeping calculations, Computational Fluid Dynamics (CFD) calculations, wind tunnel tests and the propeller open-water diagram (FORCE Technology 2016). Ship responses may be predicted using RAOs (see Sec. 5.5). By applying Simulated Annealing (Monte Carlo) (see Sec. 4.5) the voyage is optimized within a few seconds to minutes (Larsson and Simonsen 2014). The system SeaPlanner as part of the onboard SeaSuite solution can be complemented with SeaTrend for propeller and hull performance monitoring, SeaEngine for engine performance monitoring or SeaTrim for trim optimization.

MeteoGroup - SPOS Onboard Introduced at a congress in Beijing in 1994, more than 4500 vessels use the Ship Performance Optimisation System (SPOS) Onboard to support voyage optimization, ETA planning or compliance with regulatory requirements, such as SEEMP (MeteoGroup 2017b; Spaans and Stoter 2000). SPOS provides optimal routes and route alternatives based on vessel and voyage data entered by the master including speed and fuel curves, as well as weather forecasts updated four times daily (John 2018; MeteoGroup 2014a, 2017c). These are produced by an in-house model using input from three models. In addition, MeteoGroup offers the systems RouteGuard, FleetGuard Monitoring and SPOS Seakeeping. RouteGuard is applied by 5000 ships annually to improve safety of crew and cargo throughout the voyage (MeteoGroup 2017c). It provides an optimum route based on daily weather updates to reduce fuel consumption, emissions and sailing time, to avoid adverse weather conditions, to increase accuracy of ETA predictions, safety and efficiency, and to monitor and analyze a ship's performance (MeteoGroup 2017a). FleetGuard Monitoring offers real-time fleet monitoring, including fleet tracking, weather maps and warnings (MeteoGroup 2015). It can be seamlessly integrated in SPOS Onboard, as can SPOS Seakeeping. The latter is developed in cooperation with AMARCON, a member of the ABB group. It can be connected to AMARCON's Octopus system to allow real-time motion control besides motion based voyage optimization (Adegeest 2008; MeteoGroup 2014b). Accounting for ship characteristics including type, dimensions and loading conditions, weather forecasts and user-defined motion thresholds, SPOS Seakeeping aims at voyage performance opti-

mization and route alternatives by forecasting and visualizing ship responses, resonances and exceedance of limits along any route.

NAPA Group - ClassNK-NAPA GREEN NAPA Group, headquartered in Helsinki, Finland, offers software solutions for ship design and operation. It was acquired by the classification society ClassNK in 2014 (NAPA Group 2017b). Already launched in 2012, the joint ClassNK-NAPA GREEN solution addresses ship operations and their planning by trim, speed and route optimization, their monitoring in real-time, noon and voyage reporting as well as their follow-up ashore by fleet monitoring, voyage analysis and analytical services (ClassNK Consulting Service 2016, 2017; NAPA Group 2017a). Regarding speed and route optimization, NAPA Voyage Optimization provides an optimal speed profile, engine configuration and route by using a dynamic performance model and up-to-date weather and ocean forecasts (ClassNK Consulting Service 2017; NAPA Group 2017a,c). According to a functional specification for NAPA Voyage Optimization Version 2013.4 (NAPA Group 2014), the system allows to minimize fuel costs on a voyage for a given ETA, to calculate the earliest ETA or to determine the optimal voyage execution at constant RPM or at full engine load for multi-engine ships. Speed and route are optimized based on a ship specific 3D model of the hull and appendages, a propulsion machinery and engine model, the ship's loading and hull condition (draught, trim, fouling), engine configuration and condition, fuel properties, weather and ocean forecasts as well as water depths to consider shallow water effects (NAPA Group 2014, p. 6). Data on the loading condition is automatically available from the NAPA Loading Computer (NAPA Group 2014, p. 4). Constraints are given by geographical and user-defined limits for environmental conditions or ship motions, which may be maximum wave height, wind speed, roll angle and accelerations at a specified point (NAPA Group 2014, p. 6). To predict ship motions, such as the probability of slamming, propeller immersion or water on deck, a seakeeping module may be added (NAPA Group 2014, p. 9). For improved performance predictions in normal operating conditions, where data from the shipyard and sea trials are insufficient, a dynamic performance model combines this data with measured operational data from onboard sensors and applies machine learning techniques to reduce errors (NAPA Group 2014, p. 10).

The standard weather data includes wind, waves and surface pressure from the European Centre for Medium-Range Weather Forecasts (ECMWF). It has a forecast period of 14 days, is updated twice a day and is enhanced by ocean current forecasts (NAPA Group 2014, p. 11). Optionally, forecasts can be customized, e.g. the resolution or data format, by cooperation with partners, such as DMI (Denmark), National Oceanic and Atmospheric Administration (NOAA) (U.S.) or Tidetech (Australia) (see Sec. 3.4). Also the implementation is adapted to customer needs, existing navigational equipment and sensors onboard to collect and analyze operational data efficiently (ClassNK Consulting Service 2016). The system is applied by shipping companies, such as Evergreen, Stena Line (Nagata 2015) and K Line (Wingrove 2016a), but also by some shipyards, such as Namura Shipbuilding for optimized ship design (NAPA Group 2016).

SkySails - V-PER The Vessel Performance Management Toolbox (V-PER) by SkySails not only provides weather routing functionalities but also monitoring features for fuel consumption, engine performance, hull and propeller condition and bunkering. Planning functions relate to voyage scheduling, weather routing, conditional maintenance and fleet strategy. In addition, it includes documentation and analysis functions for voyage reporting, online performance, legal documentation and performance reporting. Lastly, there are optimization functions for ship speed, dynamic trim, energy management and performance consulting (SkySails 2017). All standard onboard logbooks are integrated into V-PER. Concerning weather routing, individual and multiple ship performance curves for every weather situation and for different loading conditions are used. Both, route planning and real-time monitoring, can be conducted on board or ashore. Furthermore, the system allows to calculate and optimize routes, estimated time of sailing and of arrival, fuel consumption and costs (Cameron and Brabeck 2015, p. 26). SkySails (2017) states that SkySails' performance management solutions have been installed on approximately 200 ships of different types and sizes.

StormGeo - BVS Originally, the Bon Voyage System (BVS) was offered by Applied Weather Technology, Inc. (AWT) headquartered in Silicon Valley, California. It was acquired by StormGeo, headquartered in Bergen, Norway in January 2014 (StormGeo 2017g). In 2017, AWT changed its name to StormGeo with AWT being known as the shipping division of StormGeo (StormGeo 2017a). The division routes 60 000 ship voyages annually and more than 6 000 ships use BVS for onboard route and ship performance optimization (StormGeo 2017h). A voyage can be optimized with the objective to minimize costs while sailing an optimal route, to arrive at a required ETA, to minimize risk of damage or maximize safety (StormGeo 2017i).

StormGeo (2017f) highlights eight features of BVS 8. They include position polling and track transfer to allow onshore fleet management, system compatibility with ECDIS, and automatically updated tropical storm data. Tropical cyclone proximity is given by multi-model ensemble-based probability zones (Tastula 2016). Latest weather updates are derived from global model data from various sources in combination with running and developing in-house models. They are sent highly compressed by email or broadband. Ship speed related features refer to ship-specific fuel consumption curves based on statistical curve modeling and dual speed optimization for speed adjustments in ECAs to maximize cost savings. For this purpose BVS Dual Speed Optimization considers sailing distances and speed settings inside and outside ECAs, environmental data and constraints, fuel prices and daily hire costs as well as ship data, in particular dynamic fuel consumption curves derived by regression analysis from a large database storing weather data and noon reports (StormGeo 2017b,c). Generally, speed recommendations by StormGeo, which are calm sea speeds, assume constant power rather than constant RPM as this is considered to be more fuel efficient (Shields and Weber 2015). Last but not least, features concerning seakeeping aspects are incorporated in the BVS Seakeeping module. It aims at predictive seakeeping to avoid excessive ship motions and

damage to ship, cargo or crew. The optional integration of anemometer and motions sensors allows the consideration of wind data as well as real-time seakeeping guidance and motion alerts. In addition, onshore experts provide 24/7 support.

As to E.R. Schiffahrt (2017), BVS is applied on board their ships due to customized input of ship data, such as length, breadth, design draught, fuel consumption and speed reduction curves, of safety thresholds and weather constraints as well as of voyage specific no-go areas and bunker prices. To maximize the time of running the main engine at constant power in an efficient range, BVS includes functions to adjust the ship's RPM periodically according to the environmental conditions or at least every twelve hours (E.R. Schiffahrt 2017, p. 15). An optimized route is calculated within minutes. Moreover, CPO Containerschiffreederei uses BVS and experiences a decrease in vessels' damage and weather-related accidents (StormGeo 2017d; The Maritime Executive 2017). Also at the Korean company H-Line Shipping Co.,Ltd. BVS helps masters to calculate least cost, fuel or time of a route as well as ETA (StormGeo 2017e).

WNI - OSR Weathernews Inc. (WNI), headquartered in Chiba, Japan, provides services to more than 6 000 vessels each day (Weathernews 2017). Optimum Ship Routing (OSR) uses ship-specific performance models and latest weather forecasts to optimize route and engine RPM. This enables operators to meet their objectives and business priorities, which may be minimum time, minimum fuel consumption with or without on-time or earliest arrival, maximum safety, emission control or charter party compliance. Based on the business priority, the concept of voyage planning continues with a strategic route selection, hence the shortest, best North, best mid Latitude, best South or the master's intended route, in order to run a speed reduction algorithm to allow RPM control (Weathernews 2014).

When planning a voyage, information regarding the voyage, hazards, the customer and the weather are considered (Ogata 2010, p. 35). Voyage information includes the master's report and position polling, which concerns vessel status, position, time, speed, course and RPM. Hazards can originate from geography, bathymetry, ice, tropical storms and regulations, such as military, environmental protection, fishery and piracy areas. Customers' business data refers to the vessel specification, fleet schedule, company policies regarding safety, schedule or costs and contractual requirements. Weather data is related to pressure, visibility, wind, wave, ocean and tidal currents as well as sea surface and air temperature. According to John (2018), OSR uses weather data from WNI models. WNI continuously enhances the forecast models by upgrading detailed coastal wave models and developing integrated atmosphere-ocean coupling models (Weathernews 2013). Throughout a voyage, WNI provides monitoring of the ship's schedule, performance and safety including ship motions (Ogata 2010, p. 24). 24/7 onshore assistance is ensured by a global network with service centers in the U.S., Japan and Denmark. The latter aims to serve European customers, in particular Maersk Line and Maersk Tankers, who entered into a three-year contract with WNI in 2016 (Weathernews 2016).

3 Meteorological and Oceanographic Data

Meteorological services and warnings, subject to Chapter V Rule 5 of the SOLAS (IMO 2009c), are important for the safety of navigation. Particularly those parameters of the atmosphere and ocean that influence the ship's voyage, i.e. motion and fuel consumption, are important for ship weather routing (Bowditch 2002, pp. 547f. Perez 2005, p. 17). Often, the factors considered for route selection and surveillance include wind, seas, fog, ice and ocean currents. Since primarily wind, seas and currents directly influence the ship's fuel consumption, which can be optimized by ship weather routing, these factors are addressed in Sec. 3.1 to 3.3 and their forecasting in Sec. 3.4.

3.1 Global Atmospheric Circulation and Winds

In general, all movements in the atmosphere originate from the solar radiation energy absorbed by the Earth, which is high at the equator (low pressure) and low at the poles (high pressure) (Bott 2016, p. 207). This differential heating of the Earth and corresponding pressure gradients create circulation systems in the atmosphere, thus global wind systems, that redistribute thermal energy. Wind in this context is the movement of air relative to the Earth's surface caused by vertical and horizontal differences in atmospheric pressure. Bott (2016, p. 211) states that in addition to the thermal circulation, the global atmospheric circulation is mainly affected by the Earth's rotation, the inclination of its axis of rotation resulting in seasonal variations of solar radiation, the inhomogeneous distribution of water and land surfaces with various macroscale mountain structures as well as by the momentum conservation of the Earth-atmosphere-system.

Due to the Coriolis effect caused by the Earth's rotation, the direct flow along the pressure gradients is deflected. In the free atmosphere above the friction layer, the impact of both forces may be balanced leading to a flow parallel to the isobars known as the geostrophic flow or wind (Bouws 1998, p. 23). Generally, the isobars are not straight but curve around highs and lows, which leads to a flow crossing the isobars called gradient wind (Bowditch 2002, p. 482). At the Earth's surface, surface friction additionally diverts winds towards low pressure areas. As the wind speed tends to zero when approaching the Earth's surface and the wind profile in the boundary layer is influenced by friction effects, the altitude for which a weather forecast is given is not to be neglected.

The large scale global circulation patterns and wind systems resulting from the above factors are schematically shown in Fig. 3.1. In each hemisphere, three cells of circulation can be defined, namely the Hadley cell, the Ferrel cell and the Polar cell. Within the

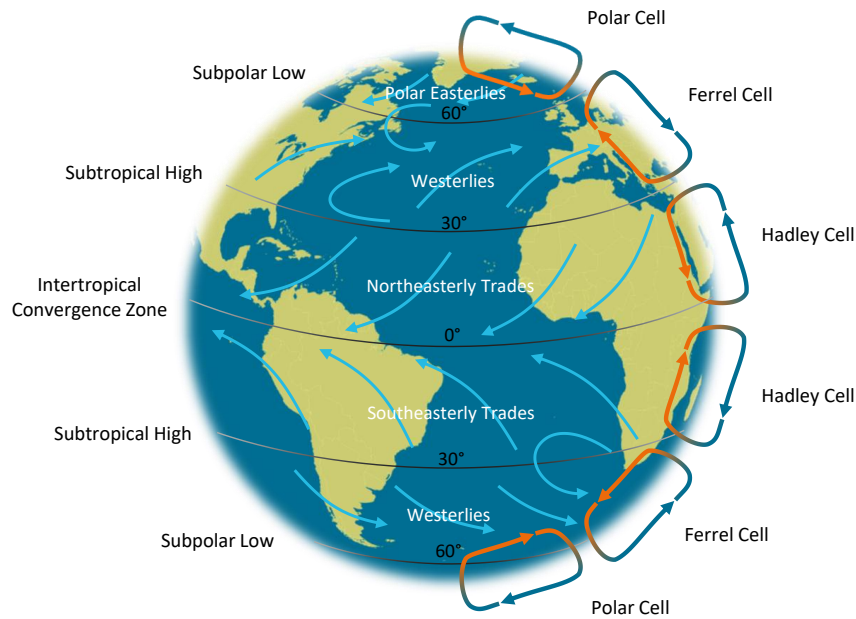


Figure 3.1: Schematic of Global Atmospheric Circulation, based on Bott (2016, p. 212), Bowditch (2002, p. 483), Met Office (2017a), and Wells (2012, p. 169)

Hadley cell the air ascends at the equator, cools down when moving in northeasterly direction in the upper troposphere¹ and sinks down at approximately 30° latitude. From these subtropical high pressure belts in the so called horse latitudes the air flows back to the equator in the lower troposphere causing the northeasterly and southeasterly trade winds. These merge in the Intertropical Convergence Zone (ITCZ) and have been particularly important in shipping due to their persistence (Bott 2016, p. 207). The area between the two trade winds known as the doldrums is characterized by light variable winds similar to the horse latitudes. The near calms used to be a problem for sailing merchant ships. In the adjacent Ferrel cell, the circulation system is mainly formed by the prevailing westerlies in the lower troposphere and ascending air in the subpolar low pressure belts at approximately 60° latitude that flows back to the subtropical high pressure belts at high altitudes. In comparison to the Hadley cell, the circulation system is rather volatile and inconsistent. Particularly due to large landmasses present in the northern hemisphere secondary wind circulations distort the pattern considerably (Bowditch 2002, p. 485). In the rather landless southern hemisphere, the different atmospheric pressure pattern leads to greater speed and persistence of the westerlies, which are called roaring forties in 40° to 50° southern latitude. In the Polar cell, part of the air ascending in the subpolar low pressure belts flows towards the poles, where it is cooled down, sinks and flows back in the lower troposphere resulting in the polar easterlies.

¹The troposphere is the atmospheric layer from the Earth's surface up to a height of 10 to 15 km. (Malberg 2007, p. 20)

Further common circulation patterns include winds associated with cells of relatively low pressure, known as cyclones with counterclockwise circulation, and those of high pressure, known as anticyclones with clockwise circulation in the northern hemisphere (Bowditch 2002, p. 492). Circulation is reversed in the southern hemisphere. In an anticyclone, winds are rather light resulting from the comparatively large distance between successive isobars. The relatively small distance in case of a cyclone causes stronger winds and usually stormy weather. Migratory (extratropical) cyclones and anticyclones, developing over land and sea, commonly occur in the region of the prevailing westerlies. Strong tropical cyclones² originating in the subtropics or tropics are infrequent but generally more violent due to the high energy concentration in a rather small area (Bowditch 2002, pp. 493, 503). Due to their violence and predominantly oceanic occurrence, they are of importance for maritime shipping. Consequently, specific hurricane forecasts (e.g. provided by National Hurricane Center (2018)) are considered by many commercial weather routing systems. Also in academic research, attention is paid to cyclone avoidance, such as by Wisniewski et al. (2009).

For maritime shipping, particularly the winds in the lower troposphere are relevant. In addition to the winds associated with the large scale global circulation pattern and those related to migratory cyclones and anticyclones, various local wind systems, such as land and sea breezes resulting from alternate cooling and heating of land bordering on water, influence the weather (Bowditch 2002, p. 493). To account for the specific weather conditions during a ship's voyage, forecasts derived from numerical models (see Sec. 3.4) are used in ship weather routing. In contrast to the general impact of wind on a ship (see Sec. 5.4), the specific consideration of hurricane forecasts and their effects on ship weather routing is not in the particular focus of this thesis.

3.2 Global Oceanic Circulation and Currents

Ocean currents can be classified based on their forcing mechanism as wind driven and thermohaline currents. Another distinction can be made as to their depth, i.e. surface, intermediate, deep or bottom currents (Bowditch 2002, p. 433). Thermohaline currents are caused by differences in water density, which is influenced by temperature and salinity taking into account a certain depth, thus pressure. Temperature differences result from heating or cooling of the water surface. The salinity increases due to evaporation processes and the formation of sea ice and decreases due to excessive precipitation, inflow of freshwater into the oceans and melting of ice (Klose 2016, p. 59). While thermohaline circulation mainly generates subsurface currents, the global surface circulation (see Fig. 3.2) is primarily wind driven caused by friction effects at the interface between water and air. Due to the water's low viscosity the surface movement is not directly transferred

²Tropical cyclones are generally classified by their form and intensity. A tropical disturbance may become a tropical depression with a rotary circulation and one or more closed isobars, then a tropical storm with distinct rotary circulation and finally a hurricane (North Atlantic) or typhoon (North Pacific) with strong rotary circulation and closed isobars. (Bowditch 2002, p. 846)

to lower layers, but is increasingly deflected by the Coriolis force the greater the water depth until about 200 m. Within this so called Ekman layer, the direction of the current consequently shifts with depth forming a spiral (Bowditch 2002, p. 433). This influence results in wind driven gyres not being symmetrical and ocean currents being narrower, stronger and deeper at the oceans' western boundaries, such as the Agulhas Current, and broad, shallow and slow-moving at eastern boundaries and mid-ocean. At eastern boundaries, e.g. in case of the California Current, water masses are transported away from the coast allowing nutrient-rich water to flow from the depths to the surface (Berking and Huth 2010, p. 296). Moreover, the total surface current is influenced among others by tidal currents, thus the periodical (cyclically changing) horizontal movement of water accompanying the rise and fall of tide (Bowditch 2002, pp. 129, 434).

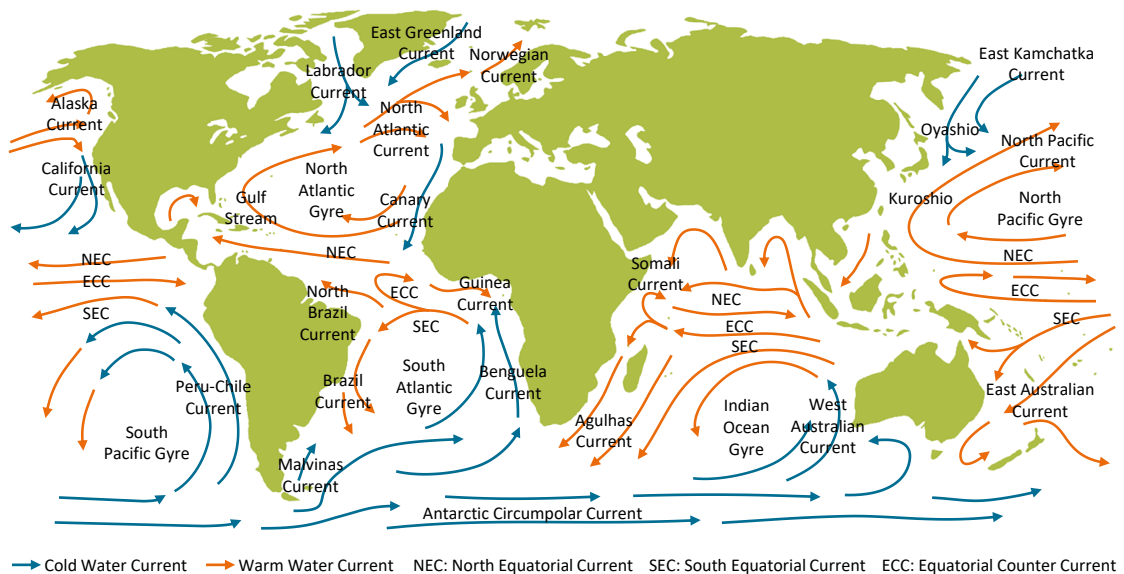


Figure 3.2: Schematic of Global Oceanic Surface Circulation, based on Berking and Huth (2010, p. 294), Siedler et al. (2013, p. 12), and Wells (2012, p. 171)

Since the global surface circulation is related to the general atmospheric circulation described in Sec. 3.1, some major warm and cold water ocean currents, schematically illustrated in Fig. 3.2, are relatively persistent throughout the year. In principle, the major surface currents move around the subtropical highs in circulatory patterns, thus the clockwise North Atlantic and Pacific Gyre as well as the counterclockwise South Atlantic, Pacific and Indian Ocean Gyre. In the equator region, the trade winds cause westward Northern (NECs) and Southern Equatorial Currents (SECs) as well as eastward Equatorial Counter Currents (ECCs) that transport part of the westward moving water back eastward as part of the tropical surface circulation patterns (Berking and Huth 2010, p. 295). In the Indian Ocean, the ECC only occurs in the Monsoon season from May to October. In the South, the broad, slow-moving Antarctic Circumpolar Current is mainly caused by the strong westerlies (roaring forties). It completely ex-

tends around Antarctica, as there are no major boundaries, and serves as conveyor belt to exchange water between the oceans. This cold water current extends to the North feeding the Peru-Chile, Malvinas, Benguela and West Australian Currents. In turn, it is fed by the Brazil, Agulhas and East Australian Currents (Bowditch 2002, p. 434). Together with the SEC these currents form the gyres of the southern hemisphere.

In the northern hemisphere, the North Atlantic Gyre is mainly formed by the cold Canary Current, the warm NEC and the warm, rather narrow and fast Gulf Stream with maximum speeds of 2 to 4 knots off the coast of Florida (Bowditch 2002, pp. 435f.). The Gulf Stream continues northeastward following the prevailing westerlies as vast, slow-moving North Atlantic Current and then Norwegian Current. It meets the cold Labrador Current carrying large amounts of ice and the East Greenland Current. The Canary Current partly forms the NEC and partly the Guinea Current. In the North Pacific, the main part of the NEC curves northwards becoming the Kuroshio (Black Stream), which is similar to the Gulf Stream in many respects, until it continues widened and slower as North Pacific Current (Bowditch 2002, p. 436). The minor part of the North Pacific Current curving northwards becomes the Alaska Current and then the (East) Kamchatka Current. The major part continues clockwise as California Current and deflects westward at the end of Baja California to substantially form the NEC. Similar to the Labrador Current in the North Atlantic, the Oyashio comes from the North bringing sea ice and turns southward and then eastward when encountering the Kurashio.

Ocean currents considered to be particularly important for maritime shipping are the Gulf Stream and the Agulhas Current (Berking and Huth 2010, p. 296). When the warm Gulf Stream meets the cold Labrador Current eddies may break off as there is little mixing of the waters and the Gulf Stream meanders and shifts position (Bowditch 2002, p. 435). These cold and warm eddies continue as separate, circular flows and may have a diameter of up to 50 to 150 nautical miles. Passing through them can reduce or increase the ship's speed by 2 knots (Berking and Huth 2010, p. 296). The warm, narrow and fast Agulhas Current with speeds up to 5 knots along the South African east coast often encounters strong winds in the area of the Cape of Good Hope that originate from southern ocean storms. Due to the opposing directions of current and wind, dangerously large seas are created (Berking and Huth 2010, p. 296; Bowditch 2002, p. 438). Considering the effect of ocean currents on a ship and its voyage in ship weather routing (see Sec. 5.3) can reduce transit times and fuel consumption and increase safety (Bowditch 2002, p. 433).

3.3 Ocean Surface Waves and Natural Seaway

In principle, ocean surface waves are caused by natural forces acting on the ocean. These forces primarily relate to pressure or stress from the atmosphere, thus winds, but also to forces due to earthquakes, the gravity of Earth, Moon and Sun as well as surface tension (Bouws 1998, p. 1). The resulting natural motion of the water in the form of ocean sur-

face waves is also referred to as seaway (Berking and Huth 2010, p. 288; Bowditch 2002, p. 826). Ocean waves can be classified by their wave period, which is the time between the passage of two successive wave crests at a fixed point. Depending on the wave period it can be distinguished between capillary waves (< 0.1 s) resulting from surface tension, gravity-capillary waves (0.1 - 1.0 s), ordinary gravity waves (1.0 - 30.0 s) caused by winds, infra-gravity waves and wave groups (30.0 s - 5.0 min), long-period waves (5.0 min - few hours), such as seiches³, storm surges and tsunamis, as well as ordinary tidal waves (12 h - 24 h) and trans-tidal waves (> 24 h) (Bouws 1998, p. 1).

Particularly important for maritime shipping and subject to forecasting are wind-generated gravity waves. They are almost always present at sea, may significantly affect a ship's behavior and other coastal and offshore activities, and are more difficult to predict than e.g. tidal waves due to their irregularity resulting from winds considerably varying in space and time (Bouws 1998, pp. VII, 1). With respect to these waves, it can be distinguished between wind sea and swell. While the first propagates approximately as fast as the present wind speed and is often short-crested, the latter originates from stronger wind elsewhere and is rather long-crested (Bertram 2012, p. 156). For wave forecasting and seakeeping investigations of ships, the natural wind-generated seaway is typically approximated by superposition of many regular (harmonic) waves, i.e. sinusoidal, long-crested, progressive waves with an infinite number of troughs and crests (Bertram 2012, p. 144; Bouws 1998, pp. 1f.). It is illustrated in Fig. 3.3.

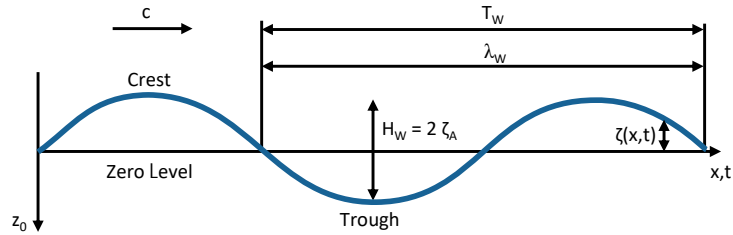


Figure 3.3: Parameters of a Regular Wave, based on Bouws (1998, p. 2) and Perez (2005, p. 21)

The wave height H_W is defined as the vertical difference between trough and crest, which is double the wave amplitude ζ_A . The wave length λ_W is the horizontal distance between two successive crests and the wave number k is $2\pi/\lambda_W$. A regular wave is further described by its period T_W or (circular) frequency ω which is $2\pi/T_W$. The speed of the wave propagation, i.e. the advancing speed of a wave crest or trough, is denoted as the phase velocity or celerity c which is λ_W/T_W . In contrast, the energy of waves in deep water, potential and kinetic energy, does not move with the speed of an individual wave but with the speed of wave groups. These even occur in regular swell due to the presence of many different wave lengths that tend to be grouped together (Bouws

³As to Bowditch (2002, p. 827) a seiche is a “stationary wave usually caused by strong winds and/or changes in barometric pressure. It is usually found in lakes and semi-enclosed bodies of water. It may also be found in areas of the open ocean.”

1998, p. 8). In deep water, the group velocity c_g of waves is half of the phase velocity. The ratio of wave height to wave length is defined as the steepness of a regular wave. The momentary elevation of a regular wave $\zeta(x, t)$ is generally given as a sine or cosine function of position x and time t and considering an initial phase ϵ (Perez 2005, p. 21):

$$\zeta(x, t) = \zeta_A \sin(\omega t - kx + \epsilon) \quad (3.1)$$

The superposition of many regular waves of different wave lengths and propagation directions yields an irregular seaway (Bertram 2012, p. 153). The phase shifts between the regular waves vary with time and space and are chosen randomly at time zero. This leads to a random irregular seaway corresponding to the natural wind-excited one. Initial assumptions to apply this superposition principle relate to a stationary seaway as well as small wave heights and small steepness, thus linear wave theory or Airy theory (Bertram 2012, p. 144). Due to the random, irregular nature, natural seaway and wave records are often approached using statistical descriptions (Perez 2005, p. 25). A wave record, i.e. a record of the wave elevation at a specific location for a certain time period, can be decomposed by Fourier analysis to derive a wave spectrum, or energy-density spectrum. Giving the distribution of wave energy over frequency (and direction), this is the most common description of a wave field (Bouws 1998, p. 12). A one-dimensional, only frequency dependent spectrum is given when assuming that all regular waves propagate in the same direction, which is typical for long-crested seaways, such as swell. In case of short-crested seaways, which rather represent natural seaways, the energy is distributed over frequency and direction. Thus, the spectrum is directional or two-dimensional. The two-dimensional spectrum $S_\zeta(\omega, \mu)$ can be described by a one-dimensional one $S_\zeta(\omega)$ multiplied with a function f giving the distribution of wave energy over the direction μ to both sides of the main propagation direction μ_0 (Bertram 2012, p. 156):

$$S_\zeta(\omega, \mu) = S_\zeta(\omega) \cdot f(\mu - \mu_0) \quad (3.2)$$

A wave spectrum can be derived in good approximation when the wind field and its recent history are known. Although swell and sometimes wind sea can significantly change a spectrum's form, a wind sea spectrum can be rather uniform after a 0.5 to 1.0 hour period of constant wind (in space and time) (Bertram 2012, p. 156). But the parameters of the spectrum, in particular the significant wave height H_S , i.e. the mean wave height of the one-third highest waves, and the period can also reach constant values only after hours or days. At the peak frequency ω_P (correspondingly the peak period T_P), the spectrum has its maximum, thus maximal energy density. Together with the significant wave height it is frequently used to characterize a specific sea state by codes from 0 to 9 (Fossen 2011, p. 200). Consequently, particularly accurate surface wind analyses and forecasts need to be available for reliable wave forecasting (Bouws 1998, p. 15, 35). In addition, the processes of wave generation and decay have to be analyzed and considered, since they influence the form of the spectrum. These processes include wind driven wave generation, dissipation e.g. due to breaking waves or shallow water,

convection, i.e. transport of wave energy, and nonlinear wave-wave interaction causing a redistribution of wave energy within the wave spectrum. Moreover, importance is attached to the propagation of surface wave energy, which is strongly related to the group velocity of waves. Although these processes are fundamental for state-of-the-art numerical wave modeling, fully calculating all processes and explicitly treating all components in an operational environment is usually not computationally viable. Thus, outputs of operational numerical wave models used to consider the effect of seaways on ships in weather routing (see Sec. 5.5) may differ. The superordinate complexity of forecasting systems is briefly discussed in the next section, while a detailed introduction to numerical wave modeling and operational models is given by Bouws (1998, pp. 57–80).

3.4 Meteorological and Oceanographic Forecasting

Marine meteorological and oceanographic (metocean) information and services need to be adequately available to meet the requirements established under the SOLAS convention and to consider winds, ocean currents and waves in ship weather routing. Relevant services are offered by numerous national centers continuously producing metocean forecasts as well as by private companies. As the overview of commercial weather routing systems in Fig. 2.7 indicates, data is among others provided by the European Centre for Medium-Range Weather Forecasts (ECMWF 2018), the UK Met Office (UKMO) (Met Office 2018), the National Oceanic and Atmospheric Administration’s (NOAA) National Centers for Environmental Prediction (NCEP 2017), the Danish Meteorological Institute (DMI 2018) as well as the U.S. Navy (2018). An example of a private company is Tidetech from Australia (Tidetech 2017). Metocean data supplied by Tidetech is used by weather routing systems, such as ClassNK-NAPA Green. Also the developed weather routing system can handle data from Tidetech (see Sec. 6.4.5), which is used for the evaluations in Chpt. 7.

Data Format Although metocean information is provided by numerous institutions, an internationally standardized binary code named GRIB introduced by the WMO is typically used to exchange observed or processed metocean data (WMO 2015). It may be distinguished between two editions. While GRIB Edition 1 (GRIB1) stands for GRIDded Binary data, or processed data in the form of grid-point values expressed in binary form, GRIB Edition 2 (GRIB2) refers to General Regularly-distributed Information in Binary form. General advantages of the code are related to self-description, flexibility and expandability. GRIB2 has been introduced to overcome weaknesses in particular for transmission and archiving of spectral data, multi-dimension data, long-range and climate products as well as ensemble products (WMO 2003, p. 1). A detailed specification of both editions is given by WMO (2003, 2015).

Forecasts, Hindcasts, Reanalyses and Climatologies Forecasts used by the commercial weather routing systems listed in Fig. 2.7 are valid for periods of 9 to 16 days. They

are updated two to four times a day, since the forecast accuracy deteriorates with increasing forecast period (ECMWF 2012a). Instead of using specific forecasts at the time of voyage, routes can also be selected for climatological reasons (WMO 2001, p. 2-7). Among others, climatologies may be applied to provide weather routing advice outside the forecast period when a ship's (remaining) voyage duration is longer than the latest available forecast. Based on the forecast periods, meteorological forecasting ranges are defined by the WMO (2010, p. I-4). It is distinguished between nowcasting (0-2 h), very short-range (< 12 h), short-range (12-72 h), medium-range (72-240 h), extended-range (10-30 days) and long-range (30 days-2 years) forecasts as well as climate forecasts (>2 years). Depending on the definition, extended-range forecasts are sometimes considered to be long-range ones. In other cases, long-range weather forecasts are referred to as climate forecasts.

While a forecast presents an estimate of future conditions, a hindcast “is a numerical model integration of a historical period where no observations have been assimilated” (Met Office 2016). In contrast, when data assimilation techniques are applied to historical periods the process is called reanalysis. Reanalyses not only provide information for a specific position, like observations, but across a complete region giving a more coherent picture. Relating this for example to waves, Bouws (1998, p. VIII) notes that “one can forecast the propagation of wave energy, but the evolution (growth) of the wave energy is dependent on the wind and so a major part of the procedure is actually referring to the forecast of the winds that cause the waves. The wave growth is in fact diagnosed from the forecast wind.” Hence, hindcasting of wave data is its diagnosis based on historical wind data. Hindcasts are often used to derive wave climatologies (WMO 2010, p. 3-4).

Numerical Models Metocean forecasts are generally derived from numerical models based on data collected from observations and measurements of the atmosphere and oceans. To generate accurate forecasts the numerical models need to account for various, complex and globally interconnected physical processes. The complexity can be illustrated by means of the ECMWF forecasting system as an example, which is explained in detail by Persson et al. (2015). It consists of an atmospheric general circulation model, a land surface model, an ocean general circulation model and an ocean wave model as well as perturbation models for the data assimilation and forecast ensembles.

The atmospheric general circulation model is formulated based on diagnostic and prognostic equations describing the “static relationship between pressure, density, temperature and height” as well as “the time evolution of the horizontal wind components, surface pressure, temperature and the water vapour contents of an air parcel” (Persson et al. 2015, p. 2). In contrast, rather small scale physical processes, such as convection and clouds, are described by means of statistical methods and simplified mathematical-physical models. Furthermore, topographical and climatological fields are considered, such as the percentage of land and water for every grid point given in a land-sea mask or the sea surface temperature and ice concentration obtained from analyses provided

daily by the Met Office. To solve the equations numerically, a discretization in space and time, thus a grid point space, is used. The larger the time steps, the more acceptable the computation time of the forecast becomes. However, the higher the resolution, the more accurate the forecasts will be, e.g. concerning coastlines or anticyclones.

The land surface model accounts for the energy and water exchange between the atmosphere and different types of natural surfaces, such as soil and vegetation. In addition, the atmosphere is coupled to the ocean through the effects of wind, heat, precipitation and evaporation. In this regard, the three-dimensional ocean general circulation model considers the circulation as well as the thermal structure of the upper ocean layers and its variations. The interaction of wind and waves is treated by the ocean wave model named WAM, which is coupled to the atmospheric general circulation model. The model “describes the rate of change of the 2-dimensional wave spectrum, in any water depth, caused by advection, wind input, dissipation due to white capping and bottom friction and non-linear wave interactions” (Persson et al. 2015, p. 6). It also considers swell propagation. However, the impact of surface currents on the sea state is not taken into account and near-coastal waves may be of lesser quality than open-ocean waves due to the present model resolution.

Regarding observations serving as input for the models, a distinction can be made between conventional and non-conventional observations. These are in-situ observations or measurements, e.g. from buoys, ships or surface weather stations, and remote-sensing observations from satellites respectively. Due to the increasing availability of particularly non-conventional observation data, advanced analysis procedures, such as four-dimensional variational data assimilation (4D-Var), gain in importance (Persson et al. 2015, p. 8). This aims to mathematically enable continuous feedback between observations and model data and to create sequences of model states for specific time windows, which best fit the observations. Uncertainties in the observations, sea surface temperature and forecast evolution are incorporated by small variations. This results in an ensemble of data assimilations producing perturbations, which are also used to construct perturbations in forecast ensembles (see below).

Similar to ECMWF, other national centers maintain several models to address the increasing need for reanalysis, numerical weather prediction (NWP), ocean models and climate prediction. In this regard, NOAA’s NCEP operate the Global Forecast System (GFS), which is a coupled model consisting of four separate models for atmosphere, ocean, land/soil and sea ice (NCEI 2018). NOAA’s NCEP also maintains the third-generation wave model WAVEWATCH III. Detailed information is published by NOAA’s National Weather Service (2018) and The WAVEWATCH III Development Group (2016). Since it is a modeling framework with contributions by various developers, it is also the basis for model configurations at the Met Office (Met Office 2017c). GFS and WAVEWATCH III are both named in Fig. 2.7.

However, differences among others in resolutions, global and regional configuration, data assimilation and the considered physics, result in a different accuracy of weather forecasts for every model. As to Chen (2013), national centers tend to provide higher accuracy in their own coastal waters than in mid-ocean areas. Moreover, most models only poorly account for complex and rapidly occurring phenomena, such as hurricanes. That is why some commercial weather routing systems listed in Fig. 2.7 consider specific hurricane forecasts. In general, the nonlinear nature implying uncertainties and often complicated interpretation of the model output, i.e. the forecasts, is inherent to forecast systems. Uncertainty due to incomplete knowledge of the initial state, unavoidable simplifications and resulting forecast errors may be sampled by probabilistic prediction using forecast ensembles (ECMWF 2012b). Furthermore, skilled human forecasters with meteorological and statistical knowhow are usually employed to interpret different numerical outputs, determine modification needs, optionally combine information from different sources and provide decision support to forecast users (Persson et al. 2015, pp. 37f.).

Deterministic and Probabilistic Forecasting Generally, a Numerical Weather Prediction (NWP) system generates a forecast based on a single initial state, which is referred to as a deterministic forecast (WMO 2012). Since uncertainty is associated with every deterministic forecast primarily due to the chaotic nature of the atmosphere, it is aimed at the prediction of forecast confidence by probabilistic weather forecasting (ECMWF 2012b, 2017a). Therefore, many centers operate Ensemble Prediction Systems to produce a set of forecasts, i.e. a forecast ensemble or ensemble forecast, representing a range of possible weather conditions on the basis of slightly different initial states, perturbed weather models and sometimes several models. To save computational time, the ensemble members are computed using a lower horizontal resolution, normally around half the resolution of the deterministic one (Persson et al. 2015, p. 25; WMO 2012, p. 1). Comparing the members to a control forecast generated without perturbations gives an estimate of the uncertainty in the forecast based on the divergence or spread.

Using ensemble forecasts for weather routing allows to assess the likeliness that an estimated time of arrival can be met at a set speed. The smaller the spread of the forecast results, the higher the confidence becomes that a lower speed will be sufficient to reach the destination in time. To increase the confidence, a higher speed may be chosen or the best of each national center’s forecast may be combined to increase the accuracy (Chen 2013, p. 27). At ECMWF (2012a), ensemble prediction based on the coupled ocean-wave, atmosphere model allows e.g. to show the uncertainty in ocean wave height along a ship’s route. Ensemble forecasts are used by some commercial weather routing services (see Fig. 2.7), such as IMS, SPOS Onboard and OSR. Furthermore, the use of ensemble weather data has been studied among others by Chu et al. (2014), Hinnenthal (2008) and Skoglund et al. (2015). However, the specific consideration of ensemble forecasts and their effects on ship weather routing is not in the particular focus of this thesis.

4 Mathematical Modeling and Optimization Approaches

The ship weather routing problem described in Sec. 2.1 is treated as an optimization problem. Hence, this chapter deals with optimization in relation to ship weather routing in Sec. 4.1 and with mathematical modeling and optimization algorithms applied in this field of research in Sec. 4.2 to Sec. 4.5. The content of this chapter is substantially based on Walther et al. (2016), who provide a slightly less extensive overview of applied approaches. Moreover, it is to be noted that the approaches are classified according to the names, terms and descriptions used by their authors. Conclusions for the development of the weather routing system are drawn in Chpt. 6.

4.1 Optimization in Relation to Ship Weather Routing

Ship weather routing typically aims at minimum fuel costs, minimum voyage time, maximum safety or a combination of these objectives, while taking into account forecasted meteorological and oceanographic information and various constraints. Constraints may not only be given by ship characteristics, geographic conditions and time restrictions, but also by safety requirements or emission regulations. Looking at all these characteristics at once, the ship weather routing problem may be seen as a rather complex real-world problem. As to Domschke et al. (2015, p. 1), the analysis of complex real-world problems within a planning process to support sound decision making by applying mathematical methods is understood as operations research (OR). Although a generally accepted standard definition for the field of OR is lacking (Eiselt and Sandblom 2010, p. 1; Schwenkert and Stry 2015, p. 1), Hillier and Lieberman (2010, p. 8), Domschke et al. (2015, p. 2), and Eiselt and Sandblom (2010, p. 4) acknowledge that OR in the narrower sense is primarily limited to quantitative models and their solution. Hence, it refers to the mathematical modeling of decision problems and the development of algorithms for the application and solution of these models.

Approach In order to approach a complex real-world problem, slightly varying six to eight steps are among others proposed by Hillier and Lieberman (2010, p. 8), Domschke et al. (2015, p. 2), Heinrich (2013, p. 8), Schwenkert and Stry (2015, p. 6), and Eiselt and Sandblom (2010, p. 9). Giving an example, Domschke et al. (2015, pp. 1f.) identify the six steps of analyzing the problem, creating a descriptive model, formulating a mathematical model, gathering data, finding a solution by using an adequate algorithm and evaluating the solution. In contrast, Finke (2008, p. ix) summarizes most of the proposed steps and

distinguishes between the phase of mathematical modeling and the solution procedure, which may be exact or approximate, and generally algorithmic. Also Domschke et al. (2015, p. 2) focus on mathematical modeling of decision problems and the development of algorithms. Accordingly, this chapter mainly focuses on these two phases.

Types of Models In general, a model is a purpose-oriented, possibly simplified and generally idealized representation of a real system or problem (Werners 2013, p. 3). As to their purpose, it can be distinguished between descriptive models to illustrate the real situation by elements and relationships, explanatory and forecast models to evaluate empirical laws or hypotheses for explaining facts and to predict future developments as well as decision models. A decision or optimization model is a formal representation of a decision or planning problem that, in its simplest form, contains at least one alternative set and an objective function that evaluates it (Domschke et al. 2015, p. 4). A decision model is developed with the aim to determine optimal or suboptimal solutions by applying suitable methods. Simulation models are often very complex optimization models, where no analytical solution method exists. While OR primarily deals with decision or optimization models and their optimal solution, descriptive, explanatory or forecast models can be used to gather information or support decision-making (Domschke et al. 2015, p. 4; Werners 2013, p. 8).

Mathematical Modeling A descriptive decision or optimization model needs to be translated into a mathematical model in order to choose an adequate method for finding an optimal solution. A mathematical model corresponds to an idealized representation formulated by using mathematical symbols and expressions (Hillier and Lieberman 2010, p. 11). Hence, mathematical modeling refers to the objective function, the decision variables, the constraints and the parameters being identified and expressed in mathematical terms. The objective function, a mathematical function of the decision variables, generally aims at minimization or maximization. The decision variables represent each of the related quantifiable decisions to be made. Thus, they are the unknowns that are varied within their co-domains for finding an optimal combination (Domschke et al. 2015, p. 5). Mathematical expressions of any restrictions on the values of the decision variables are referred to as constraints, which can be equality or inequality constraints. The constraints and the objective function can contain constants, such as coefficients, which are called parameters of the model (Hillier and Lieberman 2010, p. 11).

As to the ship weather routing problem, options for objectives, decision variables and constraints are given in this chapter as well as for the developed weather routing system in Sec. 6.2. Due to varying interpretations and definitions of the real problem, models and mathematical formulations can differ. When developing a model, an abstract idealization of the problem is created, where approximations and simplifying assumptions are generally required if the model is to be tractable, thus capable of being solved (Hillier and Lieberman 2010, p. 12). However, the model needs to remain a valid representation of the problem. This leads to the trade-off between precision and tractability of

the model. In addition to tractability, Domschke et al. (2015, p. 7) distinguish between deterministic and stochastic models, single and multiple objectives as well as linear and nonlinear models. In deterministic models, the parameters of the objective function(s) and the constraints are assumed to be known accurately. If, however, at least one parameter is to be interpreted as a random number or variable, a stochastic model is given. Often, optimization models have a single objective. Multiple objectives require the introduction of efficiency measures allowing for assessing the degree to which each objective is satisfied. Further, models can be subdivided according to the type of objective function(s) and constraints (see 'Areas of Operations Research'). In any case, importance is attached to efficient modeling, thus the construction of an adequate model, to derive an optimal solution with minimal computational effort.

Method and Algorithm To determine optimal solutions for the developed mathematical model, suitable methods are required. In this context, a method is usually understood as the procedure including modeling and problem solving by using algorithms. An algorithm can generally be regarded as a processing specification for solving a problem, which can be represented in detail by an executable program (Werners 2013, p. 9). Occasionally, method and algorithm are used synonymously. The central technique to OR is optimization, which is used as a solution tool and a modeling device. As to Nemhauser et al. (1989, p. v) "optimization deals with problems of minimizing or maximizing a function of several variables usually subject to equality and/or inequality constraints". A technique, which is widely used to analyze stochastic systems and can be seen as a key technique to OR as well, is simulation (Hillier and Lieberman 2010, p. 935).

Optimization is the determination of the valid alternative that best corresponds to a given objective of all alternatives. Therefore, optimization presupposes that all valid alternatives are taken into account, the objective is known, the alternatives are evaluated with regard to this objective and the evaluation results must be comparable with each other (Werners 2013, p. 8). In case of numerous alternatives, describing and evaluating all alternatives explicitly is too costly and complex. Instead, it is aimed at implicitly examining all alternatives by means of mathematical optimization and deriving the best alternative using an optimization algorithm. Depending on the structure of the model, efficient suitable algorithms are available. If optimization is not possible or too complex due to the model structure or size, heuristics may be suitable to determine a good solution. A heuristic is a procedure or an algorithm that uses a systematic procedure to find the best possible solution, but which usually does not achieve the optimum and cannot be mathematically proven (Werners 2013, p. 9). The quality of the solution in case of optimization methods is assessed based on the computational effort to derive the optimal solution. In case of heuristics, importance is attached to the deviation from the optimal solution or to the comparison of results using different heuristics.

Areas of Operations Research In correspondence with the approaches towards mathematical modeling and algorithmic solution procedures, it can be distinguished between

different areas or disciplines in the field of OR. Depending on the reference, such as Domschke et al. (2015, pp. 8f.), Gerdtts and Lempio (2011, p. 1), Heinrich (2013, p. 13), and Schwenkert and Stry (2015, p. 2), the number of areas and the degree of detail, i.e. the level of categorization, differ. Since none of the overviews claims to be exhaustive, the following list provides a non-exhaustive overview of areas in OR derived from the named references but mainly based on Domschke et al. (2015, pp. 8f.):

- Linear and Nonlinear Programming
- Graph Theory and Network Optimization
- Dynamic Programming
- Integer and Combinatorial Programming
- Inventory and Queuing Theory
- Simulation

Linear Programming (LP) models have one or several linear objective functions, often numerous linear constraints and variables with mostly nonnegative real values (Domschke et al. 2015, p. 8). In contrast, nonlinear optimization models have a nonlinear objective function and/or at least one nonlinear constraint. Linear and nonlinear programming are described fundamentally and with respect to ship weather routing in Sec. 4.2. The area of graph theory and network optimization has contributed to bridging the gap between linear and combinatorial programming (Nemhauser et al. 1989, p. vii). It is commonly used to approach all kinds of networks, e.g. for shortest path problems or maximum or minimum cost flows in graphs. It is treated in Sec. 4.3. Dynamic Programming (DP) models can be divided in separate stages allowing stage-wise recursive optimization for sequential decision making. Approaches from DP are subject to Sec. 4.4. Many combinatorial optimization problems can be expressed as integer or binary (linear) optimization problems, but solving these models is often far more difficult than solving linear models with continuous variables (Domschke et al. 2015, p. 9). Finke (2008) presents various solution techniques for combinatorial problems and mainly distinguishes between exact methods, such as dynamic programming, and approximate methods, i.e. heuristics. In recent years effective heuristic algorithms, also called metaheuristics, have gained popularity for various combinatorial problems (Hillier and Lieberman 2010, p. 490). Also in ship weather routing metaheuristics have been applied more frequently lately and are addressed in Sec. 4.5. The last two areas, namely inventory and queuing theory as well as simulation⁴, do not play a significant role in ship weather routing and are disregarded. In the following, the relevant areas are used to categorize and provide an extensive but not exhaustive overview of mathematical modeling and optimization approaches applied with regards to ship weather routing. It is to be noted that the approaches are classified according to the names, terms and descriptions used by their authors.

⁴Queuing theory is mainly used to analyze the handling behavior of service and operating stations. Simulation may be deterministic or stochastic and is often applied to analyze different alternatives within complex stochastic optimization models. (Domschke et al. 2015, p. 9, 246)

4.2 Linear and Nonlinear Programming

Linear Programming (LP) has become a standard tool with diverse areas of applications that range from production planning to agricultural planning as well as from portfolio selection to selecting shipping patterns (Hillier and Lieberman 2010, p. 23). Models in LP require all mathematical functions to be linear functions. They generally have one or several linear objective function(s), often numerous linear constraints and variables with real values (mostly only nonnegative) (Domschke et al. 2015, p. 8). The most important and remarkably efficient solution procedure for linear programming problems is called the simplex method⁵, described in detail among others by Domschke et al. (2015, p. 26) or Hillier and Lieberman (2010, p. 89). Variations and extensions of the simplex method can also be used to perform postoptimality analysis on the model, which includes sensitivity analysis (Hillier and Lieberman 2010, p. 89). Sensitivity analysis can be described as the testing of a model's optimal solution regarding reactions to changes in the initial data by identifying and varying sensitive parameters (Domschke et al. 2015, p. 48). Despite the fact that sensitivity analyses may be used in the area of ship weather routing, e.g. to analyze routes in different weather conditions or with regards to different ship characteristics, LP can hardly be applied to solve the ship weather routing problem as all mathematical functions need to be linear functions.

In contrast to linear programming, nonlinear programming aims to get hold of the numerous real-world problems with nonlinear interrelationships, such as transport costs influenced by transport volume and distance. Hence, nonlinear optimization models have a nonlinear objective function and/or at least one nonlinear constraint. Depending on the characteristics of the objective function and constraints, various different types of nonlinear optimization problems exist. Types of problems described by Domschke et al. (2015, p. 183) include unconstrained problems with one or several variables that can or cannot easily be solved by differentiation, general constrained problems as well as constrained problems with specific characteristics, such as quadratic programming with linear constraints and a quadratic objective function, convex and separable programming⁶. As there is no single universal algorithm to solve all types of problems like the simplex method in linear programming, algorithms for various different types have been developed (Hillier and Lieberman 2010, p. 546). Depending on the type, problems with rather simple functions may be solved efficiently, while other small problems might lead to significant increases in computational effort (Domschke et al. 2015, p. 9; Hillier and Lieberman 2010, p. 537). The widespread general distinction between methods de-

⁵The simplex method is an incremental technique starting with a feasible solution which is improved, tested and increased in case of a non-optimal solution. Thus, it moves “on the boundary of the feasible set from one extreme point to an adjacent extreme point” (Eiselt and Sandblom 2010, p. 69).

⁶Convex programming commonly refers to minimization of a problem with a convex ('curving upward') objective function or to maximization of a problem with a concave objective function (Domschke et al. 2015, p. 191). Separable programming is a special case of nonlinear convex programming, where each term of a function involves just a single variable, so that the objective function can be separated into a sum of functions of individual variables (Hillier and Lieberman 2010, p. 549).

signed for unconstrained optimization problems and those for constrained optimization problems is used to classify the methods applied in ship weather routing in the following (Domschke et al. 2015; Luenberger and Ye 2008; Nemhauser et al. 1989).

4.2.1 Unconstrained Optimization Methods

Often, importance is attached to unconstrained optimization problems, because in many procedures for solving more complex problems they occur as sub-problems and constrained problems are sometimes easily transformed into unconstrained ones (Domschke et al. 2015, p. 192; Luenberger and Ye 2008, p. 3). It is to be noted that although methods are developed for unconstrained optimization in particular, the concepts are fundamental to nonlinear programming and may be applied or extended to constrained optimization methods (Bertsekas 1999, p. 22).

Conjugate Direction Method As an algorithmic approach particularly for unconstrained minimization, conjugate direction methods are iterative methods and “are most simply presented as methods for minimizing strictly convex quadratic functions” (Nemhauser et al. 1989, p. 55). However, they can also be used to solve nonquadratic optimization problems (Bertsekas 1999, p. 131). A method from this class is presented by Powell (1964) “for finding the minimum of a function of several variables without calculating derivatives”. In ship weather routing, Ishii et al. (2010) apply this method to derive a minimum time route based on a predetermined ship’s route given as a Bézier curve along which the voyage time is calculated by numerical ship maneuvering motion simulation. Kobayashi et al. (2015) use the same approach to find a minimum fuel route. The aim now is to minimize a cost function consisting of N variables by applying Powell’s method instead of optimizing the route. This is initially given by a Bézier curve defined by N control points along the great circle route between origin and destination. The costs are calculated by performing a maneuvering simulation accounting for hull and rudder forces, propeller thrust as well as wave and wind forces. Planned improvements refer to the consideration of constraints, such as voyage time or safety limits.

Nelder-Mead-Method The Nelder-Mead-Method (NMM) or Downhill Simplex Method was proposed by Nelder and Mead (1965) as a simplex method for function minimization. It is popular for solving nonlinear problems in a multidimensional space for which the derivatives are not available in explicit form or only in form of very complicated expressions. Thus, NMM belongs to the class of nonderivate methods. Considering a function of n variables without constraints, the method starts with a simplex defined by $n+1$ nodes, which is iteratively adapted until it contracts on to the final optimum (Nelder and Mead 1965). Although NMM as well as other methods of this type are fairly simple to implement, they are direct search methods with a rationale bordering on heuristics and theoretical convergence properties that are often unsatisfactory (Bertsekas 1999, p. 162). In ship weather routing, NMM is applied by Hinnenthal (2008) to solve a nonlinear problem with minimum time and fuel consumption as objectives and several

constraints due to engine limitations and critical ship responses (see Sec. 5.5.3). The various constraints may force the objective functions into multi-modal shapes, i.e. functions with local optima. Hence, the applied deterministic method based on a convex solution space may or may not deliver the optimal result (Hinnenthal 2008, p. 17). Due to this risk, Hinnenthal (2008) also employs the stochastic method of a genetic algorithm (see Sec. 4.5.2). A similar approach is used by Pipchenko (2011) to minimize a time-integral of variable main engine power inputs required to maintain a specified ship's speed under consideration of added resistance due to environmental influences and ship's safety (see Sec. 5.5.3). To avoid adverse weather conditions and allow the generation of alternative routes intermediate points between origin and destination are introduced. In case of four or less points NMM is used. Otherwise a genetic algorithm is applied.

DIRECT Method As to observations by Nemhauser et al. (1989, p. 631), many nonlinear programming methods aim for a local optimum of a continuous real valued objective function, but have difficulties to determine the best of possibly several local optima, which leads to a global optimization problem. Methods to solve these problems may be stochastic or deterministic (Nemhauser et al. 1989, p. 633). A deterministic method belonging to a category of global optimization methods, where the objective function is replaced by an approximation that is iteratively updated until its global optimum is sufficiently good, is proposed by Shubert (1972). It assumes that the so called Lipschitz constant is known, i.e. "a bound on the rate of change of the objective function" (Jones et al. 1993, p. 158), such as the maximum possible acceleration in case of the function being a velocity (Shubert 1972, p. 380). In case of a one-dimensional function, the method improves a piecewise linear approximation with directional derivatives equal to the constant in each iteration. Due to practical problems with regards to specifying a Lipschitz constant, convergence speed and computational complexity in higher dimensions, a modified and extended algorithm and direct search technique called DIRECT (DIviding RECTangles) is presented by Jones et al. (1993). The algorithm balances local and global search and is deterministic without requiring derivatives and multiple runs. The need to specify a Lipschitz constant is eliminated by simultaneous searches with all possible Lipschitz constants, which allows simultaneous local and global search by small and large constants respectively. High-dimensional spaces can be handled by partitioning the space into hyperrectangles. Fast convergence is achieved by finding the basin of convergence by global search and exploiting it by local search.

Regarding ship weather routing, the DIRECT method is investigated by Larsson and Simonsen (2014) for finding a minimum fuel route subject to soft and hard constraints imposed by landmasses, maximum wave height and arrival time. Since information about the decision variables (latitude, longitude and speed) is assigned to each waypoint, three dimensions are added to the problem with each additional waypoint, which increases computation time and complexity. Consequently, the method only uses four intermediate waypoints. This may be seen as the main deficiency in addition to an unacceptably long computation time for finding a local optimum despite fast convergence regarding the

global optimum. This is also experienced by Hameed (2015), who applies the DIRECT method to approach a multi-objective optimization problem. Objectives are related to time, fuel consumption and safety and constraints are imposed by landmasses and arrival time. Hameed (2015) considers it to be less suitable for high-dimensional problems with 75 dimensions. It is also compared to the discrete 3D graph based approach proposed by Andersson (2015) (see Sec. 4.3) and has been found inferior due to the computational effort and the possibility of discontinuities when considering constraints.

4.2.2 Constrained Optimization Methods

In practice, many complex problems cannot be treated in its entirety considering all possible choices but need to be restricted in its scope. Hence, they are formulated as constrained problems (Luenberger and Ye 2008, p. 3). Usually, a constrained nonlinear problem involves continuous functions and variables as well as constraints that can be equality and inequality constraints. Among others depending on the type of constraints, different algorithmic approaches can be applied (Nemhauser et al. 1989, p. 171).

Augmented Lagrangian Method Augmented Lagrangian Methods (ALM) belong to a class of computational methods for nonlinear problems with equality or inequality constraints that use a penalty function. In case of methods based on a penalty function, the constrained problem is transformed into a series of unconstrained problems (Bertsekas 1999, p. 370). Some or all constraints are eliminated and a penalty term is added to the cost function prescribing a high cost to infeasible points. Thus, a penalty parameter determines the degree to which the original constrained problem can be approximated by the unconstrained one (Bertsekas 1999, p. 388). ALMs additionally aim to minimize the augmented Lagrangian function successively by introducing an estimate of the Lagrange multiplier. Bertsekas (1999) describes the Lagrange multiplier theory and algorithms in detail. Using an ALM, the Weather Adaptive Navigation (WAN) system by Tsujimoto and Tanizawa (2006) aims to minimize fuel consumption by controlling ship position and engine revolutions and considering weather forecasts and ship responses. Constraints refer to geographical boundaries, the range of engine revolutions, ship movements, safety limits and the scheduled arrival time. Tsujimoto and Tanizawa (2006, p. 4) state that the applied method is superior to an Isochrone Method (see Sec. 4.4.2) as to the handling of the objective function and constraints. As to Bertsekas (1998, p. 384), ALMs “are among the most reliable and practically useful methods in nonlinear programming”.

4.3 Graph Theory and Network Optimization

The term ‘network’ is used in many contexts and can refer to physical networks (transportation, communication or electrical) as well as logical networks (project planning, resource management or distribution) (Finke 2008; Hillier and Lieberman 2010; Nemhauser et al. 1989). When analyzing or designing these large systems, naturally network flow problems arise, which constitute “one of the most important and most frequently en-

countered class of optimization problems” (Bertsekas 1998, p. 2). As to Nemhauser et al. (1989, p. vii), network optimization has contributed to bridging the gap between linear and combinatorial programming. The link between both “can be traced to the representation of the constraint polyhedron as the convex hull of its extreme points” (Bertsekas 1998, p. ix). In case of networks, these points are integer and solutions of combinatorial problems. Partly due to this structure, network models are suitable to explain fundamentals in both, continuous and discrete optimization.

To describe and mathematically model network flow problems, typically, graph-related notions are used. The following definitions are based on Bertsekas (1998, pp. 3–4), Finke (2008, pp. 30–36), Nemhauser et al. (1989, pp. 228–229), and Turau (2009, pp. 20–26). Graphs consist of nodes, also called vertices, corresponding to points, such as depots, cities or clients, and of lines (edges or arcs) connecting these nodes and representing e.g. routes or cables. The set of nodes connected to a node by an edge or arc is called neighbors. Furthermore, there is generally an origin and a destination, also referred to as the start node and end node or the source and sink. It can be distinguished between directed graphs with ordered pairs of distinct nodes connected by an arc and undirected graphs with unordered ones connected by an edge. It is referred to a path as a sequence of nodes. Accordingly, a directed path is a sequence of distinct nodes connected by arcs, while an undirected path (also called chain) only contains edges. A directed (or undirected) path is a directed (respectively, undirected) cycle when origin and destination are equal. A graph without cycles is acyclic. A graph is said to be connected if at least one undirected path exists between any two nodes of the graph, otherwise it is called disconnected. A subgraph of a graph is a subset of nodes and of edges/arcs. It is a spanning subgraph, if the subset of nodes corresponds to the set of nodes of the graph. A spanning subgraph that is a tree, i.e. a connected acyclic graph, is a spanning tree, which incorporates a unique path between any two nodes. Finally, a directed graph can be a directed network when numerical values are associated with its nodes or arcs (Nemhauser et al. 1989, p. 228), such as available merchandise with nodes or maximum capacities as constraints with arcs (Finke 2008, p. x).

To solve problems modeled using graph-related notions, the algorithmic graph theory provides solution procedures, i.e. graph algorithms (Turau 2009, p. 1). Various algorithms are available for a range of problems. Important and classical combinatorial problems are shortest path problems (Bertsekas 1998, p. 52). Nemhauser et al. (1989, p. 215) states that the “shortest path problem is to determine directed paths of smallest cost from a given node 1 to all other nodes.” They are said to be “the most fundamental and also the most commonly encountered problems in the study of transportation and communication networks” (Nemhauser et al. 1989, p. 249). Thus, when aiming for the shortest, fastest, cheapest or safest path between selected pairs of nodes in a network, as in ship weather routing, a shortest path problem may be existent. Since these problems are applied in a broad variety of contexts, the design and test of efficient algorithms has been a major research area in network optimization. As to Nemhauser et al. (1989,

p. 249), solution difficulty depends on the type of shortest path problem. This is among others determined by the number of origins and destinations, the negativity or nonnegativity of arc weights as well as constraints, such as turn penalties or specified nodes, i.e. fixed waypoints on a ship's route. It can be distinguished between label setting methods for nonnegative arc weights and label correcting methods for both, negative and nonnegative arc weights. While the first assign permanent (optimum) labels to the nodes, the latter assign temporary ones that become permanent only in the final step. Costs, distances or times usually assigned to arcs in ship weather routing are typically nonnegative. Applied graph based approaches are described in the following.

It is to be noted that shortest path problems can also be formulated as dynamic programming problems (see Sec. 4.4.2) and vice versa, which presents an "important connection between shortest path problems and problems of deterministic discrete-state dynamic programming, which involve sequential decision making over a finite number of time periods" (Bertsekas 1998, p. 53). A dynamic programming problem can be converted to a shortest path problem by introducing a graph with arcs equivalent to transitions between states at successive stages and an associated cost (Bertsekas 1998, p. 54). The final stage is handled by an artificial terminal node, where each state of the final stage is connected to by an arc. While control sequences in general are represented by paths from the initial state to one of the nodes substituting the final stage, the optimal one is equivalent to the shortest path. Keeping this in mind, those ship weather routing problems and approaches described by stages and states for sequential decision making are outlined in Sec. 4.4.2 although they may also be treated in this section.

Dijkstra's Algorithm The most popular label setting algorithm to approach shortest path problems is Dijkstra's algorithm (Nemhauser et al. 1989, p. 250). Often, it is described as a greedy algorithm but also a dynamic programming perspective on the algorithm is presented by Sniedovich (2006). First published by Dijkstra (1959), it finds shortest paths between an origin and all other nodes in a directed graph. It fans out from the origin to adjacent nodes and labels the nodes according to their distances from the origin. In a next step, it fans out from the adjacent node with the total shortest distance from the origin. Since several paths may lead to the same node, the label is temporary until the shortest path is found and the label becomes permanent. Thus, the method continuously scans adjacent nodes and updates labels. It terminates when all nodes are permanently labeled. This procedure leads to the optimal path based on the idea that "it is always possible to designate the node with the minimum temporary label as permanent" (Nemhauser et al. 1989, p. 250).

Takashima et al. (2009) employ Dijkstra's algorithm to derive a sub-optimal minimum fuel route for coastal merchant ships by controlling the ship's heading. The propeller revolutions are constant and only adjusted iteratively in every optimization run to finally meet a given arrival time. The graph is defined by nodes two miles apart located on lines perpendicular to a standard route, similar to that shown in Fig. 4.1c. In com-

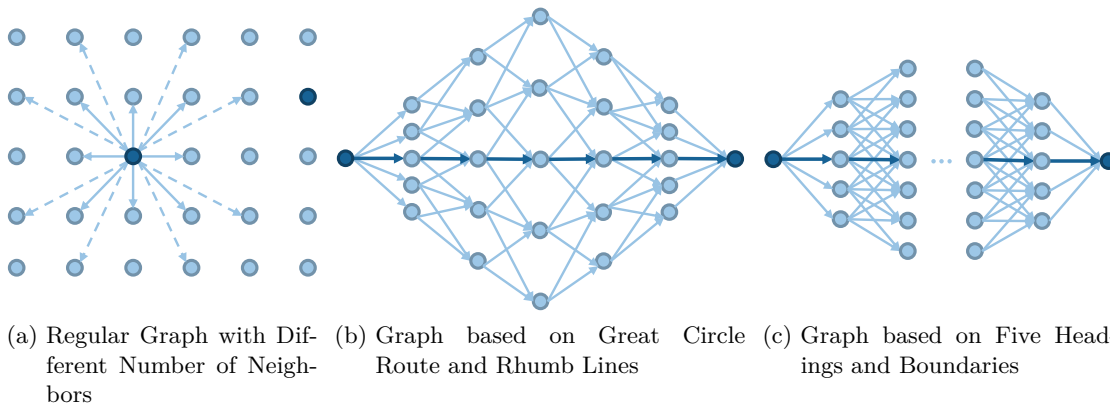


Figure 4.1: Examples of Graph Designs

parison, Sen and Padhy (2010, 2015) use Dijkstra's algorithm to calculate a minimum time route in the North Indian Ocean. Assuming a two-dimensional, usually $1^\circ \times 1^\circ$, grid with weather data available at each node, the travel time at constant engine power is assigned as weight to each arc. The speed is involuntarily reduced by the prevailing weather conditions and voluntarily by safety limits (see Sec. 5.5.3). Geographic constraints and unfavorable weather conditions are considered through large weights. The method's main deficiency is the smoothness of the final path which results from the regular graph and eight neighbors, as indicated by the solid lines in Fig. 4.1a. Also Mannarini et al. (2013) apply Dijkstra's algorithm to calculate a minimum time route by controlling the ship's heading at constant speed constrained by landmasses and MSC.1/Circ. 1228 (see Sec. 5.5.2). Focusing on the Mediterranean Sea, the prototype is based on a regular graph with thirty nodes at a distance of four nautical miles and twenty-four instead of eight neighbors per node. These are located at the end of the dashed lines in Fig. 4.1a as well as in the same square when extending the solid lines. Moreover, Vettor and Guedes Soares (2016) apply Dijkstra's algorithm to generate an initial population for an evolutionary approach (see Sec. 4.5.2).

Eskild (2014) uses Dijkstra's algorithm to minimize the fuel consumption, which is assumed as a function of the heading only due to constant engine power. Constraints are imposed by criteria for slamming, deck wetness, roll motions and vertical accelerations. The graph is defined by nodes located on rhumb lines connecting the origin and destination and points at a distance of 1° on a line perpendicular to the great circle route, as shown in Fig. 4.1b. To reduce the computational effort the number of neighbors of a node (except origin and parents of destination) is restricted to a maximum of three. The fuel costs for each arc are assigned as weight. Although the application of this weather routing approach does not lead to any fuel savings compared to the great circle route, extreme weather conditions are avoided. A shortcoming is that landmass avoidance, ocean currents and ship speed optimization are not considered. Dijkstra's algorithm is also applied by Montes (2005) and Chu et al. (2014) for navy vessels. Montes (2005)

aims to derive a minimum time route using a grid with 0.5° resolution in the western Pacific Ocean, speed reduction and fuel consumption curves as well as weather and speed limits. Chu et al. (2014) aim to determine a minimum cost route by creating a 3D grid (latitude, longitude, time) based on user-specified departure and arrival locations and times as well as minimum and maximum ship speed. An optimal path is computed by controlling speed and heading and considering (ensemble) weather conditions and the ship's hull, power curve and loading condition.

Finally, Chen (2013) and Jeffery (2015) state that variations of Dijkstra's algorithm are often employed to approach the problem by considering a ship sailing with full power at different headings while neglecting speed management. This, however, is critical for exploiting fuel saving potentials, reducing weather risks and ensuring safe ship operation. Combined route and speed optimization allows the ship to slow down to avoid severe weather conditions in addition to changing the route. Consequently, latest approaches employing Dijkstra's algorithm use a 3D graph in a spatial and temporal domain.

Multi-objective Optimization with Dijkstra's Algorithm In contrast to the single-objective applications of Dijkstra's algorithm, Böttner (2007) and Skoglund et al. (2012) aim at multi-objective optimization. Böttner (2007) suggests to use a generalization of Dijkstra's algorithm for finding the shortest and fastest route to a refuge or harbor in case of limited maneuverability and propulsion capacity. It is based on Aneja et al. (1983) formulating a special case of a minimal cost-flow problem with side constraints and presenting an implicit enumeration algorithm. It first introduces operations to reduce the network (e.g. deleting edges leading to unfeasible turning angles) and second applies a multiple vectorial labeling scheme, which is a generalization of Dijkstra's algorithm. Thus, a multidimensional cost vector is assigned to each arc containing e.g. distance and time values. The graph is discretized in space and time, generated automatically based on the ship's current position, and refined the closer the ship is to the coast.

Skoglund et al. (2012) additionally use the concept of Pareto optimality. When moving from the origin to the destination and evaluating the arcs, the algorithm saves all Pareto optimal labels for each node, thus the set of values for each objective, such as arrival time and fuel consumption (Skoglund et al. 2012, p. 5). Hence, it allows to compute Pareto optimal solutions to a multi-objective routing problem. It can be applied using both deterministic and ensemble forecasts (see Sec. 3.4), but requires improvements as to the ship performance model and investigations to determine an appropriate spatial and temporal resolution and structure of the graph.

Combined Shortest Path and Gradient Approach Aiming at a minimum cost solution of the ship weather routing problem, Weber (1995) considers the ship voyage process as a finite sequence of temporal and local state changes. Therefore, Weber (1995, p. 64) introduces a state vector, a control vector, a vector containing all constraints and an admissible region. The state vector contains state variables and describes the state of

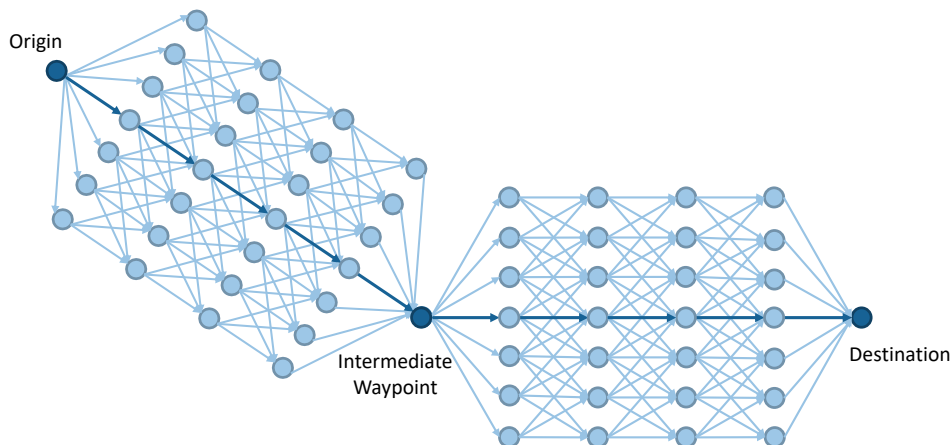


Figure 4.2: Graph with Intermediate Waypoint, adapted from Weber (1995, p. 76)

the process in a defined number of stages, while the control vector contains decision variables and guides the process from one state to the next or one stage to the next. Constraints need to be satisfied by the state and decision variables at all times. The aim is to find the optimal control vector and corresponding optimal state vector from the set of admissible vectors that connect the initial and the final state with minimal costs. The discrete mathematical model is based on a directed graph with nonnegative arc weights that has a geometrical shape of a hexagon and stretches from the origin to the destination (Weber 1995, pp. 68f.), as depicted in Fig. 4.2. The figure also shows that several hexagons may be connected to allow the specification of intermediate waypoints.

The optimization problem is approached by solving a combinatorial problem, i.e. a shortest path problem, to calculate the state vector for a given control vector and by solving a nonlinear problem to calculate the control vector for a given state vector. Both methods are applied alternately to determine the shortest path and the optimal control, where the result of one method is input to the succeeding other (Weber 1995, p. 74). Due to the objective of minimal costs, the state vector for a given control vector must be a shortest path, thus total costs are minimal (Weber 1995, p. 77). The shortest path is derived by employing Dijkstra's algorithm and considering landmasses. As long as the objective can still be improved or a termination criterion is not fulfilled, the iterative procedure is continued. After termination, i.e. if two identical state vectors are determined in succession, a smoothing algorithm is used since discretization effects are a drawback of Dijkstra's algorithm. The nonlinear optimization problem with the objective of minimal costs is approached by an iterative gradient method, whose linear convergence speed is considered to be sufficient and which is less dependent on the initial guess (average number of propeller revolutions) compared to Newton's method. The aim is to decrease a differentiable objective function until its minimum is reached by iteratively improving the current estimated solution based on the gradient, which is the vector of partial derivatives and indicates the direction of improvement (Eiselt and

Sandblom 2010, p. 65). Constraints, that include time restrictions, engine characteristics and a maximum wave height and wind speed, are considered by penalties in the objective function and by inadmissibility of vectors violating constraints (Weber 1995, p. 88). The convergent approach is said to be independent of the initial guess and to yield a continuous ship's route without unintentional discontinuities.

A* Algorithm The A* algorithm is a generalization of Dijkstra's algorithm and similarly determines the shortest path (Turau 2009, p. 270). The aim is to reach a destination as fast as possible, which is equivalent to minimizing the number of nodes visited. The main feature of the A* algorithm is a heuristic function that is used to estimate the shortest path from each current node to the destination. Thereby, it is determined which node is visited next. Admissible heuristic functions always underestimate the length of the shortest path to the destination (Turau 2009, p. 271). Dijkstra's algorithm is a special case of the A* algorithm with the heuristic function set to zero.

A time-dependent A* algorithm is employed within this thesis to find a route of minimum fuel costs, as outlined in Sec. 6.3.1, and by Meyer (2014), Walther (2015), and Walther et al. (2015) for an unmanned autonomous and a wind-driven hybrid merchant ship. When comparing this to a genetic algorithm, it appears to be superior for the considered problem since the results are more reliable and do not depend on the initial population, population size and number of variables (Walther et al. 2017). Also Bentin et al. (2016) apply it to minimize and analyze the fuel consumption of a ship with and without wind assistance at a given speed on an optimized route. Thus, it is accounted for the impact of wind, waves and wind assisted propulsion as well as constraints by a maximum passage time and safety limits. The nodes of the graph are arranged along and symmetrically to each side of the orthodrome, i.e. the great circle route, connecting origin and destination. Since the nodes are specified by a ship traveling with a certain speed and heading for a certain time (Bentin et al. 2016, p. 160), it may be considered similar to the Isochrone Method (see Sec. 4.4.2) including a heuristic.

Veneti et al. (2015b, 2017) consider a bi-objective time-constrained ship weather routing problem formulated as a shortest path problem. The aim is to minimize fuel consumption and safety risks based on IMO (2007), MSC.1/Circ. 1228 (see Sec. 5.5.2), while controlling the ship's heading at constant speed and respecting a given arrival time. A variable speed is assumed to be less important in coastal shipping, such as in the examined Aegean Sea. To efficiently return the whole Pareto set, Veneti et al. (2017, p. 221) propose "(i) a dynamically partitioned grid for reduced graph size as well as an alternative reduction technique where grid is pruned along a given voyage plan, (ii) a heuristic function used to transform the initial algorithm into a bi-objective A* algorithm thereby reducing the search space and (iii) a technique for deriving loopless ship routes". Some techniques are presented by Makrygiorgos et al. (2015). The static grid has a regular structure and a node has sixteen neighbors, as indicated by the solid and dashed lines in Fig. 4.1a. The dynamically partitioned grid is based on the idea of removing nodes

so that the reduced grid still yields most solutions of the original Pareto set. It can only be applied to static graphs with constant costs assigned to arcs, i.e. in static weather conditions assumed for short routes (Veneti et al. 2017, p. 228). Loops can be avoided by remembering all intermediate nodes of each path or by initially defining an acyclic graph (Veneti et al. 2017, p. 228). According to experiments, the heuristic function leads to a significant increase in computational speed (Veneti et al. 2017, p. 225). However, the lack of speed as decision variable and a simple ship model can be seen as shortcomings. The approach is compared to an evolutionary one outlined in Sec. 4.5.2.

Other Graph Search Approaches The following approaches are based on graphs and are mostly called grid based or grid search approaches by the authors. They may also be considered as dynamic programming approaches, but little information is given on mathematical modeling and the algorithmic solution procedure. The approach proposed by Skoglund et al. (2012) inspired the 3D Grid Search Method applied by Andersson (2015) to solve a single-objective optimization problem using a 3D grid (longitude, latitude and time) with different stages along the longitudinal direction. Since an existing implementation only considers a single objective, the three objectives of minimum time, wave impact and fuel consumption are considered individually and trade-off solutions are determined using Pareto optimality. Due to long computation times for long voyages (e.g. transatlantic), it is more suitable for short voyages or may require sampling the Pareto front and running it on a cluster (Andersson 2015, pp. 22f.). The approach is also used by Hameed (2015) in addition to the DIRECT method (see Sec. 4.2.1).

Cui, Howett, et al. (2016) and Cui, Turan, et al. (2016) present a grid based method with the network formed by points that are reachable along five headings from each point, as shown in Fig. 4.1c. The points are located within defined boundaries and on lines perpendicular to the great circle route between origin and destination. By varying the random discretized speed assigned to each leg, a Pareto front can be provided for decision support that displays arrival time versus fuel consumption accumulated for all legs of one route. Potential for improvement mainly concerns the ship's resistance and land avoidance. Lu et al. (2015) employ a similar graph, where a possible route, such as the great circle route, is divided into stages at which nodes are distributed equally in latitudinal direction with a unique longitude. The minimum fuel route at a given average speed and variable heading is defined as the optimum. The user can weigh the attributes, such as fuel consumption, safety or passage time, as to their importance.

4.4 Dynamic Programming

Dynamic Programming (DP) focuses on situations, more specifically dynamic systems, in which decisions are made in stages (Bertsekas 2005, p. 2). Often, dynamic systems are classified into continuous and discrete dynamic systems. As to Domschke et al. (2015, p. 169), a discrete dynamic system, thus the corresponding discrete model, is given when decisions or changes of states are made at discrete points in time (or in

discrete steps). Hence, the states are represented by a discrete state variable, otherwise the model is continuous. In the case of systems represented by continuous models, state changes are possible through continuous decision making (= control), which is subject to control theory. Besides the differentiation between continuous and discrete models, DP problems and their corresponding models can be classified according to three further aspects. These are related to deterministic and stochastic models, to state and decision variables being single variables or vectors as well as to a finite or infinite number of stages, states or decisions. In deterministic models, the current state and policy decision at the current stage completely determine the state at the next stage. In case of a stochastic model, either the state or decision is only known as a probability function (Poler et al. 2014, p. 329). Furthermore, Hillier and Lieberman (2010, p. 432) categorize deterministic DP problems by the form of their objective function, which generally aims at minimization or maximization. When differentiating between continuous and discrete dynamic systems, the former are usually approached by methods from optimal control, solutions of the latter are typically obtained using a DP algorithm. Both are addressed in detail by Bertsekas (2005) and concerning ship weather routing in the following.

4.4.1 Continuous Dynamic Programming

As to Bertsekas (2005, p. 106), a continuous-time dynamic system can be described by a state vector at a time, a vector of first order time derivatives of the states at that time, a control vector at that time, which are all viewed as column vectors, as well as a control constraint set, and a terminal time specifying the maximum for all times. It is assumed that the system function is continuously differentiable with respect to the state vector and is continuous with respect to the control vector. The control trajectories, thus the admissible control functions, are the piecewise continuous functions. A state trajectory corresponds to the unique solution of the system of differential equations that is assumed to exist for any admissible control trajectory. The aim is to determine an admissible control trajectory and corresponding state trajectory that minimize a cost function.

Pontryagin's Minimum Principle To approach deterministic continuous-time optimal control problems, the analog of the DP algorithm (see Sec. 4.4.2) is the Hamilton-Jacobi-Bellman equation (Bertsekas 2005, p. 109). It is a partial differential equation that is satisfied by the optimal cost-to-go function considering certain assumptions. It is a sufficient condition, while Pontryagin's Minimum Principle, also referred to as maximum principle, is a necessary condition for optimal control (Wit 1988). Pontryagin's theory on optimally controlled processes is applied by Wit (1968, 1970, 1976) to mathematically treat optimal ship routing as a minimum time problem. In order to, among others, search for a global solution, Wit (1968) additionally introduces time fronts, which are the boundaries of regions of points reachable within a given time. The use of time fronts is similar to the Isochrone Method described in Sec. 4.4.2. The minimum principle of optimal control theory and its connection to the method of DP are discussed for the case that ship weather routing is treated as a continuous process as well as in relation to the objective of minimum fuel consumption by Bijlsma (2002).

Calculus of Variations Problems from calculus of variations relate to finding (possibly multidimensional) curves with certain properties concerning optimality. This can be a curve of minimum length from a given point to a given line (Bertsekas 2005, p. 108). They can be transferred into problems from optimal control with the aim to find an optimal control trajectory. In general, calculus of variations aims to find extremals, thus minima or maxima, of functionals by varying the parameters that control the trajectory, such as time or speed in ship weather routing. A functional can be a rule that associates numerical values with curves. It can be an integral or derivative (Dreyfus 1965, p. 27). Key to calculus of variations is the Euler-Lagrange equation, which is a necessary condition. To derive a minimum time route, Haltiner et al. (1962) and Hamilton (1961) apply calculus of variations by numerically solving the associated Euler-Lagrange equation using relaxation methods and assuming the ship's speed to be a time-independent function of direction and position. Deficiencies are related to the assumption of a steady wave field and stationary form of the differential equation.

The method by Haltiner et al. (1962) has been extended by Faulkner (1963) to take into account time-dependent wave height and direction. It aims at minimum time courses by assuming the speed to be a known function of position, heading and time, and applying a different method to solve differential equations (Bliss 1918). Developments have been continued by Bleick and Faulkner (1965) using a series of semidaily wave analyses provided by a numerical weather facility. Haltiner et al. (1968) extrapolate these forecasts for a longer time period and refine the method to achieve rapid convergence when iteratively determining an admissible track by variation of time extremal ship tracks.

In comparison to Hamilton (1961), Bijlsma (1975) considers three additional conditions (Weierstrass, Legendre and Jacobi) when numerically computing a ship's least-time track. An arc satisfying the four necessary conditions yields only a relative minimum. Hence, the time front is considered, which represents the boundary of a set of points reachable within a specific time given by the temporal resolution of the wave data. After initialization, the points attainable along the extremals, the great circle and rhumb line within every time step are computed until the destination is reached or a boundary, such as land, requires the introduction of an intermediate point to start a new extremal, as shown in Fig. 4.3. To minimize the fuel consumption, speed may be introduced as new decision variable. However, due to the insufficient accuracy of the applied empirical fuel functions and an arising inhomogeneity of equations, Bijlsma (1975) favors suitable approximations to estimate fuel costs. Nevertheless, the method is not only extended for limited maneuverability (Bijlsma 1999), but also for minimum fuel consumption (Bijlsma 2001), for a pre-specified fuel consumption on a minimum time route to meet emission requirements (Bijlsma 2008) as well as for consideration of ocean currents (Bijlsma 2010).

Papadakis and Perakis (1990) approach a minimum time ship routing problem in stationary or time-dependent environments by calculus of variations and optimal control considerations. The ship's speed is a function of either direction or time and direction.

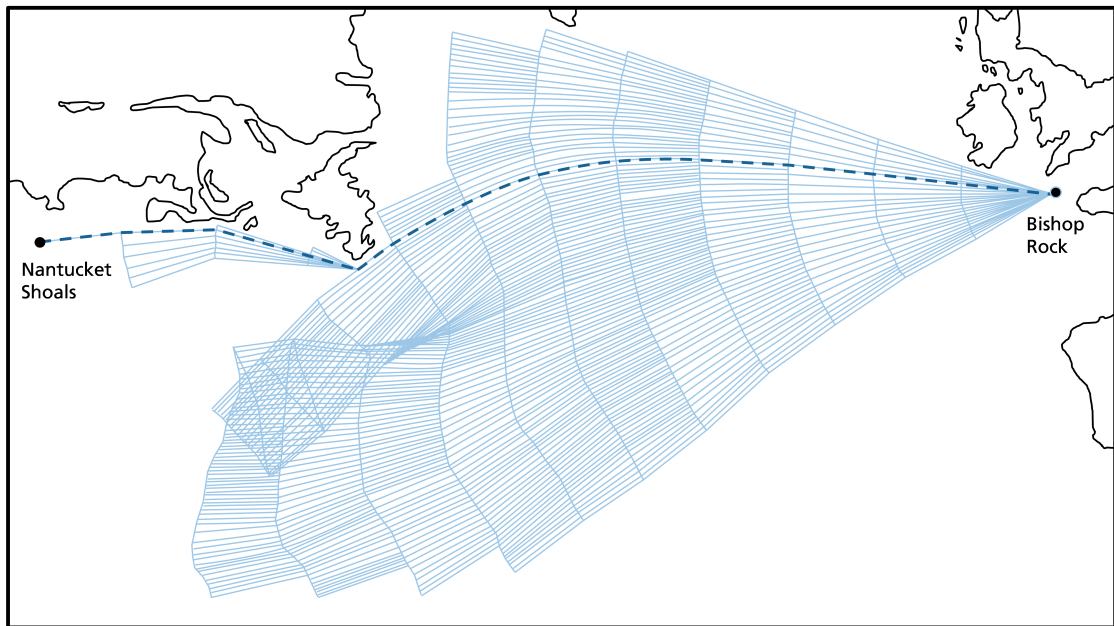


Figure 4.3: Minimum Time Route derived by Calculus of Variations, adapted from Bijlsma (1975, p. 40)

Perakis and Papadakis (1989) extend the approach and use a more general vessel performance model and constraint set to express the ship's dynamics within the 2D routing space. The heading and power setting are considered as decision variables. The routing space is discretized into a finite number of subregions, where the ship's speed is assumed to be only time dependent. A 'broken extremal' approach based on local optimality and global boundary conditions is introduced to achieve piecewise continuous optimal policies.

4.4.2 Discrete Dynamic Programming

Dynamic programming provides a systematic solution procedure for decision problems in which a sequence of interrelated decisions has to be made in order to achieve an optimum combination of decisions as a solution for the problem (Bertsekas 2005, p. 2; Domschke et al. 2015, p. 165; Hillier and Lieberman 2010, p. 424). DP problems can typically be divided into several stages. Each stage is composed of a number of associated states describing the possible conditions of the system at this stage. Moreover, each stage requires a policy decision which aims "to transform the current state to a state associated with the beginning of the next stage" (Hillier and Lieberman 2010, p. 429). By determining the optimal policy decision for each state at each stage, an optimal policy for the overall problem can be found. Considering the current stage, the optimal policy for the following stages does not depend on the policy decisions of former stages. This is known as Bellman's principle of optimality (Bellman 1952, 1954, 1957), which constitutes the

basis of DP (Bertsekas 2005, p. 18; Gerdtts and Lempio 2011, p. 465). Accordingly, the last stage does not depend on any previous stages and is solved first. Based on the optimal policy for this stage, a recursive relation allows to determine optimal policies for the previous stages by moving backwards stage by stage until reaching the initial one and yielding the optimal solution for the entire problem. Hillier and Lieberman (2010, p. 431) state that many problems, in particular those with stages corresponding to time periods, require solution procedures moving backwards. In ship weather routing, forward and backward methods can be found.

Challenges when applying DP can be related to appropriate modeling of the problems, to the required design of the solution method as there is no universal method, such as the simplex method in linear programming, and to the possibly stochastic character often given in practical applications (Domschke et al. 2015, p. 165). Although a universal formulation for problems that are to be solved by DP can be given, mathematical modeling may be rather difficult for some problems and demands considerable experience to develop a valid model. Since there is no universal method but only a general solution principle, a problem-specific implementation into a solution procedure is required.

It is to be noted that DP, particularly discrete deterministic models, can also be used to determine shortest paths in a graph, as indicated in Sec. 4.3. In case DP cannot be successfully applied to a discrete DP problem, procedures from linear or nonlinear programming may help since every discrete DP problem is a very large but structured finite-dimensional problem (Gerdtts and Lempio 2011, p. 457). The following paragraphs are dedicated to those ship weather routing problems and approaches that are described in some way by stages and states for sequential decision making. Also the so called isochrones described below may be seen as stages. Moreover, recent approaches, which are referred to as isochrone methods by their authors, show minor or major similarities to those approaches that explicitly relate to dynamic programming. Approaches rather using typical graph related notions are discussed in Sec. 4.3.

Original Isochrone Method The first developments of the so called Isochrone Method are generally attributed to James (1957). The deterministic method is used to manually derive least-time tracks by variation of the ship's heading at constant engine power. It assumes a ship traveling straight ahead with various headings for a specified time. The points reachable from the origin within this time under consideration of weather impacts constitute the first time front, i.e. isochrone. The second isochrone is formed by points reachable on lines perpendicular to the first isochrone. The process is repeated and terminated when reaching the destination. The optimal path can be determined by tracing back the route that passes through the least number of isochrones from the destination to the origin in a recursive manner. Disadvantageous for computerized calculation is the possible occurrence of so called isochrone loops, which are irregularities "in shape of an isochrone caused by non-convexity of speed characteristic for given weather data" (Szlapczynska and Smierzchalski 2007, p. 3).

Modified Isochrone Method Improvements of the Isochrone Method for computerized calculation are among others presented by Hagiwara and Spaans (1987), Hagiwara (1989), Spaans (1985), and Spaans and Hagiwara (1987). Hagiwara (1989) describes the Modified Isochrone Method applied to single-objective deterministic minimum time, fuel and cost routing and stochastic minimum time and fuel routing. Instead of treating ship weather routing as a continuous optimization problem, it is considered as a multistage decision process with discretized time to be more convenient for computerized calculation. The proposed method is also regarded to be superior to DP methods due to reduced computational effort particular in stochastic routing. Referring to Shao et al. (2012) and Spaans and Stoter (2000), the Modified Isochrone Method is also applied by the Ship Performance System Optimisation (SPOS) described in Sec. 2.5.

For minimum time routing the procedure presented by Hagiwara (1989) is similar to that of James (1957), but with the ship traveling along great circle routes (GCRs) with various discretized headings. To limit the number of points per isochrone, a set of sub-sectors around the reference GCR between origin and destination is introduced, as illustrated in Fig. 4.4a. Decreasing the sub-sector width may increase the method's accuracy. In each sub-sector marked by two GCRs departing from the origin, only the point with maximum distance is selected. After reaching the destination, the optimal path may be traced back, as exemplified in Fig. 4.4b. For minimum fuel and cost routing, the method is applied at a varying number of propeller revolutions to iteratively determine the optimum route meeting a given arrival time or time window. It is only a sub-optimal result, since the propeller revolutions are constant throughout the whole voyage. For stochastic routing, information on environmental forecast errors is incorporated in the method to estimate standard deviations of passage time and fuel consumption.

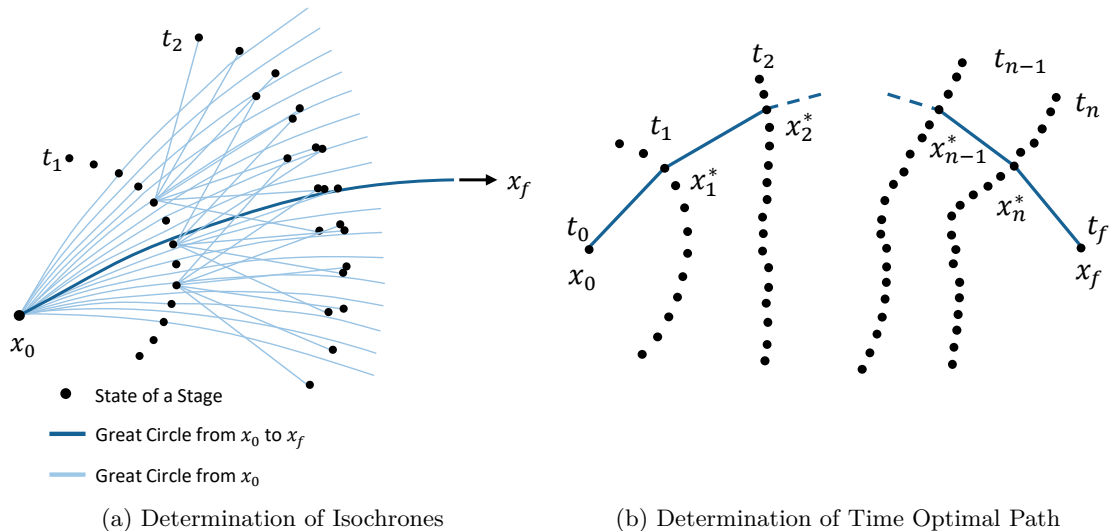


Figure 4.4: Principle of the Modified Isochrone Method, adapted from Hagiwara (1989, p. 21, 24)

According to Szlapczynska and Smierzchalski (2007), the method proposed by Hagiwara (1989) only provides a general solution for land avoidance. This is why an isochrone method is presented with area partitioning. It not only requires origin and destination to be in water but also the lines connecting one point and its predecessor. This is achieved by a bitmap-based algorithm. The method is used to generate an initial population for an evolutionary approach that allows multi-objective optimization (see Sec. 4.5.2).

3D Modified Isochrone Method A three-dimensional Isochrone Method proposed by Fang and Lin (2015), Lin et al. (2013), and Lin and Fang (2013) aims at minimum fuel consumption or passage time. It controls the ship's heading and speed, meets a given arrival time and considers constraints related to land avoidance and safety (roll motion). It is said to be a recursive forward algorithm based on stages consisting of states (see Fig. 4.5). The use of voyage progress as a stage variable suggests similarities to the 3D dynamic programming methods described below.

2D Dynamic Programming A 2-dimensional Dynamic Programming (2DDP) approach has been proposed e.g. by Nagle (1972), Wit (1990) and Zoppoli (1972) to solve a discrete ship weather routing problem. While assuming a constant number of propeller revolutions, the ship's heading is varied to find a minimum time or fuel route.

3D Dynamic Programming In contrast to 2DDP, 3-dimensional Dynamic Programming (3DDP) considers the ship's speed or propeller revolutions as a variable in addition to the heading. This allows route and speed optimization. It is among others applied by Aligne et al. (1997), Calvert (1990), Chen (1978), and Petrie et al. (1984) with preceding research done by Motte (1981) and Motte and Calvert (1988, 1990). While Aligne et al.

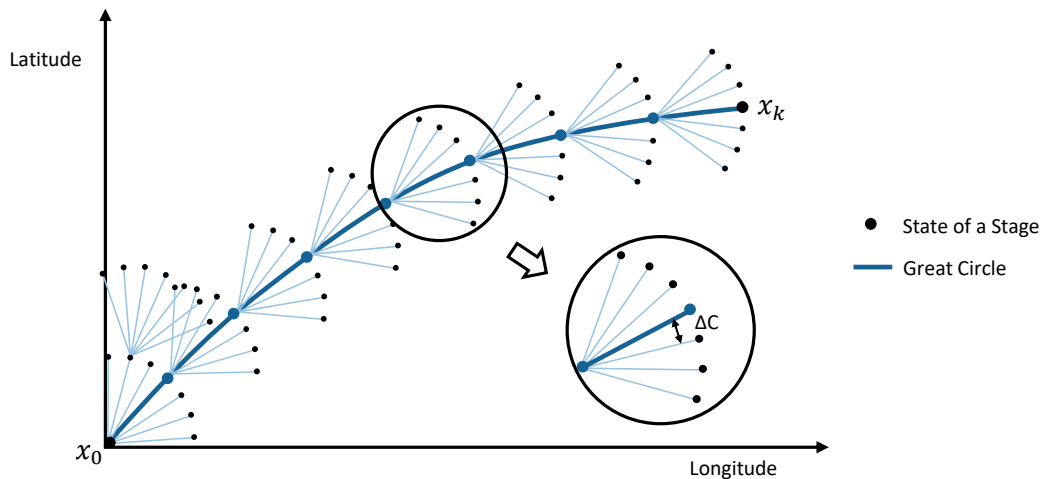


Figure 4.5: Principle of the 3D Modified Isochrone Method with Stages along the Great Circle Route, adapted from Lin et al. (2013, p. 186)

(1997) and Petrie et al. (1984) use a forward algorithm, Calvert (1990) and Chen (1978) apply a backwards one. For instance, Chen (1978) has developed a dynamic program for minimum cost ship routing under uncertainty using a stochastic DP algorithm. It not only considers ship dynamic response characteristics but also probabilistic environmental conditions, which may result in probabilistic travel time and hence may effect the choice of optimal control policies. Constrained by ship operational requirements, the ship's trajectory and its corresponding heading and power output are computed. The method has been improved over the years (also see Sec 2.5). Chen (2013) suggests a 3DDP method to minimize fuel consumption under safety constraints and for a range of arrival times. The grid may be user-defined. Including the computation of ship responses and engine overload, the problem is said to be solved within a few minutes. The set-up allows application on board as well as ashore.

Also Shao and Zhou (2011, 2012) and Shao et al. (2012) solve a single-objective discrete optimization problem deterministically by 3DDP. The aim is minimum fuel consumption under consideration of several constraints. In contrast to Chen (1978), Shao et al. (2012) employ a forward algorithm with a fixed initial time of departure, while the arrival time at each stage is flexible. A path is considered to be optimal if and only if the choice of the previous path is optimal for any intermediate stage. The voyage progress is used to describe the stages that have a spatial layout perpendicular to the great circle route as shown in Fig. 4.6. A state is specified in three dimensions by location (grid point) and time (arrival time). Between two consecutive stages, the values of the decision variables, namely ship's heading and engine power, are assumed to be constant. First, the ship's heading is computed from the initial state to each grid point on the second stage. For each heading and calm water speed, the fuel consumption and voyage time are derived

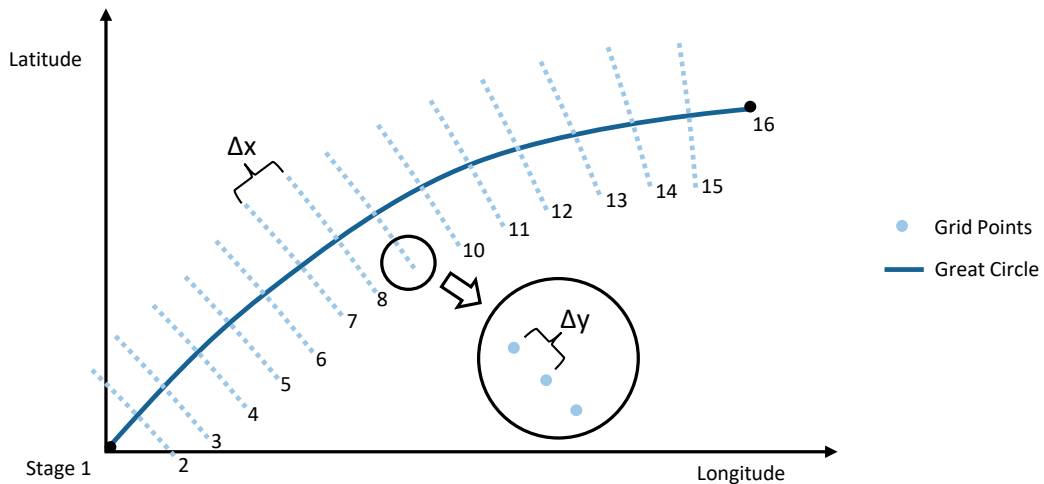


Figure 4.6: Principle of the 3D Dynamic Programming Method with Stages Perpendicular to the Great Circle Route, adapted from Shao et al. (2012, p. 244)

for the passage between two consecutive stages within a specified time interval. Any ship's heading, speed, engine power, or passage time violating constraints is abandoned. Finally, at each location a set of routes with minimum fuel consumption corresponding to different arrival times can be obtained. Once the state of the final stage is reached, the optimal route can be reconstructed easily. Shao and Zhou (2011) compare the proposed 3DDP to the traditional 2DDP as well as to three types of genetic algorithms with minimum fuel consumption and passage time as objectives. In all cases, the same grid system is used. It is concluded that 3DDP is to be favored over 2DDP due to the variation of the ship's heading and engine power. It is also said to be superior to all three genetic algorithms since less parameters need to be defined and it is able to determine a global optimum particularly in harsh weather conditions. However, adequate parameter settings for the genetic algorithms are not studied and information about the computational effort is not given.

Figari et al. (2017), Ottaviani et al. (2016), Zaccone and Figari (2017), and Zaccone et al. (2018) apply 3DDP coupled with a dynamic ship propulsion model (see Sec. 5.6.4) to derive a minimum fuel route and speed profile constrained by ETA and ship motion thresholds (see Sec. 5.5.3). The underlying three dimensional space-time-grid is arranged along the great circle route, similar to Fig. 4.6. It is assumed that deviations from this shortest route are ideally only caused by harsh weather. Geographically, ten stages with ten steps each are assumed on an exemplary transatlantic route. Weather impacts only refer to wind and waves. Ocean currents are neglected. The developed method is available in form of SmartNautilus, a web application (On AIR 2018a,b).

Iterative Dynamic Programming Avgouleas (2008) presents an improved DP approach, i.e an Iterative DP (IDP) algorithm (Luus 2000), to solve a deterministic nonlinear fuel minimization problem while controlling speed and heading and taking into account safety constraints. Standard DP methods require a fine grid to ensure convergence to the global optimum inducing significant computational effort. Hence, the applied IDP method utilizes an iterative procedure of piecewise constant control with a single grid point instead of a complete grid of admissible states. After initially guessing the optimal control and defining the number of controls (allowed speeds and headings) and the increment, an optimal control policy is determined and the solution improved in each iteration. The procedure avoids using fine grids for standard DP methods as well as derivatives for variational methods. It is considered to be suitable for the highly nonlinear minimum fuel problem lacking convexity or other optimality conditions, both locally and globally.

Isopone Method The so called Isopone Method is proposed by Klompstra et al. (1992). It is based on the Modified Isochrone Method presented by Hagiwara (1989) with the time fronts being replaced by energy fronts. This boundary of a set of points is reachable with a specific amount of fuel in a three-dimensional space (location and time). The method is based on a recursive description of the optimization problem which is key to DP (Finke 2008, p. 96). The first isopone is determined by the set of points reachable

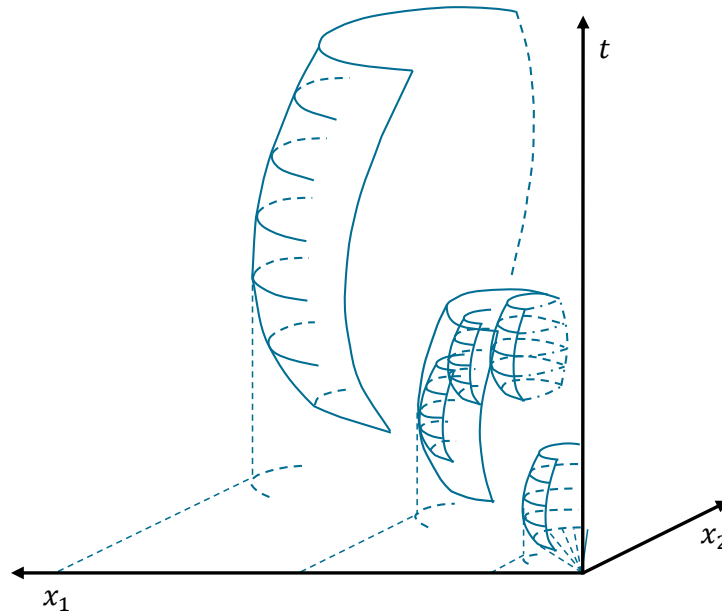


Figure 4.7: Illustration of Isopones reachable with a Specified Amount of Fuel in Constant Weather Conditions, adapted from Klompstra et al. (1992, p. 289)

from the initial state roughly along the great circle. Each point of the first isopone is an initial point of further energy fronts, whose envelope forms the second isopone, as illustrated in Fig. 4.7. The depicted barrel-shaped energy fronts result from uniform weather conditions. Initial points for the third isopone are the boundary points closest to the destination in each of the constructed subsectors, which are defined by parabolic planes parallel to the x_1 - x_2 -plane. The final isopone needs to meet the destination, otherwise recalculation with a smaller amount of fuel or calculation of the minimum fuel route from the second-last isopone is required. When the final isopone is plane, the resulting path is not only fuel optimal but also time optimal.

4.5 Metaheuristic Methods

Commonly, heuristic methods are used to search for a good feasible solution reasonably close to the optimum of the specific problem. For many years, these methods have been designed to fit specific problems rather than a variety. Efficient general solution methods called metaheuristics have gained popularity in recent years. They aspire to provide “both a general structure and strategy guidelines for developing a specific heuristic method to fit a particular kind of problem” (Hillier and Lieberman 2010, p. 607). A metaheuristic aims to enable a robust search of a feasible region and to escape local optima by combining local improvement procedures with higher level strategies (Hillier and Lieberman 2010, p. 610). Sophisticated algorithms, such as tabu search, simulated annealing and genetic algorithms, can also be employed for integer nonlinear program-

ming problems with local optima far from the global optimum as well as for various combinatorial problems (Hillier and Lieberman 2010, p. 491). Metaheuristics applied to the ship weather routing problem include simulated annealing, genetic algorithms and other evolutionary methods. Due to the combination of local and global search also the DIRECT method outlined in Sec. 4.2.2 may be named here.

4.5.1 Simulated Annealing

Simulated annealing is a widespread metaheuristic that aims to perform a process able to escape from a local optimum. Originally, it is inspired from metallurgy and annealing metals, which may have defects if cooled too quickly (Finke 2008, p. 87). The method assumes an initial solution and searches for another solution in the neighborhood that may become the current solution. The underlying idea behind this method to escape local optima relates to the possibility of arriving at a lower quality neighboring solution with a probability not equal to zero. A parameter related to the temperature is introduced that regulates the acceptance probability of solutions of worse costs, thus deteriorating solutions. Typically, the parameter is large in the beginning and decreases towards zero throughout the process. The rule of decrease, thus cooling, determines the performance of simulated annealing, since rapid cooling might lead to a low quality local optimum and slow cooling may induce high computational effort.

In ship weather routing, simulated annealing is employed by Kosmas and Vlachos (2012) to minimize a cost function, which is the weighted sum of voyage time and comfort (including safety) and dependent on environmental influences. This is done by defining several initial routes represented by smooth curves, which are approximated by polygonal lines and divided into segments. Hence, sets of waypoints are introduced that are iteratively moved during the process until a minimum is found. Evaluated optimal routes seem to be in line with results obtained by genetic algorithms. Commercially, simulated annealing is applied by FORCE Technology in the system SeaPlanner, as stated by Larsson and Simonsen (2014) and indicated in Fig. 2.7.

4.5.2 Evolutionary Methods

Inspired by the process of natural evolution, evolutionary methods are usually composed of three key elements: A population consisting of several individuals that represent candidate solutions of the problem, an evaluation mechanism to measure an individual's quality and an evolutionary mechanism to select and produce individuals (Finke 2008, p. 224). Typically, an initial population generated in the beginning is followed by an evolutionary process. The evaluation mechanism is applied to measure the quality of the specific solution and assign a fitness to each individual. The part with the highest quality is selected to produce a new generation of individuals using the evolutionary mechanism. The selection process aims to conserve the best-adapted, fittest individuals while eliminating less-adapted ones. Mutation, crossover or recombination are used to modify individuals and create further generations with potentially superior individuals.

When a preset termination condition is met, such as a maximum number of evaluations or generations, the process is exited. Evolutionary methods, particularly genetic algorithms, are used in particular if the function to be minimized does not possess sufficient continuity or differentiability properties or if a global minimum is sought (Gerdt and Lempio 2011, p. 500). The application of evolutionary algorithms often yields good initial results, i.e. existing solutions are rapidly improved, but it might be difficult to achieve an optimum with high accuracy. In addition, these algorithms have stochastic components, so there is no guarantee that an optimum will actually be achieved. In this regard, Finke (2008, p. 225) notes that random operators (random mutation, random crossovers, etc.) are suggested by the theory of classical genetic algorithms. However, careful adaptation is rather critical for such an algorithm to be competitive. Finke (2008, p. 225) states that “genetic algorithms provide a general framework that, combined with other methods of specific or general solution, can lead to extremely powerful hybrid methods”.

In the field of ship weather routing, evolutionary approaches become increasingly popular to solve multi-objective optimization problems mainly aiming at minimum time, fuel consumption and/or heavy weather damage. This is endorsed by Chen (2011, p. 6), but the advantages are also contrasted with disadvantages. These may be related to the risk of not reaching the optimum, the choice of a stopping criterion, such as a marginal rate of improvement after further iterations, and potentially long run times. Further challenges refer to properly presenting resulting routes, which are influenced by weather uncertainties, to the master for making a sound final decision. Also Walther et al. (2017) conclude from a comparison of a genetic algorithm with the A* algorithm that results derived by employing a genetic algorithm are influenced by the initial population, population size and number of variables. Moreover, it is suggested to further study the impact of mutation rate, crossover mechanisms or other operators.

Real-Coded Genetic Algorithm Maki et al. (2011) propose a Real-Coded Genetic Algorithm (RCGA) to solve a multi-modal function problem with the waypoints’ latitudes and propeller revolutions as variables. The objectives minimum fuel consumption and minimum risk of parametric rolling are combined in one function by a weight ratio that may be varied. Apart from handling the objective function and other minor differences, this method is understood as an extension of the Augmented Lagrangian Method by Tsujimoto and Tanizawa (2006) (see Sec. 4.2.2). When formulating the weather routing problem as an optimization problem in a continuous domain, a bit-string or a real-coded genetic algorithm is considered to be suitable. Due to strongly intervariable dependencies in weather routing, the bit-string approach with the genotype being a binary string is less efficient and inferior compared to the real-coded approach based on real-valued vectors (Maki et al. 2011, p. 313). Crucial for RCGAs are a crossover operator to generate new candidate solutions and a selection model to determine the new population. As the results depend on the initialization and the weight ratio, the great circle route as initial solution and the choice of appropriate weights are recommended.

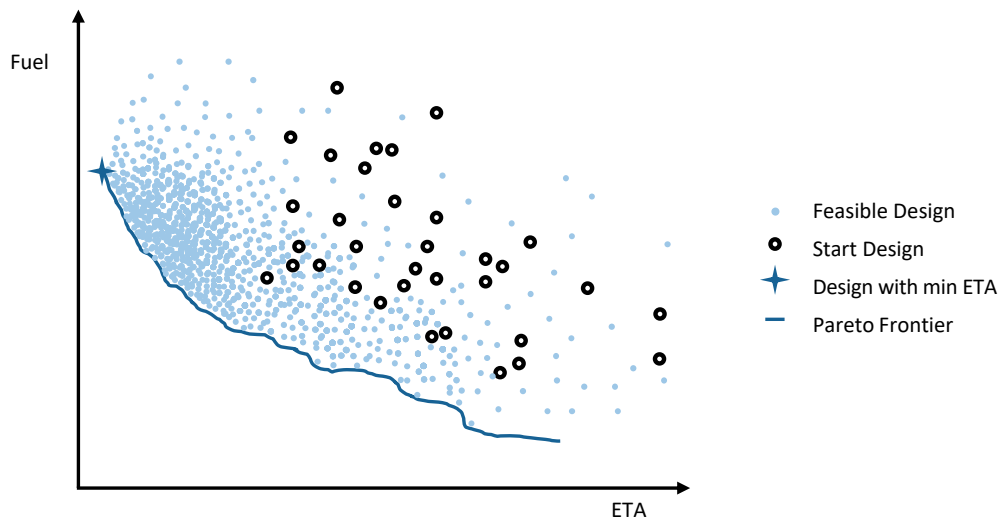


Figure 4.8: Solution Space for the Objectives Minimum Arrival Time and Fuel Consumption, adapted from Hinnenthal (2008, p. 60)

Multi-Objective Genetic Algorithm In addition to the Nelder-Mead-Method (NMM) subject to Sec. 4.2.1, Hinnenthal (2008) applies a Multi-Objective Genetic Algorithm to stochastically solve the discretized nonlinear optimization problem with minimum estimated time of arrival and minimum fuel consumption as objectives and several constraints (see Sec. 5.5.3). Although the stochastic method leads to the tenfold number of required designs with half of them being necessary to determine the global optimum (Hinnenthal 2008, p. 113), it is aimed at improving the genetic method due to the risk of NMM converging to a local optimum. To reduce the computational effort, the number of designs, thus the number of free variables, objectives and route evaluation points, needs to be reduced. Therefore, the route including course and speed is modeled using a B-spline technique. Standard spectra are used to describe the seaway and linear superposition is applied to assess ship responses. Furthermore, ensemble weather forecasts are taken into account to identify Pareto optimal routes, as shown by the Pareto frontier in Fig. 4.8, as well as to further increase the accuracy and robustness of the resulting routes and provide decision support to the master. The method described by Hinnenthal and Harries (2004) and Hinnenthal (2008) is also considered for intact weather routing, i.e. for ships with normal maneuvering and propulsion capacity, by Böttner (2007).

In comparison to Hinnenthal (2008), Marie and Courteille (2009a) aim to reduce the number of free variables in their Pareto-optimized Multi-Objective Genetic Algorithm with the objectives minimum time and consumption by proposing a “method for spatial and temporal generation of route variants based on a generic and automatic meshing method” (Marie and Courteille 2009a, p. 140). The discretization is based on physical parameters, such as the geographical environment, meteorological data and ship charac-

teristics. Marie and Courteille (2009b) apply the method to a sail-assisted motor vessel, while Marie and Courteille (2014) add a fuzzy logic model to derive the ship's fuel consumption on a route by using data collected from onboard measurements.

Tsou and Cheng (2013) combine a genetic algorithm with an Ant Colony Algorithm. It is inspired by the interactive process of ants searching for food by emitting pheromones. The more ants pass by a point, the higher the concentration and the closer the optimal path. Computational performance is among others improved by introducing a maximum course deviation, a maximum route length segment, a ship's critical speed in different wave conditions, a range of information quality as well as crossover and mutation operations. Crossover operations are used when two ants or ships pass by the same grid point to combine both halves of the route to achieve two new ones. To avoid local optima, mutation randomly exchanges a point from the currently optimal route with a non-passed one. Experiments from Yokohama to San Francisco show that results reducing fuel consumption, safety risks and/or passage time by controlling ship's course and speed can be achieved within five minutes. However, appropriate choice of the number of ants and parameters is critical for algorithm's efficiency.

A Distance-based Pareto Genetic Algorithm (DPGA) with three objectives (minimum voyage time, fuel consumption and wave height) and two decision variables (latitude and speed) is introduced by Andersson (2015). It is compared to the previously described grid search method (see Sec. 4.3) and uses the same grid to generate the initial population. To reduce computational time, an upper boundary limits the number of elite sets. It is concluded that the DPGA achieves a good result in approximately 1% of the computation time required by the grid search approach. However, it is limited to east-west routes due to the longitude not being defined as a decision variable. Moreover, it lacks the critical constraint for maximum available engine power.

Veneti et al. (2015a) apply a Non-dominated Sorting Genetic Algorithm (NSGA-II). It includes a niching method to achieve population diversity and a fast ranking method to find non-dominated solutions, and thus to fully retrieve the Pareto optimal set. The initial population comprises routes optimized regarding the single objectives of minimum fuel consumption, maximum safety and distance from obstacles as well as historically popular routes. Further generations are created by three mutation operators and a node based crossover operator. Assuming minimum fuel consumption and risk as objectives, a given arrival time as constraint and a constant ship speed, the comparison of this approach with an exact algorithm (see Sec. 4.3) shows that this approach is faster but cannot retrieve the whole Pareto set.

Multi-Objective Evolutionary Algorithm In order to find a trade-off between the often conflicting maximum economic efficiency and maximum ship safety, Szlapczynska (2007) suggests to combine evolutionary algorithms and ranking methods to select the most suitable route out of the Pareto set. Thus, Szlapczynska and Smierzchalski (2009)

present the Multicriteria Evolutionary Weather Routing Algorithm (MEWRA) incorporating the Strength-Pareto Evolutionary Algorithm (SPEA) and a multicriteria ranking method. It aims to solve a constrained multicriteria optimization problem with minimum passage time, fuel consumption and voyage risks as objectives and the waypoint's coordinates and engine settings as variables. Krata and Szlapczynska (2012, 2018) adapt the method designed for ships with hybrid propulsion to motor-driven ones and improve it by integrating MSC.1/Circ. 1228 (see Sec. 5.5.2 and 5.5.3). Szlapczynska (2013) further enhances the multicriteria ranking method to remove deficiencies, such as complex configuration and long computation time. Moreover, the concept of compensation may lead to non-acceptably poor ship safety being compensated with short passage time. Hence, the Fuzzy TOPSIS (Technique for Order Preference by Similarity to an Ideal Solution) is replaced by the non-compensatory Zero Unitarization Method. It allows "normalization of the diagnostic variables by the gap between the variable's value and the most or the least suitable variable value" (Szlapczynska 2013, p. 64).

An advanced version of MEWRA by Szlapczynska (2015) focuses on completely customizable optimization criteria and constraints. These include dynamically changing, i.e. time-dependent, constraints, such as wind speed, wave period and angle of encounter, as well as static time-independent constraints, such as landmasses, shallow waters and piracy areas. First, the method randomly generates an initial set of routes based on a loxodrome, a great circle and a reflected great circle from origin to destination as well as routes from an isochrone method (see Szlapczynska and Smierzchalski (2007) and Sec. 4.4.2) and an A* algorithm (Szlapczynska 2015, p. 343). Second, it applies the SPEA to derive the Pareto set of optimal solutions accounting for user-defined optimization criteria. Last, the multicriteria ranking method is employed to select the best suitable route. Results for two examples are obtained in two and six minutes respectively (Szlapczynska 2015, p. 353). The first example considers passage time and voyage safety as objectives and landmasses and shallow waters as constraints. The second one adds fuel consumption as objective as well as piracy areas and a wind speed threshold.

Vettor and Guedes Soares (2015a,b, 2016) apply an upgraded version of the Strength-Pareto Evolutionary Algorithm (SPEA2) to derive a Pareto set of optimal solutions regarding the three objectives of fuel consumption, voyage duration and safety. Safety may be considered as an objective or by constraints. Decision variables are speed and heading. To reduce the computational effort and the total number of generations, the initial population is generated using Dijkstra's algorithm for single-objective optimization. Thus, fuel consumption, voyage length and duration at several different ship speeds are optimized. Further generations are created by crossover, mutation and migration operators. To select the most favorable route, a ranking method has been developed that allows to define the importance of each objective and of some constraints after instead of before an optimization run. Future improvements may relate to substituting Dijkstra's algorithm with the A* algorithm to increase efficiency, since creating the initial population consumes 85 % of the computational time.

5 Aspects of Ship Performance

In addition to the metocean data from numerous providers and the various optimization approaches applied in ship weather routing, the third major aspect refers to the ship's performance during a voyage. As a basis to describe ship motions, Sec. 5.1 is dedicated to reference frames and equations of motion. The motion of a ship, thus its performance, significantly depends on the service conditions, particularly the influence of ocean currents, wind and seaway addressed in Sec. 5.2 to 5.5, as well as on the ship itself, e.g. its geometry, loading conditions and propulsion system. Adequate modeling of a ship's propulsion, treated in Sec. 5.6, is critical to ensure safe and efficient operation and navigation of ships in particular against the background of efficiency regulations. However, many systems aim to provide routing support to various types of ships. Thus, simplified methods with a wide scope of application are popular to avoid the need for detailed ship data. Inherent to the range of methods, the dynamics and propulsion of a ship are considered with varying level of detail, which influences performance and safety prediction accordingly. Approaches used in ship weather routing are individually pointed out in line with the different sections.

5.1 Reference Frames and Equations of Motion

For ship weather routing and route planning particular importance is attached to earth related reference frames. When studying ship motion dynamics, however, generally ship related reference frames are used to specify the ship's motion in six degrees of freedom. According to the considered degrees of freedom, equations of motion can be formulated. The reference frames as well as the equations of motion are treated in the following.

5.1.1 Earth Related Reference Frames

In case a ship is operating in a local area, thus at approximately constant latitude and longitude, a coordinate system (x_0, y_0, z_0) relative to the Earth's reference ellipsoid is often used with its x axis pointing northwards, its y axis eastwards and its z axis downwards normal to the Earth's surface (Fossen 2011, p. 17). This is shown in Fig. 5.1 together with the World Geodetic System 1984 (WGS 84). This coordinate system is particularly important in the context of ship navigation and weather routing. Its origin is determined by the Earth's center of mass, which is the origin of the Earth's reference ellipsoid, also called WGS 84 ellipsoid (National Imaginery and Mapping Agency 2000, p. 2-2). Its x axis intersects with the International Earth Rotation Service (IERS) reference meridian (zero meridian). Its z axis points towards the IERS reference pole and serves as rotational axis to follow the Earth's rotation, while its y axis completes

the Earth-centered, Earth-fixed, right-handed and orthogonal coordinate system. Correspondingly, locations are specified by latitude Φ and longitude λ . As to the National Imaginery and Mapping Agency (2000, p. 1-1), WGS 84 is the most common and best worldwide geodetic reference system for the Earth that is available for applications such as mapping, geopositioning and navigation. In terms of navigation and ship weather routing, it is usually the reference frame used when providing weather data or voyage plans. Thus, the reference ellipsoid including its definitions and mathematical transformations is used to calculate distances and azimuths between two waypoints of a ship's voyage.

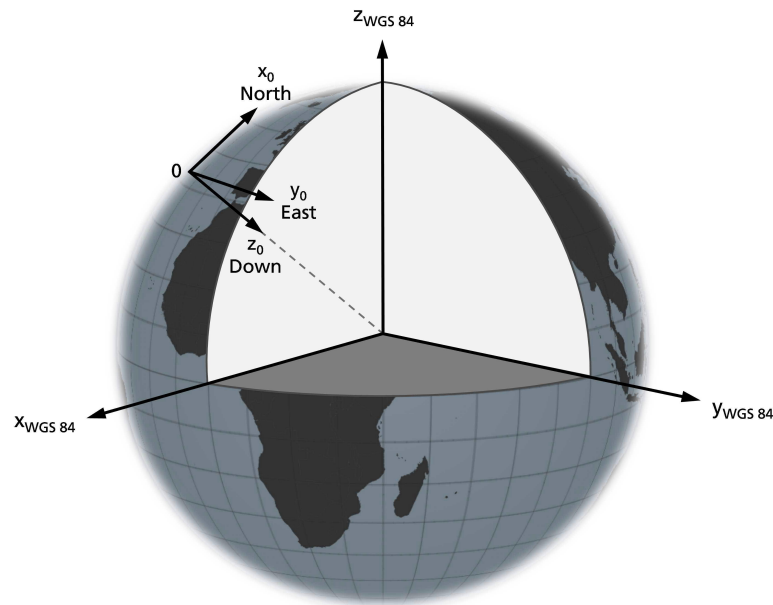


Figure 5.1: North-East-Down and Earth-fixed Earth-centered WGS 84 Coordinate Systems, based on (Fossen 2011, p. 17; National Imaginery and Mapping Agency 2000, p. 2-1)

5.1.2 Ship Related Reference Frame

In addition, a ship-fixed reference frame is required when studying ship motion dynamics. Since a ship may experience motion in six degrees of freedom (DOF), six independent coordinates to specify position and orientation in a ship-fixed reference frame (x, y, z) are introduced, as shown in Fig. 5.2 and listed in Tab. 5.1. The location of its origin C is usually chosen to be located midships in the waterline. The first three coordinates describe the position along the x , y and z axes. Their time derivatives represent the translational motion, defined as surge, sway and heave (Fossen 2011, pp. 15–16). Equivalently, the last three coordinates p , q and r correspond to the orientation, and their time derivatives to the rotational motion components roll, pitch and yaw.

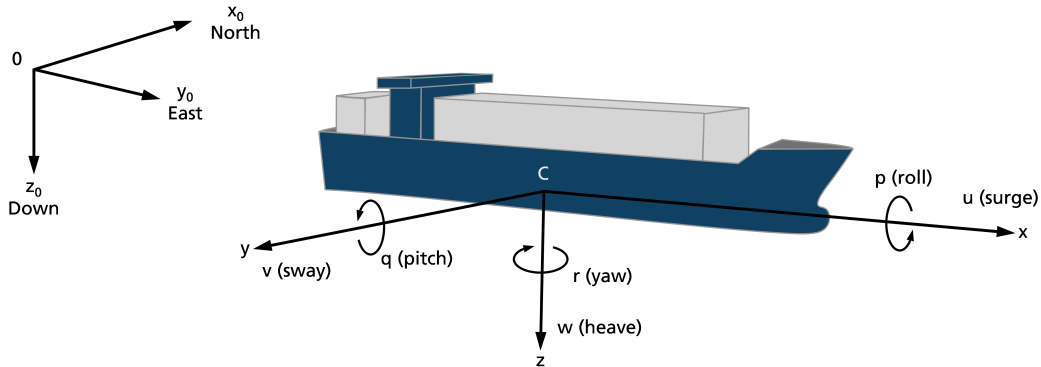


Figure 5.2: Definition of 6 DOF Motions in Ship-fixed Reference System, adapted from Fossen (2011, p. 16)

Principally, the influence of environmental forces due to ocean currents, wind and waves takes place in six DOF (Fossen 2011, p. 7). However, available weather data is commonly limited to the ocean surface. In addition, the focus of this research is on merchant surface vessels rather than on underwater vehicles. Hence, relations addressed in the following are generally expressed regarding the water surface neglecting the underwater space, i.e. vertical or subsurface thermohaline ocean currents relevant for underwater vehicles moving in a three-dimensional space.

Table 5.1: Notation for Ship Motion Components, according to Fossen (2011, p. 16) based on SNAME (1950)

	Surge	Sway	Heave	Roll	Pitch	Yaw
Degree of freedom	1	2	3	4	5	6
Forces and moments	X	Y	Z	K	M	N
Linear and angular velocities	u	v	w	p	q	r
Positions and Euler angles	x	y	z	Φ	Θ	ψ

In relation to the ship's movement in a two-dimensional space and on the basis of the introduced reference frames, Fig. 5.3 provides the notations regarding the three most important environmental influences, i.e. ocean currents, wind and waves. Ocean currents (velocity vector \mathbf{V}_C , direction against North α_C) present the relation between the ship's motion through water (velocity vector \mathbf{V}_S , velocity in longitudinal u and transverse direction v , course angle χ) and over ground (velocity vector \mathbf{V}_G , angle against North α_G , angle against ship longitudinal axis β_G) (see Sec. 5.3). The course angle χ is the sum of the heading angle ψ , which is the angle between the x_0 (North) and the x axis, and the drift angle β_D . The ocean current and the geographic wind (speed U_G , direction against North α_W) influence the true wind (speed U_T , direction against North α_T , angle

against ship longitudinal axis γ_T), which induces the apparent wind (speed U_A , direction against ship longitudinal axis β_A) (see Sec. 5.4).

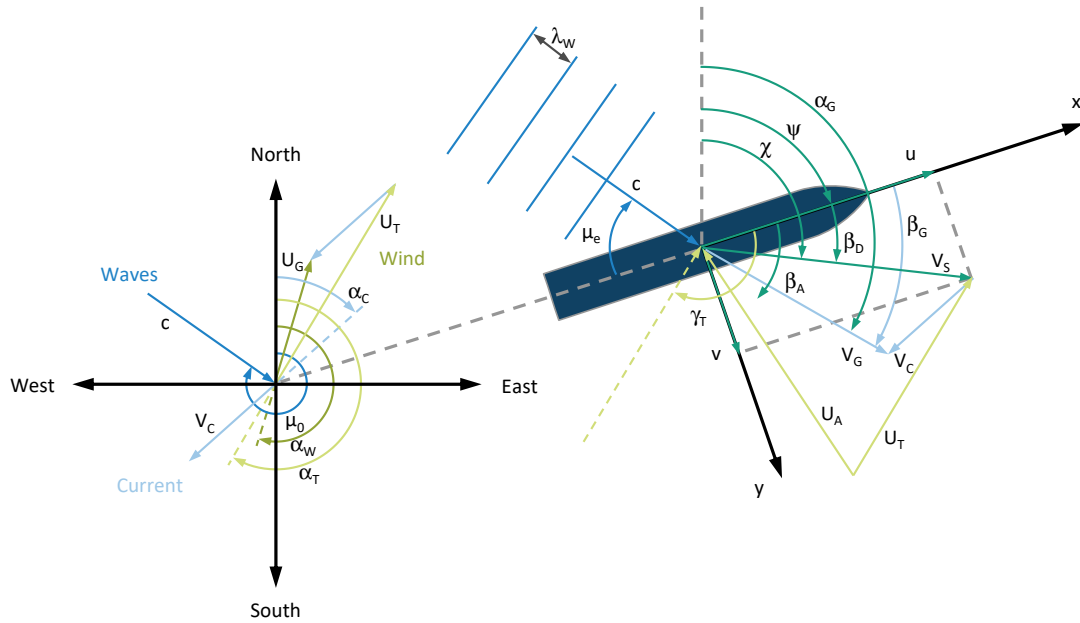


Figure 5.3: Definition of Angles and Motion Components in the Horizontal Plane, based on Abdel-Maksoud et al. (2016, p. 28) and Fossen (2011, p. 40)

The encounter of waves (velocity c , wave length λ_W , main propagation direction μ_0) is visualized in greater detail in Fig. 5.4, which shows the encounter angle μ_e as well as the usual denomination of the sailing conditions in waves (see Sec. 5.5). The environmental influences on the ship according to Fig. 5.3 and 5.4 are elaborated in the following sections. It is to be noted that bold type notation indicates vectors and regular type notation absolute values.

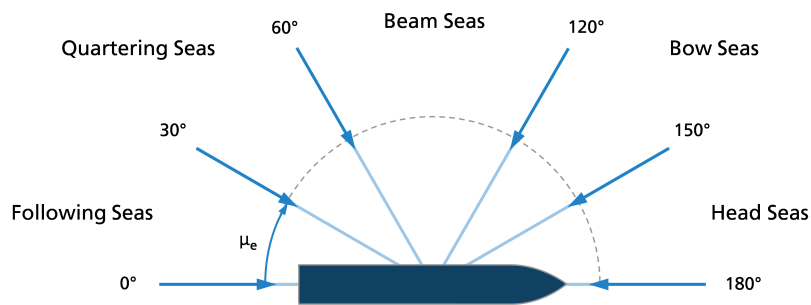


Figure 5.4: Definition of Encounter Angle and Sailing Conditions, based on Fossen (2011, p. 209) and Perez (2005, p. 24)

5.1.3 Equations of Motion

In seakeeping theory, the movement of a ship in a seaway in six degrees of freedom is generally described using a reference frame, which is not fixed to the hull but with respect to the equilibrium of motion and which moves at the ship's average speed along its path. The ship motion is studied assuming the ship to move on a steady course at a constant-average forward speed (Perez 2005, p. 50). Accordingly, equations of motion for all six degrees of freedom can be formulated. In ship maneuvering theory, where a ship is assumed to move at constant speed in calm water without wave excitation, and motion control problems, as treated by Perez (2005, p. 80), pitch and heave components are commonly neglected leading to models with four degrees of freedom, thus surge, sway, roll and yaw. As to Fossen (2011, p. 9), also models limited to three degrees of freedom considering surge, sway and yaw motion are applied. For example, Shigunov (2017, p. 66) presents an approach based on these three equations of motion to predict the required added power for a ship in a seaway. The accurate prediction is key to sound weather routing as indicated by the following statement (Shigunov 2017, p. 65):

Operational assistance concerning optimal speed, course and trim, as well as ship- and weather-specific route optimisation (routing) is gaining increasing interest; its usefulness depends on the accuracy of weather data and predicted added power vs. seaway parameters and ship geometry, loading condition, speed and course.

This is endorsed by Bertram and Couser (2014, p. 15) stating that:

For practical purposes, added power rather than added resistance should be considered. This requires at least a simple model of maneuvering, propeller and wind forces. This should be taken into account for a range of applications involving 'added resistance', such as route optimization, hull optimization, or hull performance management.

In order to apply these recommendations, the equations of motions required for the maneuvering model need to be formulated and taken into account. In line with Shigunov (2017, p. 66) and Abdel-Maksoud (2009, p. 42), the following equilibrium equations for surge, sway and yaw may be given:

$$(1 - t)T + X_{Hull} + X_{Wind} + X_{Drift} + X_{Rudder} = (1 - t)T - R_T = 0 \quad (5.1)$$

$$Y_{Hull} + Y_{Wind} + Y_{Drift} + Y_{Rudder} = 0 \quad (5.2)$$

$$N_{Hull} + N_{Wind} + N_{Drift} + N_{Rudder} = 0 \quad (5.3)$$

where the indices *Hull*, *Wind*, *Drift* and *Rudder* denote the forces (X , Y) and moments (N) at the hull in calm water as well as due to wind loads, waves (averaged) and the rudder. T is the propeller thrust and t the thrust deduction fraction. In this regard, the negative longitudinal force $X_{Hull} + X_{Wind} + X_{Drift} + X_{Rudder}$ is the ship's total resistance R_T including the added resistance due to wind, waves and the rudder.

In ship weather routing, commonly not even the three equations of motion for surge, sway and yaw but only the equation of motion in longitudinal direction, thus surge, is considered for reasons of simplicity. Hence, the ship's total resistance (see Sec. 5.2) needs to be balanced with an adequate propeller thrust. Generally, transverse drift forces influencing the heading and the required rudder angle, which induces rudder forces and may further increase the resistance, are neglected. Applied approaches, though, differ in particular as to the way the calm water resistance and the added resistance among others due to wind and waves (see Sec. 5.2, 5.4 and 5.5) are calculated. Moreover, propeller and engine characteristics are considered with different degrees of detail if considered at all (see Sec. 5.6). The general approach is schematically indicated in Fig. 5.5.

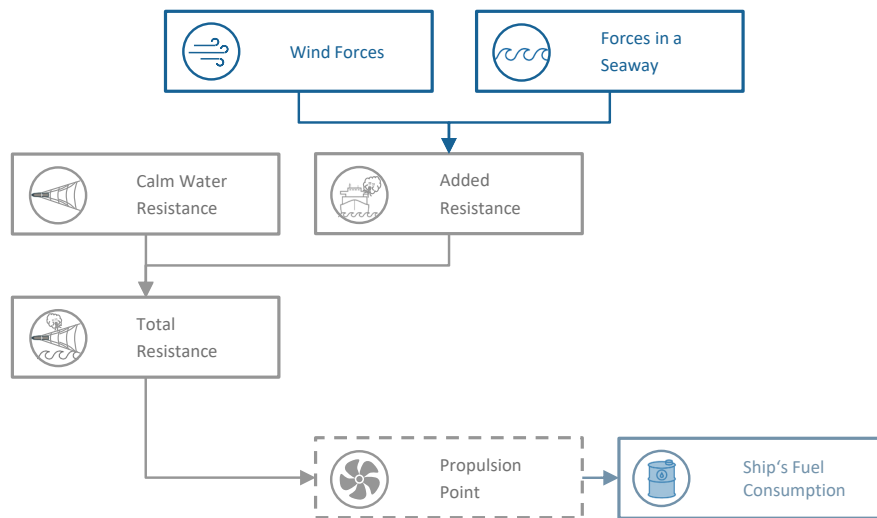


Figure 5.5: Model based on Longitudinal Ship Motion with or without Propeller

In contrast to the approaches focusing on the ship's resistance and motion in longitudinal direction, only few approaches also account for transverse motions. Hagiwara (1989) addresses weather routing of (sail-assisted) motor vessels and consequently pays specific attention to the wind resistance as well as heel, drift and rudder angle. Thus, not only the equation of motion considering longitudinal forces but also those regarding lateral forces, yawing moments and heeling moments are taken into account. These equations include aerodynamic and hydrodynamic forces and moments as well as added resistance due to waves, rudder forces and moments, propeller thrust and the hull's righting moment due to heel. Once the ship's speed is obtained by solving the equations, the engine power is determined taking into account the propeller and engine characteristics. Transverse motions may also be considered by integrating a maneuvering motion model, such as by Ishii et al. (2010) and Kobayashi et al. (2015). Costs along a route are calculated by performing a maneuvering simulation with solving horizontal differential equations of motion, such as yaw, sway, and surge, and accounting for hull and rudder forces, propeller thrust as well as wave and wind forces.

In general, the integration of a maneuvering model into weather routing systems must be weighed up against the resulting added value. However, the improvements are often expected to be small and more importantly they are often not quantifiable without previous implementation and validation. This is in line with the conclusion of Sec. 2.4 that case by case evaluations based on computational methods are required for quantitative assessments. Thus, the integration of a maneuvering model is frequently omitted right from the beginning due to the associated development expenditures on the one hand and the expected increased computational efforts and data requirements on the other hand. As a consequence, this situation encourages the development of a system that can optionally consider a simple maneuvering model, i.e. more than one equation of motion, in order to investigate the impact of added resistance and added power on ship weather routing. While the ship's resistance is addressed in Sec. 5.2, a method for added power prediction applied in this thesis is described in Sec. 5.6. It has been developed by Abdel-Maksoud et al. (2016) within a research project concerning the performance of ships in a seaway.

5.2 Ship Resistance in Service Conditions

Traditionally, ships are designed and optimized for performance in calm water (Shigunov 2017). However, service conditions differ, since effects due to hull roughness, shallow water and weather impacts, such as wind and seaway, cause an additional resistance (Bertram 2012, p. 94). Also the loading condition plays an important role. Hence, the total resistance of a ship R_T (see Eqn. 5.1) may be decomposed into its resistance in calm water and the added resistance in service conditions. In ship weather routing, considered impacts are often limited to wind and seaway.

5.2.1 Calm Water Resistance

The calm water resistance R_0 of a ship generally refers to the ship's resistance in trial conditions, thus without waves, wind, shallow water or fouling. Appendages and wind resistance induced by the ship's own speed, though, may be included (Krüger 2006, p. 2). It is the negative longitudinal hydrodynamic force in calm water X_{Hull} (see Eqn. 5.1) and can be expressed as a polynomial function of the ship's speed u . The calm water resistance curve of a post-panmax container ship is shown in Fig. 5.6. Using the nondimensional coefficient c_T , the ship's wetted surface S and the water density ρ , the calm water resistance R_0 can also be given as:

$$R_0(u) = 0.5 \cdot \rho \cdot c_T(u) \cdot u^2 \cdot S \quad (5.4)$$

The calm water resistance can be derived among others from model tests or empirical formulae. Model tests are still considered as the most useful way to accurately predict the ship's resistance and power requirements in calm water, since the resistance of a ship can hardly be measured in full-scale and despite continuous improvements and

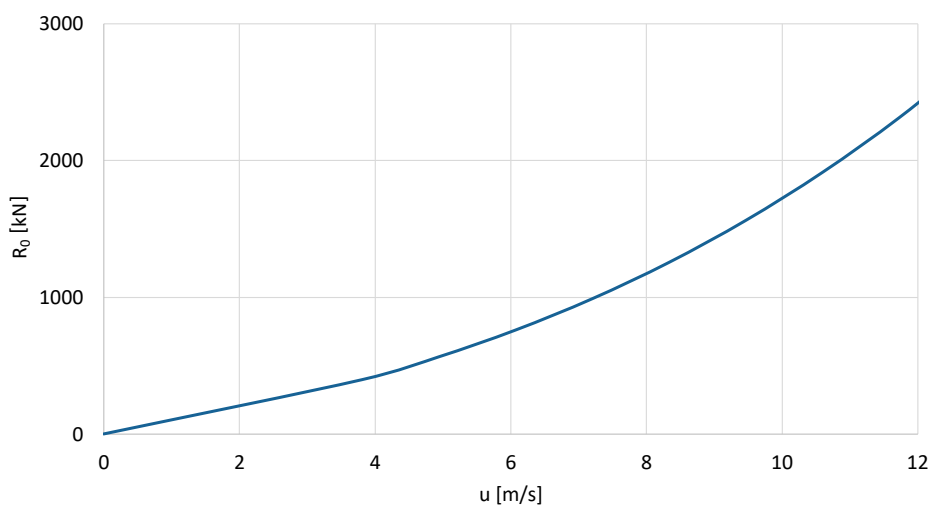


Figure 5.6: Approximated Calm Water Resistance Curve for Post-Panmax Container Ship (DTC), derived from Riesner et al. (2016, p. 29)

increasing availability of numerical methods (Bertram 2012, pp. 76–77, 80). Several methods are available to derive the full-scale ship resistance from the model resistance, which are discussed among others by Bertram (2012), Krüger (2006), and Schneekluth and Bertram (1998). However, particularly in early stages of the ship design as well as in ship weather routing, rather simple, time and cost efficient estimates of the ship’s resistance are required. Therefore, a variety of largely empirical methods exists that allow to predict the ship resistance more or less accurately without model tests but with comparably few global design parameters. Bertram (2012), Krüger (2006), and Schneekluth and Bertram (1998) describe methods, which are among others based on resistance data from similar ships or the evaluation of (systematic) model tests. For example, the method presented by Holtrop and Mennen (1978, 1982) and Holtrop (1984) is based on evaluating the database of the Dutch Model Basin MARIN by regression analysis.

In ship weather routing, often empirical methods are applied, either due to the lacking availability of calm water resistance data or because it is aimed at wide applicability for various ship types without high data requirements. In this regard, the Holtrop-Mennen method is popular and applied among others by Aligne et al. (1997), Böttner (2007), Calvert (1990), Cui, Turan, et al. (2016), Hinnenthal (2008), Lu et al. (2015), Shao et al. (2012), Vettor and Guedes Soares (2016), and Zaccone and Figari (2017). Bentin et al. (2016) either use the Holtrop-Mennen approach or calm water resistance data measured in a model basin as well as a constant factor to consider appendages and hull roughness (fouling). An advantage is the rather simple application of these methods requiring only some global design parameters. At the same time, Krüger (2006, p. 35) points out the disadvantage that the predictions are usually not very accurate and vary widely. Thus, it is recommended to determine the resistance on the basis of reference ships.

5.2.2 Added Resistance Components

Generally, the added resistance of a ship in service conditions relates to effects due to appendages, hull roughness, shallow water, wind and seaway (Bertram 2012; Schneekluth and Bertram 1998). The loading condition influences both, the calm water resistance as well as the added resistance. In commercial weather routing systems summarized in Sec. 2.5, it is often taken into account by information provided on the ship's trim, draught and *GM*. The environmental impacts on the added resistance may also include effects due to ice. In the described commercial systems, ice areas are rather considered as hazards and are integrated as restrictions influencing the planned route.

Appendages and wind resistance induced by the ship's own speed are sometimes included in the calm water resistance, since this is subject to the contract between shipyard and owner (Krüger 2006, p. 2). As to the influence of appendages, Schneekluth and Bertram (1998, p. 200) indicate that bilge keels may increase the ship's resistance by 1% to 2%, transverse thrusters in the aftbody by 1% to 6%, bow thrusters by a non-significant amount, shaft brackets and bossings by 5% to 12%, long propeller shafts of twin-screw ships by 20% and rudders by only 1% in neutral position but 2% to 6% at moderate angles. Chen (1978, p. 92) accounts for appendages by augmenting the calm water resistance estimate by 3% in case of a single screw ship. Hull roughness may add up to 5% to the ship's frictional resistance, while fouling can contribute much more (Bertram 2012, p. 96). Concerning a very moderate influence of shallow water, the speed loss can be estimated using respective diagrams. For a strong impact on the ship's resistance, physical interactions of wave-breaking, squat and free surface deformation become complex (Schneekluth and Bertram 1998, p. 200).

The impact of wind and waves is elaborated in Sec. 5.4 and 5.5. In principle, the added resistance due to waves increases approximately by the square of the significant wave height in case of a constant wave period. Similarly, wind induced forces are proportional to the square of the apparent wind speed (Shigunov 2017, p. 70; ABS 2013, p. 14). In normal operational conditions with typically large forward speeds and low sea states, waves contribute less than wind to the added resistance, according to Shigunov (2017, p. 74). At lower speeds and in higher sea states (container ship at 14 kn in more than 4.5 to 5.0 m), however, the influence of waves is dominant. Moreover, it is indicated that considering the rudder is important as its contribution to added resistance in high beam waves seems to be significant. For ocean going vessels, typical operational conditions are sea state 3 (0.5 to 1.25 m wave height) or higher (ABS 2013, p. 14). Sea state 3 is exceeded with a probability of approximately 60% in the North Atlantic and sea state 7 with 10%. Referring to Smith et al. (2014, p. 108), the fuel consumption of low speed vessels, such as bulkers and tankers, can increase by 2% in sea state 2 and 6% in sea state 5 when comparing head wave conditions to following waves. From sea state 2 to 5, the increase amounts to 6% to 12%. Thus, Smith et al. (2014, p. 108) draw the conclusion that weather routing is crucial for saving fuel.

5.2.3 Speed Reduction Approach

Instead of considering metocean impacts on the ship by added resistance, the effects are often integrated by so called speed reduction curves, which are functions of wave height and wave direction relative to the ship's speed. An example is given in Fig. 5.7.

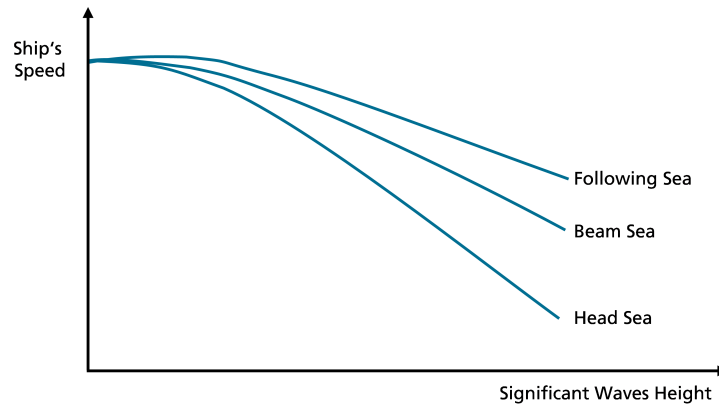


Figure 5.7: Concept of Speed Reduction Curves, adapted from Bijlsma (1975, p. 10) and Wit (1968, p. 70)

Speed reduction curves can often be found in early weather routing approaches or as simplifications, e.g. by Bijlsma (1975), Bleick and Faulkner (1965), Montes (2005), Motte (1981), Nagle (1972), Takashima et al. (2009), Tsou and Cheng (2013), Wit (1968), and Zoppoli (1972). While usually curves as presented in Fig. 5.7 are used, Bijlsma (1975) and Bleick and Faulkner (1965) provide the speed reduction in waves as function of the encounter angle in a polar velocity diagram for each wave height. Also Chen (1978) mentions an empirical approach with simple speed curves for various power settings and headings under different sea conditions which are derived from statistical curve fitting through recorded data. To increase accuracy, Chen (1989) describes an enhanced version where ship speed and power requirements in realistic sea states are predicted by a semi-empirical performance model that utilizes ship motions, speed, RPM, horsepower and environmental conditions recorded by shipboard sensor technology.

Another method is proposed by Kwon (1981) (also see Townsin and Kwon (1983)), thus also referred to as Kwon's method. It aims to estimate the speed reduction taking into account the weather conditions by the Beaufort number, to which the wave height is correlated, and a few ship characteristics, such as ship type, block coefficient and loading condition. This approximate approach is applied in weather routing among others by Lu et al. (2015), Meyer (2014), and Shao et al. (2012) and considered for further developments by Veneti et al. (2017). Lu et al. (2015) and Shao et al. (2012) estimate the final reduced speed in the prevailing wind and sea conditions and predict a corresponding engine power and propeller's rotational speed. Instead of Kwon's method, Shao and Zhou (2012) prefer to use data from sea trial, model tests and numerical simulations

to estimate the ship's resistance in calm water and due to wind and waves relative to ship speed over the ground, draught and trim. Meyer (2014) compares weather routing results based on Kwon's method to those using data from PDSTRIP and concludes that Kwon's method yields a comparably low fuel consumption in all studied cases. This is attributed to limited weather data and a maximum Beaufort number of 6. Based on a review of some semi-empirical approaches for added resistance prediction (see Sec. 5.5.1), Lu et al. (2015) modify Kwon's method to allow ship type specific added resistance estimation with increased accuracy. This is combined with noon reports and sea trial data to develop a semi-empirical model for ship operational performance prediction in dependence of the ship's draught, speed, engine degradation conditions, hull and propeller fouling as well as sea states and encounter angles.

The impact of methods ranging from simple speed loss approaches up to a developed ship resistance and powering algorithm is studied by Calvert (1990). This algorithm uses ship motion and added resistance databases produced by seakeeping computer models by British Maritime Technology. Concerning speed loss curves, routing studies are conducted by integrating the empirical approaches of Babbedge (1975) and James (1957) based on regression analyses performed on recorded data as well as Aertssen (1969) and Townsin and Kwon (1983) based on the Beaufort number (Calvert 1990, pp. 30–32). It is concluded that simple methods may be suitable for rough route estimates but that more sophisticated methods are superior. A higher degree of complexity, however, increases computational time and often requires more ship information. For detailed information on the studies and conclusions, it is referred to the complete thesis of Calvert (1990).

5.3 Influence of Oceanic Surface Currents

The global oceanic circulation and surface currents including particularly important currents for maritime shipping are outlined in Sec. 3.2. In particular, strong ocean currents have a decisive influence on the actual speed profile of a ship during a voyage. Considering a geographically fixed reference frame, as indicated by the cardinal points in Fig. 5.2, oceanic surface currents cause a translatory motion of the ship against the ground in the x-y-plane. Correspondingly, the current velocity \mathbf{V}_C presents the correlation between the ship's speed through water \mathbf{V}_S and the ship's speed over ground \mathbf{V}_G . Eqn. (5.5) expresses this relation in a general form in a two-dimensional space in line with Fig. 5.3:

$$\mathbf{V}_S = \mathbf{V}_G - \mathbf{V}_C \quad (5.5)$$

Since meteorologists generally provide wind data relative to the land, a geographic or ground wind against the earth is provided by weather forecasts. In that case, the true wind relative to the water \mathbf{U}_T depends on the current \mathbf{V}_C and the ground wind \mathbf{U}_G , as given by Schenzle (2016):

$$\mathbf{U}_T = \mathbf{U}_G - \mathbf{V}_C \quad (5.6)$$

While navigation, and thus weather routing, usually takes place in geographically fixed coordinate systems, ship hydrodynamics pays more attention to the ship speed through water. That is why ocean currents are generally neglected in research related to maneuvering or seakeeping of ships.

5.4 Influence of Wind and Ship Aerodynamics

The influence of wind on a ship, thus the wind forces and moments acting on the hull and superstructure, may have significant impact on the balance of forces and the required power to meet a certain speed. The ship's speed through water V_S and the true wind speed U_T result in an apparent wind U_A . The angle between the vector of the apparent wind speed U_A and the ship's center line is defined as the apparent wind angle of attack β_A . The definitions of the angles and speeds are shown in Fig. 5.3. Taking into account the angle γ_T between the center line of the ship and the true wind vector, the absolute apparent wind U_A and angle of attack β_A can be determined in the ship-fixed reference system by:

$$U_A = \sqrt{V_S^2 + U_T^2 + 2V_S U_T \cos(\gamma_T)} \quad (5.7)$$

$$\beta_A = \tan^{-1} \left(\frac{U_T \sin(\gamma_T)}{V_S + U_T \cos(\gamma_T)} \right) \quad (5.8)$$

Along the x axis the apparent wind causes a force X_{Wind} . In case of head wind, this is an additional resistance, while in case of tailwind, the ship's resistance is reduced. Side wind mainly leads to a drift force Y_{Wind} along the y axis and a yaw moment N_{Wind} . Since the yaw moment is dependent on the angle β_A and the longitudinal distribution of the lateral wind projection area, which can cause inaccuracies in case of approximation, e.g. Abdel-Maksoud et al. (2016) neglect the influence of the yaw moment. Nevertheless, based on Fossen (2011, p. 191) and Shigunov (2017, p. 66) they can be expressed as:

$$X_{Wind} = 0.5 \cdot \rho_{Air} \cdot U_A^2 \cdot C_X(\beta_A) \cdot A_F \quad (5.9)$$

$$Y_{Wind} = 0.5 \cdot \rho_{Air} \cdot U_A^2 \cdot C_Y(\beta_A) \cdot A_L \quad (5.10)$$

$$N_{Wind} = 0.5 \cdot \rho_{Air} \cdot U_A^2 \cdot C_N(\beta_A) \cdot A_L \cdot L_{OA} \quad (5.11)$$

where ρ_{Air} denotes the air density, L_{OA} the overall ship length, A_F and A_L the ship's frontal and lateral projected area above sea level. C_X , C_Y and C_N are nondimensional coefficients, which may be determined experimentally by wind-tunnel tests or numerically. Since generic methods, though, are often favored over ship specific coefficients to increase applicability of weather routing developments, estimations using empirical formulae are common practice (Fossen 2011, pp. 191–199; Schneekluth and Bertram 1998, p. 221). Applied approaches include formulae presented by Blendermann (1994, 1996), Fujiwara et al. (1998), and Isherwood (1972).

Isherwood (1972) has analyzed experimental data from tests with a range of merchant ships at different laboratories. Using multiple regression techniques, empirical formulae for the wind force coefficients in surge, sway and yaw have been derived. These are among others applied by Aligne et al. (1997), Calvert (1990), and Pipchenko (2011). Also Blendermann (1994, 1996) provides empirical formulae to estimate the coefficients in surge, sway, yaw and roll for different types of ships, which are among others used by Bentin et al. (2016) and Zacccone et al. (2018). In order to increase accuracy compared to previous methods, Fujiwara et al. (1998) propose a new method to estimate wind forces and moments. A linear regression model is used to fit experimental results of various ships. It is applied by Ishii et al. (2010) and Kobayashi et al. (2015).

Although approaches, such as the empirical formulae mentioned, do not only refer to one DOF, i.e. surge, the consideration of wind effects in ship weather routing is often limited to the added resistance. Particular importance is attached to the influence of wind and ship aerodynamics generally in those cases, where sailing ships or ships with wind assistance are taken into account, such as by Bentin et al. (2016), Howett et al. (2016), Smith et al. (2013), Traut et al. (2014), and Walther et al. (2015).

5.5 Influence of Waves and Ship Seakeeping

Ocean waves may be considered as the dominant environmental disturbance leading to undesirable motions of the ship in a seaway (Perez 2005, p. 17). The effect of seaways on the behavior of ships and their responses in waves is referred to as seakeeping. The specific ship responses not only depend on the sea conditions fundamentally addressed in Sec. 3.3, but also on the type of ship, its loading condition, the speed and heading. As to Bertram (2012, pp. 143–144), seakeeping investigations of ships may refer to aspects, such as added resistance in waves, ship safety and comfort, as well as wave induced loads on the ship’s hull structure. The added resistance in waves leads to an involuntary speed reduction, which directly affects the fuel consumption and compliance with given arrival times. In contrast, ship safety and comfort may be enhanced by a voluntary speed reduction, e.g. to avoid excessive ship motions, or other operational limits. Aspects related to wave induced loads on the ship’s hull structure, such as critical stresses or bending moments, as well as hull vibrations may also be considered in ship weather routing and in the developed system, but are not addressed in this thesis. Following a brief introduction to the numerical prediction of the ship’s behavior in waves and computational methods, it is focused on ship safety and comfort as well as their consideration in weather routing approaches.

5.5.1 Prediction of Ship Motions in Waves

Linear Wave Theory Seakeeping investigations of ships usually assume linear wave theory (see Sec. 3.3). For each harmonic wave, individual ship responses are computed where one wave is not influenced by another wave, i.e. all responses are proportional to

the wave height. By applying the superposition principle, the total ship response may be obtained from all individual responses to waves of different wave lengths, phases, amplitudes and propagation directions. This implies that studying a ship in incident regular sinusoidal waves of small steepness is sufficient (Faltinsen 2005, p. 229). Assuming a steady-state condition, i.e. a harmonic oscillation of motion and loads on the ship with the same frequency as the waves, the problem may be subdivided. The first problem concerns a body forced to oscillate in calm water resulting in added mass, damping and restoring forces and moments. The second problem relates to a restrained body in incident regular waves that induce so-called wave excitation forces. Due to linearity, the derived forces may be added to the total hydrodynamic forces.

Considering linear wave theory and gravity waves (see Sec. 3.3), which are particularly important for seakeeping and dominated by gravity effects, other effects are generally neglected and an ideal fluid (incompressible, inviscid) without surface tension is assumed. This leads to the potential theory (constant, irrotational and incompressible flow) being applicable to describe waves. Potential flow solvers can be applied to compute ship responses. Using the wave elevation in Eqn. 3.1, the potential of a deep water wave Φ_W (at $\mu_e=0$) in a coordinate system moving with ship speed may be given as (Perez 2005, p. 22):

$$\Phi_W(t, x, y, z) = c \cdot \zeta_A \cdot e^{-kz} \cos(\omega t - kx + \epsilon) \quad (5.12)$$

As a gradient of the potential function, the fluid velocity vector can be obtained. The pressure can be derived based on the deep water wave potential, the velocities and the linearized Bernoulli-equation. Integrating the pressure distribution along the hull yields the hydrodynamic forces (Fossen 2011, p. 84). Although this approach is often sufficient, it is, for example, not valid for roll motions due to the dominance of nonlinear viscous damping. The development of numerical and experimental methods for the determination of roll damping has been among others addressed by Abdel-Maksoud et al. (2013). Similarly, the added resistance shows significant dependence on wave height. Since this can be attributed to nonlinear effects, the superposition principles possibly cannot be applied (Bertram and Couser 2014, p. 15). For strongly nonlinear problems, such as roll motions, capsizing, breaking waves, slamming or green water on deck, either model tests are performed or computationally expensive Reynolds-Averaged Navier-Stokes (RANS) solvers are required.

Prediction Methods In general, ship seakeeping may be predicted by expensive and time consuming model tests or increasingly performed but challenging full-scale measurements. Furthermore, predictions may be based on computations in the most popular frequency domain, the computationally expensive time domain or the statistical domain aiming at long-term assessments for a given ocean region or seaway, as stated by Bertram (2012, p. 144) and Bertram and Couser (2014, p. 8). Both publications provide an overview of computational methods for seakeeping with particular importance attached to added resistance in waves. The overview includes simple design estimates,

linear and nonlinear strip methods, strip methods especially for high-speed or multihull ships, the 3D Green Function Method (GFM) and Rankine Singularity Method (RSM) as well as RANS solver. Due to lower computational efforts, potential methods, such as GFM and RSM, are favored over methods based on RANS. Although there are a number of commercial codes using 3D GFM and RSM and despite several shortcomings, (linear) strip methods as fast, cheap and often sufficiently accurate methods represent the most popular and standard approach for seakeeping investigations and are explained below.

Based on studying the different approaches, Bertram and Couser (2014, p. 12) conclude that a simple formula does not exist that yields the added resistance in waves with sufficient accuracy for all types of ships. This should be kept in mind in terms of their application in ship weather routing. Considering potential flow methods and RANS simulations, Bertram and Couser (2014, p. 8) further draw the following conclusion:

While heave and pitch for conventional ships are predicted well by virtually all approaches, motions in oblique waves and second-order forces such as added resistance are much more difficult to predict.

In summary, it is generally difficult to predict added resistance but methods with comparably low computational effort are principally preferred in the context of ship weather routing. As a consequence, semi-empirical and strip methods are popular to consider the impact of waves and are briefly addressed in the following. The concept of speed reduction curves to take into account the influence of waves is subject to Sec. 5.2.3.

Semi-empirical Methods As indicated above, a simple formula for sufficiently accurate added resistance prediction of all ships is said to be not available (Bertram and Couser 2014, p. 12). Often, simple formulae only have a limited range of application. Furthermore, their application in ship weather routing may occasionally show good agreement but lacks reliability due to the large scatter of results shown in investigations. Nevertheless, some semi-empirical methods are applied in ship weather routing.

Two methods to estimate the added resistance due to waves often mentioned in this context, e.g. by Bertram and Couser (2014) and Journée and Meijers (1980), are proposed by Boese (1970) and Gerritsma and Beukelman (1972). Boese (1970) integrates the pressure due to the relative motions in regular waves over the wetted surface of the hull. It is among others used by Pipchenko (2011). The approach by Gerritsma and Beukelman (1972) is based on the radiated energy caused by the ship's motion. It is applied among others by Alexandersson (2009) including a simplification and by Cui, Turan, et al. (2016). It also appears in a summary by Lu et al. (2015) in addition to other semi-empirical approaches for added resistance prediction proposed by Fujii and Takahashi (1975), Kuroda et al. (2008), and Salvesen (1978). Salvesen (1978, pp. 31–32) states that the approach based on expressing “the added resistance in oblique waves as the sum of products of first-order terms” achieves better agreement with experiments

than applying the theory of Gerritsma and Beukelman (1972). Fujii and Takahashi (1975) consider the ship's motion as well as the wave reflection at the blunt bow. An improved expression is presented by Kuroda et al. (2008) and a simplified version by Sasaki et al. (2008), which is applied by Ishii et al. (2010) and Kobayashi et al. (2015). Nevertheless, Lu et al. (2015) decide to modify the speed loss method proposed by Kwon (1981) (see Sec. 5.2.3) to allow a ship type specific added resistance estimation with increased accuracy. Last but not least, Bentin et al. (2016) calculate the added resistance in a sea wave spectrum using the tool SBRIN by the Hamburg Ship Model Basin. It has been originally developed by Blume (1977), who has systematically performed parametric model tests with different hull shapes. Further simple approaches are mentioned by Bertram and Couser (2014). Details on the specific methods can be found in the corresponding references.

Strip Theory and PDSTRIP Strip methods are potential flow methods based on linear wave theory. Assuming an advancing slender body in waves, the flow variation in the body's transverse direction is much larger than in the longitudinal one. Hence, the complex 3D flow problem can be simplified to a 2D one by dividing the hull into transverse strips, as shown in Fig. 5.8. Flow computations are performed for each individual strip and integrated over the body's length to derive the solution for the 3D problem. In principal, strip methods are valid for long and slender bodies with length to breadth ratios greater than three (Journée 1992, p. 10), for almost all types of large displacement ships with Froude numbers up to 0.4 (Bertram and Couser 2014, p. 9) as well as for long waves with lengths greater than approximately 40% of the ship's length (Söding and Bertram 2009, p. 40).

Besides some commercial strip methods, a popular public-domain hydrodynamic strip code for seakeeping often used in academia is PDSTRIP. Also the added power prediction method by Abdel-Maksoud et al. (2016) described in Sec. 5.6.3 provides an interface to consider results from PDSTRIP. It may be used to compute ship motions for monohulls including sailing boats in the frequency domain. Furthermore, it is capable to consider unsymmetrical bodies including heeled ships, shallow water, stabilizer fins and suspended loads. Information is published in particular in the documentation by Söding and Bertram (2009), but also by Bertram et al. (2006).

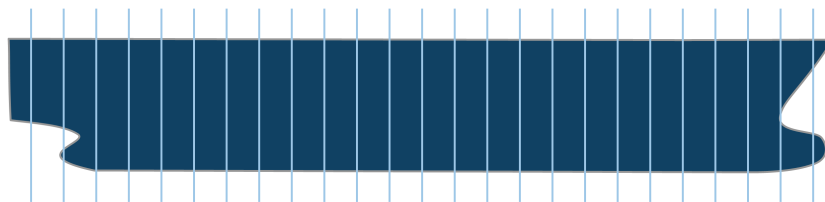


Figure 5.8: Schematic of a Ship's Hull Subdivision in Strip Theory

PDSTRIP applies the so called patch method to solve the potential flow problem. Here, potential point sources are placed on each segment of a strip to represent the hull geometry. Their superposition is used to approximate the potential. Integrating the pressure distribution derived from the potential along the hull yields the three-dimensional forces and moments acting on the hull due to the ship's motion, i.e. added mass, (non-viscous) damping and restoring forces. In addition, the wave excitation forces can be calculated by use of a wave potential (see Eqn. 5.12) and the resulting pressure, again integrated along the hull. It can be distinguished between a so-called Froude-Kriloff force and a diffraction force. The former is the force due to the unsteady pressure of the undisturbed wave, while the latter results from pressure changes caused by the ship section (Söding and Bertram 2009, p. 7). Based on these forces, PDSTRIP can calculate so-called RAOs, which are transfer functions that linearly relate the excitation due to regular waves to the ship's response. Generally, there are Force RAOs as well as Motion RAOs either mapping the wave elevation to force or motion (Perez 2005, p. 59). Assuming the wave elevation in Eqn. 3.1 at the origin ($x = 0$), the following relation as to Faltinsen (2005, p. 231) can be given:

$$x_i = RAO_i \cdot \zeta_A \sin(\omega_e t + \epsilon) , \quad i = 1, \dots, 6 \quad (5.13)$$

where x_i denotes the response for the i -th degree of freedom, either one of the translational (surge, sway, heave) or rotational (roll, pitch, yaw) ones (see Fig. 5.2 and Tab. 5.1) when the ship encounters a wave with amplitude ζ_A and encounter angle μ_e (see Fig. 5.4). Since a ship with a forward speed e.g. moving in head seas experiences waves with an increased frequency, the so-called encounter frequency ω_e (in deep water), is introduced:

$$\omega_e = \omega - kV_s \cos \mu_e = \omega - \frac{\omega^2}{g} V_s \cos \mu_e \quad (5.14)$$

More precisely, the transfer function or RAO for a specific motion mode i is the ratio $|x_i|/\zeta_A$, where $|x_i|$ is the amplitude of the steady-state motion and ζ_A the wave amplitude. The RAO is a function of encounter frequency ω_e and angle μ_e . Furthermore, it depends on the ship form and mass distribution. The RAOs are calculated by solving the classical linear equations of motion in the frequency domain for each degree of freedom of interest. By superimposing and combining the RAOs with the wave spectrum, i.e. the prevailing irregular seaway, time-averaged drift forces on the ship can be obtained. The negative longitudinal part of these drift forces is the mean added resistance in waves, which is proportional to the square of the wave amplitude (Söding and Bertram 2009, p. 30). PDSTRIP overestimates the added resistance, especially in the peak values. To improve added resistance calculations, the corresponding formulations in this method have been enhanced by Valanto (2016) as part of a research project. Moreover, since the strip theory is based on linearity, ship motion amplitudes are supposed to be small compared to cross sectional dimensions. When exceeded, drift force calculations also become incorrect due to the use of the ship's vertical motions.

A strip method to compute the added resistance is applied among others by Aligne et al. (1997), Hinnenthal (2008), and Zacccone et al. (2018). To calculate the total resistance due to irregular waves and wind for each sea-state Vettor and Guedes Soares (2016) apply a time-domain method presented by Prpić-Oršić and Faltinsen (2012), where the relative ship motion is computed by a strip theory method and the added resistance by a pressure integration method. While Zacccone et al. (2018) use PDSTRIP, Hinnenthal (2008) applies a strip-theory code called SEAWAY to calculate the added resistance. It includes the methods by Boese (1970) and Gerritsma and Beukelman (1972), of which the first is chosen due to a better quality of numerical results. Also Böttner (2007) derives the added resistance in waves by using SEAWAY.

5.5.2 Aspects of Ship Safety and Comfort

Adverse weather and sea conditions can endanger the safety of ship, cargo, crew or passengers or limit the comfort. As outlined in Sec. 2.2, the IMO has published a guidance to the master in MSC.1/Circ. 1228 applicable for all types of merchant ships to avoid dangerous situations in adverse weather and sea conditions (IMO 2007). These conditions refer to some combinations of wave height and wave length under specific operational conditions that may lead to heavy rolling or even capsizing of the ship. The considered phenomena, the occurrence criteria and the proposed actions are summarized in Tab. 5.2. Hazards related to slamming, shallow water effects, or collision and stranding risks are excluded. It is to be noted that an encounter angle in line with the IMO definition $\mu_{e,IMO} = \mu_e - 180^\circ$ with $0^\circ < \mu_{e,IMO}, \mu_e < 360^\circ$ is introduced, since $\mu_{e,IMO} = 0^\circ$ corresponds to head seas. This is opposite to the definition of μ_e in Fig. 5.4 commonly used for seakeeping investigations (see Sec. 5.5).

Table 5.2: Guidance according to MSC.1/Circ. 1228, (IMO 2007)

Condition	Critical when	Action
Surf-riding and broaching to	$135^\circ < \mu_{e,IMO} < 225^\circ$ $\wedge V_s > \frac{1.8\sqrt{L_{PP}}}{\cos(180 - \mu_{e,IMO})}$	Speed and/or course outside dangerous region
Successive high-wave-attack	$(\lambda_W > 0.8 \cdot L_{PP})$ $\wedge H_S > 0.04 \cdot L_{PP})$ $\vee 1.8 \cdot T_P < T_E < 3.0 \cdot T_P$	Speed and/or course outside dangerous region
Synchronous rolling and parametric rolling motions	$T_E \approx T_R$ $\vee T_E \approx 0.5 \cdot T_R$	In following, quartering, head, bow or beam seas adjust course and speed adequately

First, surf-riding relates to the ship traveling on a steep wave crest in following waves and being accelerated to ride on a wave. In case of insufficient stability, the ship may experience large roll angles or even capsize (IMO 2011, p. 8). In the same situation,

broaching-to refers to the danger of capsizing due to a change of heading. As to the guidance, both may occur when the ship speed V_s exceeds a certain critical speed and the encounter angle $\mu_{e,IMO}$ is in a critical range.

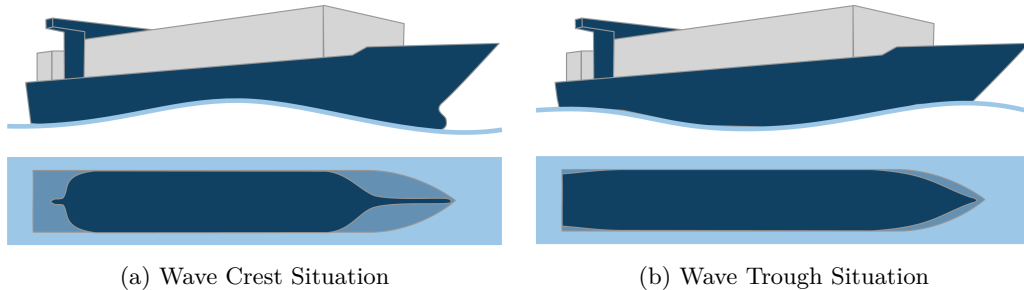


Figure 5.9: Schematic of a Ship's Changing Water Plane Area in Waves

The second criterion aims to avoid the successive encounter of higher waves, since this can result in pure loss of stability, synchronous or parametric rolling or in a combination. Pure loss of stability may particularly occur in head or following seas. In a wave crest situation indicated in Fig. 5.9a, a significantly reduced ship's water plane area can lead to vanishing stability and thus to capsizing. Fig. 5.9a and Fig. 5.9b in comparison indicate the variation in buoyant distribution and thus stability, which can cause large roll angles (IMO 2011, p. 5). A situation may be critical when the waves exceed a critical length λ_W and height H_S in relation to the ship length L_{PP} . This corresponds to the encounter period T_E being a certain multiple of the wave period T_P .

Third, synchronous and parametric rolling motions concern large roll motions induced by direct excitation or the varying stability in the wave crest and trough situation described above. Accordingly, situations shall be avoided where the encounter period T_E coincides with the ship's natural roll period T_R , which can be approximated by:

$$T_R = \frac{2\pi \cdot i}{\sqrt{g \cdot GM}} \quad \text{with} \quad i = \sqrt{\frac{I_{xx}}{\Delta}} \approx 0.4B \quad (5.15)$$

where GM denotes the metacentric height of the ship, g the Earth's gravitational acceleration and i the gyration radius, which can be approximated using the mass moment of inertia I_{xx} , the ship's displacement Δ and breadth B (IMO 2011, p. 22). Usually, 0.4 times the ship's breadth is assumed to approximate the radius of gyration. However, this can increase up to $0.45B$ for large ships with high superstructures or deck cargo.

In order to avoid the described hazards and the corresponding potentially dangerous zones, the IMO proposes mainly speed and/or course alterations. However, the vulnerability and the probability that a ship encounters these dangerous phenomena in a certain sea state not only depend on ship size and speed, but also on hull geometry and actual stability parameters. This implies that the guidance may be too generous for

ships with insufficient stability but too restrictive for certain other ships (IMO 2007). This is endorsed by the IMO (2011) based on the study of eight capsizing accidents in following seas, where additional information provided by applying the IMO guidelines could not have aided their prevention. Despite these deficiencies regarding the guideline's applicability to ensure ship safety, this rather simple approach is widely implemented in academic as well as commercial weather routing systems. To roughly assess whether a ship may encounter these dangerous situations during a voyage, the developed weather routing system also offers the option to apply the guidance (see Sec. 6.2).

In addition, further aspects related to ship safety and comfort may be considered by adequate restrictions and improved methods. This includes criteria, such as those by Nordforsk (1987) concerning roll motion, vertical and lateral accelerations, as well as the probability of slamming and deck wetness limiting human effectiveness and the general operability of ships. Furthermore, to improve the applicability of the IMO guidelines regarding roll motions at least slightly, an effective metacentric height may be used to calculate the roll period (see Eqn. 5.15). Linearizing the vessel's stability is only valid for small inclinations and can lead to significant deviations when large motion amplitudes occur. In case of the effective metacentric height, the discretized righting levers need to be numerically integrated to obtain the area of the lever arm curve which is equivalent to the energy stored by one roll motion (IMO 2011, pp. 22–23). Moreover, ship specific polar plots derived from nonlinear simulations may be used to assess the ship's safety in adverse sea conditions depending on course, speed and trim (Krüger et al. 2003). Also results e.g. from numerical and experimental methods for the determination of roll damping by Abdel-Maksoud et al. (2013) may improve ship safety assessment.

Despite many options to account for ship safety and comfort in simplified or sophisticated ways, the study of safety constraints in weather routing is not in the particular focus of this research but of others, as outlined in the next section.

5.5.3 Ship Safety in Weather Routing

Ship motions due to waves affecting the ship's safety, comfort and/or resistance are considered in lesser or greater detail in many academic developments concerning ship weather routing. The basis for the summary of approaches related to ship safety and comfort is the overview of mathematical modeling and optimization approaches applied in ship weather routing in Chpt. 4. As to the consideration in commercial weather routing systems, it is referred to Sec. 2.5.

Often, ship motions influencing the ship's safety or comfort are taken into account by constraints. Applied criteria refer to vertical and lateral accelerations at specific points, such as the bow, in holds or accommodation areas, to bending moments, slamming, deck wetness, propeller racing and emergence as well as to roll motions, specifically parametric rolling, and to motion sickness. Limits are given in terms of absolute values or nondimensional indices or regarding the probability of occurrence. Threshold values for different

phenomena are among others introduced by Avgouleas (2008), Böttner (2007), Calvert (1990), Chen (1978), Hagiwara (1989), Hinnenthal (2008), Petrie et al. (1984), Shao and Zhou (2012), Tsujimoto and Tanizawa (2006), Vettor and Guedes Soares (2016), and Zaccone et al. (2018). Frequently, the corresponding ship motions are computed using RAOs, such as by Böttner (2007), Chen (1978), Hinnenthal (2008), Petrie et al. (1984), Sen and Padhy (2015), Vettor and Guedes Soares (2016), and Zaccone et al. (2018). Also Cui, Howett, et al. (2016) and Eskild (2014) use RAOs to apply the criteria by Nordforsk (1987) (see Sec. 5.5.2). To derive RAOs, methods presented in Sec. 5.5.1 can be utilized, such as the strip codes PDSTRIP used by Zaccone et al. (2018) and SEAWAY deployed by Hinnenthal (2008). However, RAOs may not only vary for different computational methods but also significantly influence the optimization results (Zaccone and Figari 2017).

Apart from ship motion constraints, limits can also concern the weather conditions themselves. Larsson and Simonsen (2014) (see Sec. 4.2.1) only take into account a maximum wave height, while Bentin et al. (2016) assume threshold values for wind and waves. Furthermore, Chu et al. (2014) incorporate control bounds regarding maximum allowable wave heights in head, beam, and following seas (see Fig. 5.4), maximum allowable true and relative wind speeds as well as tropical cyclone avoidance limits.

Instead of considering safety aspects by constraints leading to certain headings or speeds being excluded, they may also be part of the objective function or an objective itself. Weber (1995, p. 88) considers constraints, that include maximum wave height and wind speed, by penalties in the objective function and by inadmissibility of vectors violating constraints (see Sec. 4.3). Pipchenko (2011) compares different criteria limiting the operability of ships, among others those by Nordforsk (1987). From the comparison and a survey of navigators it is concluded that simple threshold values are ineffective for safety assessment. Hence, Pipchenko (2011, p. 386) integrates a fuzzy logic system correlating ship motion parameters, particularly roll amplitude, and a risk level, which is included in the objective function. Also the objective function of Kosmas and Vlachos (2012) includes a scalar that characterizes the safety during the voyage and is calculated based on vectors containing the wind and wave conditions on the route and corresponding ship responses. Maki et al. (2011) treat a minimum risk of parametric rolling as objective in addition to minimum fuel consumption. However, a maximum roll angle and the duration of excitation are neglected. In the multi-objective optimization problem solved by Hameed (2015), safety, thus minimizing the encountered wave height, is one objective. Depending on the choice of optimization criteria, Vettor and Guedes Soares (2016) account for ship safety in their evolutionary algorithm either as objective, thus a single risk coefficient influenced by all responses, or by constraints (see above).

Either as constraints or within the objective function, many developments integrate the guidance to the master given in MSC.1/Circ. 1228 to avoid dangerous situations in adverse weather and sea conditions (IMO 2007), which is indicated in Sec. 5.5.2. While

Shao and Zhou (2011) and Shao et al. (2012) apply all criteria, Mannarini et al. (2013) focus on preventing surf-riding and parametric rolling. Krata and Szlapczynska (2012) go one step further and compute a nondimensional safety index considering the accumulated area of all dangerous zones arising from the guidance. To improve the method, Krata and Szlapczynska (2018) incorporate a so called equivalent metacentric height, which corresponds to the effective metacentric height. Hence, the approach allows to include MSC.1/Circ. 1228 either as objective in terms of the safety index or in the constraint set. In the time-dependent bi-objective shortest path algorithm presented by Veneti et al. (2017), certain arcs are deleted when critical as to the guidance. In addition, the risk of a possible ship accident (collision or grounding) is predicted using a Bayesian model. It is proposed by Koromila et al. (2014) and based on ship parameters and data from the Automatic Identification System (AIS).

Last but not least, dangerous zones can be found in the approaches by Bijlsma (1975) and Zoppoli (1972). While Zoppoli (1972) introduces sea zones forbidden during certain time intervals to avoid dangerous situations in rough seas, Bijlsma (1975) uses a polar velocity diagram. This provides the speed reduction in waves and indicates forbidden courses, i.e. those causing heavy roll motions of the ship.

5.6 Principles of Ship Propulsion

The performance of a ship during a voyage not only significantly depends on the service conditions including the influence of ocean currents, wind and seaway but also on the ship itself and among others its geometry, loading condition and propulsion system. Accounting for the total resistance or speed reduction in service conditions, the required engine power to achieve a given ship's speed or an attainable speed assuming a given power can be determined and the fuel consumption calculated. In this regard, propeller and engine characteristics play an important role to provide sound routing support. A more sophisticated method to predict the added power is proposed by Abdel-Maksoud et al. (2016). However, due to computational efforts and data requirements, relations such as speed dependent efficiencies or power dependent specific fuel consumptions are often simplified, i.e. neglected or assumed to be constant. Hence, approaches with different levels of detail are applied in ship weather routing.

5.6.1 Propeller Characteristics

In line with the most popular approach in ship weather routing shown in Fig. 5.5 based on solving the equation of motion in longitudinal direction (Eqn. 5.1), the ship's total resistance needs to be balanced with the thrust delivered by the propeller. In addition, the "torque required by the propeller must be in equilibrium with the torque delivered by the engine" (Journée and Meijers 1980, p. 5). Hence, propeller characteristics need to be taken into account when determining the propeller's operational point including torque and rate of revolutions, and when predicting the required engine power. It is

to be noted that it is focused on the characteristics of conventional propellers, more precisely fixed pitch propellers.

Since the propeller load, i.e. the required thrust, changes with varying added resistance throughout a ship's voyage, which affects the required power, the complete propeller characteristics need to be available (Abdel-Maksoud et al. 2016, p. 36). These are generally given in an open-water diagram. Usually, this is obtained from model tests and adequate correction for full-scale application or alternatively from numerical calculations. In ship weather routing, also empirical data is used (see Sec. 5.6.4). An example of such a diagram for a Post-Panmax container ship is shown in Fig. 5.10.

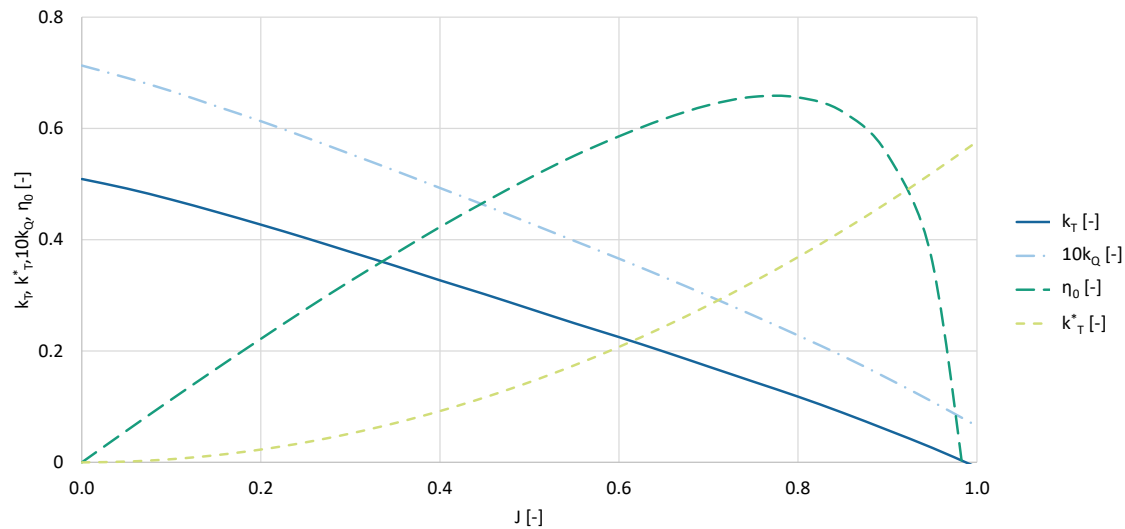


Figure 5.10: Open-Water Diagram for a Post-Panmax Container Ship (DTC), adapted from Riesner et al. (2016, p. 16) and Moctar et al. (2012, p. 53)

The propeller thrust T and torque Q_0 are usually expressed by the nondimensional thrust and torque coefficients k_T and k_Q as a function of the rate of revolutions n and using the propeller diameter D_p and the water density ρ :

$$k_T = \frac{T}{\rho \cdot n^2 \cdot D_p^4} \quad (5.16)$$

$$k_Q = \frac{Q_0}{\rho \cdot n^2 \cdot D_p^5} \quad (5.17)$$

Another important parameter is the so-called advance coefficient J . At the same advance coefficient the nondimensional thrust and torque values of a propeller are the same, which is why the propeller curves are presented as a function of it. Thus, in principle, the characteristic values for a model propeller can be transferred directly to full scale (Krüger 2005, p. 17). The advance coefficient is defined as:

$$J = \frac{u_a}{n \cdot D_p} \quad (5.18)$$

where $u_a = u(1 - w)$ denotes the propeller inflow, i.e. the speed of advance of the propeller. Due to effects, such as flow separation, it is generally observed to be lower than the ship's longitudinal speed u , which is expressed by the wake fraction w that largely depends on the hull shape. The increased resistance due to the propeller is taken into account by the so-called thrust deduction fraction t . Some empirical formulae to estimate both are summarized by Schneekluth and Bertram (1998, pp. 181–183). The given wake fraction w and thrust deduction fraction t , the relation of thrust T and total resistance R_T in Eqn. 5.1 as well as Eqn. 5.16 and 5.18 provide the basis to eliminate the unknown torque and rate of revolutions and derive the following curve:

$$k_T^*(J) = \frac{R_T}{u^2} \cdot \frac{1}{(1-t)(1-w)^2 \rho \cdot D_p^2} \cdot J^2 \quad (5.19)$$

Hence, the advance ratio J can be found as the intersection of this curve with a known open-water propeller curve k_T often using an iterative procedure. The curve for calm water conditions based on ship data given by Abdel-Maksoud et al. (2016) is depicted in Fig. 5.10. Varying weather conditions cause the curve, and thus the intersection to change, which requires a recalculation of the operating point. The propeller rate of revolutions n can be derived using Eqn. 5.18 and the open-water propeller torque Q_0 from Eqn. 5.17. With a known relative rotative efficiency η_R or propeller torque Q the delivered power at the propeller P_D can be obtained (Abdel-Maksoud et al. 2016, p. 35):

$$P_D = 2\pi \cdot Q \cdot n = 2\pi \cdot \frac{Q_0}{\eta_R} \cdot n \quad (5.20)$$

According to Schneekluth and Bertram (1998, p. 184), “the relative rotative efficiency η_R accounts for the differences between the open-water test and the inhomogeneous three-dimensional propeller inflow encountered in a propulsion test. In reality, the propeller efficiency behind the ship cannot be measured and all effects not included in the hull efficiency, i.e. wake and thrust deduction fraction, are included in η_R .” Empirical formulae for its estimation are given by Schneekluth and Bertram (1998, p. 184).

Alternatively, the delivered power at the propeller P_D can be obtained using the propeller curve of the open-water efficiency η_0 . It is given in the open-water diagram in Fig. 5.10 and is defined as:

$$\eta_0 = \frac{T \cdot u_a}{2\pi \cdot n \cdot Q_0} = \frac{k_T \cdot J}{k_Q \cdot 2\pi} \quad (5.21)$$

With the relative rotative efficiency η_R and the hull efficiency η_H , which considers the thrust deduction fraction t and the wake fraction w , the propulsive efficiency η_D can be calculated:

$$\eta_D = \eta_H \cdot \eta_0 \cdot \eta_R = \frac{1-t}{1-w} \cdot \eta_0 \cdot \eta_R \quad (5.22)$$

Consequently, the delivered power at the propeller P_D can be obtained from the propulsive efficiency η_D and the effective power P_E , which is the power required to tow the ship without a propulsive system, i.e. the product of the total resistance R_T and the speed u :

$$P_D = \frac{P_E}{\eta_D} = \frac{R_T \cdot u}{\eta_D} \quad (5.23)$$

To account for the ship's propulsion in ship weather routing (see Sec. 5.6.4), the ITTC Performance Prediction Method (ITTC 1978) presents a popular approach. It is “an analytical method to predict delivered power and rate of revolutions for single and twin screw ships from model test results” (ITTC 1978, p. 3). Therefore, it requires data from a resistance and self-propulsion test as well as the model propeller characteristics.

5.6.2 Engine Load and Fuel Consumption

The fuel consumption is significantly influenced by the ship speed, since the required propulsive power is proportional to approximately the third or fourth power of the speed depending on the ship (ABS 2013, p. 54). Hence, slowing down by 10% can reduce the fuel consumption by about 20% with only a slightly longer voyage time. As a consequence of this slow steaming, particularly mechanically controlled engines are not operated in an optimal operating point but at rather low loads. This “can cause accelerated wear of the engine and auxiliary components if not properly planned and executed” (ABS 2013, p. 56). For electronically controlled engines the operational range is higher. Moreover, Chen (2011, p. 4) notes that engine overload in service conditions may also be caused by propulsion systems being optimized for calm weather conditions. Thus, consideration of the engine characteristics in weather routing is recommended.

When deriving the fuel consumption from the previously calculated delivered power at the propeller, an important aspect refers to the efficiency losses between the engine and propeller. The delivered power P_D is generally less than the brake power P_B directly at the ship's engine. The efficiency losses due to shaft and bearings typically amount to 1.5% to 2.0% (Bertram 2012, p. 76), thus the transition or shaft efficiency η_S is typically 0.98 to 0.985 (Schneekluth and Bertram 1998, p. 181). Sometimes also a gear efficiency η_G (IMO 2016a, Annex, p. 25) or other ship specific efficiencies are considered. Using a simplified definition of the shaft efficiency η_S , the brake power P_B can be expressed as:

$$P_B = \frac{P_D}{\eta_S} \quad (5.24)$$

The brake power P_B required to achieve a given speed has to match the engine characteristics and be within its limits. The power and speed limits of an engine for continuous and overload operation are generally given in an engine load diagram. Since a ship of equivalent size to the previously mentioned Post-Panmax container ship is equipped with the electronically controlled MAN B&W 9S90ME-C10.2 type engine with nine cylinders, the corresponding engine load diagram is shown in Fig. 5.11 (MAN Diesel & Turbo 2014; Zaitoun et al. 2014).

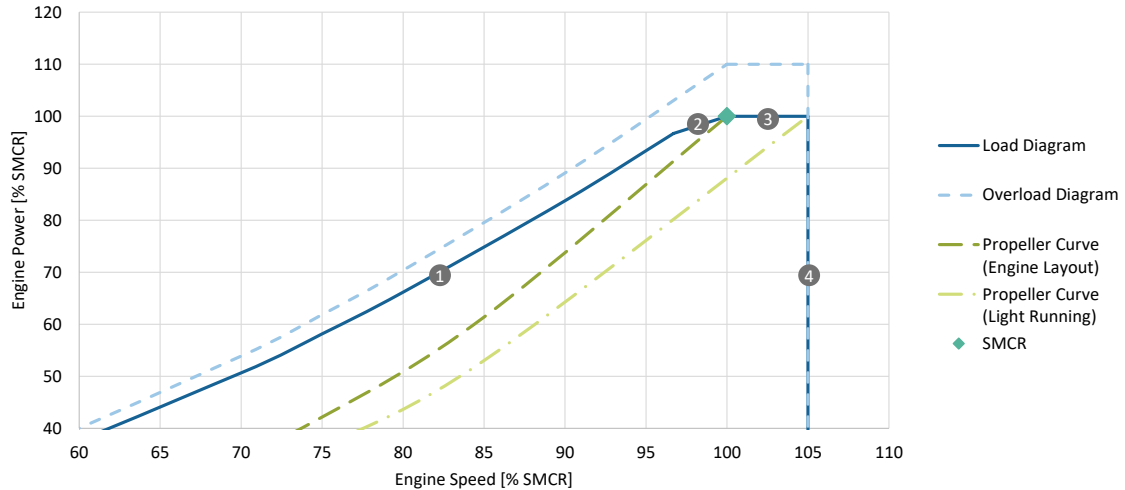


Figure 5.11: Engine Load Diagram of MAN B&W 9S90ME-C10.2 (MAN Diesel & Turbo 2014; MAN Energy Solutions 2018)

When the required engine power for a ship is determined, extra power margins are usually added. The sea margin of typically 15% accounts for added resistance due to weather effects, while the engine margin of 10% to 15% presents an operational margin for the engine (MAN Diesel & Turbo 2011, pp. 28–29). The point corresponding to the optimum for the ship, the operating profile and the requirements of yard or owner for continuous operation of the engine is the specified maximum continuous rating (SMCR). At SMCR the power output amounts to 37 620 kW at a speed of 72.0 rpm (MAN Diesel & Turbo 2014; Zaitoun et al. 2014).

The according propeller curve through SMCR, i.e. the engine layout curve, is shown in Fig. 5.11. It accounts for heavier running of the propeller due to fouling or heavy weather. In contrast, the light running propeller curve considers a clean hull and calm weather, which may be used for the propeller layout. Due to effects such as fouling of hull and propeller, which can increase resistance by 25% to 50% throughout a ship's lifetime, the curve shifts to the left as the time in operation progresses (MAN Diesel & Turbo 2011, pp. 12, 22–23, 31). This causes different limits to be critical for continuous operation or for temporary overload running. Particularly in adverse weather conditions, considering the reduced available power is essential (IMO 2016a, Annex, p. 26).

The range for continuous operation, as indicated by the load diagram in Fig. 5.11, is typically limited by the maximum combination of torque and speed to ensure ample air supply for combustion (Line 1) as well as by maximum mean effective pressure (Line 2), maximum power (Line 3) and maximum speed (Line 4, 105 % of SMCR) (MAN Diesel & Turbo 2011, pp. 29–30). While the propeller curve for a fixed pitch propeller is based on a power demand proportional to the third power of the engine speed, i.e. rate of revolutions n , the power is proportional to n^2 for Line 1 and to n for Line 2. Further details are given by MAN Diesel & Turbo (2011, 2014). Similarly, the overload diagram can be derived, where the maximum overload limit corresponds to 110 % of SMCR. It “may be permitted for a limited period of one hour every 12 hours” (MAN Diesel & Turbo 2014, Sec. 1.04). Furthermore, at certain shaft speeds excessive torsional vibrations can occur resulting in many shaft lines having a barred speed range (MAN Diesel & Turbo 2015, p. 4). Thus, additional restrictions especially concerning the time taken for passing the speed range may be considered, which are omitted here.

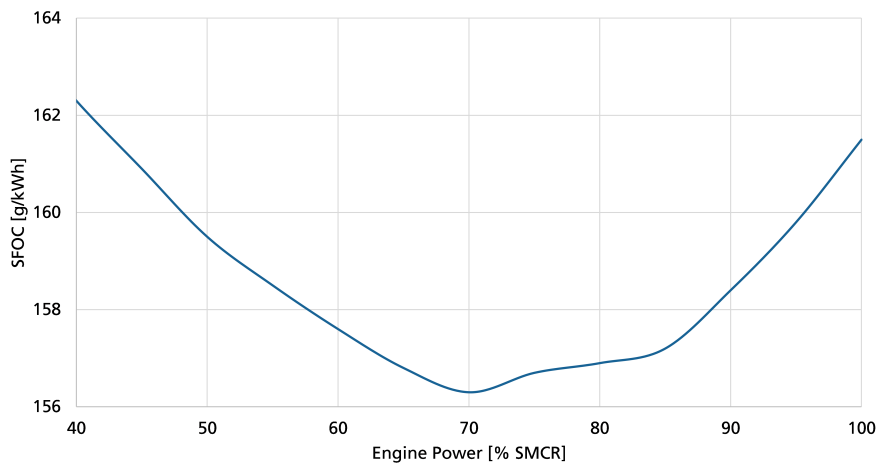


Figure 5.12: Specific Fuel Oil Consumption of MAN B&W 9S90ME-C10.2 (MAN Energy Solutions 2018)

In addition, the specific fuel oil consumption as a function of power needs to be taken into account, as this may increase at low loads. According to ABS (2013, p. 56), the increase can amount to 10 % more fuel for each kilowatt. The curve of the specific fuel oil consumption of the MAN B&W 9S90ME-C10.2 is shown in Fig. 5.12 (MAN Energy Solutions 2018). Hence, the derived brake power P_B , the corresponding specific fuel oil consumption SFOC and the voyage time t_{ij} between the two waypoints or nodes i and j provide the basis to calculate the absolute fuel consumption m_{Fuel} as well as the fuel costs C_{ij} using the current price per ton of fuel P_{Fuel} :

$$m_{Fuel,ij} = P_B \cdot SFOC \cdot t_{ij} \quad (5.25)$$

$$C_{ij} = m_{Fuel,ij} \cdot P_{Fuel} \quad (5.26)$$

The consumption of any auxiliary engines as well as of lubricating oil has to be obtained separately if required but is neglected within this research. Even the engine characteristics are only rarely considered explicitly in ship weather routing. Hinnenthal (2008) takes into account the main engine characteristics including boundary lines for engine overload, maximum allowable mean effective pressure, nominal power and maximum rate of revolution at nominal power. Also the specific fuel oil consumption is given as function of the main engine's rate of revolution.

5.6.3 Added Power Prediction Method

The general approach shown in Fig. 5.5 is often applied in academic ship weather routing developments. However, among others Bertram and Couser (2014) and Shigunov (2017) highlight the importance of considering added power in weather routing systems. Added power approaches typically integrate at least a simple maneuvering model, thus consider more than one equation of motion and may include transverse drift and rudder forces. A fast method for added power prediction named *ProWe* has been developed by Abdel-Maksoud et al. (2016) within a research project concerning the performance of ships in a seaway. The approach is schematically visualized in Fig. 5.13. The method is developed in Python and is briefly explained in the following. For a detailed description of the method including all functions, input and output parameters, it is referred to Abdel-Maksoud et al. (2016). Further information on the integration into the weather routing system developed within this research is given in Sec. 6.4.4.

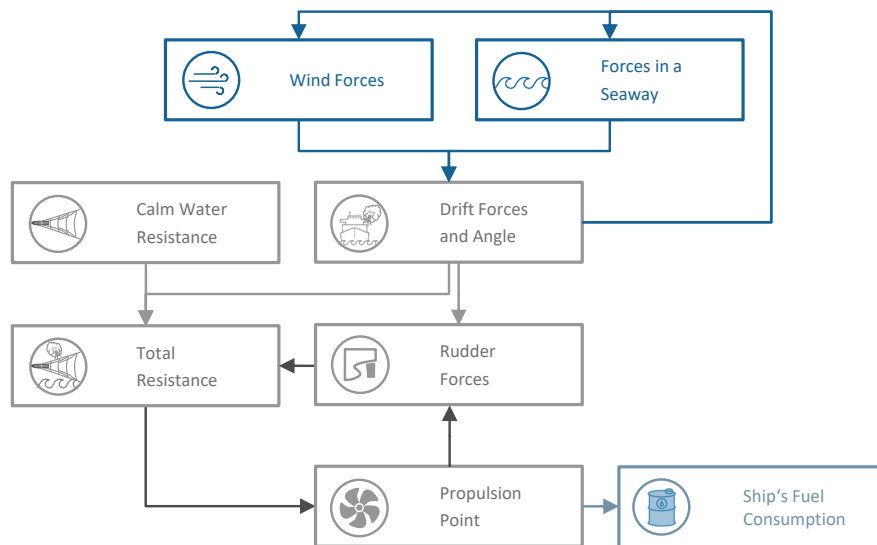


Figure 5.13: Model including Transverse Drift Forces, Rudder and Propeller, based on Abdel-Maksoud et al. (2016)

In principle, the method is based on the three equilibrium equations given by Eqn. 5.1 to 5.3 and definitions similar to those in Fig. 5.2 and 5.3. Wind forces and drift forces in a seaway are calculated in line with Sec. 5.4 and 5.5.1 respectively. To consider the drift forces, the method provides interfaces to load results from the Rankine Singularity Method GLRankine and the strip code PDSTRIP. As to the propeller characteristics, the relations according to Sec. 5.6.1 are applied. Since the varying open-water efficiency due to a shifting operating point has the greatest influence on the added power, the impact of wake and thrust coefficients is comparably small and time-averaged values are used. The ship's engine is integrated by a simplified model based on a boundary curve of the available engine power. In addition, hydrodynamic hull forces as well as rudder forces are taken into account by Abdel-Maksoud et al. (2016, pp. 31–33). The longitudinal force due to an oblique inflow of the hull is neglected, since it is expected to be small in case of small transverse velocities. Moreover, the yaw velocity is omitted. Thus, the linearized transverse hull force Y_{Hull} and yaw moment N_{Hull} can be derived in dependence of the transverse velocity v and the nondimensional manoeuvring coefficients Y_v and N_v as to Abkowitz (1964):

$$Y_{Hull} \approx Y_v \cdot v \quad (5.27)$$

$$N_{Hull} \approx N_v \cdot v \quad (5.28)$$

Concerning the rudder, formulations in line with the semi-empirical method from Brix (1993) are applied. It is assumed that the resistance (drag) and lift forces of the rudder are 60% higher compared to an airfoil where no plane, i.e. hull, perpendicular to the span is arranged at one end. Due to the assumption of small rudder angles, the rudder drag is assumed to act along the x axis and the lift along the y axis (see Fig. 5.2). These assumptions, the flow u_R , the submerged projected rudder area A_R as well as semi-empirically estimated drag and lift coefficients, C_D and C_L , provide the basis to derive the longitudinal and transverse rudder forces, X_{Rudder} and Y_{Rudder} :

$$X_{Rudder} = -0.5 \cdot \rho \cdot C_D \cdot A_R \cdot u_R^2 \quad (5.29)$$

$$Y_{Rudder} = 0.5 \cdot \rho \cdot C_L \cdot A_R \cdot u_R^2 \quad (5.30)$$

$$N_{Rudder} = -Y_{Rudder} \cdot L_{CG} \quad (5.31)$$

The yaw moment N_{Rudder} results from the side force and the lever L_{CG} , which is the longitudinal center of gravity from the aft perpendicular. Since the propeller increases the flow and changes the lift coefficient of the rudder, the corrected flow $u_{R,corr}^2$ and the correction factor λ_{Lift} may be introduced, which leads to:

$$Y_{Rudder} \cdot \lambda_{Lift} = 0.5 \cdot \rho \cdot C_L \cdot A_R \cdot u_{R,corr}^2 \quad (5.32)$$

When applying the added power prediction method, the ship's speed, thus the state of motion, as well as the wind and wave conditions are assumed to be constant for ev-

ery leg of a given route. Initially, the corresponding wave spectrum and the propulsion point for calm water conditions, i.e. without wind resistance induced by the ship's own speed, are determined. As indicated by Fig. 5.3 and Eqn. 5.9 to 5.11, the wind forces are influenced by the ship's drift angle β_D . Similarly, this is applicable to the forces in a seaway. However, the drift velocity is not only affected by the hydrodynamic hull forces but also by the impact of wind and waves. Thus, for a considered state of motion the corresponding wind and wave forces are calculated and the drift velocity is estimated using the equations of motion for sway and yaw. This results in an updated drift angle and accordingly new wind and wave forces. The iterative procedure, represented by the first loop in Fig. 5.13, terminates when the change in wind force is sufficiently small.

In order to obtain the added power, the propulsion point, i.e. the operational point of propeller and engine, needs to be determined. This requires the ship's total resistance (see Sec. 5.2) including the impact of the rudder, which is assumed to be behind every propeller. The rudder inflow, though, is not only influenced by the ship's drift but also by the propeller. While the basic relations have been treated above, the iterative procedure to derive the equilibrium between propeller load and rudder force is visualized by the second loop in Fig. 5.13. The rudder angle is estimated iteratively using the semi-empirical formulae for the drag and lift coefficients. Consequently, the rudder resistance is calculated and the total resistance is updated, which leads to a new curve in the open-water diagram (see Fig. 5.10) based on Eqn. 5.19. Its intersection with the curve of the thrust coefficient gives the propeller's operational point. Finally, under consideration of the engine characteristics, the added power on each leg can be calculated, which is used to derive the ship's fuel consumption.

The method is validated within the research project by Abdel-Maksoud et al. (2016, pp. 49–52). It is applied to a 238 meter long cruise ship, different routes and weather conditions. It is concluded that the method considers the input data as expected and allows to predict the added power in real weather conditions in accordance with the accuracy of the input data.

5.6.4 Approaches in Weather Routing

Apart from different approaches to derive the total ship's resistance, which is typically composed of the calm water and added resistances due to waves and wind, also propeller and engine characteristics are taken into account with different levels of detail if considered at all. This applies to their integration in academic developments and commercial systems concerning ship weather routing. The brief summary of approaches related to ship propulsion is based on the overview of mathematical modeling and optimization approaches applied in ship weather routing in Chpt. 4. As to the consideration in commercial weather routing systems, it is referred to the overview in Sec. 2.5. It is to be noted that most approaches refer to solving the equation of motion in longitudinal direction. The few approaches also accounting for transverse motions are mentioned in Sec. 5.1.

Approaches that consider the propulsion system of a ship and the interaction between hull, propeller and rudder in lesser detail often aim at reducing data requirements or computational effort. Sometimes, the ship's propulsion is even neglected completely as in the case of simple speed reduction curves. Also Pipchenko (2011) neglects the propeller for calculating the engine load, but considers propeller racing by an operational limit. In some cases, the propulsive efficiency is assumed to be constant, such as by Bentin et al. (2016) and Sen and Padhy (2015). Sen and Padhy (2015) apply Dijkstra's algorithm and note that determining the ship speed under consideration of the total resistance and open-water propeller characteristics for every possible path between two nodes of a grid implies high time and computational efforts. Consequently, the speed reduction due to environmental impacts is assumed to be small, and thus the effective thrust to be constant within the considered speed range. This assumption is said to be acceptable for the studied North Indian Ocean region. But it is rather inappropriate for regions like the Atlantic Ocean.

In contrast, ship specific propeller characteristics are considered among others by Avgouleas (2008), Böttner (2007), Calvert (1990), Cui, Turan, et al. (2016), Hinnenthal (2008), Vettor and Guedes Soares (2016), and Zaccone et al. (2018). In some cases, a propeller with publicly known open-water characteristics is assumed. For example, Calvert (1990) and Vettor and Guedes Soares (2016) use data published by Oosterveld and van Oossanen (1975). Cui, Turan, et al. (2016) use the propeller open-water performance characteristics to calculate the open-water efficiency and derive the brake power. The engine's specific fuel oil consumption is assumed to be constant. In case of Böttner (2007), Hinnenthal (2008), Marie and Courteille (2009a), and Marie and Courteille (2009b), the ITTC (1978) power prediction method is applied to obtain the propeller's operating point and finally the fuel consumption. The approach of Calvert (1990) is said to be similar to the ITTC (1978) method. It considers engine characteristics based on full-scale test bed data. Marie and Courteille (2009a, p. 138) note that the approach is not generic and requires specific knowledge of the ship. Hence, a fuzzy logic model is suggested to derive the ship's fuel consumption on a route by using data collected from onboard measurements.

In order to avoid the integration of propeller data into the performance calculation, pre-calculated curves or databases are favored. In this regard, Klompstra et al. (1992) use a performance prediction model consisting of a resistance, a propeller and an engine module to solve the equation of motion in longitudinal direction. Based on the obtained power and the specific fuel consumption given as a polynomial function of the power, speed-fuel-curves can be derived. Thus, the fuel consumption is given as a function of speed, distance, loading and weather condition (incl. ocean current). Similarly, Aligné et al. (1997) determine the power based on curves relating the power for different speeds to the total added resistance. Also Tsujimoto and Tanizawa (2006) use a pre-calculated database with ship speed, fuel consumption per hour and vertical acceleration data in dependence of engine revolution, displacement and eight weather parameters.

Instead of obtaining the engine power and fuel consumption in accordance to the ship's speed, Fang and Lin (2015) and Lin et al. (2013) assume a constant effective power and derive an attainable speed in the prevailing weather conditions (ocean currents, wind and waves). Fang and Lin (2015, p. 131) state that lateral forces and yawing moments are neglected, since maneuverability is not considered in the present mathematical model and the rudder's "influence is complicated and needs to be further judged in the future." Also Eskild (2014) iteratively calculates the attainable speed in a given sea state at constant brake power. In case the wind is calculated from waves, a speed loss input file is considered. Otherwise, in case of wind and wave forecasts, calm water resistance data from towing tests, propulsion data from open-water tests as well as measured wind coefficients and pre-computed added resistance data due to waves are read. Furthermore, Shields and Weber (2015) state that speed recommendations by StormGeo (see Sec. 2.5), which are calm sea speeds, generally assume constant power. It is considered to be more fuel efficient than constant RPM.

Last but not least, insufficient data or less detailed hydrodynamic and propulsion models may be compensated by the use of operational data and techniques from machine learning or artificial intelligence. Thus, Chen (1989) utilizes onboard sensor data. Also Weber (1995) develops a model to integrate the influence of wind and waves on the ship's behavior based on an experimental process analysis of measurements on board of a container ship. Similarly, the method proposed by Szlapczynska (2015, p. 342) uses "data gathered from a set of ships belonging to a sea carrier company" to allow estimation of ship speed, fuel consumption and safety of the voyages based on IMO's MSC.1/Circ. 1228 (Krata and Szlapczynska 2012). Also commercial systems, such as ClassNK-NAPA GREEN (see Sec. 2.5), include measured operational data from onboard sensors and apply machine learning techniques to reduce errors. This allows improved performance predictions in normal operating conditions, where data from the shipyard and sea trials are insufficient (NAPA Group 2014, p. 10).

In conclusion, it is often claimed that adequate modeling of a ship's propulsion and steering ability is required to avoid engine overload or to ensure manoeuvring capabilities in a seaway (see Sec. 2.2, 2.3 and 5.5.1). Nevertheless, it is to be noted that the actual influence of differently detailed approaches on ship weather routing has rarely been systematically investigated so far. As summarized in Sec. 5.2.3, Calvert (1990) conducts routing studies comparing the impact of methods ranging from simple speed loss approaches up to a developed ship resistance and powering algorithm. Yaw and steering effects are neglected, since they are assumed to be less important compared to calm water and added resistances (Calvert 1990, p. 59). The lack of detailed studies on the influence of propulsion and steering in ship weather routing suggests further investigations in this regard, especially against the background of the attributed importance.

6 Design and Implementation of the Weather Routing System

The ship weather routing system is designed taking into account the influence of weather in maritime shipping addressed in Chpt. 2 and the fundamentals of meteorological and oceanographic data described in Chpt. 3. Furthermore, the design and implementation is inspired by the applied optimization approaches that are outlined regarding commercial systems in Sec. 2.5 and academic developments in Chpt. 4. The aspects of ship performance treated in Chpt. 5 are of particular importance for investigating the object of research, i.e. the impact of added resistance and added power on ship weather routing. Considering these aspects, the descriptive model of the weather routing problem is derived in Sec. 6.1 and the mathematical model in Sec. 6.2. The chapter continues with the solution procedure in Sec. 6.3. The developed system including its architecture is subject to Sec. 6.4. It also provides details on the ship performance model and its implementation as well as on the handling of weather data.

6.1 Description of the Weather Routing Problem

The first steps when approaching a complex real-world problem before formulating the mathematical model and finding a solution procedure refers to analyzing the problem and creating a descriptive model. On the basis of some generic requirements relevant for ship weather routing, the scope and assumptions of the developed system are described and the considered problem is classified.

6.1.1 Generic Requirements

The aspects treated in Chpt. 2 concerning voyage planning, maritime safety and energy efficiency provide the basis to outline requirements relevant for ship weather routing. In particular, the *Guidelines for Voyage Planning* adopted by the IMO (1999) in resolution A.893(21) emphasize the importance of a well planned ship's voyage for safety of life at sea, safe and efficient navigation and environmental protection. In line with the IMO (1999) and Berking and Huth (2010, pp. 32ff.), the following key items should be taken into consideration when planning a ship's voyage:

- Ship data
 - Ship's condition and state including information on stability and equipment as well as any required documents
 - Operational limitations

- Permissible draught at sea as well as in fairways and ports
- Maneuvering data including restrictions
- Type and distribution of cargo
- Navigational information
 - Up-to-date charts, relevant notices to mariners, navigational warnings, mariners' routing guides and other relevant routing information
 - Ships' routing and reporting systems and vessel traffic services
 - Marine environmental protection measures
 - Required port information
 - Traffic conditions and volumes of traffic
- Environmental data
 - Current and tidal atlases as well as tide tables
 - Climatological, hydrographical and oceanographic data and other appropriate meteorological information
 - Availability of weather routing services
- Voyage data and plan
 - Intended route including plot on an appropriate chart
 - Voyage schedule including time of departure, estimated time of arrival and estimated times of arrival at all intermediate points or at least at critical points (e.g. regarding tide flow and heights)
 - Safe speed and necessary speed alterations along the intended route
 - Minimum required under keel clearance in areas with critical water depth
 - Course alteration points considering ship speed and required turning circle
 - All time availability, continuous monitoring and adaptability to changing circumstances of the voyage plan
 - Specific instructions or restrictions given by the shipping company (e.g. slow steaming or full speed in piracy areas)

The output of a weather routing system is a voyage plan. It provides the intended route and voyage schedule, which covers the entire voyage from berth to berth. Each voyage plan has to be approved by the ship's master prior to the commencement of the voyage (IMO 1999, p. 4). Assistance to the master for voyage planning to safely and efficiently navigate the ship is provided by the route planning function of an Electronic Chart Display and Information System (ECDIS). It also includes a route check function, such as the NavStation by NAVTOR (2019). Since the take-over of a pilot is important for voyage planning, the voyage should be planned and approved for arrival at the respective pilot point in the first instance (Berking and Huth 2010, p. 36).

6.1.2 Scope and Assumptions

In line with Sec. 4.1, a model is a purpose-oriented, possibly simplified and generally idealized representation of a real system or problem. Creating this abstract idealization of the problem requires approximations and simplifying assumptions to ensure tractability of the model. With regard to the considered weather routing problem and the developed system, the scope and assumptions are elaborated on the basis of the requirements given in the previous section. Accordingly, the input and output model in Fig. 6.1 is derived. The categories of input data comprise ship data, navigational information, voyage and weather data. The output of the weather routing system shall be a voyage plan covering the ship's voyage between given departure and arrival points. This particularly comprises the intended route, i.e. a list of waypoints, and the voyage schedule as well as the speed profile throughout the voyage and the estimated fuel consumption of the main engine required for propulsion. The categories are briefly explained in Sec. 2.1. More details are given in the context of the mathematical model as well as the input and output data in Sec. 6.2 and 6.4.2 respectively.

The weather routing system itself needs to be able to read, load and handle all the required input data. Associated challenges relate to high resolution and multidimensional weather and ship data, as well as to the generation and visualization of the requested output. Moreover, a key requirement refers to minimum fuel consumption as objective. It is the most important aspect for many users and can be chosen to measure the impact of the different ship performance methods. To achieve this objective, the ship's route and speed shall be optimized. Flexibility concerning potential user preferences and evaluation possibilities can be increased by offering additional options for voyage optimization at constant speed or along a specified route, such as the shortest route or a predefined one. Tab. 6.1 summarizes the three optimization problems that can be solved by the developed weather routing system. Accounting for the respective constraints, either route and/or speed are optimized by varying position and/or time at a waypoint.

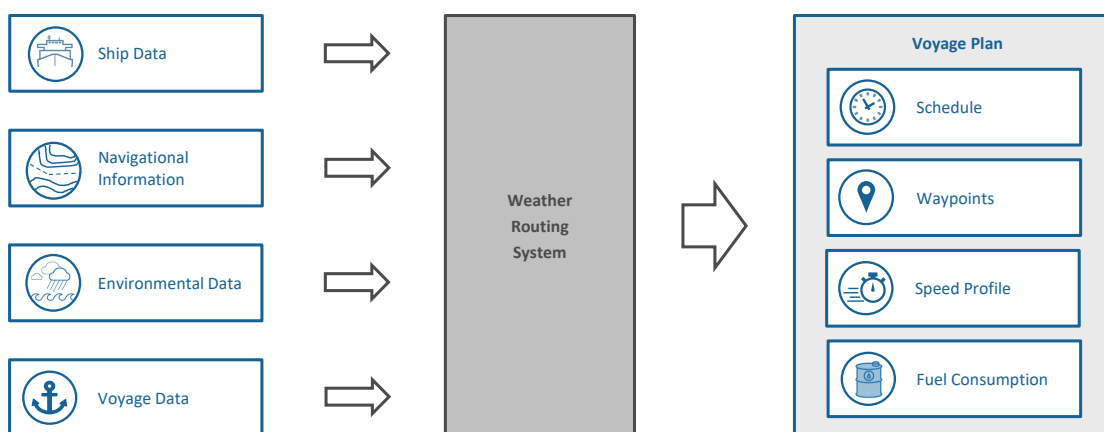


Figure 6.1: Input and Output Model of the Weather Routing System

Table 6.1: Optimization Problems solvable by the Ship Weather Routing System

Case	Objective	Decision Variables	Constraints
1	Minimum fuel	Position, time	On-time arrival
2	Minimum fuel	Position	Constant speed
3	Minimum fuel	Time	On-time arrival, predefined route (e.g. shortest route)

Future implementation of further aspects concerning weather data, safety or navigational restrictions, among others named in Sec. 6.1.1, shall be allowed by a modular design of the weather routing system. However, the more aspects are taken into account, the more complex and likely the more computationally intensive the system becomes. This leads to the trade-off between precision and tractability. In order to ensure tractability, approximations and simplifying assumptions, which do not compromise the valid representation of the problem, are required. Thus, the present system for investigating the object of research is based on the following requirements, assumptions and limitations. In summary, the weather routing system shall

- Ship data
 - Read and handle required ship data including ship information, propeller and engine characteristics
 - Consider safety restrictions in line with MSC.1/Circ. 1228 (see Sec. 5.5.2)
 - Take into account speed limits and operational limits for maximum wave heights and wind speeds
 - Provide an option to select an added resistance or added power method
 - Integrate output data from PDSTRIP for added resistance and added power calculations (see Sec. 5.5.1)
 - Compute the fuel consumption of the main engine required for propulsion
- Navigational information
 - Consider navigational restrictions limited to landmasses and shallow coastal areas without explicit consideration of minimum required under keel clearance
 - Perform weather routing from pilot point to pilot point outside each port as specified by the user
- Environmental data
 - Handle deterministic weather data (forecast/hindcast) provided in GRIB format (see Sec. 3.4)
 - Allow the use of hindcast data to ensure weather data availability throughout the travel time particularly for evaluation purposes

- Account for wind, ocean waves and currents
- Assume constant weather impacts between two subsequent waypoints
- Voyage data and plan
 - Ensure on-time arrival in line with schedule, i.e. with the user-defined input
 - Include cost aspects related to fuel costs of the main engine based on a user-defined fuel price
 - Produce output in three formats (see Sec. 6.4.2) to provide individually detailed route information and allow export to and display in an ECDIS
 - Visualize the resulting route and waypoints
- Design and implementation
 - Aim at minimum fuel consumption
 - Allow for speed and route optimization accounting for the constraints
 - Provide the functionality to solve the three optimization problems given in Tab. 6.1
 - Facilitate the addition of further options and the execution of specific processes on external servers through a modular design
 - Enable simple handling by a graphical user interface (GUI) and potential future onboard usage (e.g. by a personal computer)

6.1.3 Classification of the Problem

The overview of mathematical modeling and optimization algorithms applied in ship weather routing in Chpt. 4 reveals a broad variety of approaches. Naturally, the weather routing problem is a nonlinear problem. It has been modeled as continuous or discrete problem, as stochastic or deterministic problem and as constrained or unconstrained problem. Moreover, it has been treated as a single-objective or a multi-objective problem with one or several decision variables, such as ship's heading and engine power. When classifying mathematical models, Finke (2008, p. ix) distinguishes between two categories, which are based on algebraic and graph-related formulations.

The constructed ship weather routing problem is a single-objective deterministic and constrained optimization problem. It aims at minimum fuel consumption and is deterministic, because the parameters of the objective function and the constraints are assumed to be known accurately. The two decision variables, namely position and time, allow to optimize the ship's route, which is usually given as a list of waypoints, and its speed profile. Due to the discretization of the route by means of waypoints and the weather data that is provided in GRIB format, it appears reasonable to mathematically formulate the problem using graph-related notions.

Moreover, an optimization problem that aims for the shortest, fastest, cheapest or safest path between selected pairs of nodes in a network can be formulated as a shortest path problem. In view of this, the ship weather routing problem constructed within this thesis can also be considered as a shortest path problem. The aim is to determine the optimal path between a departure and arrival point, which is the path of minimum fuel costs. It is to be noted that one origin and one destination are taken into account and that the fuel costs assigned to the arcs are nonnegative. Both aspects influence the solution difficulty.

Shortest path problems can also be formulated as dynamic programming problems and vice versa (see Sec. 4.3). Instead of graph-related formulations based on nodes and arcs, the problem is then described by stages and states for sequential decision making. Both ways of modeling the weather routing problem belong to the most popular approaches. Here, a graph-related mathematical formulation is used.

6.2 Mathematical Model of the Problem

The previously outlined descriptive model of the considered weather routing problem has to be translated into a mathematical model in order to develop an adequate approach for deriving a solution to the problem in the next step. This includes the objective function, the decision variables, and the constraints, which are identified and formulated using graph-related notions.

6.2.1 Objective Function

In a decision or optimization model, the objective function, i.e. a function of the decision variables, aims at minimization or maximization. Given a directed graph $G = (N, A)$ with a set of nodes N and a set of arcs A , a traveling time t_{ij} and a time-variant positive fuel cost C_{ij} (see Eqn. 5.26) are associated with each arc $(i, j) \in A$ between nodes i and j and times t_i and t_j at the nodes with $t_{ij} = t_j - t_i$. Further, a directed forward path r is a time-variant sequence of nodes (i_1, i_2, \dots, i_k) with corresponding times (t_1, t_2, \dots, t_k) . In terms of ship weather routing, it is a simplified voyage plan comprising waypoints and times. Here, i_1 and i_k are called start node s (or origin) and end node d (or destination), which are equivalent to departure and arrival port or pilot point. The time t_1 corresponds to the departure time and t_k to the arrival time, i.e. ETD and ETA. The set of all feasible paths, thus all directed paths from the start i_1 to the destination i_k meeting all constraints, is denoted as P . The cost $C(r)$ of a path $r \in P$ then is:

$$C(r) = \sum_{n=1}^{k-1} C_{i_n i_{n+1}}(t_{i_n i_{n+1}}) \quad (6.1)$$

According to the aim of the weather routing problem, the path r^{min} is said to be optimal if it has minimum fuel costs $C(r^{min})$ over all forward paths with the same start

and destination. The objective of the weather routing problem can be formulated as follows:

$$C(r^{min}) = \min , r^{min} \in P \quad (6.2)$$

6.2.2 Decision Variables

The decision variables represent each of the related quantifiable decisions to be made. Since a node is associated with a position and a time, these two decision variables are varied within their respective domains to allow route and speed optimization. As to the WGS 84 coordinate system $(x_{WGS84}, y_{WGS84}, z_{WGS84})$ in Fig. 5.2, the position of a surface ship is specified by latitude Φ ranging from 90° South (-90°) to 90° North ($+90^\circ$) and longitude λ ranging from 180° West (-180°) to 180° East ($+180^\circ$). Thus, a node i_n is defined by latitude Φ_n and longitude λ_n . Furthermore, the time at a node t_n has a range from the estimated time of departure (ETD) at the start to the estimated time of arrival (ETA) at the destination node. Accordingly, a forward path $r \in P$, which is a time-variant sequence of nodes (i_1, i_2, \dots, i_k) with times (t_1, t_2, \dots, t_k) , can also be described in terms of positions $(\Phi_n \in [-90^\circ, 90^\circ], \lambda_n \in [-180^\circ, 180^\circ])$ and corresponding times $t_n \in [ETD, ETA]$ as:

$$r = \{\Phi_1, \Phi_2, \dots, \Phi_k, \lambda_1, \lambda_2, \dots, \lambda_k, t_1, t_2, \dots, t_k\} \quad (6.3)$$

For each position-time combination (Φ_n, λ_n, t_n) that is within the range of the weather data, the data as explained in Sec. 6.4.5 and summarized in Tab. 6.3 is available. The weather conditions are considered in line with the relations in Fig. 5.3 when deriving the ship's behavior and the fuel consumption. On this basis, for a path r the speed profile $V(r)$ and the variation of the ship's heading along the path $\Psi(r)$, which are relevant for ship navigation, can be obtained:

$$V(r) = \{V_{S,1}, V_{S,2}, \dots, V_{S,k}\} \quad (6.4)$$

$$\Psi(r) = \{\psi_1, \psi_2, \dots, \psi_k\} \quad (6.5)$$

Considering Tab. 6.1, both, position and time, are varied in Case 1. Case 2, however, assumes the ship's speed to be constant, which leads to the time being determined by the speed and distance between two neighboring nodes and only the position being varied. In contrast, only the time is varied in Case 3, while the positions are defined previously. The system requires either a predefined route as input or a prior calculation of the shortest route. For the shortest route, the objective is minimum distance, while the waypoint's position is variable. The time domain is not relevant in this case.

6.2.3 Constraints

Mathematical expressions of any restrictions on the values of the decision variables are referred to as constraints, which are equality or inequality constraints. In case of the

constructed weather routing problem, constraints on the variables are related to the voyage, the ship itself, its safety and geographic conditions.

Voyage Constraints The start and destination node need to correspond to the locations specified by the user for departure and arrival:

$$i_1 = (\Phi_1, \lambda_1) = (\Phi_{\text{start}}, \lambda_{\text{start}}) \quad (6.6)$$

$$i_k = (\Phi_k, \lambda_k) = (\Phi_{\text{destination}}, \lambda_{\text{destination}}) \quad (6.7)$$

Furthermore, not only a departure time but also a specific user-defined arrival time is assumed to be obligatory, which leads to a total voyage time for the whole path:

$$t_1 = ETD \quad (6.8)$$

$$t_k = ETA \quad (6.9)$$

$$\sum_{n=1}^{k-1} t_{i_n, i_{n+1}} = ETA - ETD \quad (6.10)$$

Ship Constraints As to the ship itself, an indirect constraint on the values of the decision variables is given by the available power of the ship's engine. The brake power P_B at a specific engine speed n , that is required when traveling from one node i to the adjacent node j within the time t_{ij} , has to remain within the limits given by the load diagram for continuous operation in Fig. 5.11. More detailed relations can be found in Sec. 5.6.2. Compliance with this constraint can only be verified after the time-consuming calculation of the power P_B . Hence, the ship's maximum attainable speed in calm water V_{max} is used to constrain the range of t_{ij} prior to the power calculation. The minimum time t_{ij} required to travel the distance d_{ij} is d_{ij}/V_{max} . Moreover, the option of setting a minimum ship speed V_{min} allows to account for the need to keep course control, thus to maintain the steering ability in waves. In summary, the described limits are:

$$P_{B,ij} \leq P_{MaxLoad}(n) \quad (6.11)$$

$$V_{ij} \leq V_{max} \quad (6.12)$$

$$V_{ij} \geq V_{min} \quad (6.13)$$

Safety Constraints Optionally, the ship's safety during a voyage can be taken into account by certain operational restrictions. However, the consideration of safety constraints in ship weather routing as described in Sec. 5.5.2 is not in the particular focus of this research. If any optional safety constraint is set as input and violated during the calculation, the respective arc becomes invalid and not navigable. The considered safety constraints include the IMO guidelines as well as limits for maximum wave height $H_{S,max}$ and wind speed $U_{G,max}$. Also the limit of minimum ship speed can be regarded as a safety measure, since the steering ability is essential for the ship's safety. The latter

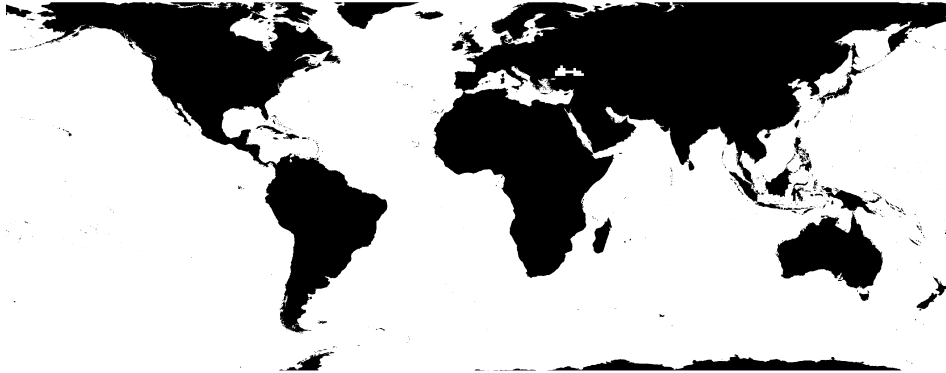


Figure 6.2: Map of the Landmasses Generated based on an Electronic Nautical Chart using the SevenCs EC2007 ECDIS Kernel

one is named above, while the guidance according to MSC.1/Circ. 1228 (IMO 2007) is given in Tab. 5.2 and is not explicitly formulated here again. The two constraints concerning waves and wind can be expressed as follows:

$$H_S(i, t_i) \leq H_{S,max} \quad (6.14)$$

$$U_G(i, t_i) \leq U_{G,max} \quad (6.15)$$

Geographic Constraints Constraints due to geographic conditions and routing restrictions primarily refer to land, but can also include shallow waters, traffic separation schemes, icebergs or mines. Due to the focus on ocean shipping and deep sea navigation, which is acceptable when comparing the impact of both ship performance methods, mainly landmasses are taken into account. This is based on the map generated from an Electronic Nautical Chart (ENC) shown in Fig. 6.2. Accordingly, every node $i \in N$ has to be located in water. In addition, every neighbor j of a node $i_n \in r$ must be in water, which ensures that no waypoint is located too close to the coastline.

6.2.4 Parameters

The constraints and the objective function can contain constants, such as coefficients. These are the parameters of the model. Since the fuel cost function in Eqn. 5.26 and also some of the constraints, such as that regarding the available power, are rather complex and more or less implicitly depend on a number of parameters, these are not described here in detail. Instead, it is referred to Chpt. 5, which elaborates on the aspects, such as wind and waves, influencing the ship's performance during a voyage.

6.3 Description of the Solution Procedure

The next step when approaching complex real-world problems refers to deriving solutions to the problem from the mathematical model by developing a solution procedure. An

algorithm is a processing specification for solving a problem, which can be represented in detail by an executable program. Turau (2009) distinguishes between the design of an algorithm and its translation into an executable program using a programming language. While the first is part of this section, the implementation in form of the developed weather routing system is subject to the next one.

6.3.1 Design of the Algorithm

An adequate algorithmic solution procedure is required to determine an optimal solution for the mathematical model. Depending on the structure of the model, efficient suitable algorithms may be available. The overview in Chpt. 4 shows that solution procedures, i.e. algorithms, employed in ship weather routing range from nonlinear approaches through graph theoretic and dynamic programming ones to metaheuristic methods.

To solve problems modeled based on graph-related formulations, the algorithmic graph theory provides solution procedures. Graph algorithms applied in ship weather routing are summarized in Sec. 4.3. The most popular algorithm to approach shortest path problems is an algorithm developed by Dijkstra (1959). However, its rather high computational effort is sometimes mentioned as a drawback for its application in weather routing. When aiming to reach a destination as fast as possible, which is equivalent to minimizing the number of nodes visited, the A* algorithm is often regarded as an alternative. In principle, it is a generalization of Dijkstra's algorithm (Turau 2009, p. 271). As to Barr and Feigenbaum (1981, pp. 58, 64), the A* algorithm, first described by Hart et al. (1968), can be classified as a heuristic state-space search method. In contrast to a blind search of a state-space with a purely arbitrary order of expanding the nodes, A* additionally uses heuristic information to reduce the search space. On the basis of Barr and Feigenbaum (1981) and Hart et al. (1968), a time-dependent version of the A* algorithm employed to solve the considered weather routing problem is described in the following.

Assuming an optimal path through node i with corresponding time t_i , the actual cost of the path is $F(i, t_i)$. It can be divided in the exact cost $G(i, t_i)$ from the start s to node i and the heuristic cost $H(i, t_i)$ from i to the destination d . Since the actual costs of the optimal path are not known a priori, an estimate $\hat{F}(i, t_i)$ is used:

$$\hat{F}(i, t_i) = \hat{G}(i, t_i) + \hat{H}(i, t_i) \quad (6.16)$$

where $\hat{G}(i, t_i)$ is the cost of the cheapest path r^{si} to reach i from s at time t_i that has been found by the algorithm so far, i.e. until the optimal path is found and $\hat{G}(i, t_i)$ becomes $G(i, t_i)$. Using Eqn. 6.1, it can be given as:

$$\hat{G}(i, t_i) = C(r^{si}) \quad (6.17)$$

The heuristic function $\hat{H}(i, t_i)$ denotes the cost estimate to reach d from i . To be admissible, $\hat{H}(i, t_i)$ should be nonnegative and a lower bound of $H(i, t_i)$. Hence, it should never overestimate the costs between nodes i and d as well as t_i and ETA. Instead, it should correspond to the lowest possible cost to travel from the current node to the destination within the remaining time. That is why the shortest possible route, i.e. the great circle distance d_{id} , is assumed and any environmental impact increasing the ship's resistance is omitted throughout the remaining voyage. One could argue that ocean currents along the ship's route or wind from aft acting over a long part of the voyage would actually accelerate the ship leading to lower actual fuel costs than estimated costs. On the one hand, though, the actual route is longer due to the discretization, and on the other hand, strong winds are usually accompanied by waves which increases the ship's resistance. Adding up the environmental impacts typically results in an increase in costs, which leads to the heuristic costs $\hat{H}(i, t_i)$ representing a lower bound. Using Eqn. 5.23, 5.24, 5.25 and 5.26, the cost estimate $\hat{H}(i, t_i)$ can be expressed as:

$$\hat{H}(i, t_i) = \frac{R_0 \cdot d_{id}}{\eta_D \cdot \eta_S} \cdot SFOC \cdot P_{Fuel} \quad (6.18)$$

where the propulsive efficiency η_D , the shaft efficiency η_S and the specific fuel oil consumption SFOC are assumed to be constant at their optimal value. Since environmental impacts are omitted, the ship's resistance is limited to its calm water resistance R_0 . This is influenced by the ship's speed $V_G = d_{id}/(ETA - t_i)$ (see Sec. 5.2, Fig. 5.3 and Eqn. 5.4) that is required to ensure on-time arrival.

In order to determine the optimal path of minimum fuel cost between start and destination, the algorithm fans out from the origin, evaluates adjacent nodes and labels them according to their estimated cost $\hat{F}(i, t_i)$. The node with minimum $\hat{F}(i, t_i)$ is expanded in every iteration. Since several paths can lead to the same node, the label is temporary until the path of minimum fuel cost is found and the label becomes permanent. Thus, the algorithm continuously scans adjacent nodes and updates labels. As the problem only considers a single destination, the algorithm terminates once the destination is reached and the voyage time between ETD and ETA is met, thus it becomes permanently labeled.

The algorithmic solution procedure has been presented by Walther (2015) and Walther et al. (2015, 2017). A popular form to describe an algorithm in a compact way is by means of a pseudocode, which can be found in Alg. 1 based on Dechter and Pearl (1985), Hart et al. (1968), and Walther (2015). It provides the basis to translate the algorithm into an executable program using a programming language in the next section.

First, the cost $\hat{F}(i, t_i)$ is calculated for the start, which is added to a so called open list. The open list contains all unexpanded nodes, while a list called closed is used for all expanded ones, whose cost values have been fully explored. As stated above, in each iteration the node i at time t_i from the open list that has the minimum $\hat{F}(i, t_i)$ and

meets all constraints given in Sec. 6.2.3 is expanded. It is removed from the open list and added to the closed list. All its admissible neighbors (see Sec. 6.3.2) or successors j at all admissible times t_j are evaluated by calculating $\hat{F}(j, t_j)$. Here, particularly the calculation of the cost $\hat{G}(j, t_j)$ from start to j depends on the ship, weather and voyage data addressed in Sec. 6.4.2. If (j, t_j) is already marked as open or closed but the new $\hat{F}(j, t_j)$ is smaller than the old one, then the assigned label is updated and (j, t_j) is moved back to the open list. Any (j, t_j) neither marked open nor closed is added to the open list with its $\hat{F}(j, t_j)$ assigned as label. Once the node selected for expansion corresponds to the destination and the time to ETA the algorithm terminates. The path with corresponding times, thus the waypoint list and voyage schedule, is generated by tracing back the arcs from the destination.

```

Data: ShipData, WeatherData, VoyageData
Result: VoyagePlan
initialization;
if OpenList created;
  ClosedList created;
  ShipData loaded;
  WeatherData loaded;
  VoyageData loaded then
     $\hat{G}(s, t_1) = 0$ ;
     $\hat{H}(s, t_1) = \text{MinCostsFromStartToDestination}$ ;
     $\hat{F}(s, t_1) = \hat{G}(s, t_1) + \hat{H}(s, t_1)$ ;
    AddToOpenList(s);
    EmptyClosedList;
    while DestinationReached = FALSE AND MaxTotalTimeElapsed = FALSE do
      Current( $i, t_i$ ) = NodeTime[ OnOpenList = TRUE AND  $\hat{F} = \text{min}$  AND ConstraintsMet
        = TRUE ];
      RemoveFromOpenList(Current);
      AddToClosedList(Current);
      for Each Neighbor j AND Each TimeAtNeighbour tj do
        Calculate  $\hat{G}(j, t_j) = \text{CostsFromStartToNeighbor}(\text{ShipData}, \text{WeatherData},$ 
          VoyageData);
        Calculate  $\hat{H}(j, t_j) = \text{MinCostsFromNeighborToDestination}$ ;
        Calculate  $\hat{F}(j, t_j) = \hat{G}(j, t_j) + \hat{H}(j, t_j)$ ;
        if OnClosedList( $j, t_j$ ) AND Updated $\hat{F}(j, t_j) < \text{Current}\hat{F}(j, t_j)$  then
          | Update  $\hat{F}$  ; RemoveFromClosedList ; AddToOpenList
        else if OnOpenList( $j, t_j$ ) AND Updated $\hat{F}(j, t_j) < \text{Current}\hat{F}(j, t_j)$  then
          | Update  $\hat{F}$ 
        else
          | Set  $\hat{F}(j, t_j)$  ; AddToOpenList( $j, t_j$ )
        end
      end
    end
  else
    | exit
  end

```

Algorithm 1: Pseudocode for the Applied, Extended A* Algorithm

When calculating the shortest route for Case 3 from Tab. 6.1, a smoothing technique is used to reduce discretization effects. Here, the weighted moving average is applied to the resulting path considering the four neighboring waypoints. A multiplying factor of two assigns a greater weight to the two direct neighbors. In case of landmasses, a waypoint's position is not affected by the smoothing.

6.3.2 Discretization and Graph Design

In the context of the considered weather routing problem, the graph consists of nodes that correspond to points of given weather data or waypoints, and of arcs connecting ordered pairs of distinct nodes that represent route legs. According to the definitions in Sec. 4.3, the graph resulting from the characteristics of the weather routing problem is connected, directed and acyclic with nonnegative arc weights as a ship's fuel costs are positive. Moreover, there is one start and one end node, i.e. departure and arrival location.

As to the generation of weather forecasts, it is indicated in Sec. 3.4 that a discretization in space and time, thus a grid-point-space, is used to solve the atmospheric and oceanic numerical models. The larger the time steps, the more acceptable the computation time of the forecast becomes. However, a higher resolution leads to more accurate forecasts, e.g. concerning coastlines or anticyclones. The same applies to the design of the graph when solving the considered weather routing problem. Nevertheless, a higher resolution than that of the applied weather data will rather increase computational effort than accuracy, because the weather impact on the ship's fuel consumption is then the same for several route legs or arcs. In contrast, a lower resolution most likely leads to a longer route due to the discretization in space. Although this can compromise the accuracy of the computed fuel consumption, it can also reduce the computational effort.

The available weather data provided in GRIB format is subject to Sec. 6.4.5. The current and wave data is provided in steps of one hour, and the wind data in steps of three hours. A ship's speed, however, can be adjusted continuously not only in discrete steps taking into account the limits of the engine and the varying efficiency (see Sec. 5.6.2). To achieve a compromise between the continuously variable speed and the computing effort, it is decided to discretize the time in steps of fifteen minutes. Thus, the time between two nodes t_{ij} is a multiple of this time step.

Furthermore, the current data has a spatial resolution of 0.1° in latitudinal and longitudinal direction. Wind and wave data have a spatial resolution of 0.5° in both directions. Thus, the latitudinal and longitudinal direction spacing is set to 0.5° . Assuming regularly arranged nodes as in Fig. 6.3 and the adjacent nodes of a node as neighbors, the ship's heading angle (see Fig. 5.3) is rather limited by these eight nodes, which is indicated in Fig. 6.3a. In order to increase the variation possibilities of the heading angle, the next but one sixteen nodes depicted in Fig. 6.3b are considered as neighbors. This applies only to the start node, since a ship's incoming and outgoing heading angles

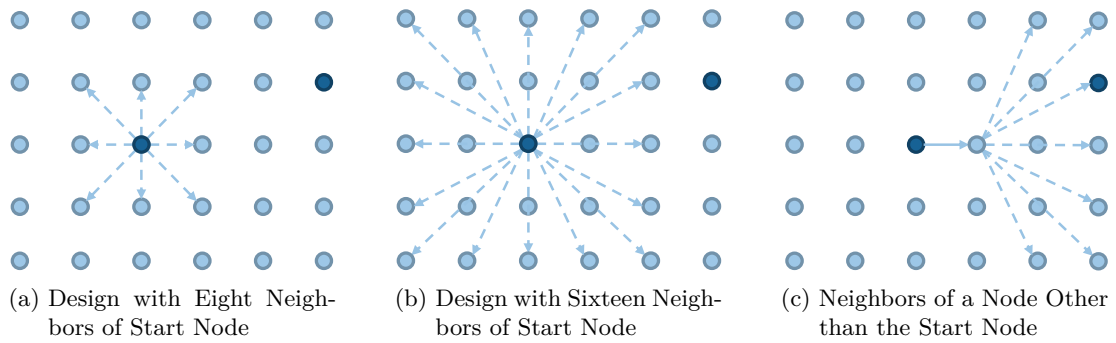


Figure 6.3: Definitions of Neighbors to Design the Graph

at a waypoint usually differ by less than $|90^\circ|$ to account for the ship's turning ability and ensure a smooth path. Hence, the number of valid neighbors of a node other than the start node is reduced from sixteen to seven. These nodes are located in the ship's sailing direction as shown in Fig. 6.3c.

The influence of the spacing and the neighbors is investigated by varying both on a route from Rotterdam to New York and vice versa using the added resistance method (see Sec. 6.4.4). The spacing can be chosen as 0.25° , 0.5° or 1.0° , while considering either eight or sixteen neighbors or the combination of both, thus twenty-four neighbors, when referring to the start node. A spacing of 0.5° and sixteen neighbors is used as reference. For eight neighbors the path is 4% longer which can be attributed to the lower variation in heading and a less smooth path. The fuel costs are approximately 12% higher, but the computation time is roughly halved. In contrast, the time increases by one third in case of twenty-four neighbors. The length and the fuel costs of the resulting path remain virtually unaffected, which also applies when varying the spacing.

In conclusion, the case of sixteen neighbors offers the best compromise concerning computation time and distance calculation. Regarding the spacing, the lowest resolution results in the lowest computation time as expected. It increases by a factor of three to four for a spacing of 0.25° instead of 0.5° and decreases to one quarter for a spacing of 1.0° . Although accuracy is not significantly compromised for a spacing of 1.0° , a smaller spacing is most likely more accurate in relation to e.g. coastlines or the influence of higher resolution weather data. Since the weather impact is important when investigating the ship's performance and the trade-off is the best, it is decided to set the spacing to 0.5° .

6.4 Development of the Weather Routing System

On the basis of the described algorithmic solution procedure to solve the considered weather routing problem, an executable program using the object-oriented programming language C++ is developed. The graphical user interface of the developed weather

routing system enables comparably simple handling and user-specific settings as to the input and output data. Its architecture allows to meet the given requirements concerning optimization objectives, variables and constraints as well as the processing of ship, navigational, environmental and voyage data. Particularly noteworthy are the ship performance model and the handling of weather data.

6.4.1 Graphical User Interface

The main window of the developed weather routing system is shown in Fig. 6.4. This graphical user interface (GUI) is designed to meet the requirements listed in Sec. 6.1.2 and to allow corresponding user-specific inputs. In this regard, the three optimization problems from Tab. 6.1 can be selected from a drop-down list. Concerning Case 3, it is distinguished between the predefined route and the shortest route, which leads to four options in the list. In the drop-down list *Weather Data Source*, weather data from a database or single GRIB files can be selected. The data can be loaded before running the weather routing system by using the button *Load Weather Data*. *Show Weather Monitor* allows to monitor and check that all required data within the specified voyage time is available and has been loaded properly.

The main window also enables the user to set input data such as departure and arrival information, speed and operational limits, fuel price and operational envelope, which are explained in Sec. 6.4.2. In addition, the ship performance method, i.e. added resistance or added power, can be selected. Accordingly, required input data can be defined in *Settings*. The optional consideration of the guidance to the master published by IMO (2007) in MSC.1/Circ. 1228 is integrated by the according checkbox. In *IMO Settings*, the user can choose the criteria to be applied and enter the required input data.

Further data can be specified in the drop-down menu *Options*. This is divided in *Set Ship Data* for specifying among others the ship's main dimensions, propeller and engine characteristics, *Set GRIB Data* for providing the path to single GRIB files if these are used, *Set Route File* for reading a predefined route and *Set Output File* for selecting one or several of the output formats and defining the output folder. Provided all specified input is correct, the button *Run!* will execute the program. The user can check the calculated voyage time and monitor the progress by information displayed at the bottom. The program can be stopped with the button *Cancel*. Once terminated, the total distance and fuel costs are also shown at the bottom. Using the drop-down menu *Help* information about the weather routing system particularly regarding aspects such as system requirements, copyright and licenses is summarized.

6.4.2 Input and Output Data

The GUI in Fig. 6.4 enables user-specific settings as to the input and output data. This relates to the ship and its safety, navigational and voyage information as well as to the components of a voyage plan as output data.

Ship Input Data The weather routing system shall read and handle ship data including its main dimensions, propeller and engine characteristics. Some data that is assumed to be static and not voyage related, such as the ship's length, its maximum engine output

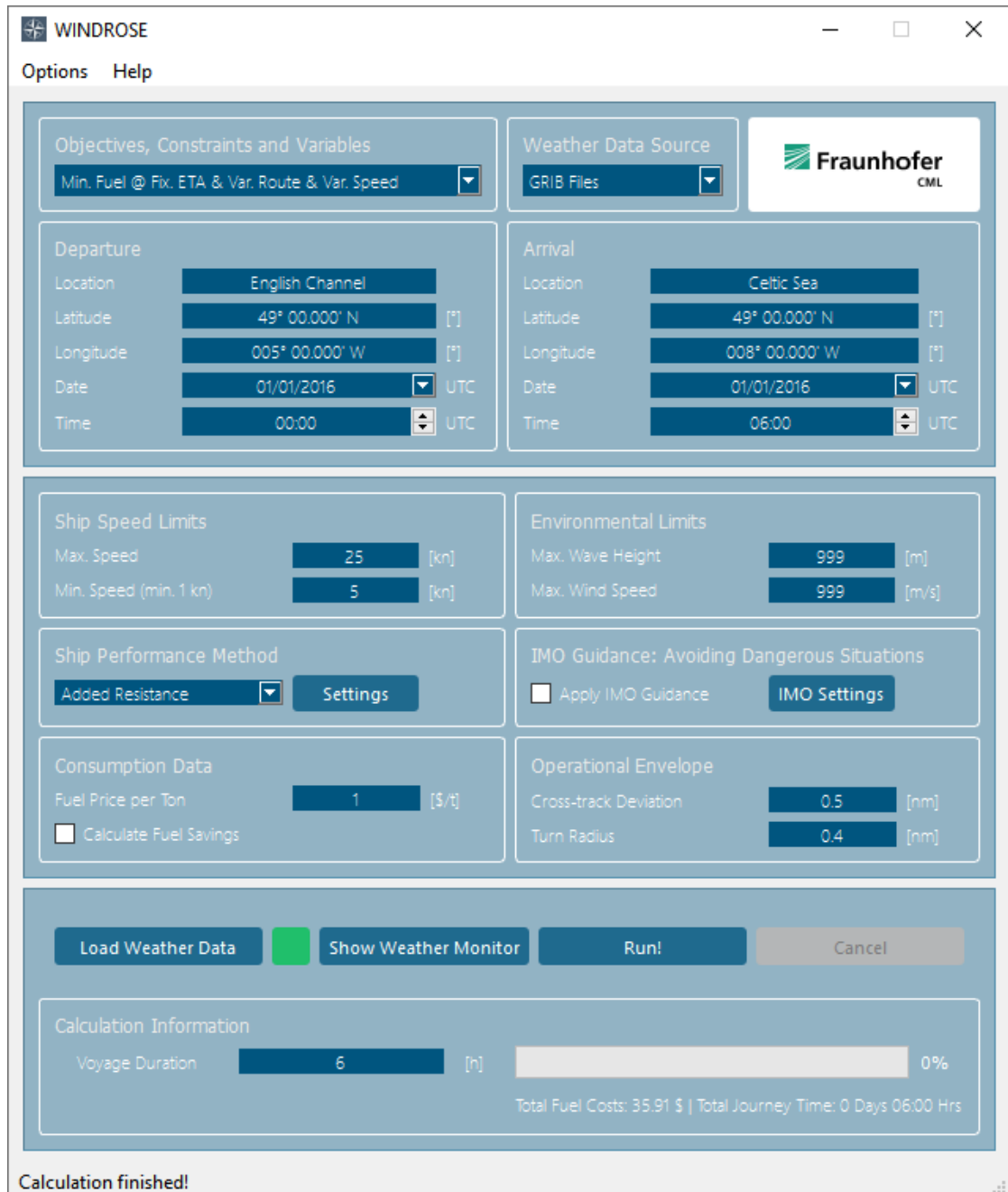


Figure 6.4: Graphical User Interface of the Weather Routing System

and its wind coefficients, is given in a text file which can be specified in **Set Ship Data** in the drop-down menu **Options**. This also allows to read a text file containing the specific fuel oil consumption as a function of the engine power as shown in Fig. 5.12. In contrast, some ship data that is voyage specific, i.e. depends on the ship's loading condition, can be defined in the main window. This includes speed limits which are explained in Sec. 6.2.3. Ship data required to apply the guidance to the master published by IMO (2007) can be entered in **IMO Settings**. It is addressed in the context of safety related input data. In addition, the ship performance method, namely added resistance or added power, can be selected. According input data can be defined in **Settings**. However, the two different methods described in Sec. 6.4.4 require different ship data to some extent. Since the method *ProWe* is developed in Python, messages are passed between both applications and the necessary ship data is directly read and handled in Python.

The added resistance method requires the ship's calm water resistance as a function of the ship's speed (see Fig. 5.6), the added resistance due to waves as well as the ship's frontal projected area above sea level which is influenced by the ship's draught. In line with the requirement that the weather routing system shall integrate output data from PDSTRIP, the added resistance due to waves is read from a text file. Sec. 7.1 provides further details on this data. With regard to the added power method *ProWe*, the input data is explained in detail by Abdel-Maksoud et al. (2016). This includes main dimensions, maneuvering coefficients and certain propulsion data, such as rudder and propeller dimensions as well as thrust deduction and wake fraction, which can be entered in a specific input file of the Python application. In addition, the calm water resistance data and the open-water propeller data as displayed in Fig. 5.10 are required in CSV format. The impact of waves is considered by providing an interface to read among others results from PDSTRIP, which should not only include longitudinal drift forces but also lateral drift forces and yaw drift moments.

Safety Related Input Data The weather routing system provides the option to also account for the ship's safety when optimizing a voyage. The guidance to the master published by IMO (2007) in MSC.1/Circ. 1228 (see Sec. 5.5.2) can be considered by the according checkbox. The user can select which criteria are to be applied (see Tab. 5.2) by further checkboxes in **IMO Settings** and enter the required input data. This includes voyage specific values such as metacentric height and radius of gyration to derive the ship's natural roll period (see Eqn. 5.15). Additionally, voyage specific operational limits regarding wave height and wind speed can be set in the main window. A default value for no operational limit is 999.

Navigational Input Data Referring to the requirements in Sec. 6.1.2, navigational information that is taken into account is limited to landmasses and shallow coastal areas without explicit consideration of minimum required under keel clearance. The focus is on deep-sea navigation from pilot point to pilot point which is relevant to compare the impact of both ship performance methods. The information about landmasses depicted

in Fig. 6.2 is stored in an image format with 3600x1800 pixels. This means that it has a resolution of 0.1° in latitudinal and longitudinal direction.

Weather Input Data It is required that the weather routing system can load and handle weather data (forecast/hindcast) provided in GRIB format. The format is briefly described in Sec. 3.4, while Sec. 6.4.5 provides information on the temporal and spatial resolution and deals with handling this data. For the years 2016 and 2017, hindcast data is available. Global combined ocean and tidal current data, global wind data as well as global wave data are provided in a file per day each. Tab. 6.3 lists all relevant parameters from the hindcast data used within the weather routing system.

Voyage Input Data Departure and arrival information is important voyage data. It includes both locations' names, positions, i.e. latitude and longitude, as well as the dates and times. If Case 3 from Tab. 6.1 is selected with a predefined route, this needs to be read using *Set Route File*. Case 3 with the shortest route does not require any route input. For Case 2, the ETA results from the optimization based on constant speed and is not required as input. To calculate the fuel costs, the fuel price per ton needs to be defined. Setting it to 1 is equivalent to providing the absolute fuel consumption in tons as output. As to the preferences of the user, the savings compared to sailing the shortest route at constant speed can also be calculated.

Last but not least, the so called operational envelope is included in the voyage plan. The cross-track deviation describes the allowed orthogonal distance of the ship's actual course to the shortest connection of two consecutive waypoints. The ship's turn radius is relevant at each course alteration point according to the requirements in Sec. 6.1.1. Both values can be set by the user and are associated with all waypoints of the resulting voyage. Starboard and portside cross-track deviation are assumed to be identical.

Voyage Plan Output Data The weather routing system shall be able to produce an output in three formats: CSV, ROUTE and RTZ format. The user can select one or more of the output formats and define the output folder in *Set Output File* in the drop-down menu *Options*. The CSV and ROUTE formats are mainly used for evaluation purposes. The CSV format is used to summarize specific configurable information. This can include the ship and its performance, the weather during the voyage or data regarding the optimization algorithm. The NAVTOR ROUTE format with the extension *.route* is mainly used for plotting the route. The weather routing output can be imported into the maritime route planning tool NavStation provided by NAVTOR (2019).

The RTZ format in line with the International Standard IEC 61174:2015 has been approved by CENELEC as a European Standard (CENELEC 2015). It is a route plan exchange format intended to be used among others between ship and shore or on board for exchange between optimization systems and ECDIS. An ECDIS includes a route planning function and a route check function. By plotting the intended route and entering the voyage schedule in the ECDIS the master and the crew are assisted to safely

and efficiently navigate the ship. A file with the extension .rtz contains an XML coded version of the route plan, which consists of a series of waypoints. Not only the geographical position, but also information associated with the leg from the previous waypoint including date and time is assigned to each of them. The RTZ format including XML schema is described by CENELEC (2015).

6.4.3 Architecture of the System

The architecture of the developed weather routing system has to correspond to the algorithmic solution procedure to solve the considered optimization problem. Furthermore, it needs to meet the requirements concerning the processing of ship, navigational, environmental and voyage data. The flowchart in Fig. 6.5 indicates that all relevant input data specified in the GUI is loaded when running the system. This includes the optimization problem, the voyage data and safety related data. In addition, the data stored in files needs to be loaded, such as ship data files, weather data files and the landmass file. The function **Optimize** executes the speed and/or route optimization depending on the input. In case of a successful optimization a voyage plan is provided as output. Otherwise, an error message is displayed to the user, which could among others result from a short voyage time combined with harsh weather conditions.

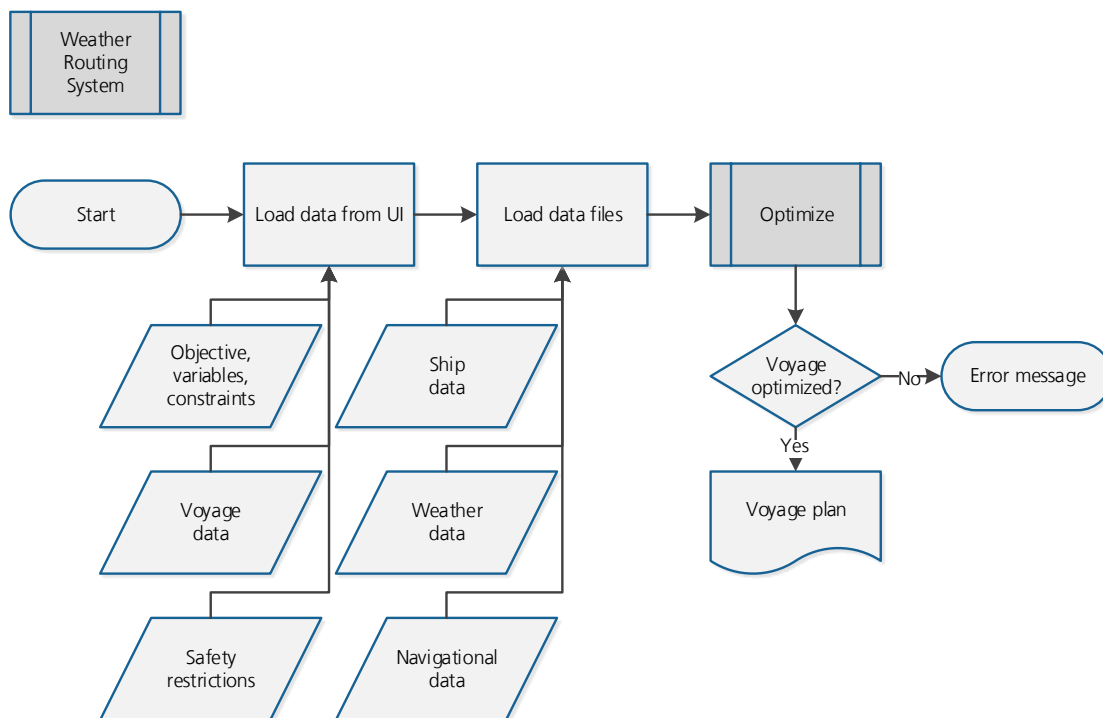


Figure 6.5: Generic Flowchart of Weather Routing System

The function `Optimize` is represented by the flowchart in Fig. 6.6. It is the visualization of the pseudocode in Alg. 1. Fanning out from the departure node s , all admissible neighbors $j \in [j_1, j_{max}]$ at all admissible times $t_j \in [t_1, t_{max}]$ with time step Δt are evaluated. In addition to time restrictions, further optional safety limits can lead to

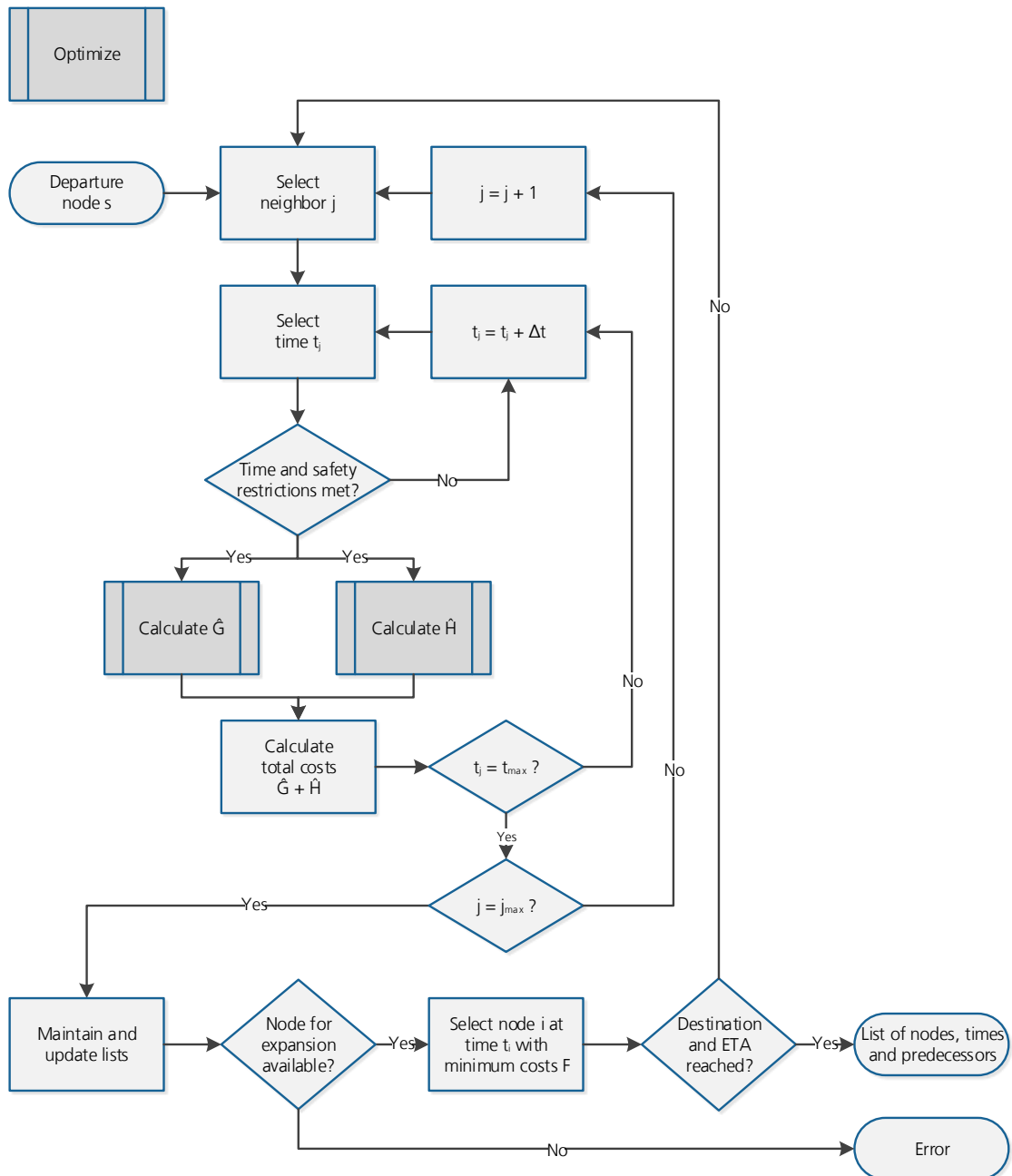


Figure 6.6: Generic Flowchart of Optimization Function

inadmissible node-time-combinations. In case the restrictions are met, the costs \hat{G} and \hat{H} are computed to derive the costs \hat{F} . Once all neighbors at all times are evaluated, the lists are updated. In each following iteration the node i at time t_i with minimum costs \hat{F} is selected for expansion. In case there is no node available for expansion, the function is terminated with an error. Once the node selected for expansion corresponds to the destination and the time to ETA, a list of nodes, corresponding times and their predecessors is provided to generate a voyage plan as output.

The functions Calculate \hat{G} and Calculate \hat{H} are visualized by the flowcharts in Fig. 6.7 and 6.8 respectively. The cost $\hat{G}(i, t_i)$ of the path r^{si} to reach node i from start s at time t_i can be derived using Eqn. 6.1 and 6.17. This is the sum of the time-variant positive fuel cost C_{ij} associated with each arc (i, j) and times t_i and t_j . The cost C_{ij} is influenced by the ship itself and the environmental impacts. Nodes i and j and their times t_i and t_j are used to calculate the speed and course over ground as well as through water accounting for the impact of the current. Together with the true wind, the speed and course through water provide the input to the selected ship performance method. Considering the ship data, particularly the specific fuel oil consumption, the absolute fuel consumption m_{Fuel} and the cost C_{ij} can be obtained from Eqn. 5.25 and 5.26 respectively. Hence, the cost $\hat{G}(j, t_j)$ at neighbor j and time t_j is the sum of the cost $\hat{G}(i, t_i)$ at the predecessor i at time t_i and the cost C_{ij} .

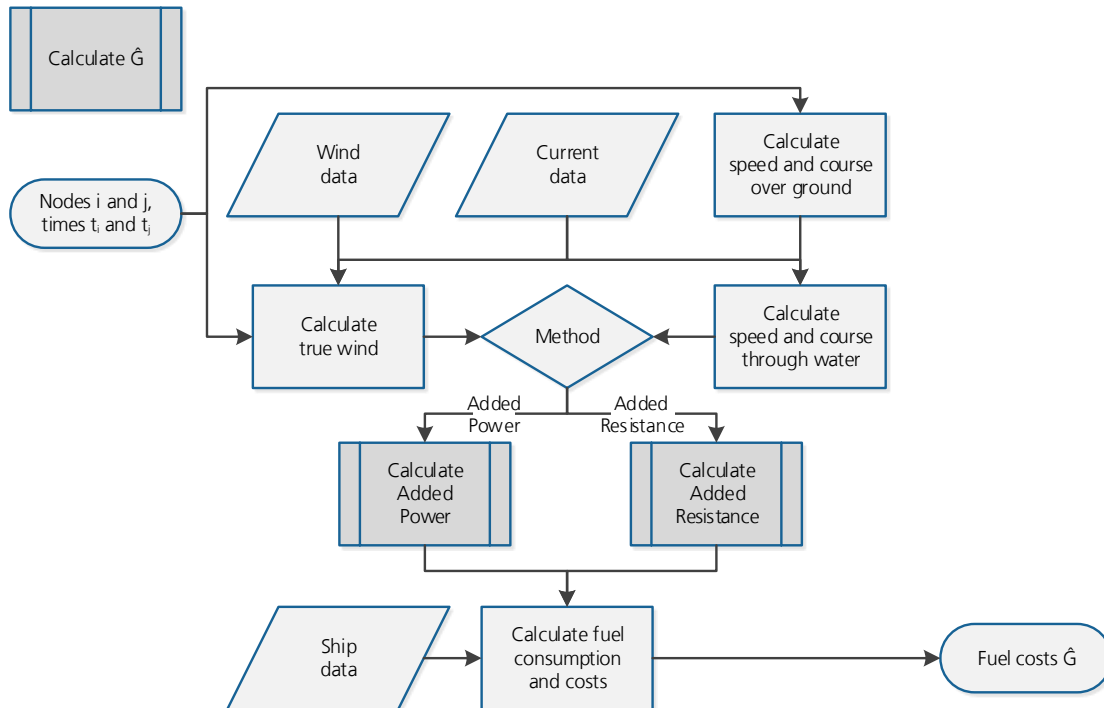


Figure 6.7: Generic Flowchart of Exact Cost Function

Similarly to Calculate \hat{G} , node i and j and the times t_i and t_j are used to calculate the speed and course over ground in the function Calculate \hat{H} . Since environmental input data is omitted here, Fig. 6.8 shows that only data referring to the ship is taken into account as input. It is used to obtain the calm water resistance R_0 , that corresponds to the ship's speed, and the specific fuel oil consumption. These are included in Eqn. 6.18 to derive the cost estimate $\hat{H}(j, t_j)$ at neighbor j and time t_j .

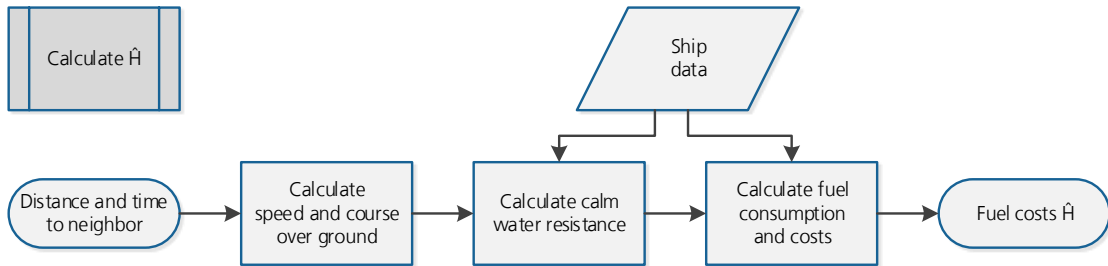


Figure 6.8: Generic Flowchart of Heuristic Cost Function

6.4.4 Ship Performance Model

The fundamentals of ship performance subject to Chpt. 5 provide the basis for the two methods implemented within the developed ship weather routing system. It is distinguished between the so called added resistance method and the added power method, which together constitute the ship performance model.

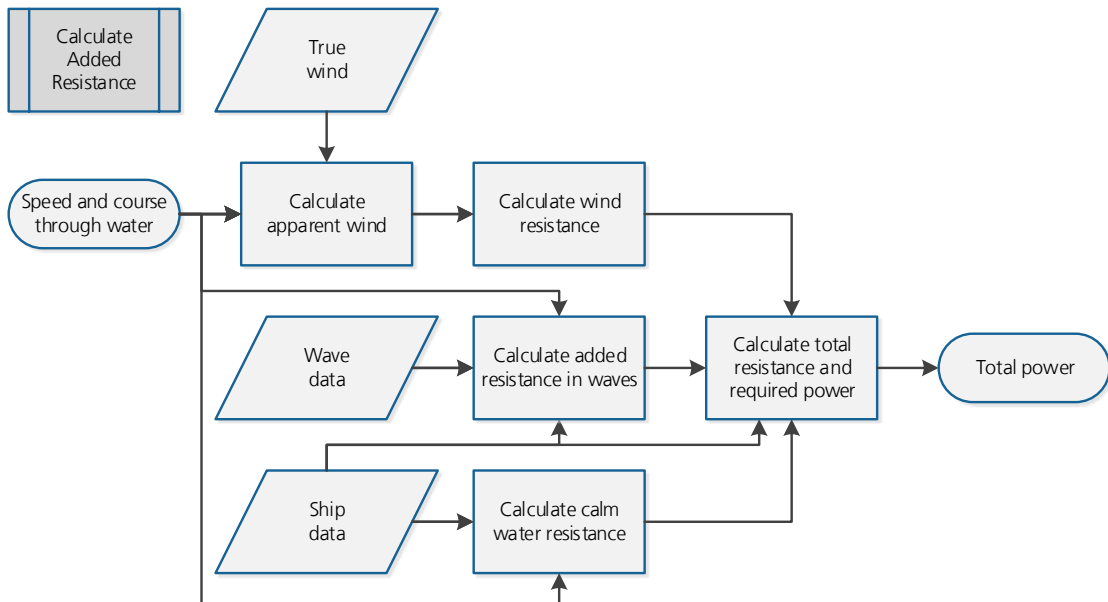


Figure 6.9: Generic Flowchart of Added Resistance Function

The flowchart of the added resistance method is shown in Fig. 6.9. It is inspired by the approach given in Fig. 5.5, which considers the equation of motion in longitudinal direction, thus surge, in Eqn. 5.1. Taking into account the previously calculated speed and course through water and the true wind, the apparent wind and wind resistance, i.e. the wind induced force along the x axis X_{Wind} , are derived. The provided wave and ship data, more precisely the PDSTRIP output for the specific ship and loading condition, are used to obtain the added resistance due to waves, i.e. the wave induced force along the x axis X_{Drift} . The sum of the added resistance due to wind and waves and the calm water resistance R_0 provided as curve of the ship's speed gives the total resistance. It is to be noted that the influences of the rudder as well as of the propeller are neglected within this approach for reasons of simplicity and computational efficiency.

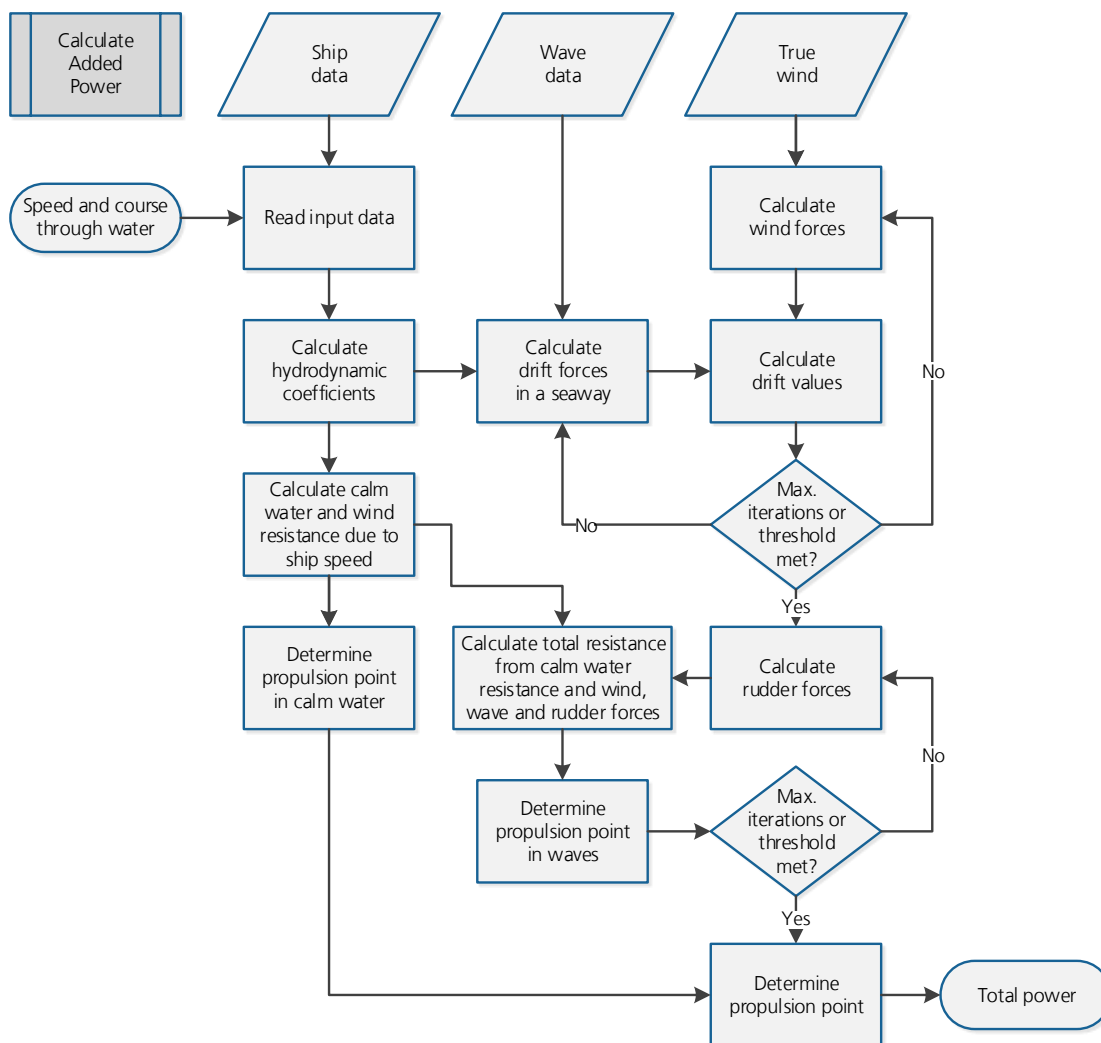


Figure 6.10: Generic Flowchart of Added Power Function

Consequently, the propulsive efficiency η_D influencing the delivered power at the propeller P_D in Eqn. 5.23 is assumed to be constant. Eqn. 5.24 and the shaft efficiency η_S lead to the brake power P_B , thus the total required power as output of this function.

The flowchart of the added power method is given in Fig. 6.10 in line with Sec. 5.6.3, particularly Fig. 5.13. Since the method *ProWe* is developed in Python, the open source message broker RabbitMQ is employed for messaging (Pivotal Software 2019). It supports several messaging protocols, such as the Advanced Message Queuing Protocol (AMQP). As an open standard for passing messages between applications or organizations, it allows to connect applications on different platforms (OASIS 2019), such as C++ and Python in this case. Consequently, the speed and course through water as well as the required wave and wind data are sent from the C++-application to Python. In contrast, the necessary ship data summarized in Sec. 6.4.2 can be entered in a specific input file and is directly loaded in the Python-application.

After reading and handling the input, the propulsion point for calm water conditions is initially determined. The interdependency of the wind and drift forces in a seaway as well as the ship's drift motion requires an iterative procedure, which terminates when the maximum number of iterations or a threshold is met as shown in Fig. 6.10. Subsequently, the total resistance including calm water, wind, wave and rudder impacts is to be calculated. Again, the interdependency of the rudder forces as part of the total resistance and the propeller load requires an iterative procedure. This also terminates when the maximum number of iterations or a threshold is met. The derived propulsion point results in the total required power as output of this function.

6.4.5 Handling of the Weather Data

In line with the requirements, the developed weather routing system shall handle deterministic GRIB data, particularly hindcast data. In the following, it is focused on data from Tidetech. It is available for the years 2016 and 2017 and used for the evaluations in Chpt. 7. Metocean data supplied by Tidetech is also used by commercial weather routing systems. To construct tidal models in-house, techniques developed at the UK National Oceanography Centre are applied (Tidetech 2019). In addition, Tidetech offers third party data procured from official and academic providers. Numerical weather model outputs are among others obtained from the GFS or the ECMWF (Tidetech 2018). Wave data is supplied from the wave model WAVEWATCH III that is maintained by NOAA's NCEP. An extract of forecast data with global coverage is given in Tab. 6.2 to outline the differences in resolution, forecast length and time step.

Historical (hindcast) data is available in form of datasets for global combined ocean and tidal currents, global wind and global waves. Although forecast as well as hindcast data are available, the latter is used within this thesis to ensure weather data availability throughout the entire duration of the voyage. Focusing on hindcast data, the u- and v-components [m/s] of global currents are given with a temporal resolution of one hour

Table 6.2: Extract of Global Data provided by Tidetech (2019)

Data	Wind Speed And Direction	Global Primary, Swell and Wind Waves	Global Wave Length	Global Combined Currents
Description	Atmospheric model displaying wind at 10 m above surface and mean sea level pressure	Wave models displaying height and direction of primary, swell and wind generated waves	Wave model displaying wave length and primary direction	Operational Analysis and Forecast Model of combined tidal and ocean currents
Resolution	0.5°	0.2°	0.2°	0.1°
Forecast Length	10 days	5 days	5 days	7 days
Time step	3 h	3 h	3 h	1 h
Longitude	180.0 W - 180.0 E	180.0 W - 180.0 E	180.0 W - 180.0 E	180.0 W - 179.9 E
Latitude	90.0 S - 90.0 N	79.0 S - 78.0 N	79.0 S - 78.0 N	70.0 S - 69.9 N
Source	NOAA NCEP GFS	Copernicus Marine Environment Monitoring Service	Copernicus Marine Environment Monitoring Service	Tidetech proprietary

and a spatial one of 0.1° in longitudinal as well as latitudinal direction. Similarly, the wind dataset includes its u- and v-components [m/s] in addition to the atmospheric pressure at mean sea level. It has a temporal resolution of three hours and a spatial one of 0.5° in both directions.

The wave dataset differentiates between wind waves, swell waves and combined wind and swell waves. It provides the corresponding significant heights [m], (primary) directions [deg] and (primary) mean periods [s]. The wave data has a temporal resolution of one hour, like the current, and a spatial resolution of 0.5° in both directions, like the wind. All three files contain information for one day from 00:00 to 21:00 or 23:00 depending on the temporal resolution. The parameters considered for ship weather routing are summarized in Tab. 6.3. The table also includes the variables corresponding to the notations introduced in Sec. 5.1.

It is to be noted that it is distinguished between a meteorological and an oceanographic convention when providing this data. In line with the meteorological convention, the u-component of wind or ocean current is positive for a flow from west to east (eastward wind/current) and the v-component is positive for a flow from south to north (northward wind/current) (ECMWF 2017b). In case a (wave) direction is given according to the meteorological convention, 0° corresponds to 'coming from north' and 90° to 'coming from east'. Following the oceanographic convention instead, directional information equal to

Table 6.3: Relevant Parameters of provided Weather Data

ID	Name	Unit	Variable
Global Combined Ocean and Tidal Current Data			
UOGRD	u-Component of current	m/s	$V_{C,East}$
VOGRD	v-Component of current	m/s	$V_{C,North}$
Global Wind Data			
UGRD	u-Component of wind	m/s	$U_{G,East}$
VGRD	v-Component of wind	m/s	$U_{G,North}$
Global Wave Data			
DIRPW	Primary wave direction	degree true	μ_0
HTSGW	Significant height of combined wind waves and swell surface	m	H_S
PERPW	Primary wave mean period	s	T_P
WVDIR	Direction of wind waves	degree true	$\mu_{0,WV}$
WVHGT	Significant height of wind waves	m	$H_{S,WV}$
WVPER	Mean period of wind waves	s	$T_{P,WV}$
SWDIR	Direction of swell waves	degree true	$\mu_{0,SW}$
SWELL	Significant height of swell waves	m	$H_{S,SW}$
SWPER	Mean period of swell waves	s	$T_{P,SW}$

“zero indicates that the waves are propagating towards the north and 90 towards the east” (ECMWF 2017c). The oceanographic convention is often used in case of wave spectra information. As stated by The WAVEWATCH III Development Group (2016, p. 93) in the documentation for version 5.16, the output parameters mean wave direction and peak direction are provided in degrees according to the meteorological convention. Tidetechnology and the Met Office (2017b), both applying WAVEWATCH III, further specify the unit of the direction [degree true], which denotes a direction relative to true north.

In order to handle the weather data available in GRIB format the use of a library is required. In this regard, the Geospatial Data Abstraction Library (GDAL) provided by GDAL/OGR contributors (2018) is used. It is available under an X/MIT style Open Source license. The Open Source Geospatial Foundation released the library to translate (all supported) raster and vector geospatial data formats. This library is used within a weather module, shown in Fig. 6.11, to read, preprocess and visualize weather data independent from the weather routing system. Thanks to the weather module, the GRIB data does not need to be handled by the weather routing system before or during each run which is time consuming. It is to be noted that the spatial resolution of the global combined ocean and tidal current data provided by Tidetechnology is reduced from 0.1° to

0.5° when it is preprocessed due to reasons of file size and handling efforts within the weather routing system.

As an example from the hindcast dataset provided by Tidetechn, Fig. 6.11 displays the global significant height of combined wind waves and swell on 01 January 2016 00:00. Similarly, Fig. 6.12 and 6.13 show the speed of global combined ocean and tidal currents and the global wind speed respectively. For each parameter from Tab. 6.3 and for each time, the values are stored in an image format which can be read by the weather routing system. It is to be noted that the u- and v-components of current and wind are converted to a vector, so that magnitude and direction are stored. The weather module is also used for verification purposes in Sec. 7.2.1.

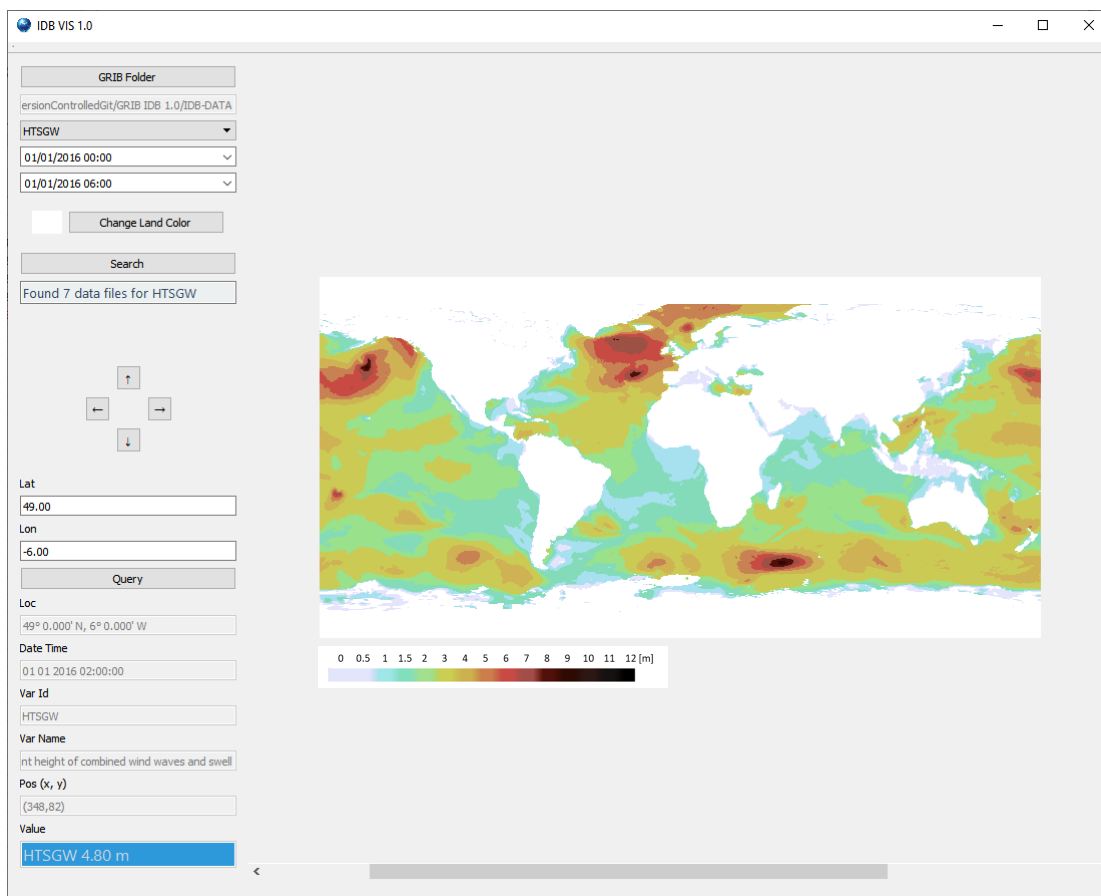


Figure 6.11: Significant Height of Combined Waves Visualized in Weather Module

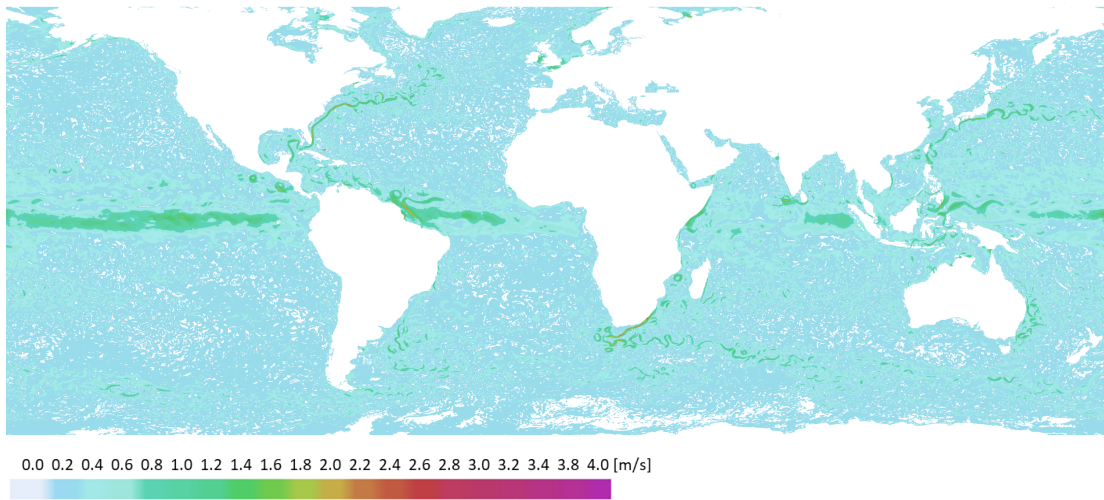


Figure 6.12: Global Combined Ocean and Tidal Current on 01 January 2016 00:00

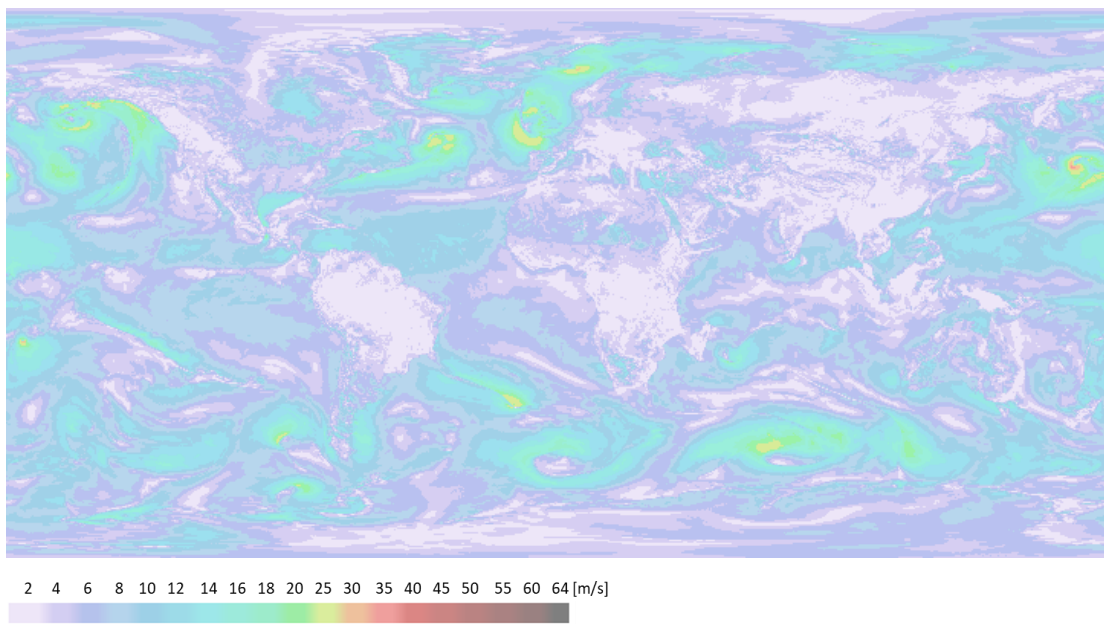


Figure 6.13: Global Wind Speed on 01 January 2016 00:00

7 Testing and Application of the Weather Routing System

The developed weather routing system needs to undergo sound testing to ensure its validity and to obtain correct results. Using the ship related input data in Sec. 7.1, the process of testing is illustrated in Sec. 7.2 by means of sample voyages. Subsequently, sensitivity analyses are conducted in Sec. 7.3 in order to evaluate the influence of the two ship performance methods on ship weather routing and to demonstrate the robustness of the results. The results are discussed in Sec. 7.4, while the limits and benefits of the weather routing system itself are subject to Sec. 7.5.

7.1 Ship Related Input Data

The ship data required as input by the developed weather routing system is described in Sec. 6.4.2. For testing and application of the system, a ship concept named Duisburg Test Case (DTC) is used. It is a “hull design of a typical 14 000 TEU container ship, developed at the Institute of Ship Technology, Ocean Engineering and Transport Systems (ISMT) for benchmarking and validation of numerical methods” (Moctar et al. 2012, p. 50). The side view of the hull geometry is displayed in Fig. 7.1. On the one hand, it is chosen due to large amounts of data being publicly available. On the other hand, actual voyage data of the A15 container ship class, which has an equivalent size, has been provided by Hapag-Lloyd (Hapag-Lloyd 2018a,b).



Figure 7.1: Side View of the Hull Geometry of the Post-Panmax Container Ship (DTC)

The main ship characteristics are summarized in Tab. 7.1. While the calm water resistance curve of the DTC is given in Fig. 5.6, Fig. 5.10 shows the open-water diagram based on Riesner et al. (2016, p. 16) and Moctar et al. (2012, p. 53). The built ship is equipped with a MAN B&W 9S90ME-C10.2 type engine, for which the engine load diagram is given in Fig. 5.11 (MAN Diesel & Turbo 2014; Zaitoun et al. 2014). Fig. 5.12 provides the corresponding curve of the specific fuel oil consumption as a function of power (MAN Energy Solutions 2018). It is to be noted that the figures given by the manufacturer consider a tolerance of 5 % (at 100 % SMCR) to 7 % depending on the

Table 7.1: Main Ship Characteristics of the Post-Panmax Container Ship - DTC and Built Ship (Hapag-Lloyd 2018a,b; Moctar et al. 2012; Riesner et al. 2016; Zaitoun et al. 2014)

Parameter	Unit	DTC	Built
Length over all	m	372.0	368.0
Length between perpendiculars	m	355.0	352.0
Waterline breadth	m	51.0	51.0
Design draught midships	m	14.5	14.5
Capacity	TEU	14 000	14 993
Power	kW	61 000	37 620
Ship speed	kn	25.0	21.2

engine load. In addition, the SFOC is “based on the use of fuel with a lower calorific value of 42 700 kJ/kg at ISO conditions” (MAN Diesel & Turbo 2014, p. 1.04). Air pressure, air temperature or cooling water temperature differing from the reference ambient conditions cause the SFOC to vary. That is why 12% are added to the given figures to meet the actual SFOC values of the container ship.

Additional ship data particularly required for the added power method is summarized in Tab. 7.2. The wind frontal and lateral areas as well as the coefficients are estimated on the basis of a general arrangement plan, the loading condition and further ship information from Hapag-Lloyd (2018a). For reasons of data consistency, among others with the available open-water diagram, the propeller and rudder data is mainly taken from Abdel-Maksoud et al. (2016, pp. 69–70) for the DTC. The thrust deduction fraction t and the wake fraction w , both used to calculate the hull efficiency η_H , as well as the relative rotative efficiency η_R result from propulsion model tests. The tests have been conducted by Moctar et al. (2012, p. 54) at a Froude number corresponding to approximately 20 kn in full scale. The open-water efficiency η_0 is derived from the open-water diagram. It is used to calculate the propulsive efficiency η_D by means of Eqn. 5.22. In line with Sec. 5.6.2 and Schneekluth and Bertram (1998, p. 181), the shaft efficiency η_S is set to 0.98. In case of the added resistance method, the propulsive efficiency η_D is assumed to be constant. It is approximated with 0.72 based on model tests by Moctar et al. (2012, p. 54). Multiplied with the shaft efficiency, the result of 0.7 corresponds to an assumption by Riesner et al. (2016, p. 26). Concerning the ship speed limits, the maximum is set to 25 kn based on ship information, while the minimum is assumed to be 5 kn taking into account regulations and investigations presented by IMO (2016a).

Last but not least, the drift forces in a seaway are derived using the public-domain hydrodynamic strip code for seakeeping PDSTRIP. The output includes the longitudinal and transverse drift force as well as the yaw drift moment in relation to wave length, encounter angle and ship speed. Figures are generally given per wave amplitude squared.

Table 7.2: Additional Ship Data of the Post-Panmax Container Ship (DTC) (Abdel-Maksoud et al. 2016, pp. 69–70; Moctar et al. 2012; Hapag-Lloyd 2018a)

Parameter	Symbol	Unit	Value
Longitudinal center of gravity from aft perpendicular	L_{CG}	m	174.07
Wind frontal area	A_F	m ²	1 800
Wind frontal area coefficient	C_X	-	0.73
Wind lateral area	A_L	m ²	12 500
Wind lateral area coefficient	C_Y	-	0.85
Rudder area	A_R	m ²	127.5
Rudder span	b	m	9.88
Wake fraction	w	-	0.264
Thrust deduction fraction	t	-	0.081
Relative rotative efficiency	η_R	-	0.959
Propeller diameter	D_P	m	10.0
Distance propeller to rudder	a	m	5.0

To assess the validity of the figures, Fig. 7.2 compares the obtained longitudinal drift force in regular waves with results from numerical and experimental investigations conducted by Sigmund and el Moctar (2017, 2018). Here, the normalized added resistance is plotted against the normalized wave frequency $\tilde{\omega} = (L_{PP}/\lambda_W)^{0.5}$. The respective added resistance coefficient C_{AW} can be expressed as follows:

$$C_{AW} = \frac{-X_{Drift} \cdot L_{PP}}{\rho g B^2 \zeta_A^2} \quad (7.1)$$

The RANS computations and measurements with the container ship DTC at full-scale speeds of 6 and 16 kn, thus Froude numbers (Fn) of 0.052 and 0.139, agree fairly well in short and long waves. At $Fn = 0.139$, computed values are 6% higher than measured added resistance coefficients in the area of peak values. Here, the wave length corresponds to the ship’s length and radiation forces caused by ship motions dominate. In short waves, where diffraction is dominant, the agreement is particularly favorable. This is said to be especially relevant for large ships that often operate under these conditions. Nevertheless, Sigmund and el Moctar (2018, p. 59) also acknowledge that “the absolute value of the added resistance is relatively small compared to, for example, the calm water resistance” in waves shorter than 20% of the ship’s length.

The comparison with values derived with PDSTRIP shows rather good agreement for waves longer than the ship’s length. But the shorter the waves, the more the results deviate. This corresponds to the statement by Söding and Bertram (2009, p. 40) that strip methods may lead to inaccurate results for wave lengths below approximately 40%

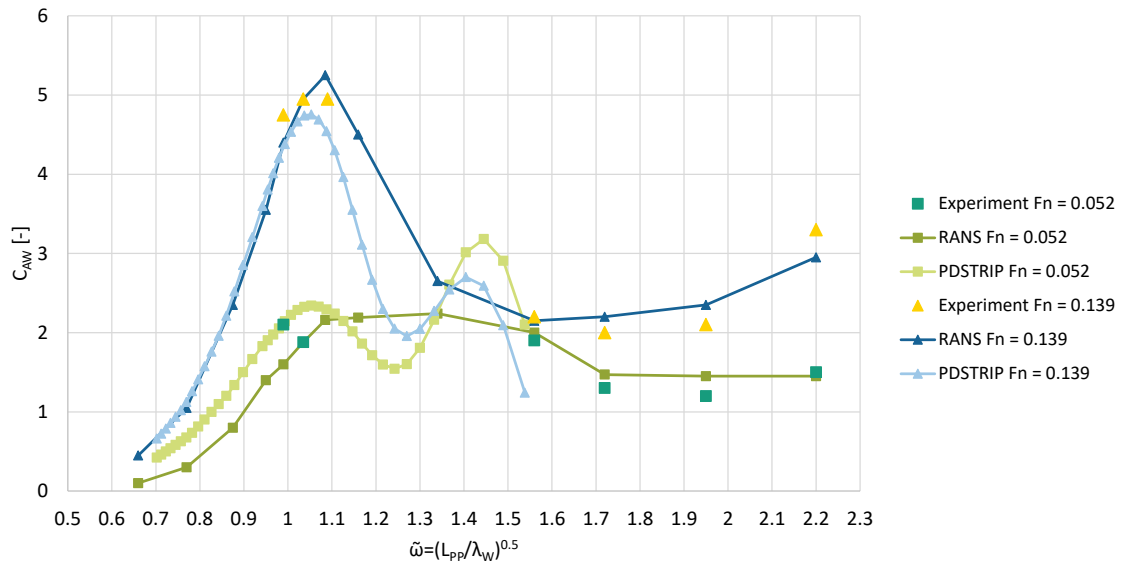


Figure 7.2: Added Resistance Coefficients of the Post-Panmax Container Ship (DTC) at Two Speeds in Regular Head Waves Compared to Experimental and Numerical Results by Sigmund and el Moctar (2018, p. 63)

of the ship's length, but are fairly accurate for long waves. Hence, the trend of the values is not unexpected. Taking into account the good agreement in long waves and the minor contribution to the total resistance in short waves, the values are assumed to be sufficiently accurate to derive the drift forces in natural seaways as input for both ship performance methods.

7.2 Testing of the System

Thorough and continuous testing has been part of the development process right from the beginning. Various routes and weather conditions as well as different ship data have been used to manually verify and validate the results. By means of sample voyages and the ship data from Sec. 7.1, the process of testing is illustrated. In this regard, results obtained with the system are verified by manual calculations. For validation, significant ship voyages are selected to compare computed results with actual data.

7.2.1 Verification

The verification of the developed weather routing system is essential to proof and ensure the functionality of the tool. The aim is to verify that the system works as expected. Therefore, only correct and plausible values are assumed as input parameters and results are computed for arbitrarily chosen sample routes. The results are compared to figures derived manually or using other software to verify the calculations.

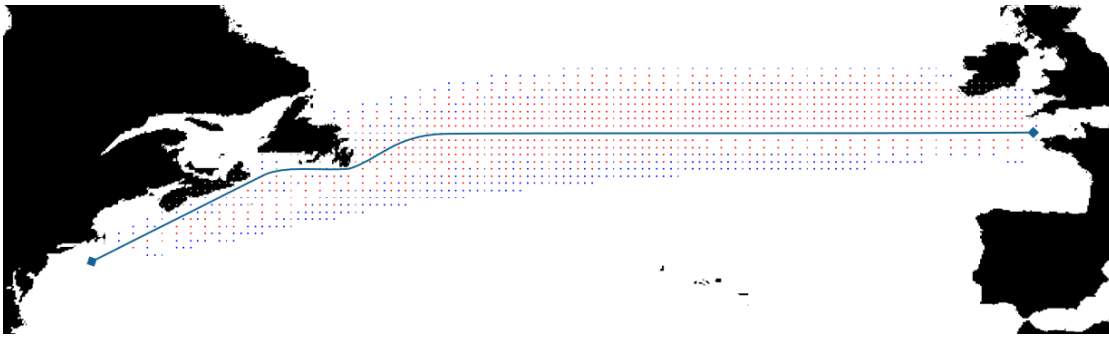


Figure 7.3: Exemplary Visualization of the Shortest Route and Spatial Search Space

A test case with a route departing from 49° North 005° West and arriving at 40° North 071° West is chosen arbitrarily. In order to increase traceability and simplify the visualization, the focus is on calculating the shortest route. As expected due to the distances on the ellipsoid, a rather northern route is derived. The resulting route as well as all visited nodes are visualized in Fig. 7.3. Blue marks indicate nodes only visited once, while the \hat{F} -value for red marked nodes has been recalculated and updated. Grey marks that may be seen on land represent invalid nodes.

The resulting route including all waypoints is also plotted in Fig. 7.4 using NavStation. Since a smoothing function is applied when computing the shortest route with the developed weather routing system, the resulting route is 2831 nm long. Previous to the smoothing, the location of waypoints is limited to the nodes of the graph in line with Sec. 6.3.2, which leads to a 2849 nm long route. The length derived by the weather routing system matches that given by NavStation and is consequently assumed to be

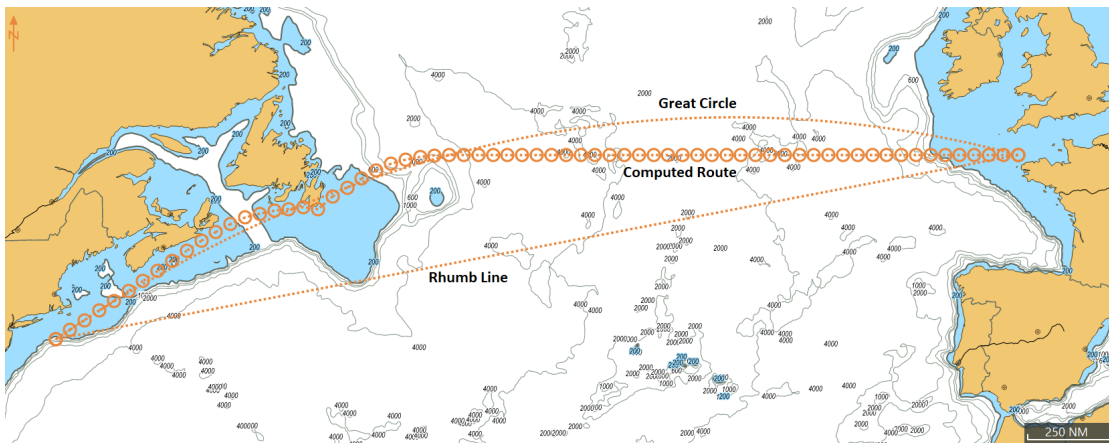


Figure 7.4: Comparison of Great Circle, Rhumb Line and Computed Shortest Route in NavStation

Table 7.3: Weather Data along Sample Route

Parameter	Unit	Waypoint 1	Waypoint 2	Waypoint 3	Waypoint 4
Time	hh:mm	00:00	02:00	04:00	06:00
Position	-	49°00.000'N 005°00.000'W	49°00.000'N 006°00.000'W	49°00.000'N 007°00.000'W	49°00.000'N 008°00.000'W
UGRD	m/s	1.6	-2.8	-3.8	-9.8
VGRD	m/s	3.4	8.0	9.0	12.3
Wind speed (U_G)	m/s	3.8	8.4	9.7	15.7
Wind direction (α_W)	degree	204.9	160.8	157.2	141.4
UOGRD	m/s	-0.2	-0.4	-0.1	0.1
VOGRD	m/s	-0.1	-0.2	0.2	0.3
Current velocity (V_C)	m/s	0.2	0.4	0.2	0.3
Current direction (α_C)	degree	61.9	64.2	143.0	199.6
HTSGW	m	4.9	4.8	4.7	4.7
DIRPW	degree	265.0	267.9	271.5	273.5
PERPW	s	11.4	11.3	11.3	13.2
SWELL	m	4.9	4.8	4.7	4.7
SWDIR	degree	261.0	261.1	262.0	261.9
SWPER	s	11.4	11.3	11.3	13.2
HTSGW	m	-	-	-	-
DIRPW	degree	-	-	-	-
PERPW	s	-	-	-	-

calculated correctly. To validate the result, Fig. 7.4 also shows the great circle with a length of 2794 nm and the 2877 nm long rhumb line connecting the departure and arrival locations. Due to the discretization and landmasses, the computed route is slightly longer than the great circle, but still shorter than the rhumb line.

In order to verify the weather data handling and the ship performance methods, it is focused on the beginning of the previously investigated long route. The departure is set to 49° North 005° West on 01 January 2016 at 00:00 and the arrival to 49° North 008° West on 01 January 2016 at 06:00. The weather data along the sample route, which is included in the output of the weather routing system, is given in Tab. 7.3. It is to be noted that the u- and v-components of current and wind are provided in the GRIB data in line with Tab. 6.3 and are converted to speed and direction. The module shown in Fig. 6.11 is used to read, preprocess and verify the data.

The consistency of the values at different times and positions is tested by means of commercial software, namely Matlab and NavStation. Matlab enables the decoding of GRIB data and its visualization as well as retrieving the values of all wind and wave

parameters listed in Tab. 6.3 at a specific time and position. The higher resolution of the current data leads to larger files affecting the processing with Matlab. Concerning the wind data, Matlab provides the u- and v-components which helps to verify the conversion in wind speed and direction given in Tab. 7.3. The converted values are verified using NavStation. In this regard, Fig. 7.5 shows the time series of current and wind speed as well as wind wave and swell wave height at a sample point, more precisely

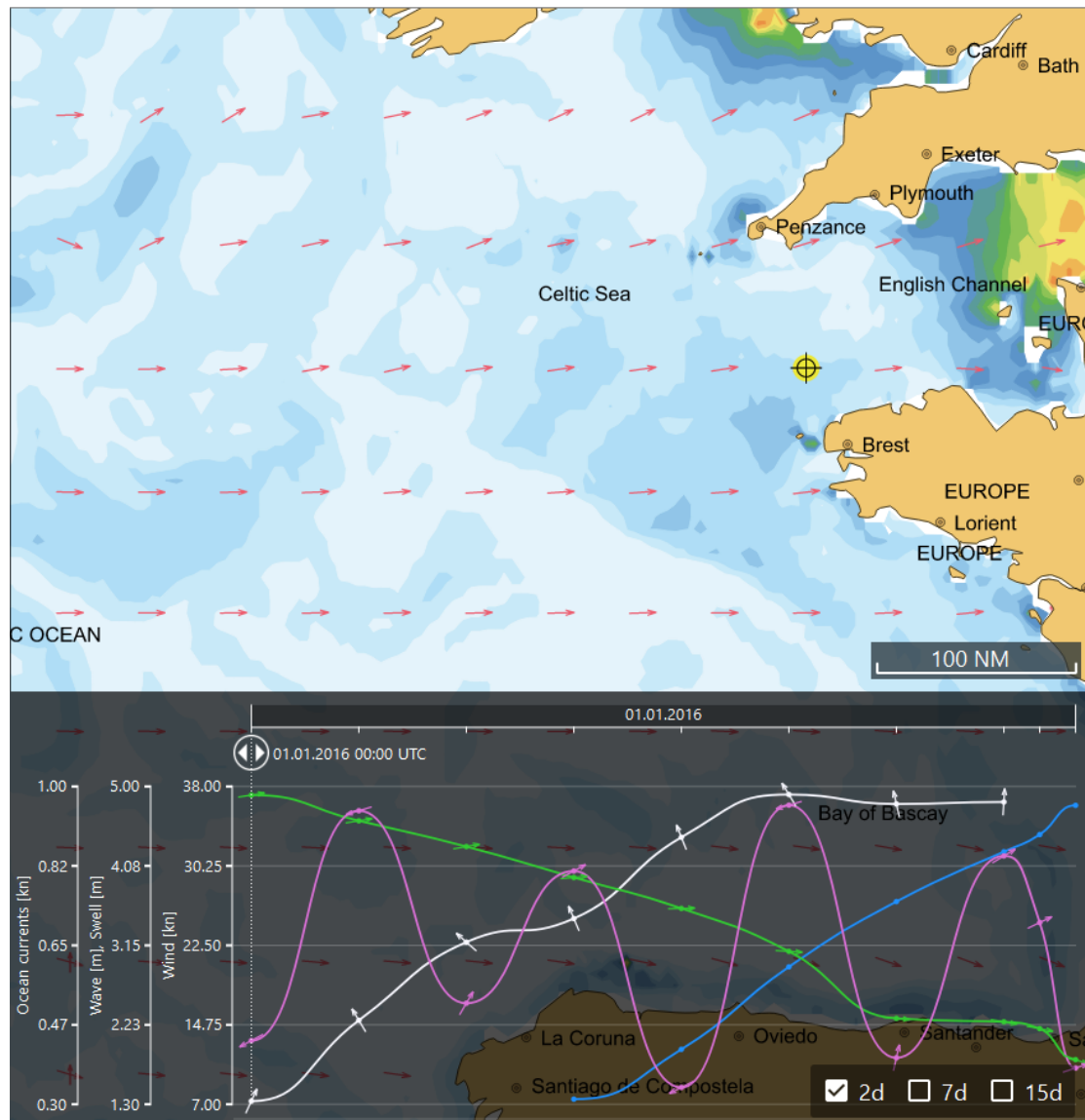


Figure 7.5: Graphical Display of Global Combined Current (Filling) and Swell (Arrows). Time Series of Ocean Current (Purple), Wind Waves (Blue), Swell Waves (Green) and Wind (White) at $49^{\circ}\text{N } 005^{\circ}\text{W}$ Visualized in NavStation

7 TESTING AND APPLICATION OF THE SYSTEM

at 49°N 005°W , for the period of one day. Additionally, the global combined current on 01 January 2016 at 00:00 is graphically displayed. Similarly, Fig. 7.6 visualizes the swell height on 01 January 2016 at 06:00 displayed in NavStation. The current speed, wind speed and the significant height of the swell waves at the beginning and end of the voyage are plotted in the time series graph. Considering slight rounding differences, comparisons show that the weather data is handled correctly.

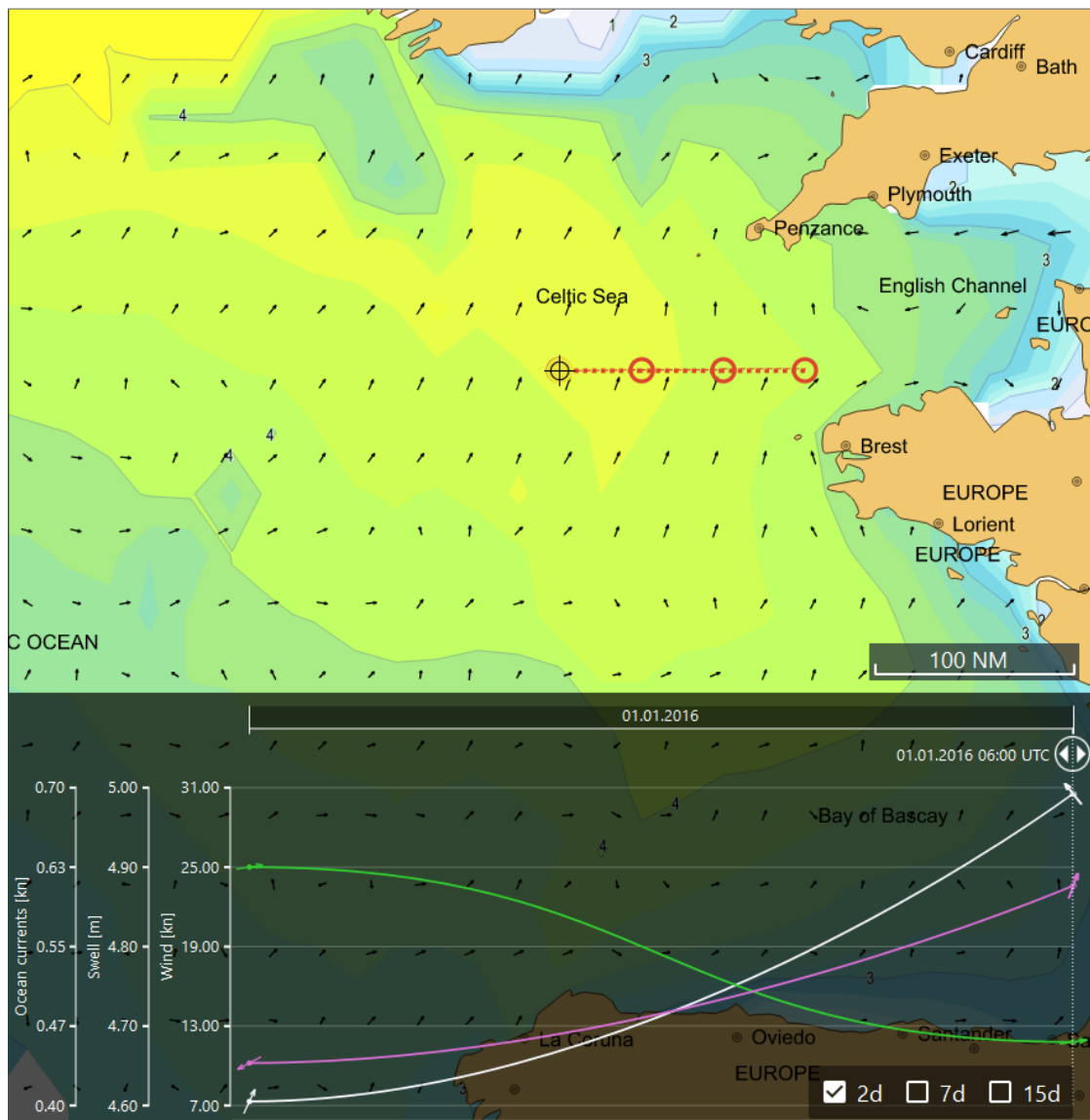


Figure 7.6: Graphical Display of Swell (Filling) and Current (Arrows). Time Series of Ocean Current (Purple), Swell Waves (Green) and Wind (White) for Sample Route Visualized in NavStation

Table 7.4: Added Resistance Data along Sample Route

Parameter	Unit	1 to 2	2 to 3	3 to 4
Time between waypoint i and j (t_{ij})	h	2.0	2.0	2.0
Distance between waypoint i and j (d_{ij})	nm	39.4	39.4	39.4
Speed over ground (V_G)	kn	19.7	19.7	19.7
Ground course (α_G)	degree	270.4	270.4	270.4
Speed through water (V_S)	kn	19.0	19.5	19.9
Heading angle (ψ)	degree	271.3	269.5	268.8
Calm water resistance (R_0)	kN	1 649.9	1 726.2	1 793.7
Added resistance due to wind (R_{Wind})	kN	42.0	33.2	0.3
Added resistance due to waves (R_{Wave})	kN	635.7	609.5	647.4
Total ship resistance (R_T)	kN	2 327.6	2 368.9	2 441.4
Delivered power (P_D)	kW	31 557.8	32 940.6	34 677.4
Specific fuel oil consumption (SFOC)	g/kWh	157.3	158.2	159.5
Fuel consumption (m_{Fuel})	t	11.3	11.9	12.6

With respect to the ship's performance, Tab. 7.4 lists figures derived with the added resistance method. The computed figures are verified by manual calculations taking into account the relations described in Chpt. 5, the ship data specified in Sec. 7.1 and the weather conditions given in Tab. 7.3. Between two consecutive waypoints the weather at the second waypoint is assumed. The derived total fuel consumption amounts to 35.9 tons, which is printed in the GUI in Fig. 6.4 after the calculation. A comparison of the resistance values, particularly the calm water resistance, with figures given by Riesner et al. (2016, pp. 29, 112) shows a fairly good agreement. As to the wind resistance, the values are reasonable bearing in mind that the wind frontal and lateral areas have been adapted. Moreover, southeasterly winds are considered in the weather routing system in addition to the wind resistance induced by the ship's own speed.

As an example, the added resistance due to waves amounts to 647.4 kN between waypoint 3 and 4 at a ship speed through water of 19.9 kn, a wave height of 4.7 m, a period of 13.2 s and an encounter angle of approximately 180° . Assuming a speed of 22.2 kn between waypoint 3 and 4, the added resistance increases to 702 kN. This matches the value of 698 kN computed with GLRankine for very similar conditions, i.e. a speed of 22.2 kn, a wave height of 4.5 m, a period of 12.5 s and the same angle, by Riesner et al. (2016, p. 112). Last but not least, the values of the engine power are within an expected range and below SMCR at 37 620 kW. It is to be noted that the margin of 12 % given in Sec. 7.1 is not yet added to the corresponding SFOC in Tab. 7.4.

The second ship performance method, i.e. the added power method, is validated within the research project by Abdel-Maksoud et al. (2016, pp. 49–52). Since the method is

Table 7.5: Added Power Data along Sample Route

Parameter	Unit	1 to 2	2 to 3	3 to 4
Calm water resistance (R_0)	kN	1 649.9	1 726.2	1 793.7
Added resistance due to wind (R_{Wind})	kN	42.0	33.2	0.3
Added resistance due to waves (R_{Wave})	kN	635.7	609.5	640.2
Added resistance due to rudder (R_{Rudder})	kN	0.8	1.1	5.4
Total ship resistance (R_T)	kN	2 328.3	2 370.0	2 439.5
Propulsive efficiency (η_D)	-	0.733	0.738	0.740
Delivered power (P_D)	kW	31 004.9	32 140.6	33 704.4
Specific fuel oil consumption (SFOC)	g/kWh	157.1	157.7	158.8
Fuel consumption (m_{Fuel})	t	11.1	11.6	12.2

said to consider the input data as expected and allows to predict the added power in real weather conditions in accordance with the accuracy of the input data, it is focused on verifying the output. When considering weather data from Tab. 7.3 as input, it needs to be kept in mind that directions are defined as 'coming from'. Based on the effective directions of the weather impacts, the computed hull, drift, wind and rudder forces and moments, more precisely their absolute values and directions, have been continuously verified during the development process. In this regard, it is noted that the drift angle (β_D) in Fig. 5.3 is opposite to that defined by Abdel-Maksoud et al. (2016, p. 28). Also the procedure of calculating the wind forces differs slightly but leads to the same results.

Values for comparison with the added resistance method can be found in Tab. 7.5. The total fuel consumption of 35.0 tons is just a little lower which results from a higher propulsive efficiency combined with the drift motion and rudder impact. Between waypoint 3 and 4, the drift angle leads to a change in the wave encounter angle, and thus to a lower added resistance due to waves. This partly compensates the added resistance due to the rudder. In summary, the results computed with both methods and presented in Tab. 7.4 and 7.5 respectively are the same, as far as comparable, and agree with manually calculated figures.

7.2.2 Validation

In order to ensure that the developed weather routing system yields reasonably valid results and adequately solves the problem, the validation mainly focuses on the comparison of computed figures with actual data collected on board of the ships of the A15 class. Initially, the resistance calculation is roughly validated based on sea trial data by Hapag-Lloyd (2018a). The data comprises information on the prevailing weather conditions, the ship's speed as well as the main resistance components. While the calm water resistance is 9 % lower, the wind resistance is increased by 5 %. Both deviations can be attributed to the difference in draught of one meter.

Table 7.6: Sample Voyages for Validation

Parameter	Voyage 1	Voyage 2	Voyage 3	Voyage 4
Departure date and time	21/01/2016 13:00	06/02/2016 18:00	06/09/2016 19:00	03/12/2016 16:00
Arrival date and time	27/01/2016 13:00	17/02/2016 06:00	12/09/2016 07:00	08/12/2016 03:00
Departure location	51°22.824'N 002°31.546'E	33°02.046'S 030°57.828'E	06°08.151'N 094°08.250'E	39°19.356'N 000°17.827'E
Arrival location	11°08.478'N 017°48.552'W	02°57.556'N 100°49.560'E	14°11.298'N 056°33.702'E	31°45.372'N 031°54.984'E
Total time	144.0 h	252.0 h	132.0 h	107.0 h
Total distance	2 738.6 nm	4 756.1 nm	2 324.1 nm	1 605.5 nm

As to the added resistance in a seaway, a deviation of 27% occurs. The forces in a seaway are derived using the strip code PDSTRIP. Strip methods are principally valid for long waves with lengths greater than approximately 40% of the ship's length, thus around 140 m (Söding and Bertram 2009, p. 40). In this case, the wave period of 3 s corresponds to a wave length of 14 m at a significant height of 0.6 m. Although results are rather inaccurate in this range, the absolute value of the added resistance is smaller than 0.2% of the calm water water resistance, and thus has a minor impact. Keeping in mind, among others, the small amount of data and the lack of information on ocean currents, the rough estimate shows sufficiently good agreement and indicates the correct order of magnitude of the resistance values.

In addition, four sample voyages are selected for validating computed figures with actual data collected on board. Key information of the voyages related to departure and arrival as well as voyage time and distance is summarized in Tab. 7.6. The routes are vi-

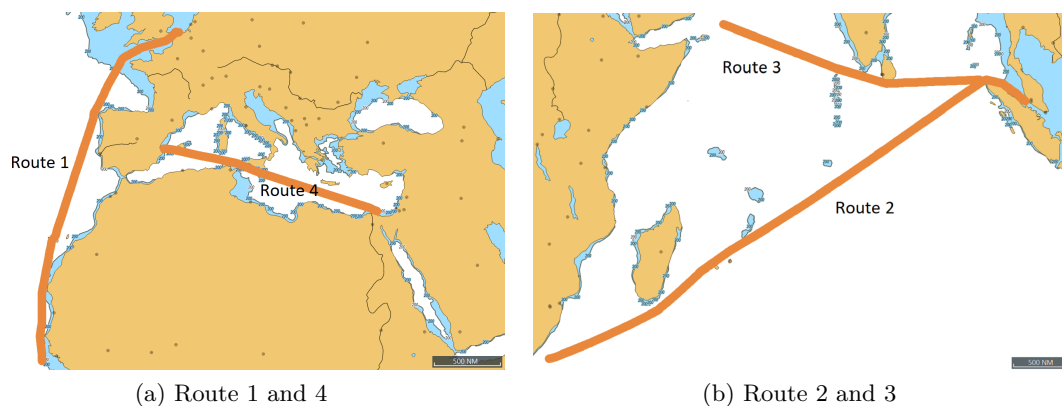
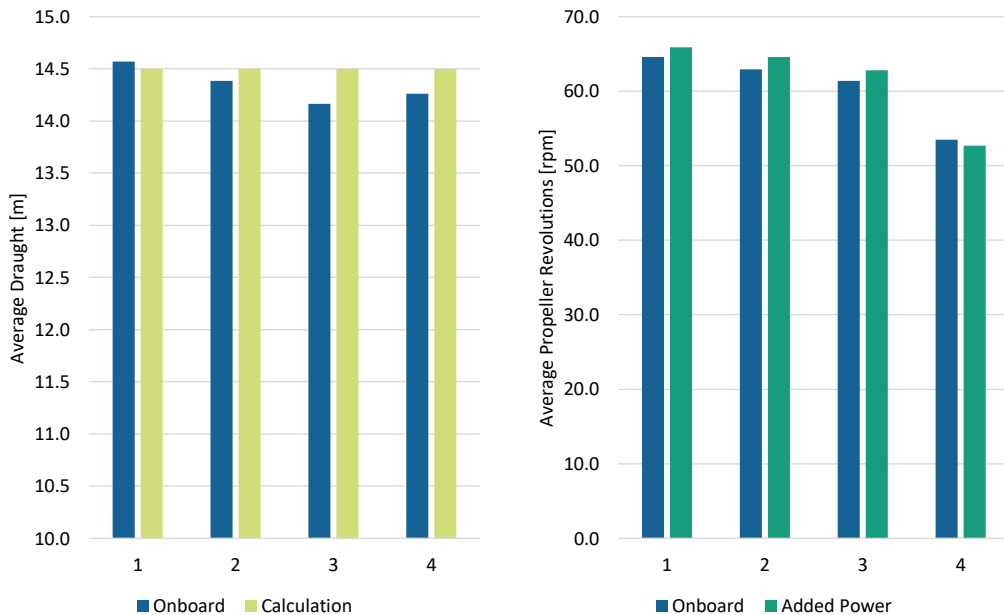


Figure 7.7: Graphical Visualization of Routes used for Validation in NavStation

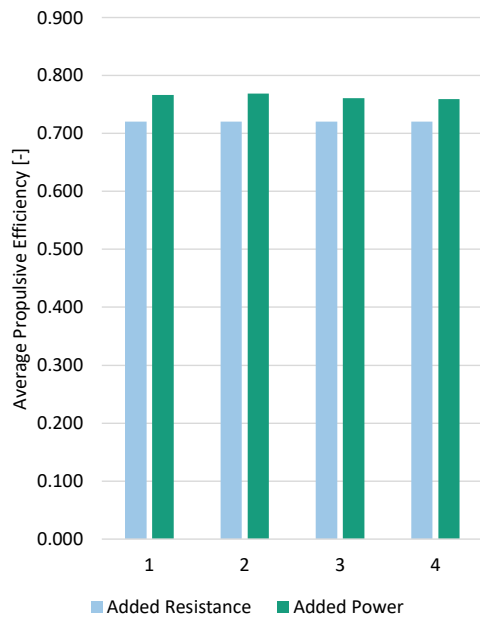
sualized in Fig. 7.7 based on data given every 15 minutes which leads to a high number of points along each route. The ship data available for calculations with the weather routing system is limited to the design condition at a draught of 14.5 m. Although draught measurements generally tend to be error-prone, they give at least an indication of a similar loading condition. The voyages are chosen in such a way that the draught deviates on average by less than 2% from the design draught, as shown in Fig. 7.8a. The influence of trim is neglected which can cause the fuel consumption to deviate by up to 3%.

For each voyage, the route and speed profile are derived from the actual data. This allows to assess the validity of the ship performance methods using the weather routing system without solving an optimization problem from Tab. 6.1. As an example, the ship's speed over ground (V_G or SOG) and through water (V_S or STW) during Voyage 1 are visualized in Fig. 7.9a. As expected, the calculated SOG derived from position and time information matches the onboard data almost exactly. In contrast, the STW deviates on average only by 2%, but in the maximum by +/-17%. This is not surprising, since the spatial resolution of the global combined ocean and tidal current data provided by Tidetech has been reduced from 0.1° to 0.5° when used by the weather routing system due to reasons of file size and handling efforts. Combined with a temporal resolution of one hour, the influence of the considered current data is substantially less accurate than that observed in the onboard data with steps of 15 minutes and less than 0.05° . The variations in STW are also reflected in the calculated propeller revolutions in Fig. 7.9b and the delivered power in Fig. 7.9c. Looking at the onboard data, both parameters fluctuate less. It is to be noted that only the added power method yields the propeller

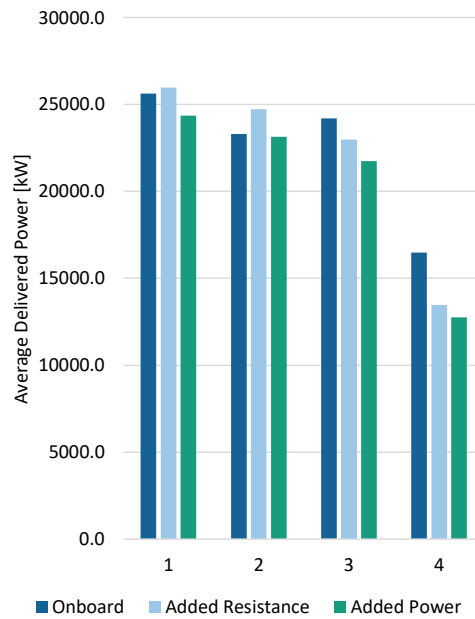


(a) Avg. Draught Midships

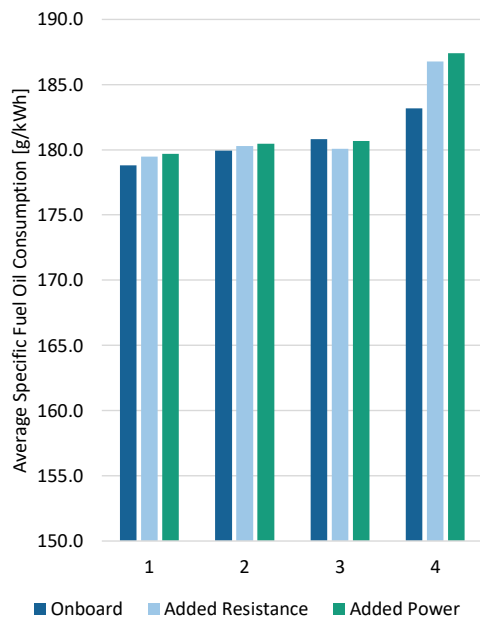
(b) Avg. Propeller Revolutions



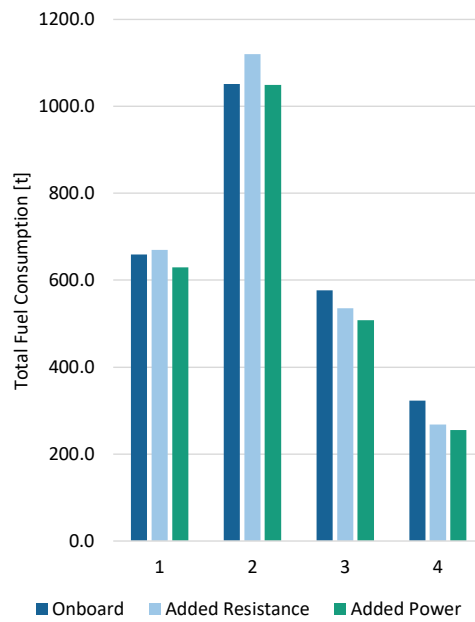
(c) Avg. Propulsive Efficiency



(d) Avg. Delivered Power



(e) Avg. SFOC

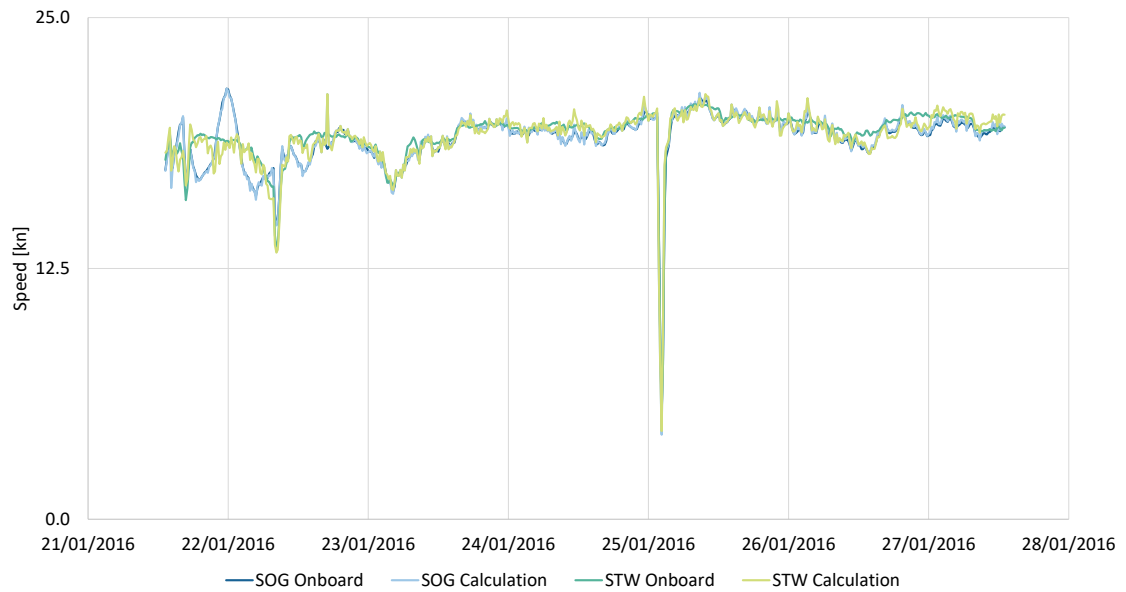


(f) Total Fuel Consumption

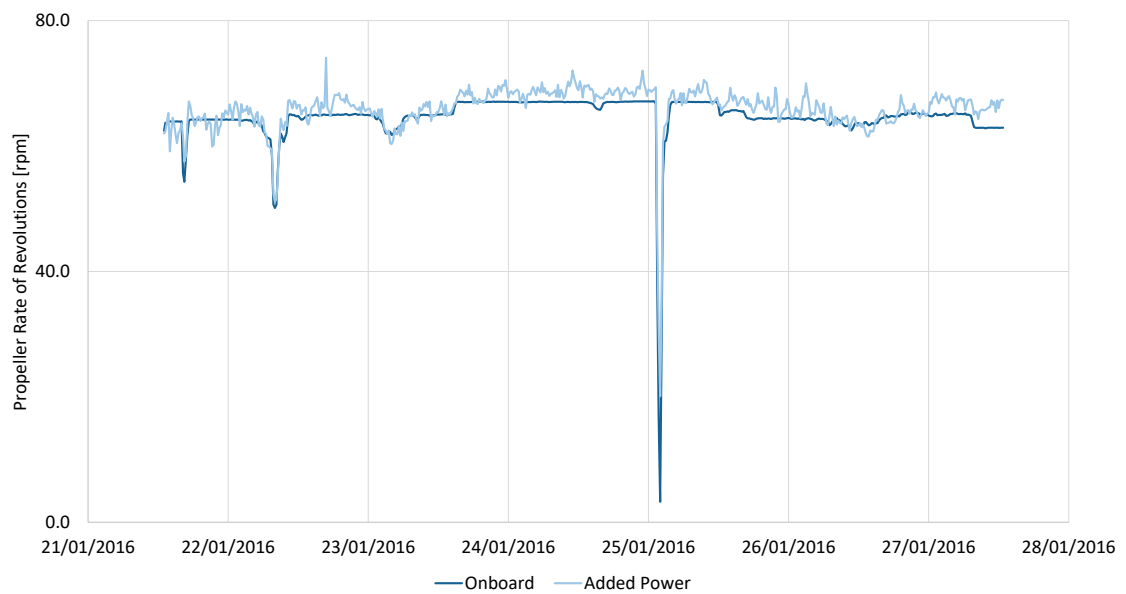
Figure 7.8: Comparison of Operational Data of Sample Voyages

revolutions. The graphs for the other three voyages showing similar effects can be found in the appendix in Fig. A.1a to A.3c.

The average propeller revolutions in Fig. 7.8b obtained with the added power method are up to 3% higher for Voyage 1 to 3 and 1% lower for Voyage 4 compared to the on-board data. Here, it needs to be pointed out that the actual propeller is slightly larger



(a) Speed Over Ground and Through Water



(b) Propeller Revolutions

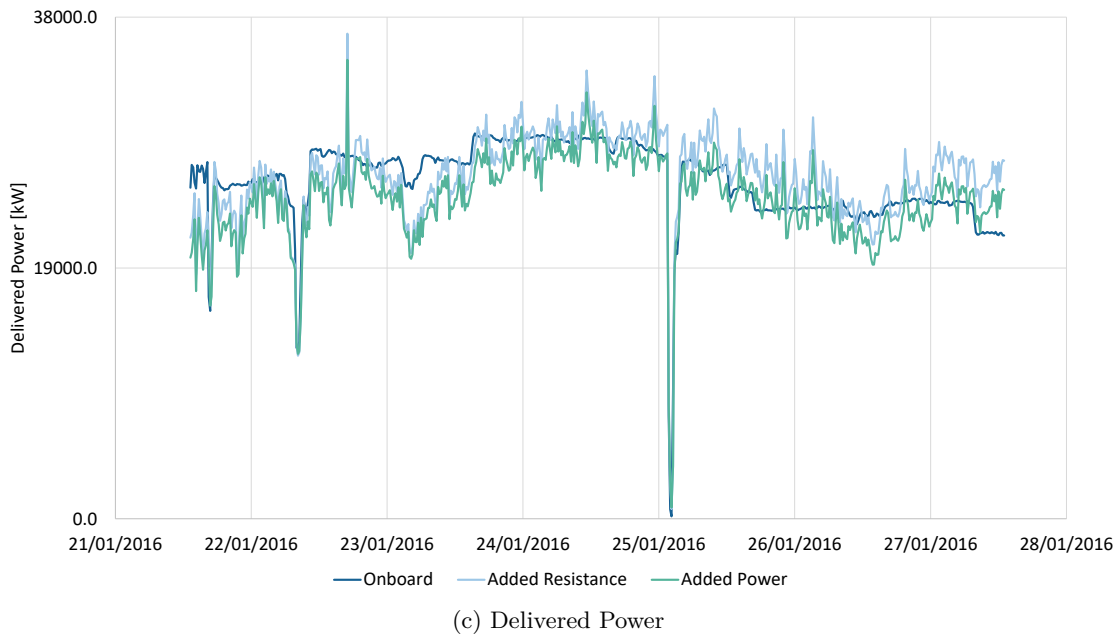


Figure 7.9: Time Series of Operational Data during Voyage 1

than the one, for which the open-water diagram is assumed. Moreover, the propulsive efficiency in Fig. 7.8c is not available for the class of built ships. While it is assumed to be constant in the added resistance method, it is influenced by the open-water diagram in the added power method. On average, the figures for Voyage 1 to 4 are 5 % to 7 % above the constant value of 0.72. Since the average SFOC value for each voyage is approximately the same, the difference of 5 % to 6 % in average delivered power can also be seen in the total fuel consumption, as indicated in Fig. 7.8d to 7.8f. Although the drift motion and rudder impact, thus an additional resistance, are taken into account, the higher propulsive efficiency leads to a lower fuel consumption. These relations are particularly interesting when comparing both methods in the next section.

Comparing the values to the onboard data in Fig. 7.8d to 7.8f, the deviation of the measured and calculated average power ranges from +5 % in case of Voyage 2 and the added resistance method to -23 % in case of Voyage 4 and the added power method. Accounting for a 2 % lower onboard SFOC value than the calculated value for Voyage 4 and about the same for the other voyages, the order of magnitude of the deviations is transferred from the delivered power to the consumption. The figures indicate that the average power requirement and consequently the total fuel consumption tend to be underestimated. Likely reasons relate to effects mentioned above and in Sec. 5.2.2, particularly metocean impacts, trim and fouling.

For Voyage 4, the difference between the onboard data and the calculation is rather large. In contrast to the comparably similar ranges of wind speed in Fig. 7.10c, the wave

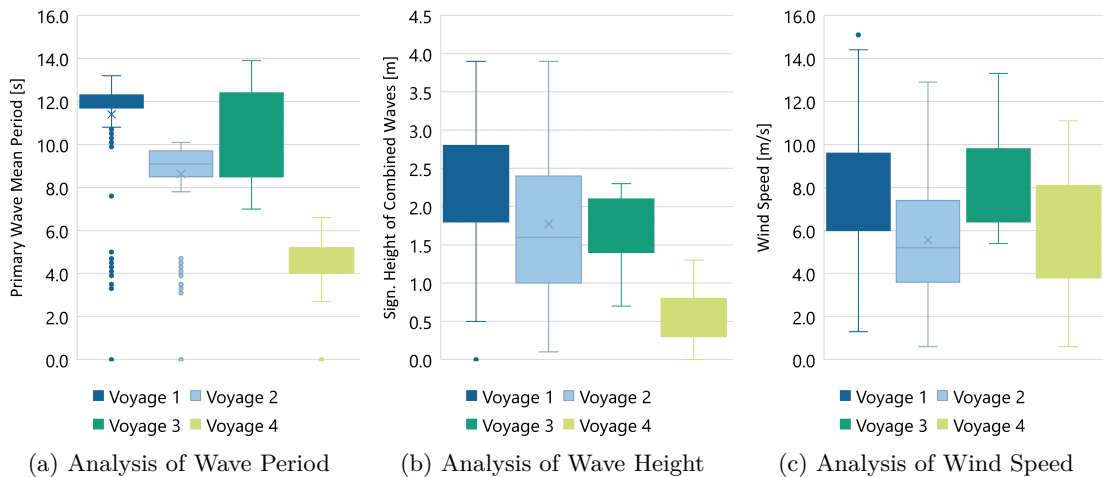


Figure 7.10: Analysis of Metocean Conditions during Sample Voyages

conditions during Voyage 4 shown in Fig. 7.10a and 7.10b noticeably differ to the other voyages. Wave lengths that correspond to the periods in Fig. 7.10a range from 3% to 19% of the ship's length. Although strip methods are principally only valid for waves longer than approximately 40% of the ship's length, it is to be noted that the impact of waves shorter than 20% with a small height on added resistance is relatively small. It is less than 2% of the calm water resistance in this case. Another notable aspect refers to the average STW of about 15 kn during Voyage 4 compared to 18 to 19 kn during the other voyages. Generally, the required power is underestimated at lower speeds.

In summary, the quality of the figures is influenced by the measurement accuracy of the onboard data as well as the limits and assumptions of the weather routing system and its input data. This includes the variation in measurements and sensor data, assumptions that cause the ship data to differ from the actual ship class and the negligence of further added resistance components. Against this background, the results derived with the weather routing system show sufficiently good agreement with the onboard data.

7.3 Evaluation of Scenarios

In order to evaluate the influence of the two ship performance methods on ship weather routing and to demonstrate the robustness of the results, sensitivity analyses are conducted. A sensitivity analysis is the testing of the optimal solution of an optimization model for reactions against changes in the initial data (Domschke et al. 2015, p. 48). Not only coefficients of the objective function but also those of the variables and the constraints can be changed. Thus, scenarios are defined to assess the influence of the ship performance methods on weather routing when varying the optimization problem, the arrival time, i.e. the ship's average speed, and the weather conditions. The obtained results are evaluated and discussed.

Table 7.7: Departure and Arrival Data of the Voyage Scenarios

Parameter	Voyage 1	Voyage 3
Departure date and time	21/01/2016 13:00	06/09/2016 19:00
Arrival dates and times	27/01/2016 21:00 28/01/2016 16:00 29/01/2016 17:00	12/09/2016 04:00 12/09/2016 20:00 13/09/2016 17:00
Departure location	51°30.000'N 002°30.000'E	06°00.000'N 094°00.000'E
Arrival location	11°00.000'N 018°00.000'W	14°00.000'N 056°30.000'E

7.3.1 Definition of Scenarios

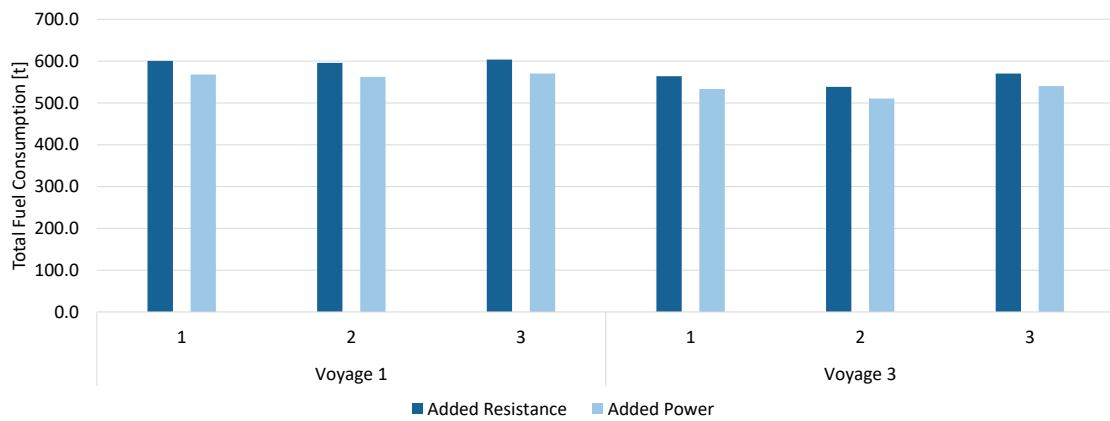
On the basis of the previous verification and validation, two scenarios are chosen to conduct sensitivity analyses. Voyage 1 and 3 shown in Fig. 7.7 are selected. The departure and arrival data is summarized in Tab. 7.7. It is to be noted that the departure and arrival locations are rounded compared to Tab. 7.6. The ship data presented in Sec. 7.1 is used as input for all calculations. Tab. 7.8 provides an overview of all calculation runs performed with the developed weather routing system. The aim to assess the influence of both ship performance methods in combination with three optimization problems and two voyages results in 12 runs. Furthermore, the ship's average speed is varied by considering three different arrival times mentioned in Tab. 7.7, which lead to an approximate speed of 14 kn and 16 kn in addition to the reference speed of 18 kn. In order to investigate the impact of weather conditions, both voyages are optimized based on weather data for each month from January to December. When varying the ship's speed and weather conditions, a minimum distance route, thus the third optimization problem, is assumed. In total, 64 runs are performed.

Table 7.8: Overview of Calculation Runs

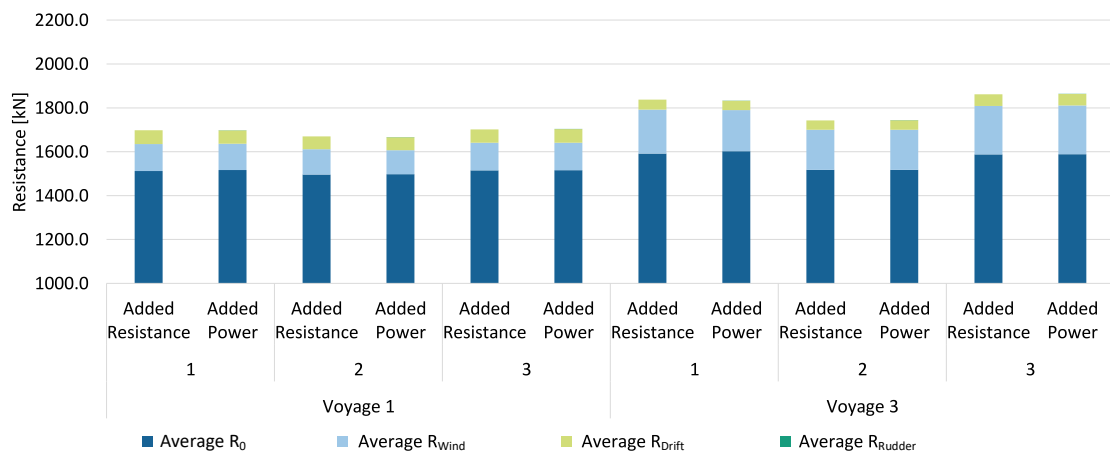
Voyage	Optimization Problem	Method	Avg. Speed	Month	Sum of Runs
1	1 and 2	Added Resistance and Added Power	18 kn	Jan	4
1	3	Added Resistance and Added Power	14 kn and 16 kn	Jan	4
1	3	Added Resistance and Added Power	18 kn	Jan-Dec	24
3	1 and 2	Added Resistance and Added Power	18 kn	Sep	4
3	3	Added Resistance and Added Power	14 kn and 16 kn	Sep	4
3	3	Added Resistance and Added Power	18 kn	Jan-Dec	24

7.3.2 Influence of the Problem

The weather routing problem can be formulated differently as to the number and type of objectives, variables, constraints and parameters, which influences the derived fuel consumption. Three optimization problems with the objective of minimum fuel consumption that can be solved by the developed weather routing system are listed in Tab. 6.1. Based on Tab. 7.8 and both voyages, the impact of the two ship performance methods in combination with the three optimization problems is analyzed. The results for Case 1 with variable route and speed, Case 2 with variable route at constant speed and Case 3 with variable speed at minimum distance are compared in Fig. 7.11. Fig. 7.12a shows the resulting routes for Voyage 1, where the westernmost route at the latitude of Morocco results from Case 3. The routes for Case 1 and 2 show slight deviations between Portugal and Western Sahara. In Fig. 7.12b, the resulting routes for Voyage 3 mainly deviate

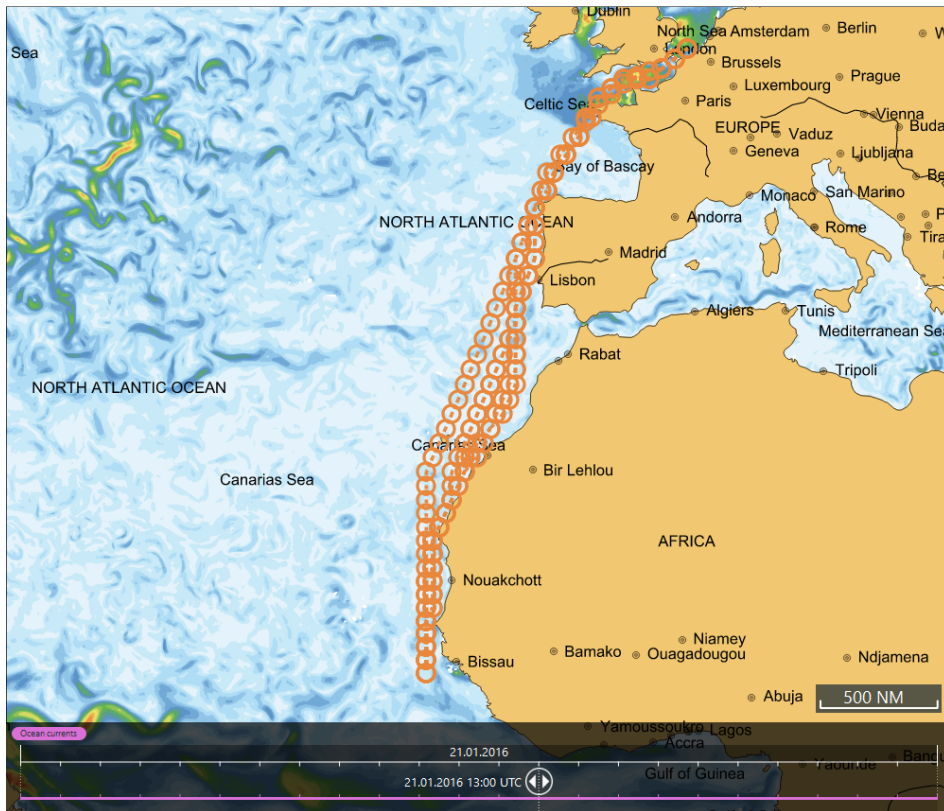


(a) Fuel Consumption

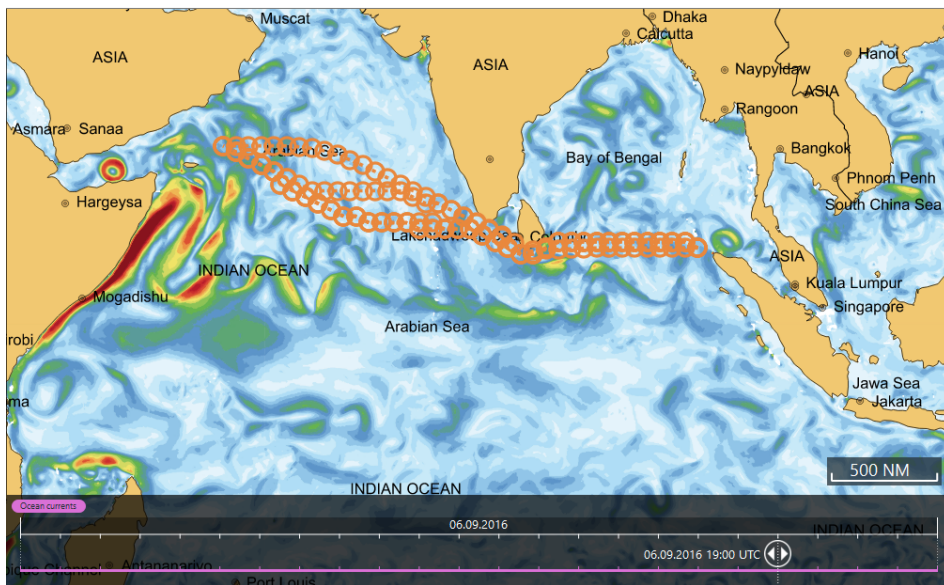


(b) Resistance Components

Figure 7.11: Impact of Optimization Problem on Consumption and Resistance



(a) Voyage 1



(b) Voyage 3

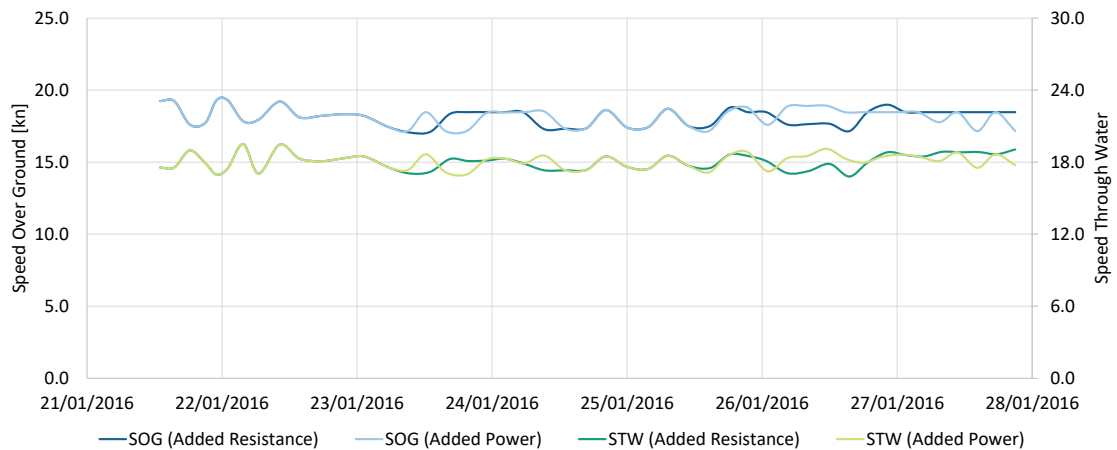
Figure 7.12: Graphical Visualization of Resulting Routes in NavStation

between India and the arrival location with the northernmost route resulting from Case 3. Case 1 with optimization of route and speed is assumed as reference.

The time series of the results for Case 1 and Voyage 1 are displayed in Fig. 7.13, while those for Voyage 3 can be found in the appendix in Fig. A.4. Fig. 7.13a indicates that the greatest impact of ocean currents causing a speed difference of up to 2 kn occurs at the beginning of the voyage. Slight deviations in the speed profile for both methods match the differences particularly in wind speed in Fig. 7.13b. The influence of the speed profile is also reflected by the time series of the propeller revolutions in Fig. 7.13c as well as the total resistance and delivered power in Fig. 7.13d.

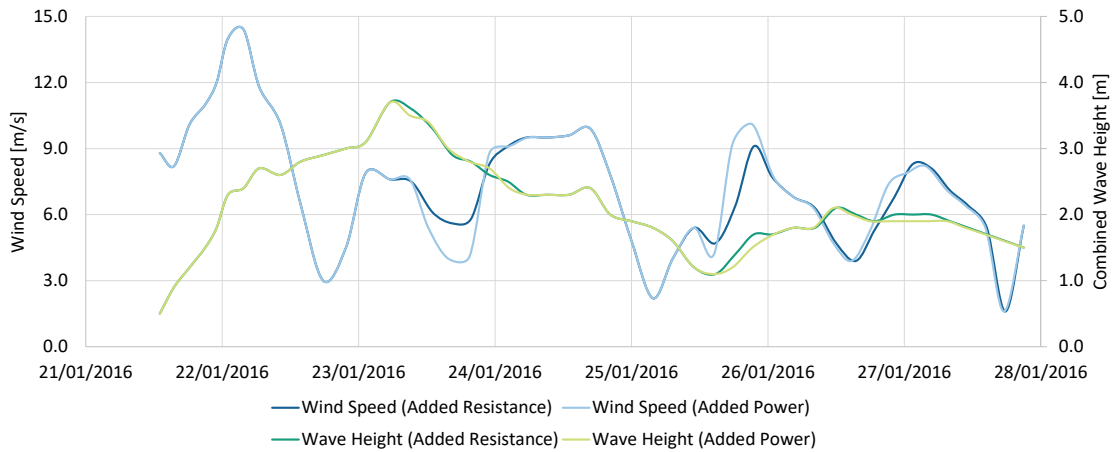
In Case 1 and 3, arrival for Voyage 1 is on 27 January 2016 21:00 and for Voyage 3 on 12 September 2016 04:00. In Case 2, it is a calculation result, which leads to an arrival at 22:33 for Voyage 1 and the added resistance method and 23:04 for the added power method. For Voyage 3 and both methods arrival is at 08:01. Due to the corresponding increase in voyage time of approximately 1 % and 3 % respectively, the average calm water resistance R_0 is reduced by 1 % and 5 % compared to Case 1, as shown in Fig. 7.11b. This results in a reduction of the total fuel consumption in Fig. 7.11a by 1 % and 4 %. In contrast, the consumption in Case 3 is roughly 1 % higher for both voyages and methods compared to Case 1. This results from an increase in the average total resistance, although the calculated minimum distance is 1 % shorter for Voyage 1 and 2 % for Voyage 3.

When analyzing the impact of the ship performance methods, the results support the trend observed during the validation in Sec. 7.2.2. For both voyages and all three problems, the propulsive efficiency for the added power method is on average 6 % above the constant value of 0.72. For Voyage 1 and Case 1, this can be seen in Fig. 7.13c. The increase is passed on to the average delivered power and to the total fuel consumption, as the specific fuel oil consumption is almost constant. Fig. 7.11b shows hardly any

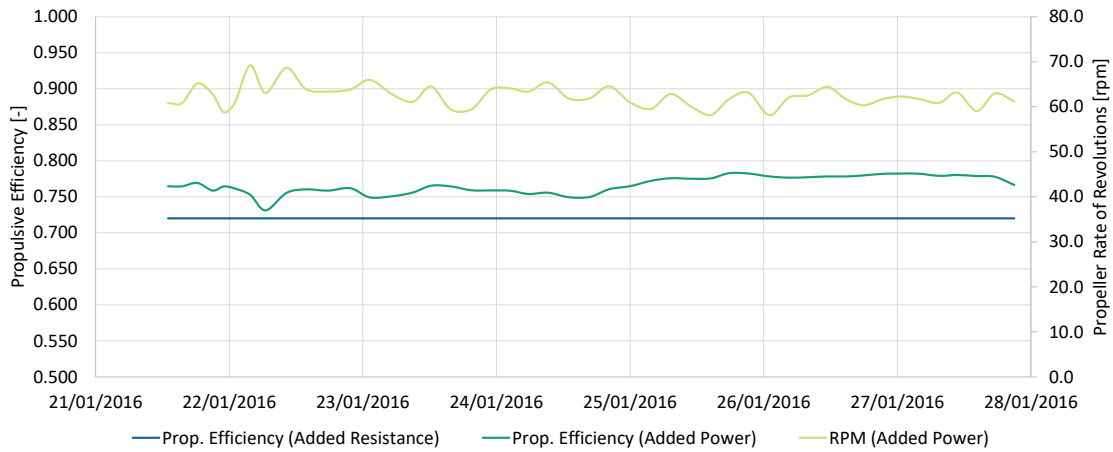


(a) Speed Over Ground and Through Water

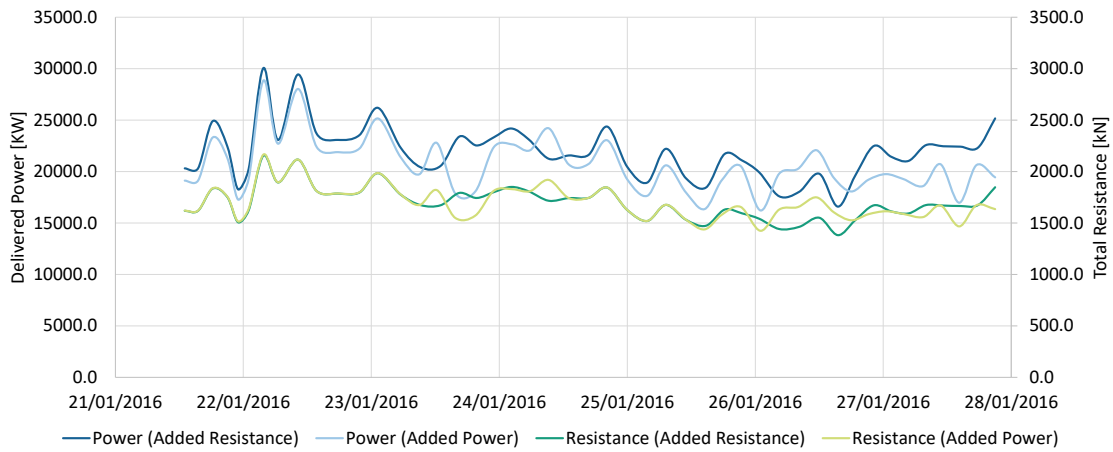
7.3 EVALUATION OF SCENARIOS



(b) Weather Conditions



(c) Propulsive Efficiency and Revolutions



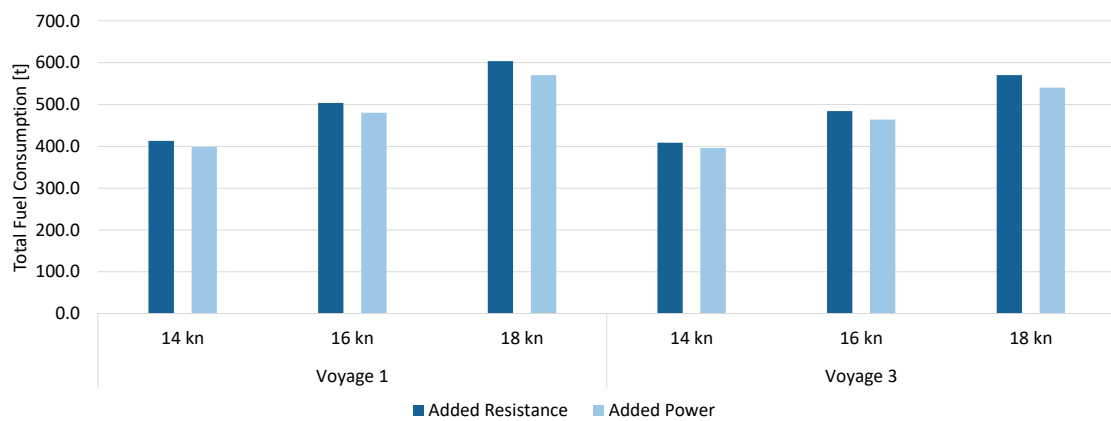
(d) Total Resistance and Delivered Power

Figure 7.13: Time Series of Optimization Results for Voyage 1

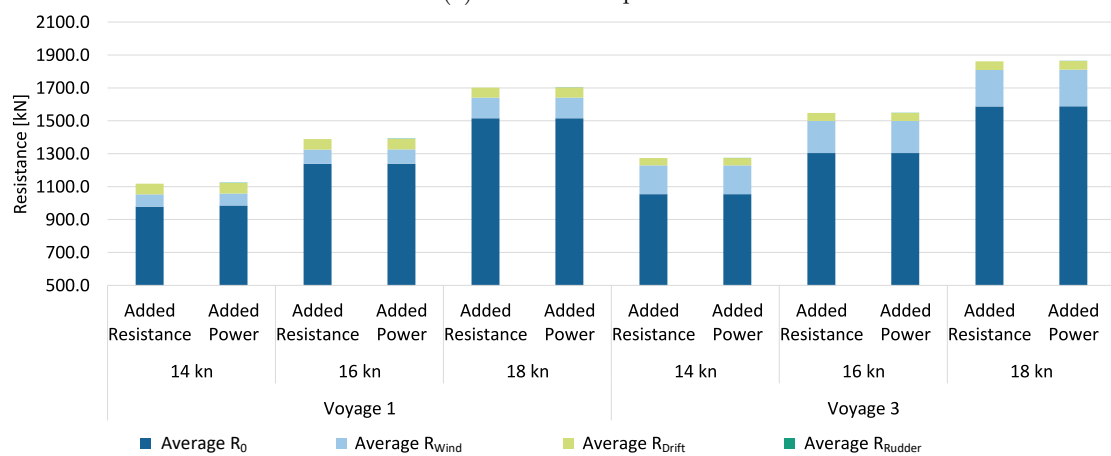
variation in resistance for the different ship performance methods, since the route and speed profile are very similar and the average additional resistance caused by the rudder is less than 1 kN. Hence, despite the consideration of drift motion and rudder impact, the lower fuel consumption can be mainly attributed to a higher propulsive efficiency.

7.3.3 Influence of Ship Speed

The ship speed significantly influences the fuel consumption, since the required propulsive power is proportional to approximately the third or fourth power of the speed depending on the ship. Hence, three different arrival times listed in Tab. 7.7 are taken into account, which lead to an approximate speed of 14 kn and 16 kn in addition to the reference speed of 18 kn. To eliminate the impact of varying routes, only the speed is optimized by solving the third optimization problem from Tab. 6.1 based on a minimum distance route. The results for both voyages are compared in Fig. 7.14 with regard to



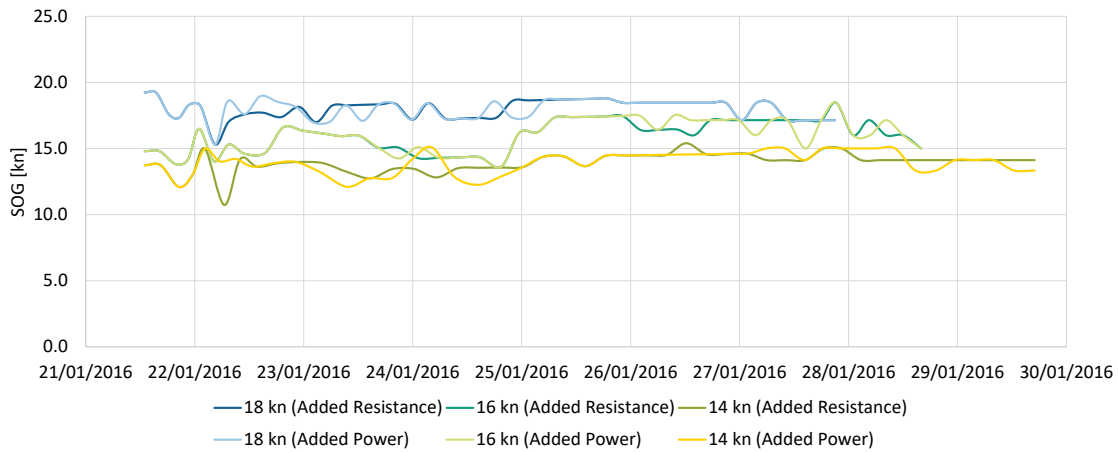
(a) Fuel Consumption



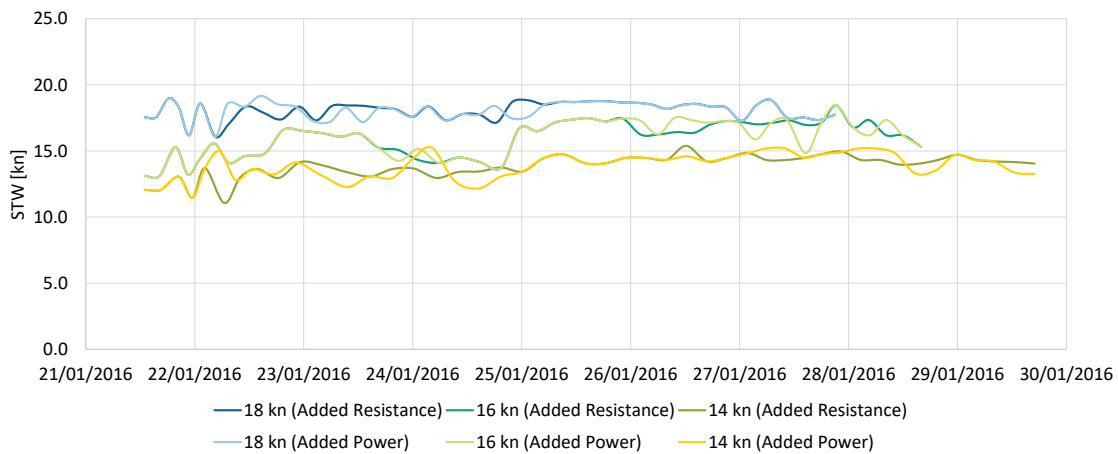
(b) Resistance Components

Figure 7.14: Impact of Ship Speed on Consumption and Resistance

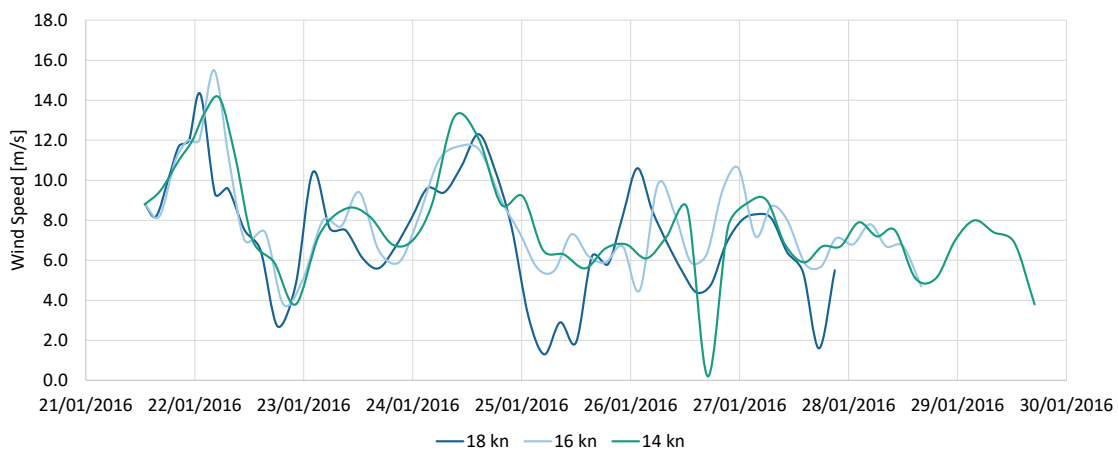
7.3 EVALUATION OF SCENARIOS



(a) Speed Over Ground



(b) Speed Through Water

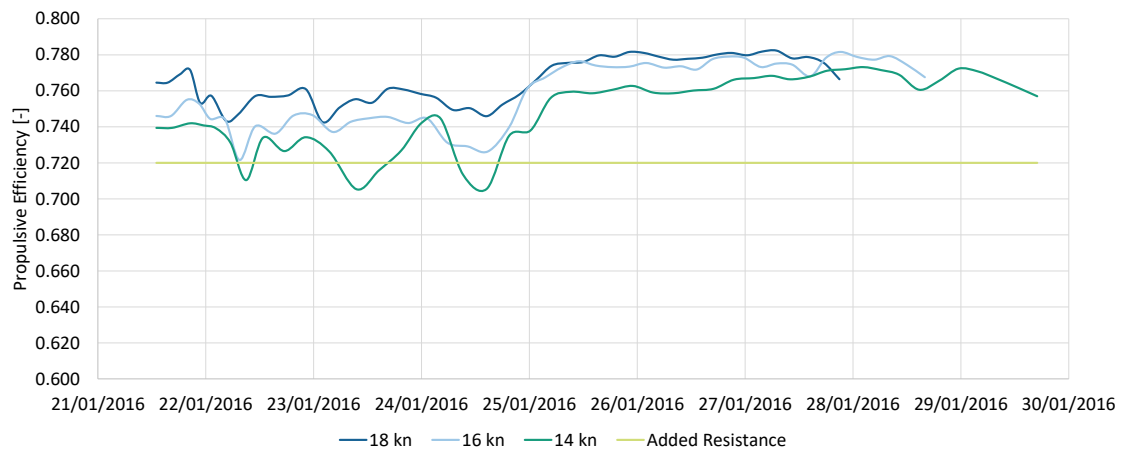


(c) Wind Conditions

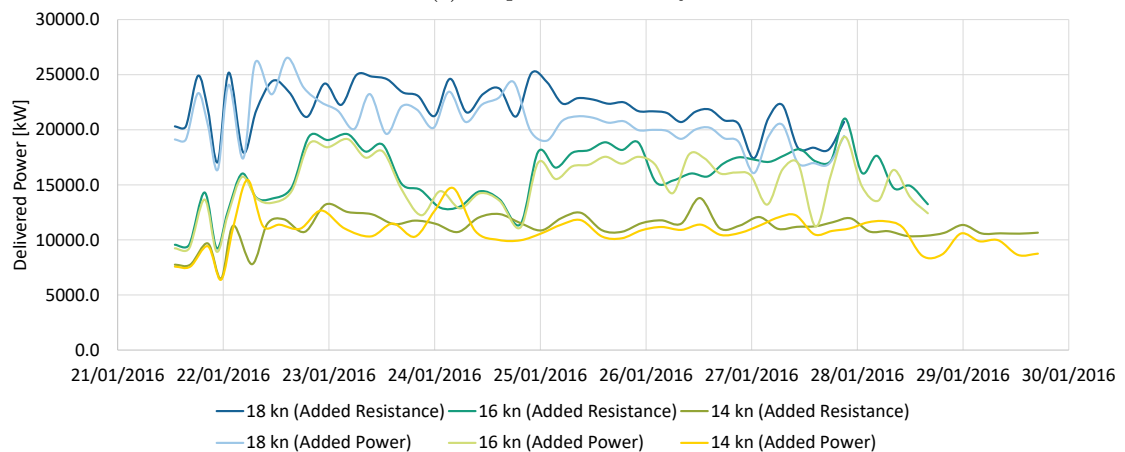
7 TESTING AND APPLICATION OF THE SYSTEM



(d) Wave Conditions



(e) Propulsive Efficiency



(f) Delivered Power

Figure 7.15: Time Series of Results for Voyage 1 with Varying Arrival Times

total fuel consumption and resistance. The time series of the results with varying arrival times for Voyage 1 are shown in Fig. 7.15. The time series for Voyage 3 are given in the appendix in Fig. A.5 and reveal the effects even more clearly.

The varying arrival time results in an average reduction of speed over ground and through water by 11 % and 22 % respectively, as indicated in Fig. 7.15a and 7.15b. Along with the slower voyage progress, the experience of stronger wind speeds or higher waves shifts in time, which can be seen in Fig. 7.15c and 7.15d as well as in the appendix. It is to be noted that the figure shows the weather conditions based on the added resistance method as both are similar. Regardless of the ship performance method, the total resistance shown by component in Fig. 7.14b decreases by 18 % and 34 % respectively for Voyage 1 and 17 % and 32 % for Voyage 3.

In case of Voyage 1, the reduction in average wind resistance of 31 % and 41 % contributes most. It is followed by the average calm water resistance decreased by 18 % and 35 %. In contrast, the average added resistance due to waves increases by approximately 5 % and that due to the rudder even by 76 % and 104 % which, however, still is below 2 kN. In case of Voyage 3, the increase in rudder resistance of 15 % and 50 % is smaller. All other components experience a decrease with the reduction in calm water resistance contributing most. While the average calm water resistance is reduced by 18 % and 34 %, the added resistance due to wind is 12 % and 21 % lower and the added resistance due to waves 8 % and 16 %.

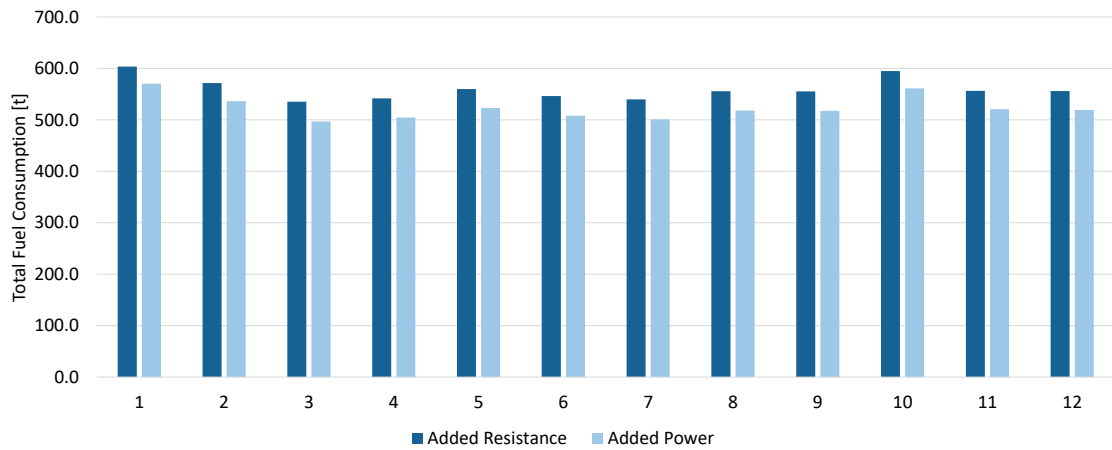
Concerning the propulsive efficiency, the added resistance method is based on the assumption of a constant value of 0.72. In case of the added power method and both voyages, the average propulsive efficiency is approximately 6 %, 5 % and 4 % higher for an average speed of 18 kn, 16 kn and 14 kn. This is indicated by Fig. 7.15e. Thus, the delivered power not only reflects the respective decrease in total resistance, but also the difference in the propulsive efficiency. Since there is almost no impact on the specific fuel oil consumption, the effect is passed on to the total fuel consumption shown in Fig. 7.14a. In summary, the fuel consumption derived with the added power method is lower regardless of the ship's average speed. This is similar to the previous comparisons. However, the lower the average speed is, the smaller the difference becomes, as the propulsive efficiency approaches the assumption of the added resistance method.

7.3.4 Influence of Weather Conditions

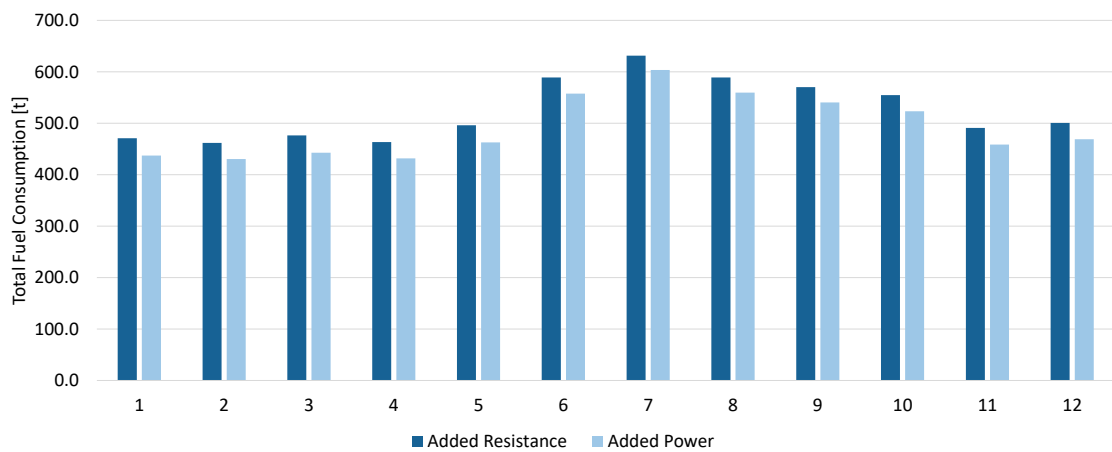
The influence of weather conditions is investigated by shifting the month of departure and arrival. Hence, both voyages are optimized for each month from January to December. To analyze the impact on the ship's speed and thus the resistance and fuel consumption, only the speed is optimized while a minimum distance route is assumed. Thus, the third optimization problem from Tab. 6.1 is solved. The results for both ship performance methods are compared for the months from January to December and for Voyage 1 and 3 in Fig. 7.16. As seen in the previous analyses, these figures emphasize

the trend that the added power method generally yields a lower total fuel consumption for a voyage. Again, the difference in consumption can be explained by the difference in propulsive efficiency which is 5 % to 8 % higher.

The speed through water during Voyage 1 is analyzed for both methods in Fig. 7.17a and 7.17b. Both figures present an almost identical picture with the same range of speed and only slight differences from one month to the other. However, Fig. 7.17c and 7.17d show a variation in wind speed and wave height throughout the year between January and December. The same trend is not only reflected by the resistance in Fig. 7.17e but also by the total fuel consumption in Fig. 7.16a. While the average calm water resistance only varies slightly in line with the speed through water, the impact of wind and waves on the respective resistance components is notable.

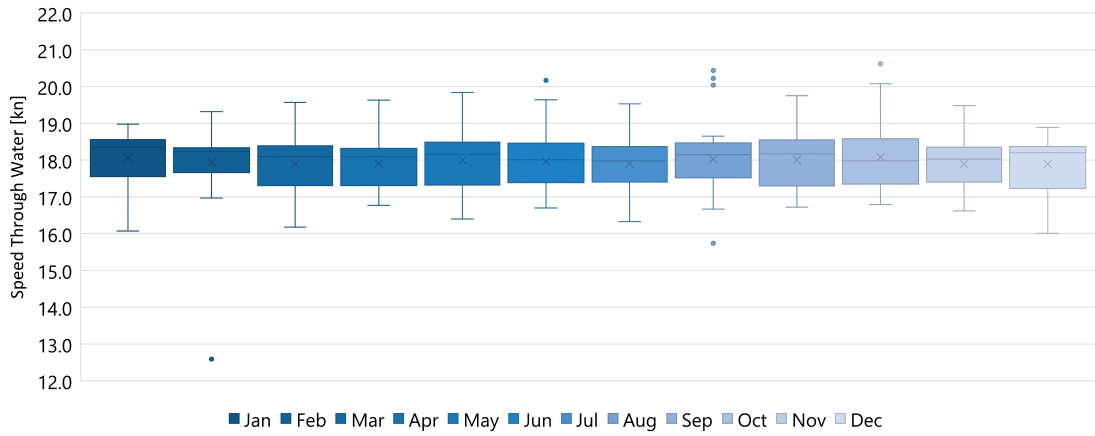


(a) Voyage 1

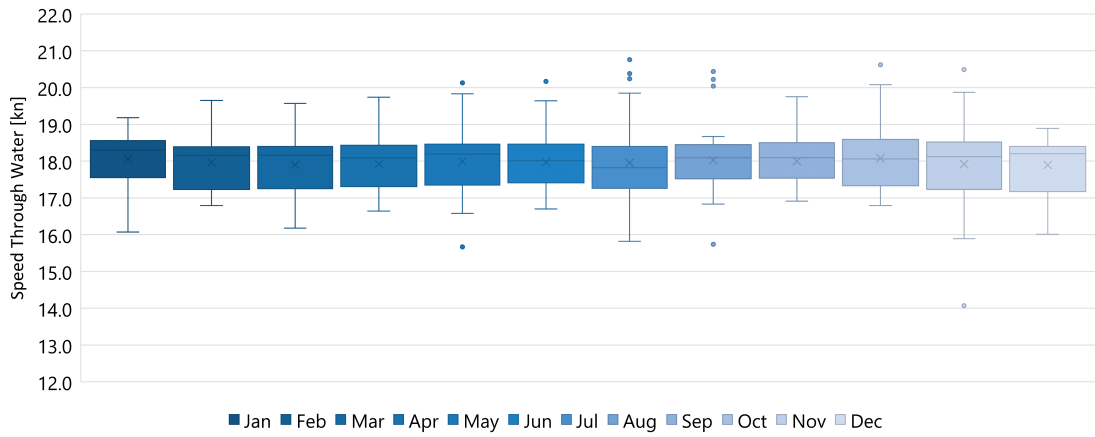


(b) Voyage 3

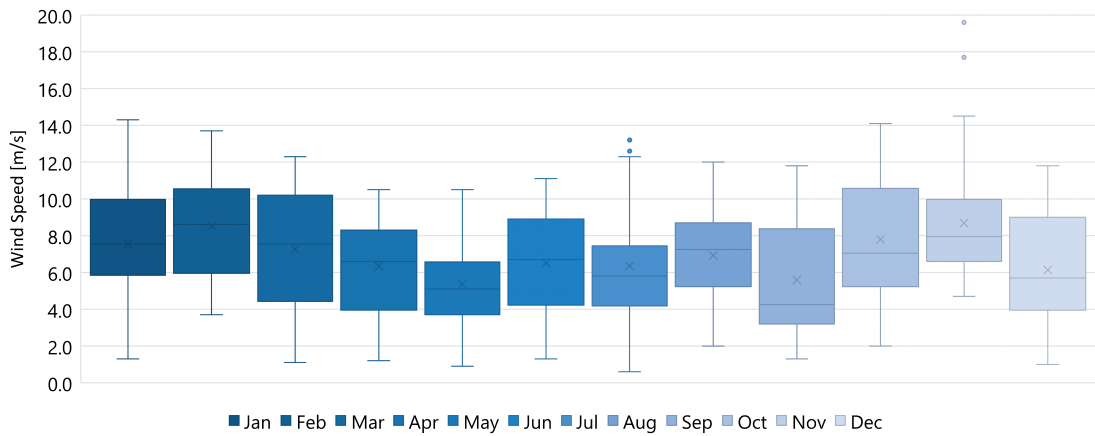
Figure 7.16: Weather Sensitivity of Total Fuel Consumption for Voyage 1 and 3



(a) Speed for Added Resistance Method

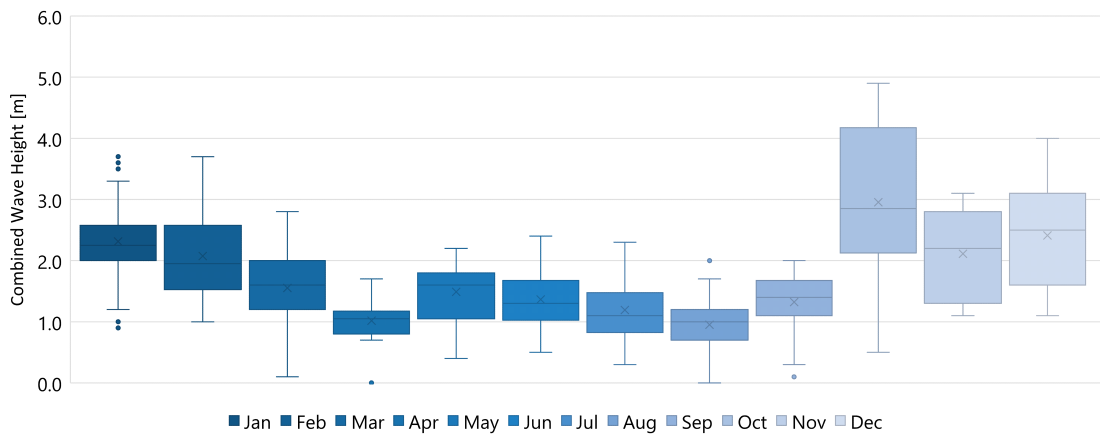


(b) Speed for Added Power Method

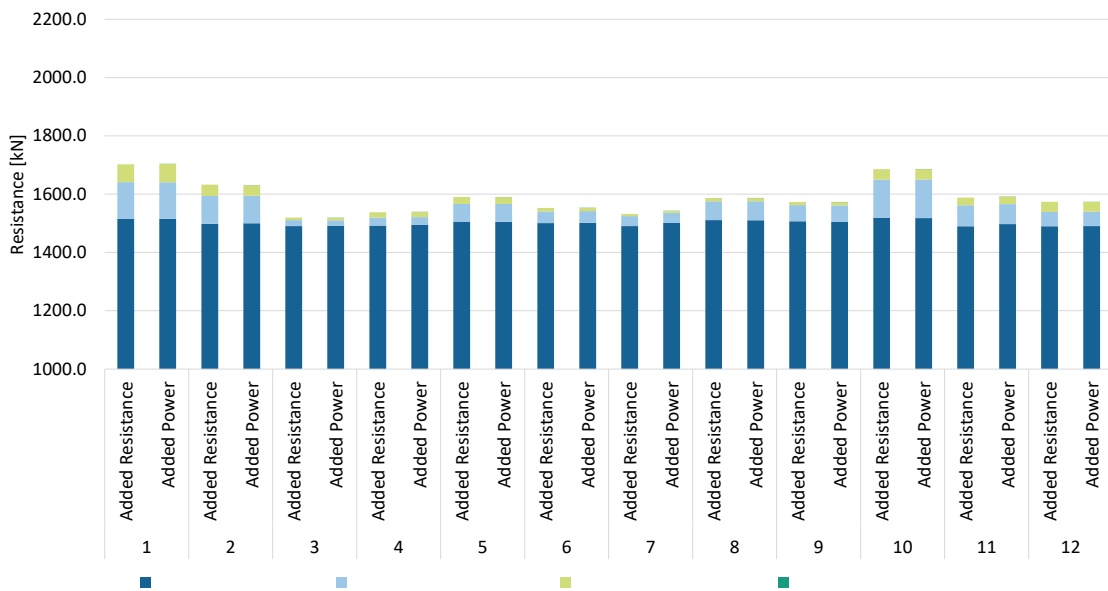


(c) Wind Speed

7 TESTING AND APPLICATION OF THE SYSTEM

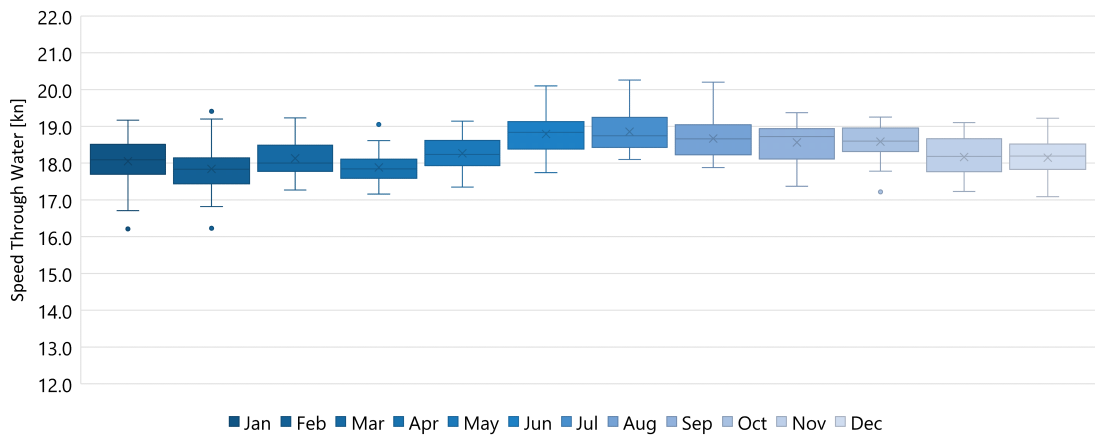


(d) Wave Height

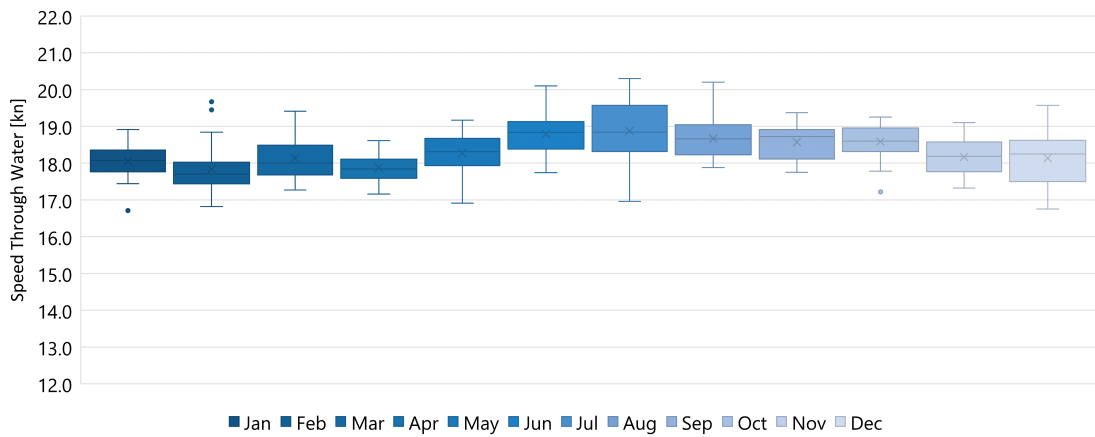


(e) Resistance Components

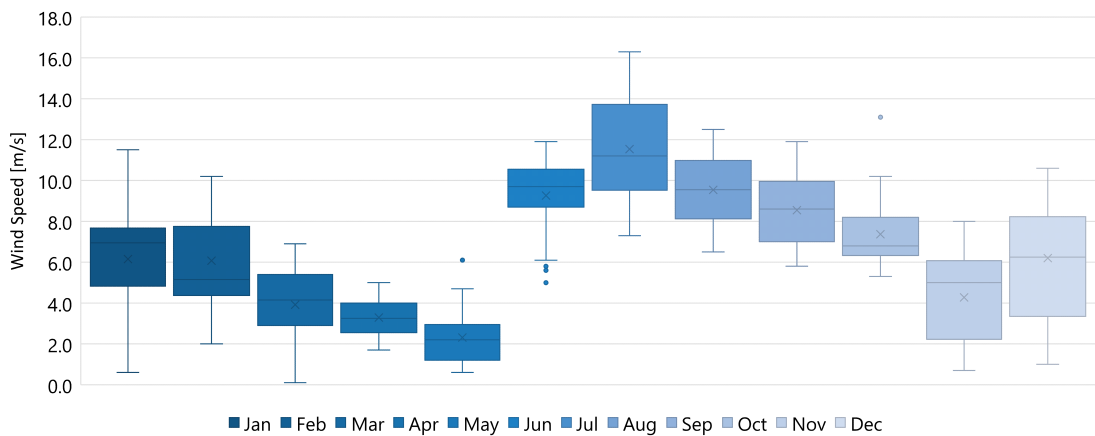
Figure 7.17: Weather Sensitivity of Voyage 1



(a) Speed for Added Resistance Method

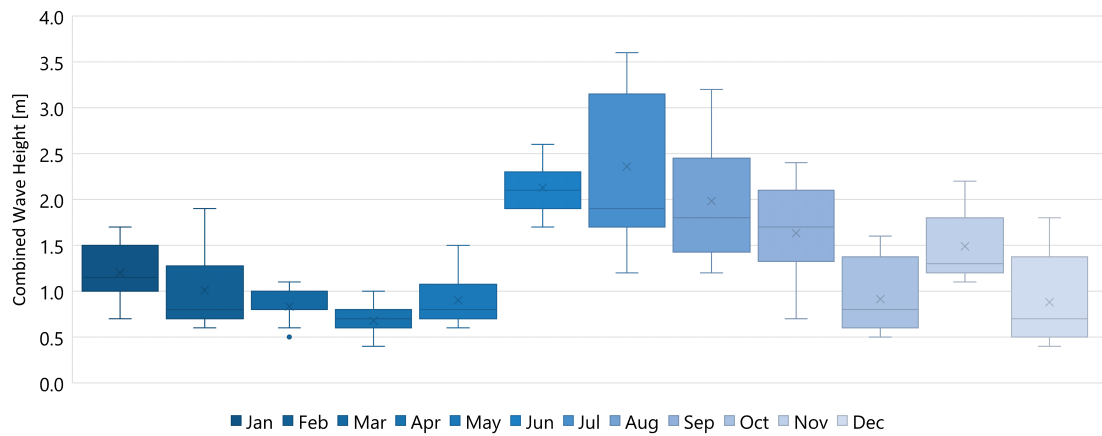


(b) Speed for Added Power Method

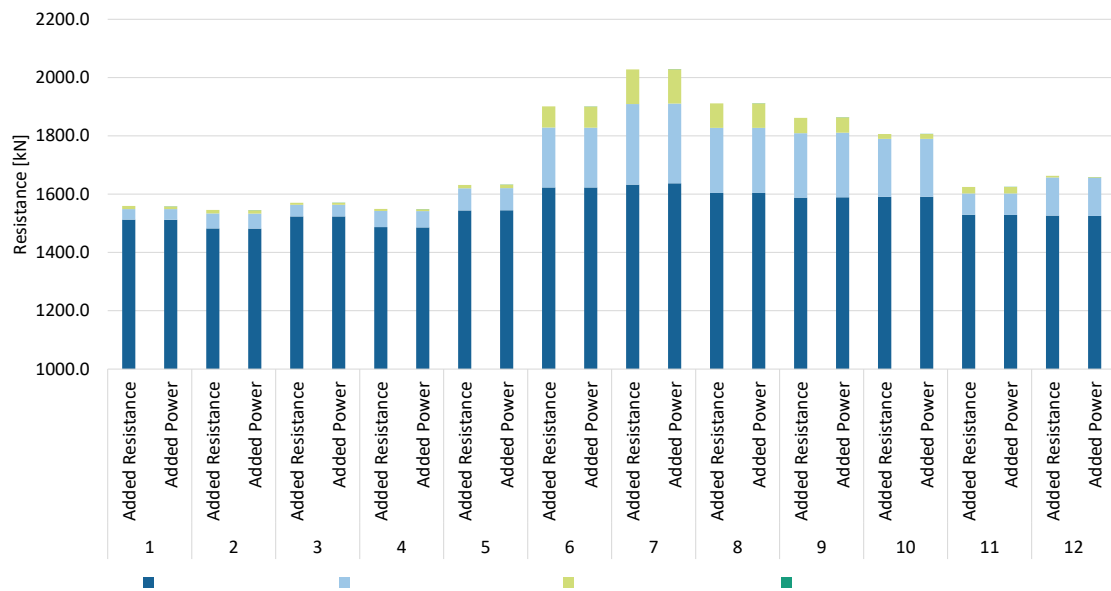


(c) Wind Speed

7 TESTING AND APPLICATION OF THE SYSTEM



(d) Wave Height



(e) Resistance Components

Figure 7.18: Weather Sensitivity of Voyage 3

The effects become even more obvious when looking at the analyses of Voyage 3 in Fig. 7.18. Although the picture regarding the speed through water is still very similar for both ship performance methods, a deviation depending on the weather conditions in the respective months can be seen. Also the analysis of the wind speed and wave height in Fig. 7.18c and 7.18d, which show very well the correlation of both metocean effects, reveals greater variations throughout the year than in case of Voyage 1. Nevertheless, the average calm water resistance in Fig. 7.18e varies along with the speed through water, while the added resistance due to wind and waves is substantially influenced by the prevailing metocean conditions.

7.4 Discussion of the Results

On the basis of the verification, the validation and the evaluation of the results derived with the developed ship weather routing system, the main findings are outlined. The verification shows that the weather routing system can handle weather data correctly with only minor rounding differences. It yields correct results for both ship performance methods based on the comparison with manually derived figures.

The validation is based on four sample voyages and the ship related input data described in Sec. 7.1. It needs to be kept in mind that the DTC and the built ships are only equivalent to a certain extent. Particularly the propulsion system as well as the wind lateral and frontal areas differ. The drift forces in a seaway are derived using the public-domain hydrodynamic strip code for seakeeping PDSTRIP. A comparison with results from RANS computations and model tests shows rather good agreement for waves longer than the ship's length but deviations in short waves. Due to the minor contribution to the total resistance in short waves, the values are assumed to be sufficiently accurate. Nevertheless, the validation and quality of according figures are influenced by assumptions regarding the ship data. Also variations in measurements and sensor data as well as the negligence of other added resistance components, such as due to trim and fouling, present influencing factors. Taking this into account, the computed figures and actual data collected on board agree comparably well for the four selected voyages. Concerning the comparison of both ship performance methods, it is to be noted that the higher propulsive efficiency leads to a lower fuel consumption for all four voyages in case of the added power method.

For evaluating the impact of the ship performance methods on weather routing systematically, two voyages are selected where the optimization problem, the arrival time, and the weather conditions are varied. All calculations emphasize the trend observed during validation that the added power method generally yields a lower total fuel consumption for a voyage than the added resistance method. This can be mainly attributed to a 5% to 8% higher propulsive efficiency resulting from changes in the open-water efficiency. The variation of the arrival time shows that the lower the average speed is, the smaller the difference becomes. This is because the propulsive efficiency approaches

the assumption of the added resistance method. Furthermore, the investigations indicate that the added resistance due to the rudder contributes on average less than 0.1 % to the total resistance. In summary, the evaluations emphasize the importance of considering engine and propeller characteristics but also demonstrate the minor contribution of integrating of a maneuvering model.

7.5 Limits and Benefits of the System

The development of the ship weather routing system including its testing and application reveals certain limits and benefits related to the mathematical modeling of the problem and the applied solution procedure.

For finding a solution to the considered weather routing problem, a solution procedure using the A* algorithm is presented. A* uses heuristic information to reduce the search space and achieve a speedup compared to algorithms such as Dijkstra's algorithm. However, Delling et al. (2009) report that the speedup is rather small for finding quickest routes in road maps especially when using the Euclidean distance between a node and the destination as conservative estimate. Furthermore, it is pointed out that significantly faster algorithms than classical approaches are available for route planning nowadays. In contrast, in case of the considered weather routing problem, computing the exact cost from the start node to any node, or between a node and its neighbor, is associated with a rather high computational effort. Consequently, the additional heuristic information leads to a speedup, which motivates the use of A*. This approach suffices the requirements within this research. Nevertheless, it cannot be denied that techniques to increase the efficiency, such as presented by Delling et al. (2009), may enhance the weather routing system. Hence, the corresponding adaptation of the algorithmic solution procedure can be seen as a meaningful subject of future research.

Due to the object of research, i.e. the question concerning the ship's performance and the adequate way of taking it into account, and the provided weather data resolution, the decision has been made to consider a graph with a static resolution and a comparably small spacing. On the one hand, this has the advantage of a more accurate consideration of changing weather conditions from one waypoint to another. Referring to the validation, it can be seen that a higher resolution of the ocean current would lead to an even better agreement with the onboard data. On the other hand, disadvantages particularly refer to the limitation of a stepwise adjustable speed and heading. Moreover, a captain generally prefers lesser waypoints requiring for example a change of speed. Hence, a dynamic grid with regard to the spatial and temporal resolution can be considered to be more favorable for practical purposes.

8 Conclusion and Outlook

Three main objectives are in the focus of this thesis to answer the research question, to which extent the integration of more extensive ship data and more complex models for ship dynamics and propulsion can be justified by an improved quality of results. The objectives relate to the determination of a suitable algorithmic solution procedure, to the design and implementation of a ship weather routing system as well as to the impact of ship performance methods on weather routing. Conclusions are drawn with respect to each objective and, correspondingly, further research potential is identified.

Weather routing is one of the most important operational measures to ensure safe and efficient navigation. It is generally supported by commercial systems offered by numerous providers. Analyzing quoted efficiency gains attributed to weather routing, though, reveals significantly varying numbers and a strong dependence on present ship operation, including climate, route and vessel performance. Accordingly, weather routing may particularly contribute to improved energy efficiency, reduced emissions and cost savings for certain routes. Since provided information on fuel savings only allows rough estimates, it is concluded that detailed case by case evaluations are required for quantitative assessments.

Particularly in harsh climates, weather routing has the greatest benefit. Environmental factors affecting a ship's voyage and its operation are generally winds, seas, currents, fog and ice. The ship's fuel consumption, thus the optimization objective, is primarily influenced by winds, waves and currents. Metocean information is provided by numerous institutions that typically use an internationally standardized binary code to exchange this data. Forecasts as well as hindcasts are generally derived from numerical models based on data collected from observations and measurements of the atmosphere and oceans. However, differences among others in resolution, global and regional configuration, data assimilation and the considered physics, result in a different output accuracy of every model and thus of weather routing systems using different input data. Within this thesis, hindcast data provided by Tidetech for the year 2016 is used for testing and application of the weather routing system.

Similar to various options regarding the choice of a weather data provider, also the weather routing problem can be formulated differently concerning the number and type of objectives, variables, constraints and parameters. Typically, ship weather routing aims at minimum fuel costs, minimum voyage time, maximum safety or a combination of these objectives, while taking into account meteorological and oceanographic information and various ship and voyage related constraints. Naturally, the weather routing problem is

a nonlinear problem. So far, it has been modeled as continuous or discrete problem, as stochastic or deterministic problem and as constrained or unconstrained problem. Moreover, it has been treated as a single-objective or a multi-objective problem with one or several decision variables. Algorithms employed in ship weather routing range from nonlinear approaches through graph theoretic and dynamic programming ones to metaheuristic methods. The evaluation of mathematical modeling and optimization algorithms as part of this thesis reveals a broad variety of approaches each with its own disadvantages and advantages. The compiled overview is one of the most comprehensive to date. Consequently, it presents a valuable contribution in the field of ship weather routing. Complementing existing studies, an interesting topic for future research relates to the detailed investigation of different algorithms applied to the same problem and the comparison of their effects on the routing results.

In accordance with the first objective, the overview aims to support the determination of a suitable algorithmic solution procedure to solve the constructed weather routing problem. Whether an approach is suitable and produces sufficient results depends largely on the specific requirements regarding accuracy and computational effort as well as the problem including optimization objectives, decision variables and constraints. The constructed ship weather routing problem is a single-objective and constrained optimization problem. It aims at minimum fuel consumption and is deterministic. The two decision variables, namely position and time, allow for speed and route optimization. The option to only vary one of the decision variables increases the number of solvable optimization problems to three.

Based on the popularity of approaches seen in the overview and the general discretization of routes and weather data, the problem is mathematically formulated using graph-related notions. The graph is connected, directed and acyclic with nonnegative arc weights. To solve the considered weather routing problem(s), a time-dependent version of the A* algorithm is employed. The applied solution approach suffices all the specific requirements related to the research objectives within this thesis. It allows to solve the three optimization problems, to consider all required constraints and to take into account the ship's performance when calculating the arc weights. Nevertheless, techniques to increase the efficiency can be seen as a meaningful subject for further improvement. Also a graph with a dynamic instead of static resolution is considered to be favorable to partly overcome the limitations associated with the spatial and temporal discretization.

In line with the second objective, the algorithmic solution procedure is translated into an executable program using the object-oriented programming language C++. The developed weather routing system including the weather data handling and the ship performance methods is successfully verified and validated. For this purpose, data from a hull design of a 14 000 TEU container ship named Duisburg Test Case, actual voyage data of a similar ship class and weather data provided by Tidetech are used. The validation is based on four sample voyages with a draught that roughly corresponds to the hull

design. It can be seen that variations in measurements and sensor data, assumptions regarding the ship data that deviate from the actual ship class and the negligence of additional resistance components influence the comparison. Keeping these assumptions, simplifications and deviations in mind, the results derived with the weather routing system show comparably good agreement with the onboard data. Furthermore, it is to be highlighted that many academic studies lack the availability of actual voyage data for a sound validation. Hence, the conducted testing presents a valuable contribution to the development of the weather routing system and encourages its future application.

Depending on the use case and application of the weather routing system, taking into account further aspects concerning weather data, safety or navigational restrictions can be desirable and reasonable. This can refer to the consideration of ensemble forecasts or statistical weather data but also of emission control areas, traffic separation schemes and shallow water effects. Furthermore, it can be related to stress and vibration monitoring or the impact of trim and fouling, which can have a notable impact on the fuel consumption of a ship. Also the integration and investigation of additional safety restrictions, e.g. related to passenger comfort and motion sickness, can be desirable. The system architecture and algorithm allow the developed system to be extended with regard to many further requirements.

In addition to the operational application, the developed weather routing system can be used during the design process of a ship. Since wind and waves cause an added resistance that reduces a ship's attainable speed, the ship's fuel consumption increases and delays can be caused. This in turn affects the profitability of a ship. To consider the expected environmental effects when designing a ship, wind and wave data from scatter diagrams is generally used. While the temporal and spatial relation of weather conditions is lost due to the statistical character of the data, hindcast data can be used to determine past best and worst case scenarios. This allows to evaluate the voyage time, fuel consumption and safety depending on the wave and wind conditions. Moreover, the likeliness of delays or the necessity to introduce measures to increase comfort can be assessed. Here, also the integrated maneuvering model may present an advantage, since among others rudder forces can be included in the optimization output to assess potential wear.

The third objective refers to assessing the impact of ship performance methods on weather routing. A ship's performance during a voyage significantly depends on the service conditions, i.e. ocean currents, wind and waves, as well as the ship itself. It is found that many weather routing systems aim to provide routing support to various types of ships. That is why simplified methods with a wide scope of application are popular to avoid the need for detailed ship data. Often, the movement of a ship is only considered based on the first equation of motion. Hence, the ship's total resistance needs to be balanced with an adequate propeller thrust. This is referred to as added resistance method where transverse drift forces and rudder forces are neglected. Only few

approaches have been published that also account for transverse motions or integrate a maneuvering model. So called added power methods generally consider three or more equations of motion and determine the required engine power accounting for the propeller and engine characteristics. The developed ship weather routing system allows to either select an added resistance method or an added power method when optimizing a ship's voyage. This is a unique feature that no other weather routing system offers in this form.

To answer the research question, sensitivity analyses are conducted to evaluate the influence of the two ship performance methods on weather routing and to demonstrate the robustness of the results. Therefore, the optimization problem, the arrival time, i.e. the ship's average speed, and the weather conditions are varied for two voyages. All 64 calculation runs show that the added power method generally yields a lower total fuel consumption for a voyage than the added resistance method. This is mainly caused by a higher propulsive efficiency. When varying the arrival time, it is found that the lower the average speed is, the smaller the difference becomes. This trend can be explained by the fact that the propulsive efficiency is approaching the constant value assumed in the added resistance method.

The evaluations point to the importance of considering engine and propeller characteristics in a ship weather routing system for reasons of accuracy. Drawing a conclusion from these assessments, it is suggested to integrate an open-water diagram or at least a speed dependent open-water or propulsive efficiency in such a system. In contrast, the integration of a maneuvering model is considered to be less important based on the evaluations. The minor impact of transverse drift and rudder forces on the resulting route, speed profile and consumption cannot compensate for the additional data requirements, development tasks and computational effort. Instead, it seems sensible to incorporate aspects such as trim and fouling and their influence on fuel consumption into the ship weather routing system.

In summary, the extensive overview of optimization approaches, the ship weather routing system itself and the conducted investigations contribute to advancing the research in the field of ship weather routing. The developed system with its optimization algorithm, its weather data handling and its ship performance methods as well as its GUI and modular structure offers various options for voyage optimization. It provides features that can keep up with commercial and academic applications and allows to consider ideas for further enhancements and extensions. In this way, various future research questions can be addressed in order to continuously improve the analysis and optimization of ship voyages.

Bibliography

- Abdel-Maksoud, M. (2009). *Manövrierfähigkeit von Schiffen. Skriptum zur Vorlesung*. Hamburg: Technische Universität Hamburg-Harburg.
- Abdel-Maksoud, M., V. Müller, and S. Handschel (2013). *Entwicklung von numerischen und experimentellen Methoden zur Bestimmung der Rolldämpfung. Teilvorhaben: Bestimmung der Rolldämpfung moderner Schiffsformen mit Hilfe von experimentellen und numerischen Untersuchungen komplexer Strömungsvorgänge; Abschlussbericht des Verbundforschungsvorhabens*. de. Schriftenreihe Schiffbau. Hamburg: Technische Universität Hamburg-Harburg. DOI: 10.2314/GBV:783227701.
- Abdel-Maksoud, M., M. Lemmerhirt, and M. Scharf (2016). *Numerische Bestimmung der Schub- und Antriebsleistung von Schiffen unter Berücksichtigung der Wechselwirkung mit dem Propeller in natürlichem Seegang*. PerSee Abschlussbericht. Hamburg: Technische Universität Hamburg-Harburg.
- Abkowitz, M. A. (1964). *Lectures on Ship Hydrodynamics: Steering and Manoeuvrability*. Lyngby: Hydrodynamics Department.
- ABS (2013). *Ship Energy Efficiency Measures. Status and Guidance*. Houston.
- Adegeest, L. J. M. (2008). “Response Based Weather-Routing and Operation Planning of Heavy Transport Vessels”. en. In: *Marine Heavy Transport & Lift II. 27-28 February 2008*. London: Royal Institution of Naval Architects. ISBN: 190504044X.
- Aertssen, G. (1969). “Service Performance and Trials at Sea”. In: *Report of the Performance Committee*. 12th International Towing Tank Conference (Rome), pp. 210–214.
- Alexandersson, M. (2009). “A Study of Methods to Predict Added Resistance in Waves”. Performed at Seaware AB. Master Thesis. Stockholm: KTH Royal Institute of Technology.
- Aligne, F., M. Papageorgiou, and J. Ramos (1997). “Fuel Minimisation for Ship Weather Routing”. In: *IFAC Proceedings Volumes 30.8*, pp. 575–580. ISSN: 14746670. DOI: 10.1016/S1474-6670(17)43882-1.
- Andersson, A. (2015). “Multi-objective Optimisation of Ship Routes”. Department of Applied Physics. Master’s thesis. Gothenburg: Chalmers University of Technology.

BIBLIOGRAPHY

- Aneja, Y. P., V. Aggarwal, and K. P. K. Nair (1983). “Shortest Chain Subject to Side Constraints”. In: *Networks* 13.2, pp. 295–302. ISSN: 00283045. DOI: 10.1002/net.3230130212.
- Avgouleas, K. (2008). “Optimal Ship Routing”. Department of Mechanical Engineering. Master’s Thesis. Cambridge: Massachusetts Institute of Technology.
- Babbedge, N. H. (1975). “Ship Speed Analysis”. M. Phil. UK: Plymouth Polytechnic.
- Bännstrand, M., A. Jönsson, R. Karlsson, and H. Johnson (2016). *Study on the Optimization of Energy Consumption as Part of Implementation of a Ship Energy Efficiency Management Plan (SEEMP)*. London: IMO.
- Barr, A. and E. A. Feigenbaum, eds. (1981). *The Handbook of Artificial Intelligence*. Vol. I. Stanford, California and Los Altos, California: Heuris Tech Press and William Kaufmann. ISBN: 0865760055.
- Bellman, R. (1952). “On the Theory of Dynamic Programming”. en. In: *Mathematics* 38, pp. 716–719.
- Bellman, R. (1954). *The Theory of Dynamic Programming*. The RAND Corporation.
- Bellman, R. (1957). *Dynamic Programming*. Rand Corporation research study. Princeton: Princeton University Press. ISBN: 9780691079516.
- Bentin, M., D. Zastrau, M. Schlaak, D. Freye, R. Elsner, and S. Kotzur (2016). “A New Routing Optimization Tool-influence of Wind and Waves on Fuel Consumption of Ships with and without Wind Assisted Ship Propulsion Systems”. In: *Transportation Research Procedia* 14, pp. 153–162. ISSN: 23521465. DOI: 10.1016/j.trpro.2016.05.051.
- Berking, B. and W. Huth, eds. (2010). *Handbuch Nautik. Navigatorische Schiffsführung*. Hamburg: Seehafen-Verl. ISBN: 3877438210.
- Bertram, V., B. Veelo, H. Söding, and K. Graf (2006). “Development of a Freely Available Strip Method for Seakeeping”. In: *Proceedings of COMPIT ’06, 5th International Conference on Computer Applications and Information Technology in the Maritime Industries. 8 - 10 May 2006, Oegstgeest, The Netherlands*. Ed. by H. T. Grimmelius. Middelburg: IMarEST Benelux Branch, pp. 356–368. ISBN: 9789081006538.
- Bertram, V. (2012). *Practical Ship Hydrodynamics*. 2nd ed. Burlington: Elsevier Science. ISBN: 0080971504.
- Bertram, V. and P. Couser (2014). “Computational Methods for Seakeeping and Added Resistance in Waves”. In: *13th International Conference on Computer and IT Applications in the Maritime Industries, COMPIT’14. Redworth, 12 - 14 May 2014*. Ed. by

- V. Bertram. Hamburg: Techn. Univ. Verl. Schriftenreihe Schiffbau, pp. 8–16. ISBN: 9783892206729.
- Bertsekas, D. P. (1998). *Network Optimization. Continuous and Discrete Methods*. Optimization and neural computation series. Belmont (MA): Athena Scientific. ISBN: 1-886529-02-7.
- Bertsekas, D. P. (1999). *Nonlinear Programming*. 2nd ed. Vol. 4. Athena scientific optimization and computation series. Belmont (MA): Athena Scientific. ISBN: 1-886529-00-7.
- Bertsekas, D. P. (2005). *Dynamic Programming and Optimal Control*. 3rd ed. Athena scientific optimization and computation series. Belmont (MA): Athena Scientific. ISBN: 1-886529-26-4.
- Bijlsma, S. J. (1975). “On Minimal-Time Ship Routing”. en. Dissertation. Delft: University of Technology Delft.
- Bijlsma, S. J. (1999). “A Computational Method in Ship Routing Using the Concept of Limited Manoeuvrability”. In: *Journal of Navigation* 57.3, pp. 357–369. ISSN: 0373-4633. DOI: 10.1017/S0373463304002899.
- Bijlsma, S. J. (2001). “A Computational Method for the Solution of Optimal Control Problems in Ship Routing”. In: *Navigation* 48.3, pp. 144–154. ISSN: 00281522. DOI: 10.1002/j.2161-4296.2001.tb00238.x.
- Bijlsma, S. J. (2002). “On the Applications of Optimal Control Theory and Dynamic Programming in Ship Routing”. In: *Navigation* 49.2, pp. 71–80. ISSN: 00281522. DOI: 10.1002/j.2161-4296.2002.tb00256.x.
- Bijlsma, S. J. (2008). “Minimal Time Route Computation for Ships with Pre-Specified Voyage Fuel Consumption”. In: *Journal of Navigation* 61.04, pp. 723–733. ISSN: 0373-4633. DOI: 10.1017/S037346330800492X.
- Bijlsma, S. J. (2010). “Optimal Ship Routing with Ocean Current Included”. In: *Journal of Navigation* 63.03, pp. 565–568. ISSN: 0373-4633. DOI: 10.1017/S0373463310000159.
- Bleick, W. E. and F. D. Faulkner (1965). “Minimal-Time Ship Routing”. In: *Journal of Applied Meteorology* 4.2, pp. 217–221. ISSN: 0021-8952. DOI: 10.1175/1520-0450(1965)004<0217:MTSR>2.0.CO;2.
- Blendermann, W. (1994). “Parameter Identification of Wind Loads on Ships”. en. In: *Journal of Wind Engineering and Industrial Aerodynamics* 51.3, pp. 339–351. ISSN: 01676105. DOI: 10.1016/0167-6105(94)90067-1.

- Blendermann, W. (1996). *Wind Loading of Ships. Collected Data from Wind Tunnel Tests in Uniform Flow*. Vol. Nr. 574. Bericht / Institut für Schiffbau der Universität Hamburg. Hamburg: Inst. für Schiffbau. ISBN: 9783892205746.
- Bliss, G. A. (1918). “Solutions of Differential Equations as Functions of the Constants of Integration”. In: *Bulletin of the American Mathematical Society* 25.1, pp. 15–27. ISSN: 0002-9904. DOI: 10.1090/S0002-9904-1918-03140-6.
- Blume, P. (1977). *Berechnung des Seeverhaltens für eine systematische variierte Formfamilie*. Bericht Hamburgische Schiffbau-Versuchsanstalt. Hamburg.
- Boese, P. (1970). *Eine einfache Methode zur Berechnung der Widerstandserhöhung eines Schiffes im Seegang*. de. DOI: 10.15480/882.648.
- Bott, A. (2016). *Synoptische Meteorologie*. Berlin, Heidelberg: Springer Berlin Heidelberg. ISBN: 978-3-662-48194-3. DOI: 10.1007/978-3-662-48195-0.
- Böttner, C.-U. (2007). “Weather Routing for Ships in Degraded Condition”. en. In: *International Symposium on Safety, Security and Environmental Protection*. Athens: National Technical University Athens.
- Bouws, E. (1998). *Guide to Wave Analysis and Forecasting*. 2. ed. Vol. No. 702. WMO-Publications. Geneva: Secretariat of the World Meteorological Organization. ISBN: 9789263127020.
- Bowditch, N. (2002). *The American Practical Navigator. An Epitome of Navigation*. 2002 bicentennial ed. Vol. 9. Pub. Bethesda (MD) and Washington (DC): National Imagery and Mapping Agency. ISBN: 9780939837540.
- Brix, J. (1993). *Manoeuvring Technical Manual*. Hamburg: Seehafen Verlag. ISBN: 3-87743-902-0.
- Buhaug, Ø., J. J. Corbett, V. Eyring, Ø. Endresen, J. Faber, S. Hanayama, D. S. Lee, D. Lee, H. Lindstad, A. Z. Markowska, A. Mjelde, D. Nelissen, J. Nilsen, C. Pålsson, W. Wanquing, J. J. Winebrake, and K. Yoshida (2009). *Second IMO GHG Study 2009*. London: IMO.
- C-MAP (2016). *Vessel and Voyage Optimization Solution*.
- C-MAP (2017). *C-MAP Integrated Maritime Suite*. URL: <http://commercialmarine.c-map.com/en/route-planning-and-fleet-management/ims> (visited on 28/08/2017).
- Calleya, J. N. (2014). “Ship Design Decision Support for a Carbon Dioxide Constrained Future”. Department of Mechanical Engineering. PhD Thesis. London: University College London.

- Calleya, J. N., Fuente, Santiago Suárez de la, R. Pawling, and T. Smith (2016). “Designing Future Ships for Significantly Lower Energy Consumption”. In: *10th Symposium on High-Performance Marine Vehicles HIPER’16, Cortona, 17-19 October 2016*. Ed. by V. Bertram, pp. 510–522.
- Calvert, S. (1990). “Optimal Weather Routeing Procedures for Vessels on Trans-Ocean Voyages”. en. Doctor of Philosophy. Polytechnic South West.
- Cameron, M. and S. Brabeck (2015). “Fuel Savings on Tankers. What Gets Measured ... Gets Done ...”. In: *International Conference on Ship Efficiency*. Hamburg: Schiffbautechnische Gesellschaft.
- CENELEC, ed. (2015). *Maritime Navigation and Radiocommunication Equipment and Systems - Electronic Chart Display and Information System (ECDIS) - Operational and Performance Requirements, Methods of Testing and Required Test Results (IEC 61174: 2015)*. European Standard. Brussels.
- Chen, H. (1978). “A Dynamic Program for Minimum Cost Ship Routing Under Uncertainty”. Department of Ocean Engineering. Ph.D. Thesis. Boston: Massachusetts Institute of Technology.
- Chen, H. (1989). “A New Approach to Ship Speed Performance Monitoring and Prediction”. In: *Spring Meeting/STAR Symposium* (New Orleans, Louisiana). The Society of Naval Architects and Marine Engineers. Jersey City (NJ).
- Chen, H. (2011). *Voyage Optimization versus Weather Routing*. Jeppesen Marine Inc. a Boeing Company.
- Chen, H. (2013). “Weather Routing vs Voyage Optimisation”. In: *Digital Ship* January/February, pp. 26–27.
- Chu, P. C., S. E. Miller, and J. A. Hansen (2014). “Fuel-saving Ship Route Using the Navy’s Ensemble Meteorological and Oceanic Forecasts”. en. In: *The Journal of Defense Modeling and Simulation: Applications, Methodology, Technology* 12.1, pp. 41–56. ISSN: 1548-5129. DOI: 10.1177/1548512913516552.
- ClassNK Consulting Service (2016). *ClassNK-NAPA GREEN. Comprehensive Software Solutions for Eco-Efficient Operations*. Tokyo.
- ClassNK Consulting Service (2017). *ClassNK-NAPA GREEN*. URL: http://www.classnk20cs.co.jp/en/napa_green/index.html (visited on 31/10/2017).
- Cui, T., O. Turan, and E. Boulougouris (2016). “Development of a Ship Weather Routing System for Energy Efficient Shipping”. In: *IAME 2016*. Annual conference of the International Association of Maritime Economists (IAME) (Hamburg, Germany).

- Cui, T., B. Howett, R. Lu, M. Y. Kim, Y. K. Demirel, O. Turan, S. Day, and A. Incecik (2016). “Voyage Optimisation towards Energy Efficient Ship Operations”. In: *Shipping in Changing Climates Conference 2016* (Newcastle, UK).
- Dechter, R. and J. Pearl (1985). “Generalized Best-First Search Strategies and the Optimality of A*”. In: *Journal of the ACM* 32.3, pp. 505–536. ISSN: 00045411. DOI: 10.1145/3828.3830.
- Delling, D., P. Sanders, D. Schultes, and D. Wagner (2009). “Engineering Route Planning Algorithms”. In: *Algorithmics of Large and Complex Networks. Design, Analysis, and Simulation*. Ed. by J. Lerner, D. Wagner, and K. A. Zweig. Lecture Notes in Computer Science 5515. Berlin, Heidelberg: Springer Berlin Heidelberg, pp. 117–139. ISBN: 3642020941.
- Deltamarin Ltd (2009). *EEDI Tests and Trials for EMSA. Report for Project 1098*.
- Dijkstra, E. W. (1959). “A Note on Two Problems in Connexion with Graphs”. In: *Numerische Mathematik* 1, pp. 269–271.
- DMI (2018). *Ocean Forecasts*. URL: <http://www.dmi.dk/en/hav/#danmark> (visited on 22/02/2018).
- DNV GL (2014). *The Future of Shipping*. Høvik.
- Dobie, G., ed. (2016). *Safety and Shipping Review 2016. An annual review of trends and developments in shipping losses and safety*. In collab. with H. Kidston, T. Chamberlain, J. Whitehead, and C. Fields. Munich: Allianz Global Corporate & Specialty.
- Dobie, G., ed. (2017). *Safety and Shipping Review 2017. An annual review of trends and developments in shipping losses and safety*. In collab. with J. Whitehead, H. Kidston, and S. Collins. Munich: Allianz Global Corporate & Specialty.
- Domschke, W., A. Drexl, R. Klein, and A. Scholl (2015). *Einführung in Operations Research*. 9., überarb. u. verb. Aufl. 2015. Berlin, Heidelberg: Springer Gabler.
- Dreyfus, S. E. (1965). *Dynamic Programming and the Calculus of Variations*. Vol. 21. Mathematics in science and engineering. Santa Monica (CA): Academic Press.
- E.R. Schifffahrt (2017). “Strategic Routing”. In: *ship & shore* 1, pp. 14–15.
- ECMWF (2012a). *Ocean Waves at ECMWF. ECMWF and Marine Forecasting*. URL: <https://www.ecmwf.int/sites/default/files/elibrary/2012/14556-ocean-waves-ecmwf.pdf> (visited on 02/02/2018).

- ECMWF (2012b). *The ECMWF Ensemble Prediction System. The rationale behind probabilistic weather forecasts*. URL: <https://www.ecmwf.int/sites/default/files/elibrary/2012/14557-ecmwf-ensemble-prediction-system.pdf> (visited on 02/02/2018).
- ECMWF (2017a). *Ensemble Weather Forecasting. Fact Sheet*. URL: <https://www.ecmwf.int/en/about/media-centre/fact-sheet-ensemble-weather-forecasting> (visited on 07/01/2018).
- ECMWF (2017b). *What is the Direction Convention for the U and V Components of Winds?* Data Services Knowledge Base. URL: <https://software.ecmwf.int/wiki/pages/viewpage.action?pageId=74768169> (visited on 29/05/2018).
- ECMWF (2017c). *What is the Direction Convention for Wave Fields?* Data Services Knowledge Base. URL: <https://software.ecmwf.int/wiki/pages/viewpage.action?pageId=76402966> (visited on 29/05/2018).
- ECMWF (2018). *Home*. URL: <https://www.ecmwf.int/> (visited on 22/02/2018).
- Eiselt, H. A. and C.-L. Sandblom (2010). *Operations Research. A Model-based Approach*. Heidelberg: Springer.
- Eskild, H. (2014). “Development of a Method for Weather Routing of Ships”. Department of Marine Technology. en. Master Thesis. Trondheim: Norwegian University of Science and Technology.
- European Commission (2017). *Reducing Emissions from the Shipping Sector - Climate Action*. URL: https://ec.europa.eu/clima/policies/transport/shipping_en (visited on 13/06/2017).
- European Union (2015). *Regulation 2015/ 757 on the Monitoring, Reporting and Verification of Carbon Dioxide Emissions from Maritime Transport, and amending Directive 2009/16/EC*.
- Faltinsen, O. M. (2005). *Hydrodynamics of High-Speed Marine Vehicles*. Cambridge: Cambridge University Press. ISBN: 0521845688.
- Fang, M.-C. and Y.-H. Lin (2015). “The Optimization of Ship Weather-routing Algorithm based on the Composite Influence of Multi-dynamic Elements (II). Optimized Routings”. en. In: *Applied Ocean Research* 50, pp. 130–140. ISSN: 01411187. DOI: 10.1016/j.apor.2014.12.005.
- Faulkner, F. D. (1963). “A General Numerical Method for Determining Optimum Ship Routes”. In: *Navigation* 10.2, pp. 143–148. ISSN: 00281522. DOI: 10.1002/j.2161-4296.1963.tb02036.x.

- Figari, M., R. Zaccone, M. Martelli, and M. Altosole (2017). *Ship Voyage Optimisation by 3D Dynamic Programming*. EPFL Valais-Wallis, Sion, Switzerland.
- Finke, G., ed. (2008). *Operations Research and Networks*. London and Hoboken: ISTE and John Wiley & Sons. ISBN: 9781282165465.
- FORCE Technology (2016). *SeaPlanner. Voyage planning*.
- Fossen, T. I. (2011). *Handbook of Marine Craft Hydrodynamics and Motion Control*. First Edition. John Wiley & Sons Ltd. ISBN: 1119991498.
- Fujii, H. and T. Takahashi (1975). “Experimental Study on the Resistance Increase of a Large Full Ship in Regular Oblique Waves”. In: *Journal of the Society of Naval Architects of Japan* 1975.137, pp. 132–137. ISSN: 1884-2070. DOI: 10.2534/jjasnaoe1968.1975.132.
- Fujiwara, T., M. Ueno, and T. Nimura (1998). “Estimation of Wind Forces and Moments acting on Ships”. In: *Journal of the Society of Naval Architects of Japan* 1998.183, pp. 77–90. ISSN: 1884-2070. DOI: 10.2534/jjasnaoe1968.1998.77.
- GDAL/OGR contributors (2018). *GDAL/OGR Geospatial Data Abstraction software Library*. Open Source Geospatial Foundation. URL: <http://www.gdal.org/> (visited on 13/05/2018).
- Gerdtts, M. and F. Lempio (2011). *Mathematische Optimierungsverfahren des Operations Research*. De Gruyter Studium. Berlin and Boston: De Gruyter. ISBN: 3110249987.
- Gerritsma, J. and W. Beukelman (1972). “Analysis of the Resistance Increase in Waves of a Fast Cargo Ship”. In: *International Shipbuilding Progress*. 19. ISBN: 0020-868X.
- Golden, A. (2016). *Digital Marine Solutions Completes Acquisition of the Marine Division of Jeppesen from Boeing*. Ed. by Digital Marine Solutions. Press Release 01/06/2016.
- Hagiwara, H. and J. A. Spaans (1987). “Practical Weather Routeing of Sail-assisted Motor Vessels”. In: *Journal of Navigation* 40.02, pp. 96–119. ISSN: 0373-4633. DOI: 10.1017/S0373463300000515.
- Hagiwara, H. (1989). “Weather Routing of (Sail-Assisted) Motor Vessels”. en. Dissertation. Delft: University of Technology Delft.
- Haltiner, G. J., H. D. Hamilton, and G. ’Arnason (1962). “Minimal-Time Ship Routing”. In: *Journal of Applied Meteorology* 1.1, pp. 1–7. ISSN: 0021-8952. DOI: 10.1175/1520-0450(1962)001<0001:MTSR>2.0.CO;2.
- Haltiner, G. J., W. E. Bleick, and F. D. Faulkner (1968). “A Proposed Method for Ship Routing using Long Range Weather Forecasts”. In: *Monthly Weather Review* 96.5,

-
- pp. 319–322. ISSN: 0027-0644. DOI: 10.1175/1520-0493(1968)096<0319:APMFSR>2.0.CO;2.
- Hameed, W. (2015). “Multi-Objective Optimization of Voyage Plans for Ships”. Department of Automatic Control. Master’s Thesis. Lund: Lund University.
- Hamilton, H. D. (1961). “Minimum-time Ship Routing by Calculus of Variations Methods”. en. Master’s thesis. Monterey (CA): United States Naval Postgraduate School.
- Hapag-Lloyd (Jan. 1, 2018a). *A15 Ship Data*. In collab. with L. Walther. Hamburg.
- Hapag-Lloyd (2018b). *Vessels with 15,000 to 18,000 TEU. A 15 Class*. URL: https://www.hapag-lloyd.com/en/products/fleet/vessel.html#anchor_c2f95c (visited on 27/12/2018).
- Hart, P., N. Nilsson, and B. Raphael (1968). “A Formal Basis for the Heuristic Determination of Minimum Cost Paths”. In: *IEEE Transactions on Systems Science and Cybernetics* 4.2, pp. 100–107. ISSN: 0536-1567. DOI: 10.1109/TSSC.1968.300136.
- Heinrich, G. (2013). *Operations Research*. 2., Überarb. Au. München: Oldenbourg Verlag. ISBN: 9783486855302.
- Hillier, F. S. and G. J. Lieberman (2010). *Introduction to Operations Research*. 9th ed. New York: McGraw-Hill Higher Education. ISBN: 978-0-07-337629-5.
- Hinnenthal, J. and S. Harries (2004). “A Systematic Study on Posing and Solving the Problem of Pareto Optimal Ship Routing”. In: *3rd International Conference on Computer and IT Applications in the Maritime Industries, COMPIT’04. Sigüenza, 9-12 May 2004*. Ed. by V. Bertram and M. Armada, pp. 27–35.
- Hinnenthal, J. (2008). “Robust Pareto-Optimum Routing of Ships utilizing Deterministic and Ensemble Weather Forecasts”. Verkehrs- und Maschinensysteme. en. Doktorarbeit. Berlin: Technische Universität Berlin.
- Holtrop, J. and G. Mennen (1978). “A Statistical Power Prediction Method”. In: *International Shipbuilding Progress* 25.290, pp. 253–256. ISSN: 0020868X.
- Holtrop, J. and G. Mennen (1982). “An Approximate Power Prediction Method”. In: *International Shipbuilding Progress* 29, pp. 166–170. ISSN: 0020868X.
- Holtrop, J. (1984). “Statistical Re-Analysis of Resistance and Propulsion Data”. In: *International Shipbuilding Progress* 31.363, pp. 272–276. ISSN: 0020868X.
- Höppner, V. (2009). “A Holistic Approach to Reduce Ship Operation Costs”. In: *International Conference on Ship Efficiency*. Hamburg: Schiffbautechnische Gesellschaft.

BIBLIOGRAPHY

- Howett, B., O. Turan, and A. H. Day (2016). "WASPP: Wind Assisted Ship Performance Prediction". In: *Shipping in Changing Climates Conference 2016* (Newcastle, UK).
- IHS Fairplay (2010). *Assessing Fuel Consumption*. URL: <https://fairplay.ihs.com/ship-construction/article/4107211/assessing-fuel-consumption> (visited on 16/10/2017).
- IMO (1983). *Recommendation on Weather Routeing*. Resolution A.528(13).
- IMO (1985). *General Provisions on Ships' Routeing*. Resolution A.572(14).
- IMO (1999). *Guidelines for Voyage Planning*. Resolution A.893(21).
- IMO (2002). *Standards for Ship Manoeuvrability*. Resolution MSC.137(76).
- IMO (2007). *Revised Guidance to the Master for Avoiding Dangerous Situations in Adverse Weather and Sea Conditions*. MSC.1/Circ.1228. en.
- IMO (2008). *Amendments to the Annex of the Protocol of 1997 to Amend the International Convention for the Prevention of Pollution from Ships, 1973, as Modified by the Protocol of 1978 Relating Thereto (Revised MARPOL Annex VI)*. Resolution MEPC.176(58).
- IMO (2009a). *Consideration of the Energy Efficiency Design Index for New Ships*. GHG-WG 2/2/22.
- IMO (2009b). *Guidelines for Voluntary Use of the Ship Energy Efficiency Operational Indicator (EEOI)*. MEPC.1/Circ.684.
- IMO (2009c). *SOLAS. Consolidated Text of the International Convention for the Safety of Life at Sea, 1974, and its Protocol of 1988: Articles, Annexes and Certificates*. Consolidated ed., 2009, 5th ed. London: International Maritime Organization. ISBN: 9280115057.
- IMO (2011). *Development of Second Generation Intact Stability Criteria. A Background Study on Application of MSC.1/Circ.1228 on the Revised Guidance to the Master for Avoiding Dangerous Situations in Adverse Weather and Sea Conditions*. SLF 54/INF.9.
- IMO (2012). *2012 Guidelines for the Development of a Ship Energy Efficiency Management Plan (SEEMP)*. Resolution MEPC.213(63).
- IMO (2013). *2013 Interim Guidelines for Determining Minimum Propulsion Power to Maintain the Manoeuvrability of Ships in Adverse Conditions*. Resolution MEPC.232(65).
- IMO (2014). *2014 Guidelines on the Method of Calculation of the Attained Energy Efficiency Design Index (EEDI) for New Ships*. Resolution MEPC.245(66).

-
- IMO (2015a). *Full Speed Ahead with Climate-change Measures at IMO Following Paris Agreement*. URL: <http://www.imo.org/en/MediaCentre/PressBriefings/Pages/55-paris-agreement.aspx> (visited on 08/06/2016).
- IMO (2015b). *Investigation of Appropriate Control Measures (Abatement Technologies) to Reduce Black Carbon Emissions from International Shipping*. London.
- IMO (2015c). *Ships' Routeing*. 12. ed. London: IMO Publishing. ISBN: 978-92-801-1625-0.
- IMO (2016a). *Air Pollution and Energy Efficiency. Results of research project "Energy Efficient Safe Ship Operation" (SHOPERA). Submitted by Denmark, Germany, Norway and Spain*. MEPC 70/INF.33.
- IMO (2016b). *Energy Efficiency Measures*. URL: <http://www.imo.org/en/OurWork/Environment/PollutionPrevention/AirPollution/Pages/Technical-and-Operational-Measures.aspx> (visited on 08/06/2016).
- IMO (2016c). *Ships' Routeing*. URL: <http://www.imo.org/en/OurWork/Safety/Navigation/Pages/ShipsRouteing.aspx> (visited on 08/06/2016).
- IMO (2017a). *Amendments to the Annex of the Protocol of 1997 to Amend the International Convention for the Prevention of Pollution from Ships, 1973, as Modified by the Protocol of 1978 Relating Thereto*. Resolution MEPC.286(71).
- IMO (2017b). *International Convention for the Prevention of Pollution from Ships (MARPOL)*. URL: [http://www.imo.org/en/about/conventions/listofconventions/pages/international-convention-for-the-prevention-of-pollution-from-ships-\(marpol\).aspx](http://www.imo.org/en/about/conventions/listofconventions/pages/international-convention-for-the-prevention-of-pollution-from-ships-(marpol).aspx) (visited on 14/05/2017).
- IMO (2018a). *Nitrogen Oxides (NO_x) – Regulation 13*. URL: [http://www.imo.org/en/OurWork/Environment/PollutionPrevention/AirPollution/Pages/Nitrogen-oxides-\(NOx\)-%E2%80%93-Regulation-13.aspx](http://www.imo.org/en/OurWork/Environment/PollutionPrevention/AirPollution/Pages/Nitrogen-oxides-(NOx)-%E2%80%93-Regulation-13.aspx) (visited on 10/03/2018).
- IMO (2018b). *Sulphur Oxides (SO_x) – Regulation 14*. URL: [http://www.imo.org/en/OurWork/Environment/PollutionPrevention/AirPollution/Pages/Sulphur-oxides-\(SOx\)-%E2%80%93-Regulation-14.aspx](http://www.imo.org/en/OurWork/Environment/PollutionPrevention/AirPollution/Pages/Sulphur-oxides-(SOx)-%E2%80%93-Regulation-14.aspx) (visited on 10/03/2018).
- Isherwood, R. M. (1972). "Wind Resistance of Merchant Ships". In: *R.I.N.A. Supplementary Papers* 115, pp. 327–338.
- Ishii, E., E. Kobayashi, T. Mizunoe, and A. Maki (2010). "Proposal of New-Generation Route Optimization Technique for an Oceangoing Vessel". en. In: *OCEANS 2010 IEEE - Sydney*. OCEANS 2010 IEEE - Sydney (Sydney, Australia,). Ed. by I. Staff. IEEE Staff. [Place of publication not identified]: I E E E, pp. 1–6. ISBN: 978-1-4244-5221-7. DOI: 10.1109/OCEANSSYD.2010.5603624.
-

- ITTC (1978). *ITTC Quality System Manual. Recommended Procedures and Guidelines. Performance prediction method for single screw ships*. The Hague, The Netherlands.
- James, R. W. (1957). *Application of Wave Forecasts to Marine Navigation*. In collab. with Navy Hydrographic Office. Washington D.C.: U.S. Naval Oceanographic Office.
- Jeffery, K. (2015). “Voyage Optimisation Supersedes Traditional Weather Routing”. In: *Tanker Operator* 14.4, pp. 28–29.
- Jeppesen (2011). *Vessel and Voyage Optimization Solution*.
- John, O. and S. Werner (2015). *Fleet Management Systems 2015. An International Market Review of Current Software Applications for Shipping Companies*. Stuttgart: Fraunhofer Verlag. ISBN: 3839609410.
- John, O. (2018). *Fleet Management Systems 2018. An International Market Review of current Software Applications for Shipping Companies*. Ed. by C. Jahn. Stuttgart: Fraunhofer Verlag. ISBN: 3839612861.
- Jones, D. R., C. D. Perttunen, and B. E. Stuckman (1993). “Lipschitzian Optimization Without the Lipschitz Constant”. In: *Journal of Optimization Theory and Applications* 79.1, pp. 157–181. ISSN: 0022-3239. DOI: 10.1007/BF00941892.
- Journée, J. M. J. and J. H. C. Meijers (1980). “Ship Routeing for Optimum Performance”. In: *Transactions IME*.
- Journée, J. M. J. (1992). “Quick Strip Theory Calculations in Ship Design”. In: *PRADS’92. Conf. on Practical Design of Ships and Mobile Structures (Newcastle upon Tyne, U.K.)*. Vol. I, pp. 1–11.
- Klompstra, M. B., G. J. Olsder, and van Brunshot, P. K. G. M. (1992). “The Isopone Method in Optimal Control”. en. In: *Dynamics and Control* 2.3, pp. 281–301. ISSN: 0925-4668. DOI: 10.1007/BF02169518.
- Klose, B. (2016). *Meteorologie. Eine interdisziplinäre Einführung in die Physik der Atmosphäre*. 3. Auflage. Berlin, Heidelberg: Springer Berlin Heidelberg. ISBN: 978-3-662-43621-9. DOI: 10.1007/978-3-662-43622-6.
- Kobayashi, E., H. Hashimoto, Y. Taniguchi, and S. Yoneda (2015). “Advanced Optimized Weather Routing for an Ocean-Going Vessel”. In: *Proceedings of 2015 International Association of Institutes of Navigation World Congress. October 20-23, 2015*. IAIN 2015 (Prague, Czech Republic). Piscataway (NJ): IEEE.
- Koromila, I., Z. Nivolianitou, and T. Giannakopoulos (2014). “Bayesian Network to Predict Environmental Risk of a Possible Ship Accident”. In: *Proceedings of the 7th International Conference on Pervasive Technologies Related to Assistive Environments*.

- PETRA'14 (Rhodes, Greece). Ed. by F. Makedon, M. Clements, C. Pelachaud, V. Kalogeraki, and I. Maglogiannis. ACM International Conference Proceedings Series. New York (NY): ACM, pp. 1–5. ISBN: 9781450327466. DOI: 10.1145/2674396.2674463.
- Kosmas, O. T. and D. S. Vlachos (2012). “Simulated Annealing for Optimal Ship Routing”. In: *Computers & Operations Research* 39.3, pp. 576–581. ISSN: 03050548. DOI: 10.1016/j.cor.2011.05.010.
- Krata, P. and J. Szlapczynska (2012). “Weather Hazard Avoidance in Modeling Safety of Motor-Driven Ship for Multicriteria Weather Routing”. In: *International Journal on Marine Navigation and Safety of Sea Transportation* 6.1, pp. 71–78.
- Krata, P. and J. Szlapczynska (2018). “Ship Weather Routing Optimization with Dynamic Constraints based on Reliable Synchronous Roll Prediction”. In: *Ocean Engineering* 150, pp. 124–137. ISSN: 00298018. DOI: 10.1016/j.oceaneng.2017.12.049.
- Krüger, S., G. Clauss, J. Hennig, and H. Cramer (2003). “Development of Safer Ships by Deterministic Analysis of Extreme Roll Motions in Harsh Seas”. In: *Proceedings of the ASME 22nd International Conference on Offshore Mechanics and Arctic Engineering*. OMAE 2003 (Cancun, Mexico). New York (NY): American Society of Mechanical Engineers.
- Krüger, S. (2005). *Schiffspropeller*. Vorlesungsmanuskript.
- Krüger, S. (2006). *Strömungsmechanische Grundlagen zum Glattwasserwiderstand von Schiffen*. Vorlesungsmanuskript.
- Kuroda, M., M. Tsujimoto, T. Fujiwara, S. Ohmatsu, and K. Takagi (2008). “Investigation on Components of Added Resistance in Short Waves”. In: *Journal of the Japan Society of Naval Architects and Ocean Engineers* 8.0, pp. 171–176. ISSN: 1880-3717. DOI: 10.2534/jjasnaoe.8.171.
- Kwon, Y.-J. (1981). “The Effect of Weather, Particularly Short Sea Waves, on Ship Speed Performance”. Department of Naval Architecture and Shipbuilding. en. PhD Thesis. Newcastle upon Tyne: University of Newcastle upon Tyne.
- Larsson, E. and M. H. Simonsen (2014). “DIRECT Weather Routing”. Department of Shipping and Marine Technology. Master’s Thesis. Gothenburg: Chalmers University of Technology.
- Lin, Y.-H., M.-C. Fang, and R. W. Yeung (2013). “The Optimization of Ship Weather-routing Algorithm based on the Composite Influence of Multi-dynamic Elements”. en. In: *Applied Ocean Research* 43, pp. 184–194. ISSN: 01411187. DOI: 10.1016/j.apor.2013.07.010.

- Lin, Y.-H. and M.-C. Fang (2013). “The Ship-Routing Optimization Based on the Three-Dimensional Modified Isochrone Method”. In: *Proceedings of the ASME 2013 32nd International Conference on Ocean, Offshore and Arctic Engineering*. OMAE 2013 (Nantes, France). New York (NY): American Society of Mechanical Engineers, pp. 1–8. ISBN: 978-0-7918-5539-3. DOI: 10.1115/OMAE2013-10959.
- Lloyd’s Register (2016a). *Low Carbon Pathways 2050*. URL: http://www.lowcarbonshipping.co.uk/files/ucl_admin/LR_Lowcarbonpathways2050_171016_web_LR.pdf (visited on 26/01/2017).
- Lloyd’s Register (2016b). *Monitoring, reporting and verification of CO2 emissions from ships. Your complete guide to Lloyd’s Register’s consultancy services*. URL: https://issuu.com/lr_marine/docs/mrv_regulation_consultancy_services (visited on 13/06/2017).
- Lu, R., O. Turan, E. Boulougouris, C. Banks, and A. Incecik (2015). “A Semi-empirical Ship Operational Performance Prediction Model for Voyage Optimization Towards Energy Efficient Shipping”. In: *Ocean Engineering* 110, pp. 18–28. ISSN: 00298018. DOI: 10.1016/j.oceaneng.2015.07.042.
- Luenberger, D. G. and Y. Ye (2008). *Linear and Nonlinear Programming*. Third Edition. Vol. 116. International series in operations research & management science. Boston (MA): Springer Science +Business Media, LLC. ISBN: 0387745033.
- Luus, R. (2000). *Iterative Dynamic Programming*. Vol. 110. Monographs and surveys in pure and applied mathematics. Boca Raton: Chapman & Hall/CRC. ISBN: 1-58488-148-8.
- Maddox Consulting (2012). *Analysis of Market Barriers to Cost Effective GHG Emission Reductions in the Maritime Transport Sector. Final Report*. CLIMA.B.3/SER/2011/0014. Brussels: European Commission.
- Maki, A., Y. Akimoto, Y. Nagata, S. Kobayashi, E. Kobayashi, S. Shiotani, T. Ohsawa, and N. Umeda (2011). “A New Weather-routing System that Accounts for Ship Stability based on a Real-coded Genetic Algorithm”. en. In: *Journal of Marine Science and Technology* 16.3, pp. 311–322. ISSN: 0948-4280. DOI: 10.1007/s00773-011-0128-z.
- Makrygiorgos, A., I. A. Vetsikas, and S. Perantonis (2015). “Accelerating Multi-objective Ship Routing Using a Novel Grid Structure and a Simple Heuristic”. In: *Proceedings of the 6th International Conference on Information, Intelligence, Systems and Applications (IISA)*. Date: 6-8 July 2015. IISA (Corfu, Greece). Piscataway (NJ): IEEE, pp. 1–6. ISBN: 978-1-4673-9311-9. DOI: 10.1109/IISA.2015.7387978.
- Malberg, H. (2007). *Meteorologie und Klimatologie*. 5th Edition. Berlin, Heidelberg: Springer Berlin Heidelberg. ISBN: 978-3-540-37219-6. DOI: 10.1007/978-3-540-37222-6.

- MAN Diesel & Turbo (2011). *Basic Principles of Ship Propulsion*.
- MAN Diesel & Turbo (2014). *S90ME-C10.2-TII. Project Guide Electronically Controlled Two stroke Engines*. Version 0.5.
- MAN Diesel & Turbo (2015). *Market Update Note. Light Running Margin (LRM)*.
- MAN Energy Solutions (2018). *CEAS Engine Data Report. 9S90ME-C10.5*.
- Mannarini, G., G. Coppini, P. Oddo, and N. Pinardi (2013). “A Prototype of Ship Routing Decision Support System for an Operational Oceanographic Service”. In: *TransNav, the International Journal on Marine Navigation and Safety of Sea Transportation* 7.2, pp. 53–59. ISSN: 2083-6473. DOI: 10.12716/1001.07.01.06.
- Marie, S. and E. Courteille (2009a). “Multi-Objective Optimization of Motor Vessel Route”. en. In: *International Journal on Marine Navigation and Safety of Sea Transportation* 3.2, pp. 133–141.
- Marie, S. and E. Courteille (2009b). *Fuel Consumption Minimization Procedure of Sail-assisted Motor Vessel based on a Systematic Meshing of the Explored Area*. Tokyo, Japan.
- Marie, S. and E. Courteille (2014). “Sail-assisted Motor Vessels Weather Routing using a Fuzzy Logic Model”. ca. In: *Journal of Marine Science and Technology* 19.3, pp. 265–279. ISSN: 0948-4280. DOI: 10.1007/s00773-013-0246-x.
- Marorka (2017). *Products - Hardware and Software powering Energy Management*. URL: <http://www.marorka.com/products/#marorka-onboard> (visited on 06/11/2017).
- McMillan, C., B. Roberts, and I. Rojon (2014). “The Weather, Back in the Driving Seat”. In: *Ship Efficiency Insight* 01, pp. 43–44.
- Met Office (2016). *Glossary of Data Terms*. URL: <https://www.metoffice.gov.uk/services/industry/energy/research-and-planning/data/glossary> (visited on 28/02/2018).
- Met Office (2017a). *Global Circulation Patterns*. URL: <https://www.metoffice.gov.uk/learning/learn-about-the-weather/how-weather-works/global-circulation-patterns> (visited on 31/01/2018).
- Met Office (2017b). *Global Wave Model*. URL: <https://www.metoffice.gov.uk/binaries/content/assets/mohippo/pdf/data-provision/global-wave.pdf> (visited on 29/05/2018).
- Met Office (2017c). *Ocean Waves*. URL: <https://www.metoffice.gov.uk/research/weather/ocean-forecasting/ocean-waves> (visited on 25/02/2018).
- Met Office (2018). *Weather and Climate Change*. URL: <https://www.metoffice.gov.uk/> (visited on 22/02/2018).

BIBLIOGRAPHY

- MeteoGroup (2014a). *SPOS Onboard*. URL: https://www.meteogroup.com/sites/default/files/sposonboard_web.pdf (visited on 12/09/2017).
- MeteoGroup (2014b). *SPOS Seakeeping. Integrated Solution for Ship Responses Optimization*. URL: https://www.meteogroup.com/sites/default/files/leaflet_seakeeping_05.pdf (visited on 12/09/2017).
- MeteoGroup (2015). *FleetGuard Monitoring. Integrated Solution for Monitoring, Planning and Optimizing your Fleet*. URL: https://www.meteogroup.com/sites/default/files/fleetguard_web.pdf (visited on 11/10/2017).
- MeteoGroup (2017a). *RouteGuard. RouteGuardOptimum Ship Routing and Performance Analysis*.
- MeteoGroup (2017b). *Vessel Performance*. URL: <https://www.meteogroup.com/vessel-performance> (visited on 12/09/2017).
- MeteoGroup (2017c). *Vessel, Crew & Cargo Safety*. URL: <https://www.meteogroup.com/vessel-crew-cargo-safety> (visited on 11/10/2017).
- Meyer, N. (2014). “Einfluss schiffsspezifischer Parameter für die wetteroptimierte Routenwahl. Entwicklung einer integrativen Methode für den Schiffsbetrieb”. Institut für Maritime Logistik. de. unpublished. Master Thesis. Hamburg: Technische Universität Hamburg-Harburg.
- Moctar, O. e., V. Shigunov, and T. Zorn (2012). “Duisburg Test Case: Post-Panamax Container Ship for Benchmarking”. In: *Ship Technology Research* 59.3, pp. 50–64.
- Montes, A. A. (2005). “Network Shortest Path Application for Optimum Track Ship Routing”. Master’s Thesis. Monterey (CA): Naval Postgraduate School.
- Motte, R. (1981). “Ship Based Weather Routeing (Using Dynamical Meteorology)”. Faculty of Science and Technology. PhD Thesis. Devon, England: University of Plymouth.
- Motte, R. and S. Calvert (1988). “Operational Considerations and Constraints in Ship-based Weather Routeing Procedures”. In: *Journal of Navigation* 41.03, pp. 417–433. ISSN: 0373-4633. DOI: 10.1017/S0373463300014909.
- Motte, R. and S. Calvert (1990). “On the Selection of Discrete Grid Systems for On-Board Micro-based Weather Routeing”. In: *Journal of Navigation* 43.01, pp. 104–117. ISSN: 0373-4633. DOI: 10.1017/S0373463300013849.
- Nagata, K. (2015). *ClassNK-NAPA GREEN. Case Studies of Optimizing Ship Operation for Increased Energy Efficiency*. ClassNK.

- Nagle, F. W. (1972). *A Numerical Study in Optimum Track Ship Routing Climatology*. Fort Belvoir (VA): Defense Technical Information Center. DOI: 10.21236/AD0761620.
- NAPA Group (2014). *NAPA Voyage Optimization. Functional Specification*. Version 2013.4. Helsinki.
- NAPA Group (2016). *Namura Shipbuilding Introduces ClassNK-NAPA GREEN*. Press Release 26/01/2016.
- NAPA Group (2017a). *ClassNK-NAPA GREEN Optimization*. URL: <https://www.napa.fi/Ship-Operations/ClassNK-NAPA-GREEN-Optimization> (visited on 31/10/2017).
- NAPA Group (2017b). *History of NAPA*. URL: <https://www.napa.fi/About-NAPA/History-of-NAPA> (visited on 31/10/2017).
- NAPA Group (2017c). *Voyage Optimization*. URL: <https://www.napa.fi/Ship-Operations/ClassNK-NAPA-GREEN-Optimization/Voyage-Optimization> (visited on 31/10/2017).
- National Hurricane Center (2018). *NHC Marine Forecasts & Analyses*. en. URL: <https://www.nhc.noaa.gov/marine/> (visited on 04/02/2018).
- National Imaginery and Mapping Agency (2000). *Department of Defense World Geodetic System 1984. Its Definition and Relationships with Local Geodetic Systems*. Version Third Edition.
- NAVTOR (2019). *NavStation*. URL: <https://www.navtor.com/navstation.html> (visited on 19/05/2019).
- NCEI (2018). *Global Forecast System (GFS)*. URL: <https://www.ncdc.noaa.gov/data-access/model-data/model-datasets/global-forecast-system-gfs> (visited on 25/02/2018).
- NCEP (2017). *Home*. URL: <http://www.ncep.noaa.gov/> (visited on 22/02/2018).
- Nelder, J. A. and R. Mead (1965). “A Simplex Method for Function Minimization”. In: *The Computer Journal* 7.4, pp. 308–313. ISSN: 0010-4620. DOI: 10.1093/comjnl/7.4.308.
- Nemhauser, G. L., A. H. G. Rinnooy Kan, and M. J. Todd (1989). *Optimization*. Vol. 1. Handbooks in operations research and management science. Amsterdam and New York (NY): North-Holland and Sole distributors for the U.S.A. and Canada, Elsevier Science Pub. Co. ISBN: 9780444872845.
- NOAA’s National Weather Service (2018). *Environmental Modeling Center / Marine Modeling and Analysis Branch home page*. EN-US. NOAA National Centers for Environmental Prediction. URL: <http://polar.ncep.noaa.gov/waves/index2.shtml?> (visited on 25/02/2018).

BIBLIOGRAPHY

- Nordforsk (1987). *Assessment of Ship Performance in a Seaway. The Nordic Co-operative Project: "Seakeeping Performance of Ships"*. Copenhagen. ISBN: 9788798263715.
- OASIS (2019). *AMQP Advanced Message Queuing Protocol*. URL: <http://www.amqp.org/> (visited on 20/01/2019).
- Ogata, M. (2010). *Optimum Ship Routeing*. Weathernews.
- On AIR (2018a). *SmartNautilus. Voyage Optimization Solution*. URL: <https://www.smartnautilus.com/> (visited on 10/08/2018).
- On AIR (2018b). *SmartNautilus. An Effective Way to Reduce Fuel Consumption and CO2 Emissions*. URL: <http://www.onairweb.com/upload/aaadz.pdf> (visited on 10/08/2018).
- Oosterveld, M. W. and P. van Oossanen (1975). "Further Computer-Analyzed Data of the Wageningen B-Screw Series". In: *International Shipbuilding Progress* 22.251, pp. 1–14. ISSN: 0020868X.
- Ottaviani, E., R. Zaccone, M. Figari, and M. Altosole (2016). *Voyage Optimization Techniques*. La Spezia: On AIR. DOI: 10.13140/RG.2.2.33042.66246.
- Papadakis, N. A. and A. N. Perakis (1990). "Deterministic Minimal Time Vessel Routing". In: *Operations Research* 38.3, pp. 426–438. DOI: 10.1287/opre.38.3.426.
- Perakis, A. N. and N. A. Papadakis (1989). "Minimal Time Vessel Routing in a Time-Dependent Environment". en. In: *Transportation Science* 23.4, pp. 266–276.
- Perez, T. (2005). *Ship Motion Control. Course Keeping and Roll Stabilisation using Rudder and Fins*. Advances in industrial control. London: Springer. ISBN: 1852339594.
- Persson, A., E. Andersson, and I. Tsonevsky (2015). *User Guide to ECMWF Forecast Products*. Version 1.2. ECMWF.
- Petrie, G. L., K. J. Bongort, and W. M. Maclean (1984). "A New Approach to Vessel Weather Routing and Performance Analysis". In: *Marine Technology* 21.1, pp. 19–40.
- Pipchenko, O. (2011). "On the Method of Ship's Transoceanic Route Planning". In: *TransNav, International Journal on Marine Navigation and Safety of Sea Transportation* 5.3, pp. 157–163. DOI: 10.1201/b11344-26.
- Pivotal Software (2019). *Messaging that just works - RabbitMQ*. URL: <https://www.rabbitmq.com/> (visited on 20/01/2019).
- Poler, R., J. Mula, and M. Díaz-Madroñero (2014). *Operations Research Problems. Statements and Solutions*. London: Springer. ISBN: 978-1-4471-5577-5. DOI: 10.1007/978-1-4471-5577-5.

-
- Powell, M. J. D. (1964). “An Efficient Method for Finding the Minimum of a Function of Several Variables without Calculating Derivatives”. In: *The Computer Journal* 7.2, pp. 155–162. ISSN: 0010-4620. DOI: 10.1093/comjnl/7.2.155.
- Prpić-Oršić, J. and O. M. Faltinsen (2012). “Estimation of Ship Speed Loss and Associated CO₂ Emissions in a Seaway”. en. In: *Ocean Engineering* 44, pp. 1–10. ISSN: 00298018. DOI: 10.1016/j.oceaneng.2012.01.028.
- Rehmatulla, N. (2012). *Barriers to Uptake of Energy Efficient Operational Measures. Survey Report*. UCL Energy Insitute.
- Rehmatulla, N. (2014). “Market Failures and Barriers Affecting Energy Efficient Operations in Shipping”. Energy Institute. PhD Thesis. London: University College London.
- Rehmatulla, N. and T. Smith (2015). “Barriers to Energy Dfficiency in Shipping. A Triangulated Approach to Investigate the Principal Agent Problem”. In: *Energy Policy* 84, pp. 44–57. ISSN: 03014215. DOI: 10.1016/j.enpol.2015.04.019.
- Riesner, M., S. Sigmund, and O. el Moctar (2016). *Entwicklung von numerischen Verfahren zur Bestimmung des Leistungsbedarfs von Schiffen im Seegang*. PerSee Abschlussbericht. Duisburg: Universität Duisburg-Essen.
- Salvesen, N. (1978). “Added Resistance of Ships in Waves”. In: *Journal of Hydronautics* 12.1, pp. 24–34. ISSN: 1555-5909. DOI: 10.2514/3.63110.
- Sasaki, N., T. Matsubara, and T. Yoshida (2008). “Analysis of Speed Drop of Large Container Ships Operating in Sea Way”. ja. In: *Conference Proceedings, The Japan Society of Naval Architects and Ocean Engineers* 6, pp. 9–12. DOI: 10.14856/conf.6.0_9.
- Schenzle, P. (2016). *Technik und Strömungsmechanik von Segelschiffen*. Vorlesungsmanuskript. de. Hamburg: Technische Universität Hamburg-Harburg.
- Schlinkert, G. (2015). *Route Spotlight: Considering EEOI and Cost Savings*. StormGeo. URL: <http://www.stormgeo.com/shipping/fleet-performance/news/route-spotlight-considering-eeoi-and-cost-savings/> (visited on 30/10/2017).
- Schneekluth, H. and V. Bertram (1998). *Ship Design for Efficiency and Economy*. 2nd ed. Oxford: Butterworth-Heinemann. ISBN: 0 7506 4133 9.
- Schwenkert, R. and Y. Stry (2015). *Operations Research kompakt. Eine an Beispielen orientierte Einführung*. 1. Aufl. 2015. Berlin and Heidelberg: Springer Gabler. ISBN: 978-3-662-48397-8.

- Sen, D. and C. P. Padhy (2010). “Development of a Ship Weather-Routing Algorithm for Specific Application in North Indian Ocean Region”. In: *Proceedings of MARTEC 2010*. The International Conference on Marine Technology (Dhaka, Bangladesh).
- Sen, D. and C. P. Padhy (2015). “An Approach for Development of a Ship Routing Algorithm for Application in the North Indian Ocean Region”. en. In: *Applied Ocean Research* 50, pp. 173–191. ISSN: 01411187. DOI: 10.1016/j.apor.2015.01.019.
- Shao, W. and P. Zhou (2011). “Development of a Dynamic Programming Method for Low Fuel Consumption and Low Carbon Emission from Shipping”. In: *Low Carbon Shipping Conference 2011* (Glasgow, UK).
- Shao, W. and P. Zhou (2012). “Development of a 3D Dynamic Programming Method for Weather Routing”. en. In: *TransNav, International Journal on Marine Navigation and Safety of Sea Transportation* 6.1, pp. 79–85.
- Shao, W., P. Zhou, and S. K. Thong (2012). “Development of a Novel Forward Dynamic Programming Method for Weather Routing”. en. In: *Journal of Marine Science and Technology* 17.2, pp. 239–251. ISSN: 0948-4280. DOI: 10.1007/s00773-011-0152-z.
- Shields, M. and T. Weber (2015). “Challenges and Solutions in Speed and Route Optimization”. en. In: *14th International Conference on Computer and IT Applications in the Maritime Industries, COMPIT’15. Ulrichshusen, 11 - 13 May 2015*. Ed. by V. Bertram. Hamburg: Techn. Univ. Verl. Schriftenreihe Schiffbau, pp. 473–479. ISBN: 9783892206804.
- Shigunov, V. (2017). “Added Power in Seaway”. In: *Ship Technology Research* 64.2, pp. 65–75. DOI: 10.1080/09377255.2017.1331953.
- Shubert, B. O. (1972). “A Sequential Method Seeking the Global Maximum of a Function”. In: *SIAM Journal on Numerical Analysis* 9.3, pp. 379–388. ISSN: 0036-1429. DOI: 10.1137/0709036.
- Siedler, G., S. M. Griffies, W. J. Gould, and J. Church, eds. (2013). *Ocean Circulation and Climate. A 21st Century Perspective*. en. Second Edition. Vol. 103. International geophysics series. Amsterdam: Academic Press. ISBN: 978-0-12-391851-2.
- Sigmund, S. and O. el Moctar (2017). “Numerical and Experimental Investigation of Propulsion in Waves”. In: *Ocean Engineering* 144, pp. 35–49. ISSN: 00298018. DOI: 10.1016/j.oceaneng.2017.08.016.
- Sigmund, S. and O. el Moctar (2018). “Numerical and Experimental Investigation of Added Resistance of Different Ship Types in Short and Long Waves”. In: *Ocean Engineering* 147, pp. 51–67. ISSN: 00298018. DOI: 10.1016/j.oceaneng.2017.10.010.

- Skoglund, L., J. Kутtenkeuler, and A. Rosén (2012). *A New Method for Robust Route Optimization in Ensemble Weather Forecasts*. Sweden: KTH, School of Engineering Sciences.
- Skoglund, L., J. Kутtenkeuler, A. Rosén, and E. Ovegård (2015). “A Comparative Study of Deterministic and Ensemble Weather Forecasts for Weather Routing”. In: *Journal of Marine Science and Technology* 20.3, pp. 429–441. ISSN: 0948-4280. DOI: 10.1007/s00773-014-0295-9.
- SkySails (2017). *V-PER by SkySails - V-PER*. URL: <http://www.v-per.com/> (visited on 26/08/2017).
- Smith, T., P. Newton, G. Winn, and A. La Grech Rosa (2013). “Analysis Techniques for Evaluating the Fuel Savings Associated with Wind Assistance”. In: *Low Carbon Shipping Conference 2013* (London, UK).
- Smith, T., S. Day, R. Bucknall, J. Mangan, J. Dinwoodie, M. Landamore, and O. Turan (2014). *Low Carbon Shipping. A Systems Approach*. Final Report. Newcastle University, University College London, The University of Hull, The University of Plymouth, University of Strathclyde Glasgow.
- Smith, T., J. P. Jalkanen, B. A. Anderson, J. J. Corbett, J. Faber, and Hanayama (2015). *Third IMO Greenhouse Gas Study 2014. Executive Summary and Final Report*. London: IMO.
- Smith, T., C. Raucci, S. H. Hosseinloo, I. Rojon, J. N. Calleya, Suarez De La Fuente, Santiago, P. Wu, and K. Palmer (2016). *CO2 Emissions from International Shipping. Possible Reduction Targets and their Associated Pathways*. Prepared by UMAS. London.
- SNAME (1950). *Nomenclature for Treating the Motion of a Submerged Body through a Fluid. Report of the American Towing Tank Conference*. Technical and Research Bulletin No. 1–5. New York (NY): Society of Naval Architects and Marine Engineers.
- Sniedovich, M. (2006). “Dijkstra’s Algorithm Revisited: The Dynamic Programming Connexion”. In: *Control and Cybernetics* 35.3, pp. 599–620.
- Söding, H. and V. Bertram (2009). *Program PDSTRIP: Public Domain Strip Method*. Updated in 2014.
- Spaans, J. A. (1985). “Windship Routeing”. In: *Journal of Wind Engineering and Industrial Aerodynamics* 19.1-3, pp. 215–250. ISSN: 01676105. DOI: 10.1016/0167-6105(85)90063-7.

BIBLIOGRAPHY

- Spaans, J. A. and H. Hagiwara (1987). “Computation of Optimum Routes for Ship Weather Routing”. In: *International Symposium on Weather-routing*. Toyko: Department of Transport and Japan Foundation for Shipbuilding Advancement.
- Spaans, J. A. and P. Stoter (2000). “Shipboard Weather Routing”. In: *Proceedings of the IAIN World Congress and the 56th Annual Meeting of The Institute of Navigation*. San Diego (CA), pp. 170–174.
- StormGeo (2017a). *AWT is Changing its Name to StormGeo!* URL: <http://www.stormgeo.com/awtworldwide> (visited on 18/10/2017).
- StormGeo (2017b). *BVS Dual Speed Optimization. Saves Fuel in ECA Zones*.
- StormGeo (2017c). *BVS Dual Speed Optimization. Saves Fuel in ECA Zones*. URL: <http://www.stormgeo.com/shipping/on-board-services/dual-speed/> (visited on 30/10/2017).
- StormGeo (2017d). *CPO Containerschiffreederei & BVS*. URL: <https://www.stormgeo.com/shipping/customers/cpo-containerschiffreederei-and-bvs/> (visited on 30/10/2017).
- StormGeo (2017e). *Customer-Story. H-Line-Shipping*. URL: <https://www.stormgeo.com/solutions/shipping/on-board-services/articles/h-line-shipping-co-ltd/> (visited on 25/10/2017).
- StormGeo (2017f). *Extending the Bridge with BVS8*. URL: <https://www.stormgeo.com/assets/ArticleFiles/StormGeo-Shipping-BVS8.pdf> (visited on 18/10/2017).
- StormGeo (2017g). *History. StormGeo has Grown to Become a Global Company with Nearly 400 People in 22 offices in 16 countries*. URL: <http://www.stormgeo.com/who-we-are/history/> (visited on 18/10/2017).
- StormGeo (2017h). *Leading the Industry. Weather Routing to Save Fuel, Time & Money*. URL: <http://www.stormgeo.com/shipping/> (visited on 18/10/2017).
- StormGeo (2017i). *Ship Routing. Getting you there safely and efficiently*. URL: <http://www.stormgeo.com/shipping/ship-routing/awt-ship-routing/> (visited on 25/10/2017).
- Szlapczynska, J. (2007). “Multiobjective Approach to Weather Routing”. In: *TransNav, International Journal on Marine Navigation and Safety of Sea Transportation* 1.3, pp. 273–278.
- Szlapczynska, J. and R. Smierzchalski (2007). “Adopted Isochrone Method Improving Ship Safety in Weather Routing with Evolutionary Approach”. en. In: *International Journal of Reliability, Quality and Safety Engineering* 14.06, pp. 635–645. ISSN: 0218-5393. DOI: 10.1142/S0218539307002842.

- Szlapczynska, J. and R. Smierzchalski (2009). “Multicriteria Optimisation in Weather Routing”. en. In: *International Journal on Marine Navigation and Safety of Sea Transportation* 3.4, pp. 393–400.
- Szlapczynska, J. (2013). “Multicriteria Evolutionary Weather Routing Algorithm in Practice”. en. In: *TransNav, International Journal on Marine Navigation and Safety of Sea Transportation* 7.2, pp. 61–65. DOI: 10.12716/1001.07.01.07.
- Szlapczynska, J. (2015). “Multi-objective Weather Routing with Customised Criteria and Constraints”. en. In: *Journal of Navigation* 68.02, pp. 338–354. ISSN: 0373-4633. DOI: 10.1017/S0373463314000691.
- Takashima, K., B. Mezaoui, and R. Shoji (2009). “On the Fuel Saving Operation for Coastal Merchant Ships using Weather Routing”. en. In: *International Journal on Marine Navigation and Safety of Sea Transportation* 3.4, pp. 401–406. DOI: 10.1201/9780203869345.ch75.
- Tastula, E.-M. (2016). *The Engine of the StormGeo Data Flow*. StormGeo. URL: <http://www.stormgeo.com/shipping/news/the-engine-of-the-awt-dataflow/> (visited on 30/10/2017).
- The Maritime Executive (2017). *Advanced Analytics Go Beyond Weather Forecasting*. URL: <https://maritime-executive.com/blog/advanced-analytics-go-beyond-weather-forecasting> (visited on 30/10/2017).
- The WAVEWATCH III Development Group (2016). *User Manual and System Documentation of WAVEWATCH III Version 5.16. Tech. Note 329*. College Park (MD): NOAA/NWS/NCEP/MMAB.
- Tidetch (2017). *Partner Solutions*. URL: <https://tidetchmarinedata.com/solutions/> (visited on 28/01/2018).
- Tidetch (2018). *Tidetch Environmental Data. Sources and Validation*. URL: <https://tidetchmarinedata.com/metocean-data/validation/> (visited on 29/05/2018).
- Tidetch (2019). *Metocean Data*. URL: <https://tidetchmarinedata.com/metocean-data/> (visited on 26/05/2019).
- Townsin, R. L. and Y. J. Kwon (1983). “Approximate Formulae for the Speed Loss Due to Added Resistance in Wind and Waves”. In: *R.I.N.A. Supplementary Papers* 125, pp. 199–207.
- Traut, M., P. Gilbert, C. Walsh, A. Bows, A. Filippone, P. Stansby, and R. Wood (2014). “Propulsive Power Contribution of a Kite and a Flettner Rotor on Selected Shipping Routes”. In: *Applied Energy* 113, pp. 362–372. ISSN: 03062619. DOI: 10.1016/j.apenergy.2013.07.026.

- Tsou, M.-C. and H.-C. Cheng (2013). “An Ant Colony Algorithm for Efficient Ship Routing”. In: *Polish Maritime Research* 20.3, pp. 28–38. ISSN: 1233-2585. DOI: 10.2478/pomr-2013-0032.
- Tsujimoto, M. and K. Tanizawa (2006). “Development of a Weather Adaptive Navigation System Considering Ship Performance in Actual Seas”. In: *Proceedings of the 25th International Conference on Offshore Mechanics and Arctic Engineering*. OMAE 2006 (Hamburg, Germany). New York (NY): American Society of Mechanical Engineers, pp. 413–421. ISBN: 9780791847497. DOI: 10.1115/OMAE2006-92376.
- Turau, V. (2009). *Algorithmische Graphentheorie*. de. 3. überarbeitete Auflage. München: Oldenbourg Verlag. ISBN: 978-3-486-59057-9. DOI: 10.1524/9783486598520.
- U.S. Navy (2018). *Naval Oceanography Portal*. URL: <http://www.usno.navy.mil/> (visited on 22/02/2018).
- Valanto, P. (2016). *Zusatzwiderstand und Propulsion von Schiffen im Seegang*. de. PerSee Abschlussbericht. Hamburg: Hamburgische Schiffbau-Versuchsanstalt. DOI: 10.2314/GBV:87788904X.
- Veneti, A., C. Konstantopoulos, and G. Pantziou (2015a). “An Evolutionary Approach to Multi-objective Ship Weather Routing”. In: *Proceedings of the 6th International Conference on Information, Intelligence, Systems and Applications (IISA)*. Date: 6-8 July 2015. IISA (Corfu, Greece). Piscataway (NJ): IEEE, pp. 1–6. ISBN: 978-1-4673-9311-9. DOI: 10.1109/IISA.2015.7388052.
- Veneti, A., C. Konstantopoulos, and G. Pantziou (2015b). “Continuous and Discrete Time Label Setting Algorithms for the Time Dependent Bi-Criteria Shortest Path Problem”. In: *Operations Research and Computing: Algorithms and Software for Analytics*. Ed. by B. Borchers, J. P. Brooks, and L. McLay. INFORMS, pp. 62–73. ISBN: 9780984337866. DOI: 10.1287/ics.2015.0005.
- Veneti, A., A. Makrygiorgos, C. Konstantopoulos, G. Pantziou, and I. A. Vetsikas (2017). “Minimizing the Fuel Consumption and the Risk in Maritime Transportation. A Bi-objective Weather Routing Approach”. In: *Computers and Operations Research* 88, pp. 220–236. DOI: 10.1016/j.cor.2017.07.010.
- Vettor, R. and C. Guedes Soares (2015a). “A Ship Weather Routing Tool to Face the Challenges of an Evolving Maritime Trade”. In: *Proceedings of the International Navigation Conference 2015* (Manchester, UK). Royal Institute of Navigation.
- Vettor, R. and C. Guedes Soares (2015b). “Multi-objective Route Optimization for On-board Decision Support System”. In: *Information, Communication and Environment. Marine Navigation and Safety of Sea Transportation*. Ed. by A. Weintrit and T.

- Neumann. London: Taylor & Francis Group, pp. 99–106. ISBN: 9780429225857. DOI: 10.1201/b18514-14.
- Vettor, R. and C. Guedes Soares (2016). “Development of a Ship Weather Routing System”. In: *Ocean Engineering* 123, pp. 1–14. ISSN: 00298018. DOI: 10.1016/j.oceaneng.2016.06.035.
- Walther, L., H.-C. Burmeister, and W. Bruhn (2014). “Safe and Efficient Autonomous Navigation with Regards to Weather”. en. In: *13th International Conference on Computer and IT Applications in the Maritime Industries, COMPIT’14. Redworth, 12 - 14 May 2014*. Ed. by V. Bertram. Hamburg: Techn. Univ. Verl. Schriftenreihe Schiffbau, pp. 303–317. ISBN: 9783892206729.
- Walther, L. (2015). “Special-Purpose Weather Routing: Autonomous and Wind-Driven Ships”. en. In: *14th International Conference on Computer and IT Applications in the Maritime Industries, COMPIT’15. Ulrichshusen, 11 - 13 May 2015*. Ed. by V. Bertram. Hamburg: Techn. Univ. Verl. Schriftenreihe Schiffbau, pp. 223–235. ISBN: 9783892206804.
- Walther, L., C. Jahn, and T. Lade (2015). “Weather Routing for a Wind Driven Hybrid Merchant Vessel”. da. In: *OCEANS 2015 - Genova. Proceedings of a meeting held 18-21 May 2015, Genova, Italy*. Piscataway (NJ): IEEE, pp. 1511–1517. ISBN: 978-1-4799-8736-8. DOI: 10.1109/OCEANS-Genova.2015.7271557.
- Walther, L., A. Rizvanolli, M. Wendebourg, and C. Jahn (2016). “Modeling and Optimization Algorithms in Ship Weather Routing”. In: *International Journal of e-Navigation and Maritime Economy* 4, pp. 31–45. ISSN: 24055352. DOI: 10.1016/j.enavi.2016.06.004.
- Walther, L., A. Rizvanolli, S. Shetty, and C. Jahn (2017). “Comparing Two Optimization Approaches for Ship Weather Routing”. In: *Operations Research Proceedings 2016. Annual International Conference of the German Operations Research Society (GOR) (Hamburg, Germany)*. Ed. by A. Fink, A. Fügenschuh, and M. J. Geiger. Cham: Springer Science and Business Media and Springer, pp. 337–342. ISBN: 3319557025.
- Weathernews (2013). *Maritime Weather and Wave Forecast Upgrade. High-resolution weather and waves model with QRT data integration for higher quality service*. Press Release 08/10/2013.
- Weathernews (2014). *Total Fleet Management Service*. URL: <https://weathernews.com/TFMS/services/vp/index.html> (visited on 02/11/2017).
- Weathernews (2016). *Maersk Line and Maersk Tankers Enter into Three Year contract with Weathernews Inc*. Press Release 23/03/2016.

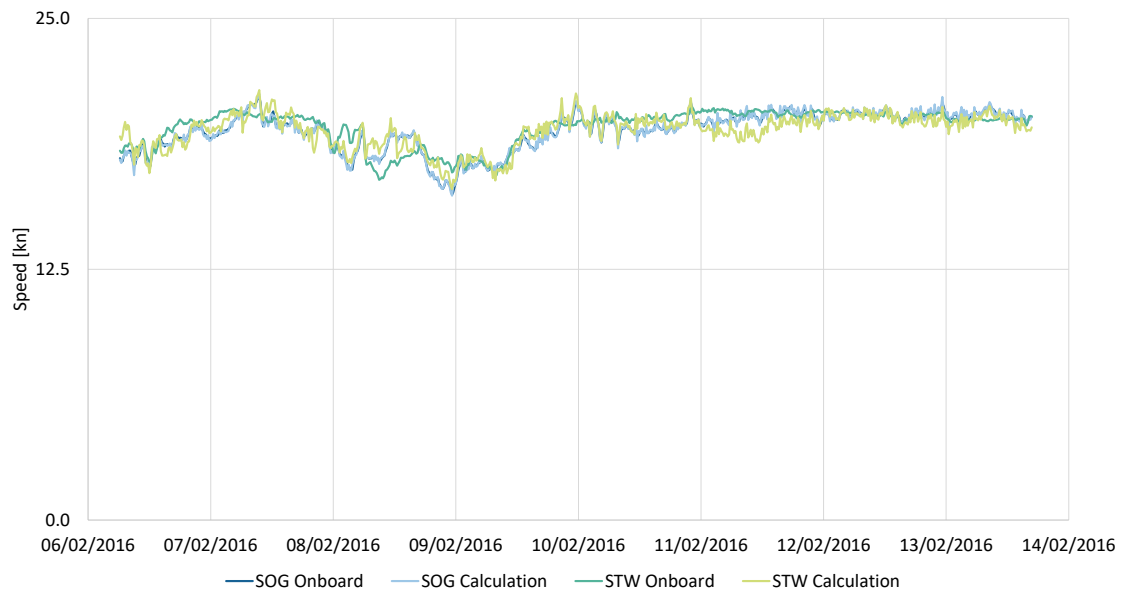
BIBLIOGRAPHY

- Weathernews (2017). *Your Industry*. URL: <https://global.weathernews.com/your-industry/> (visited on 02/11/2017).
- Weber, T. (1995). “Optimale Planung und Steuerung von Schiffsreisen”. Verkehrswesen und Angewandte Mechanik. de. PhD Thesis. Berlin: Technische Universität Berlin.
- Wells, N. (2012). *The Atmosphere and Ocean. A Physical Introduction*. 3rd ed. Advancing weather and climate science. Chichester, West Sussex and Hoboken (NJ): Wiley-Blackwell. ISBN: 9781119994596.
- Werners, B. (2013). *Grundlagen des Operations Research. Mit Aufgaben und Lösungen*. 3., überarb. Aufl. Springer-Lehrbuch. Berlin, Heidelberg: Springer Gabler. ISBN: 978-3-642-40102-2.
- Wingrove, M. (2016a). “Owners cut Fuel Costs by 10 per cent”. In: *Marine Electronics & Communications* 10.4, pp. 42–43.
- Wingrove, M. (2016b). “Passage planning should include weather routeing”. In: *The Complete Guide to ECDIS*, pp. 30–31.
- Wisniewski, B., P. Medyna, and J. Chomski (2009). “Application of the 1-2-3 Rule for Calculations of a Vessel’s Route Using Evolutionary Algorithms”. In: *TransNav, International Journal on Marine Navigation and Safety of Sea Transportation* 3.2, pp. 143–146.
- Wit, C. de (1968). “Mathematical Treatment of Optimal Ocean Ship Routeing”. en. PhD Thesis. Delft: Technische Hogeschool Delft.
- Wit, C. de (1970). *Optimal Meteorological Ship Routeing*. Delft: Netherlands Ship Research Center TNO.
- Wit, C. de (1976). “Optimal Ocean Navigation”. In: *Optimization Techniques. Modeling and Optimization in the Service of Man*. Proceedings, 7th IFIP Conference, Nice, Sept. 8-12, 1975. Ed. by J. Cea. Vol. 40. Lecture Notes in Computer Science. Berlin: Springer, pp. 748–756. ISBN: 978-3-540-07622-3. DOI: 10.1007/3-540-07622-0_508.
- Wit, C. de (1988). “Practical Weather Routeing of Sail-assisted Motor Vessels”. In: *Journal of Navigation* 41.01, p. 134. ISSN: 0373-4633. DOI: 10.1017/S0373463300009127.
- Wit, C. de (1990). “Proposal for Low Cost Ocean Weather Routeing”. In: *Journal of Navigation* 43.03, pp. 428–439. ISSN: 0373-4633. DOI: 10.1017/S0373463300014053.
- WMO, ed. (2001). *Guide to Marine Meteorological Services*. 3rd. ed. WMO-Publications No. 471. Geneva.

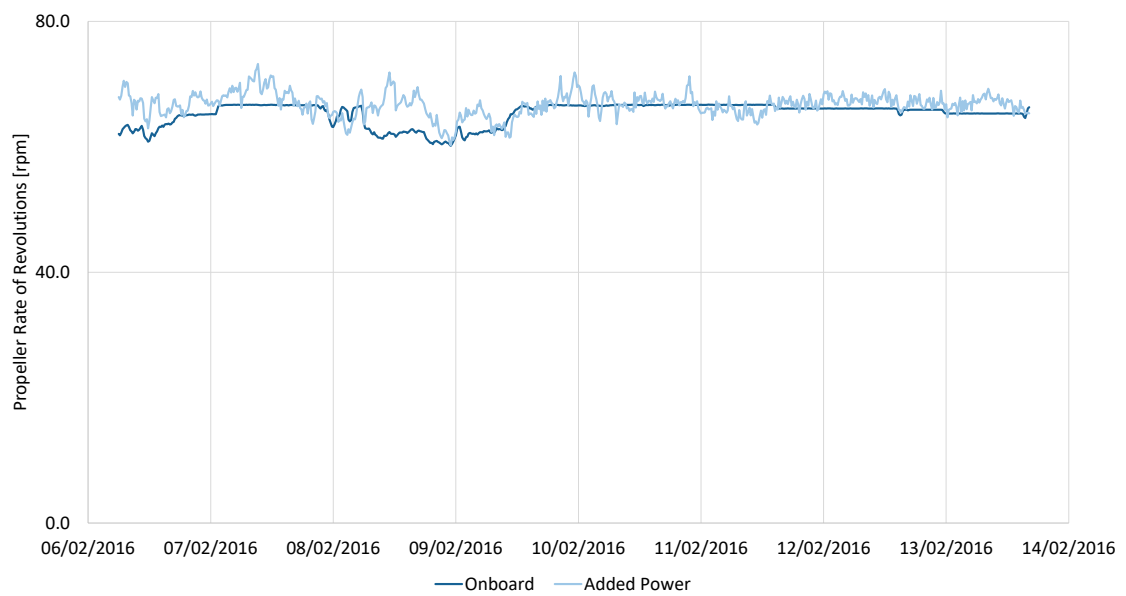
- WMO (2003). *Introduction to GRIB Edition 1 and GRIB Edition 2*. URL: https://www.wmo.int/pages/prog/www/WMOCodes/Guides/GRIB/Introduction_GRIB1-GRIB2.pdf (visited on 03/07/2015).
- WMO, ed. (2010). *Manual on the Global Data-processing and Forecasting System. Volume I - Global Aspects*. WMO-Publications No. 485. Geneva. ISBN: 978-92-63-10485-4.
- WMO, ed. (2012). *Guidelines on Ensemble Prediction Systems and Forecasting*. WMO-Publications No. 1091. Geneva. ISBN: 978-92-63-11091-6.
- WMO, ed. (2015). *Manual on Codes. International Codes. Volume 1.2*. Annex II to the WMO Technical Regulations. Part B – Binary Codes, Part C – Common Features to Binary and Alphanumeric Codes. 2015 edition. WMO-Publications No. 306. Geneva. ISBN: 978-92-63-10306-2.
- Zaccone, R. and M. Figari (2017). “Energy Efficient Ship Voyage Planning by 3D Dynamic Programming”. In: *Journal of Ocean Technology* 12.4, pp. 49–71.
- Zaccone, R., E. Ottaviani, M. Figari, and M. Altosole (2018). “Ship Voyage Optimization for Safe and Energy-Efficient Navigation. A Dynamic Programming Approach”. In: *Ocean Engineering* 153, pp. 215–224. ISSN: 00298018. DOI: 10.1016/j.oceaneng.2018.01.100.
- Zaitoun, M., A. Delius, and G.-M. Wuersig (2014). “The New Reference for LNG Propulsion. Development of Emission Reductions from 4,200 TEU to Present 18,800 TEU Ships of UASC with LNG as Fuel on Asia to Europe Trading Route”. In: *LNG as Ship Fuel* 01, pp. 14–17.
- Zoppoli, R. (1972). “Minimum-Time Routing as an N-Stage Decision Process”. In: *Journal of Applied Meteorology* 11.3, pp. 429–435. ISSN: 0021-8952. DOI: 10.1175/1520-0450(1972)011<0429:MTRAAS>2.0.CO;2.

A Additional Analyses

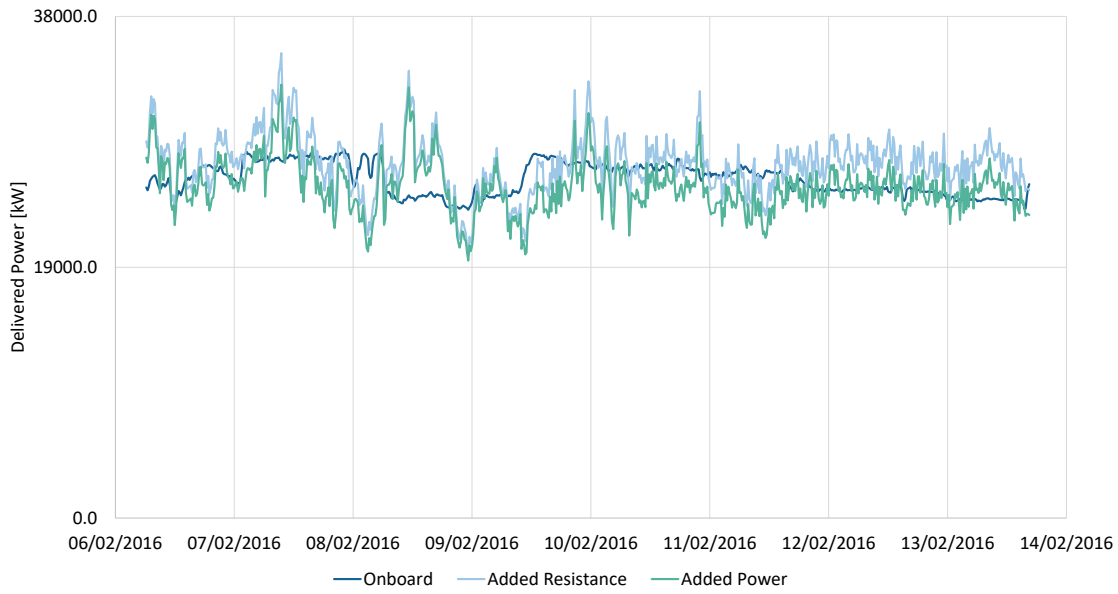
A ADDITIONAL ANALYSES



(a) Speed Over Ground and Through Water

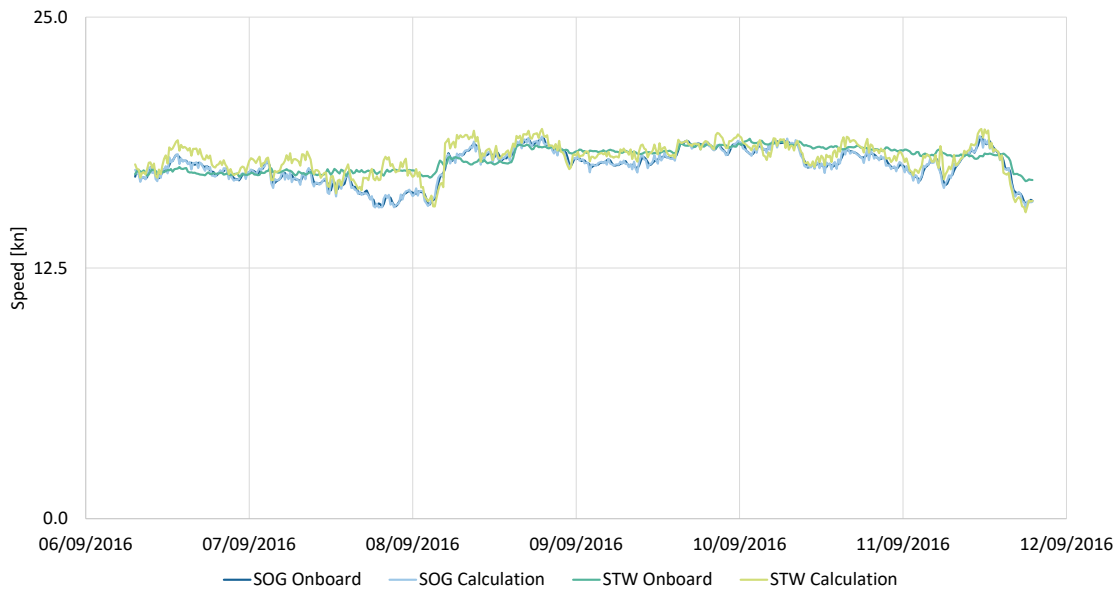


(b) Propeller Revolutions

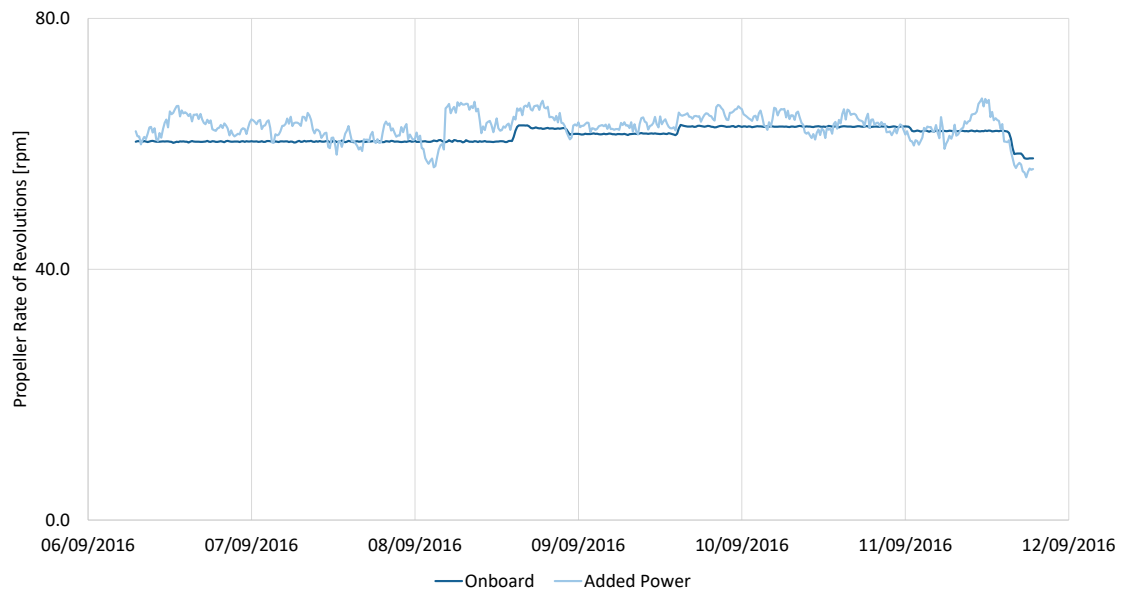


(c) Delivered Power

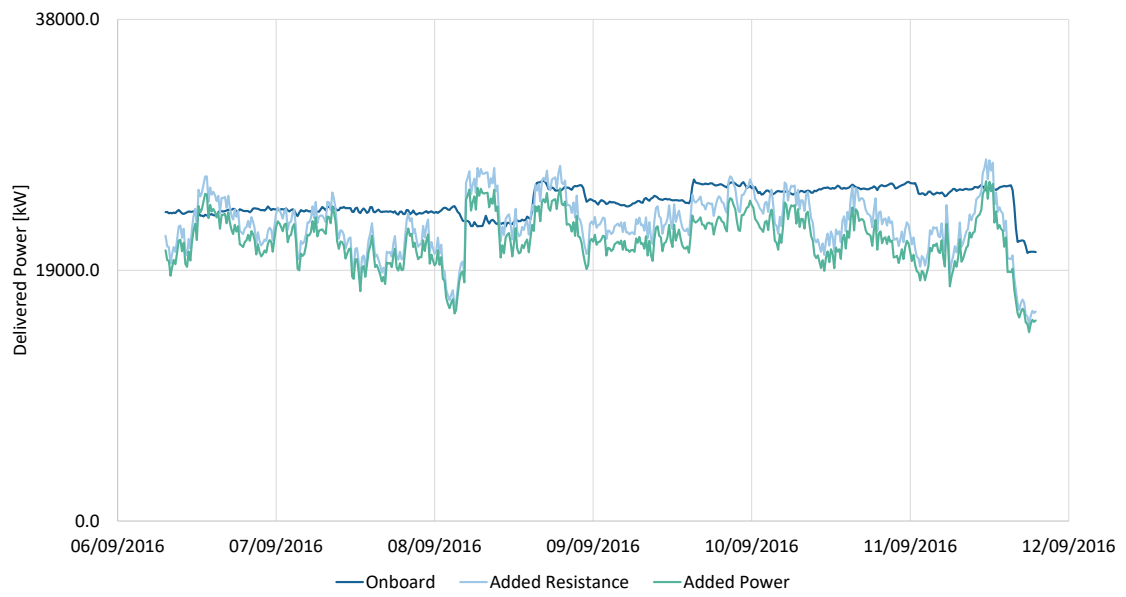
Figure A.1: Time Series of Operational Data during Voyage 2



(a) Speed Over Ground and Through Water

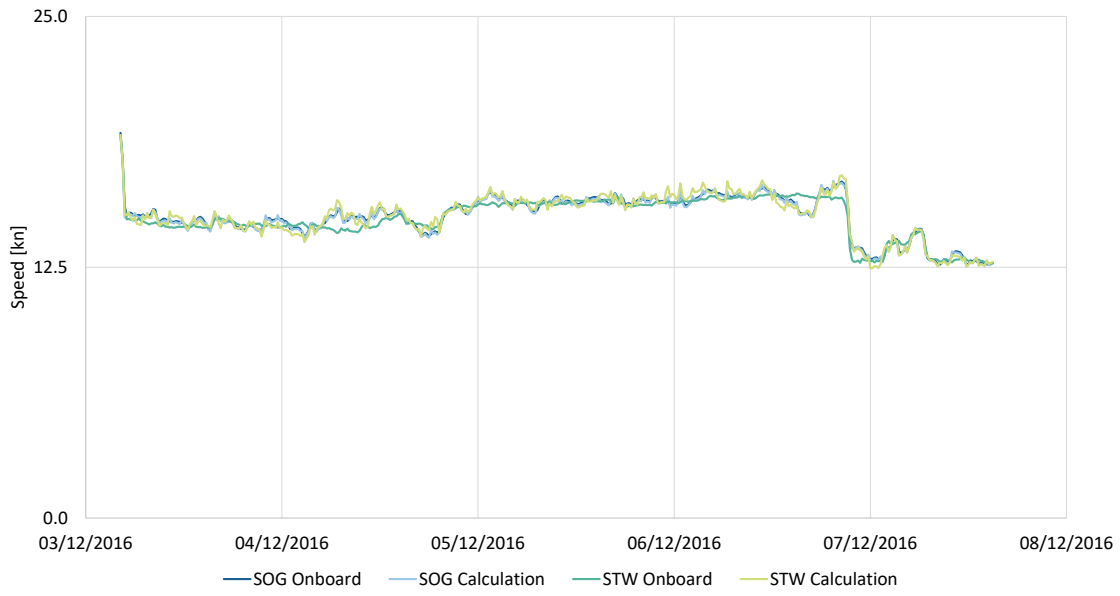


(b) Propeller Revolutions

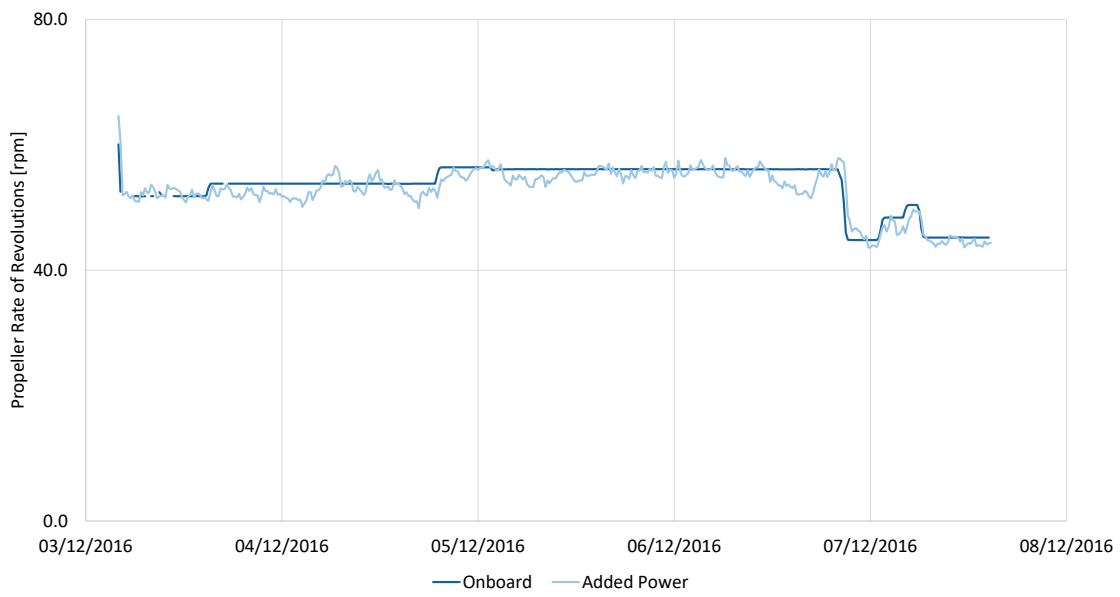


(c) Delivered Power

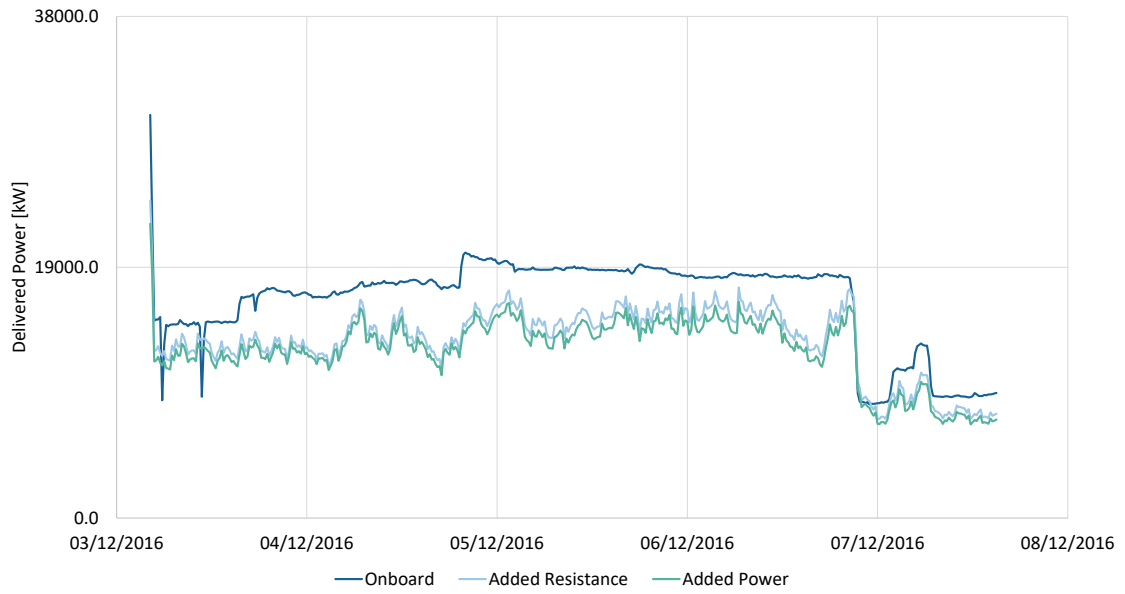
Figure A.2: Time Series of Operational Data during Voyage 3



(a) Speed Over Ground and Through Water

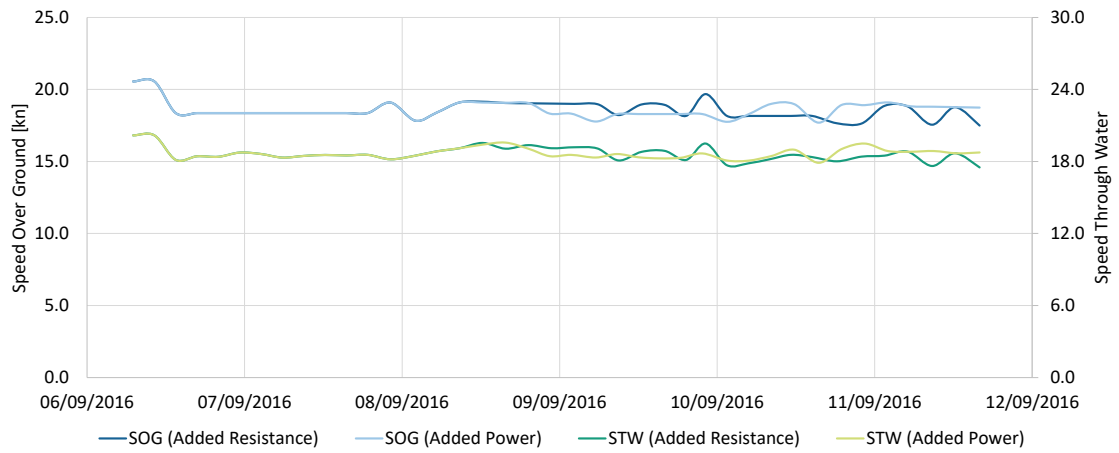


(b) Propeller Revolutions



(c) Delivered Power

Figure A.3: Time Series of Operational Data during Voyage 4



(a) Speed Over Ground and Through Water

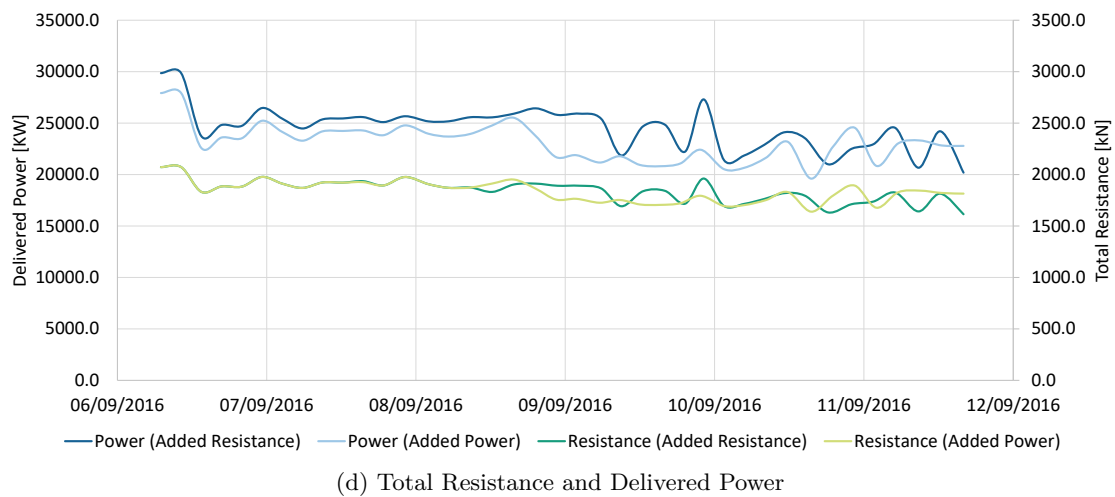
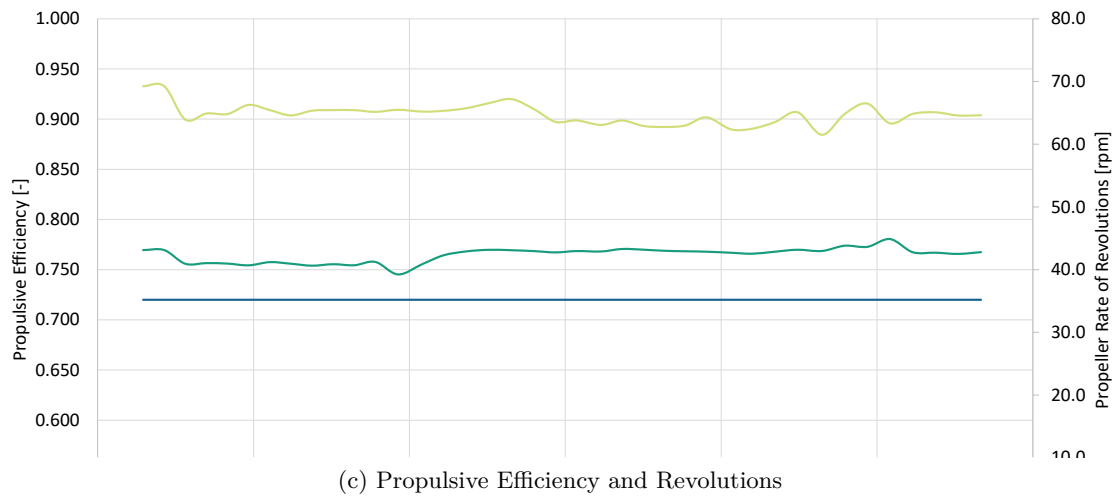
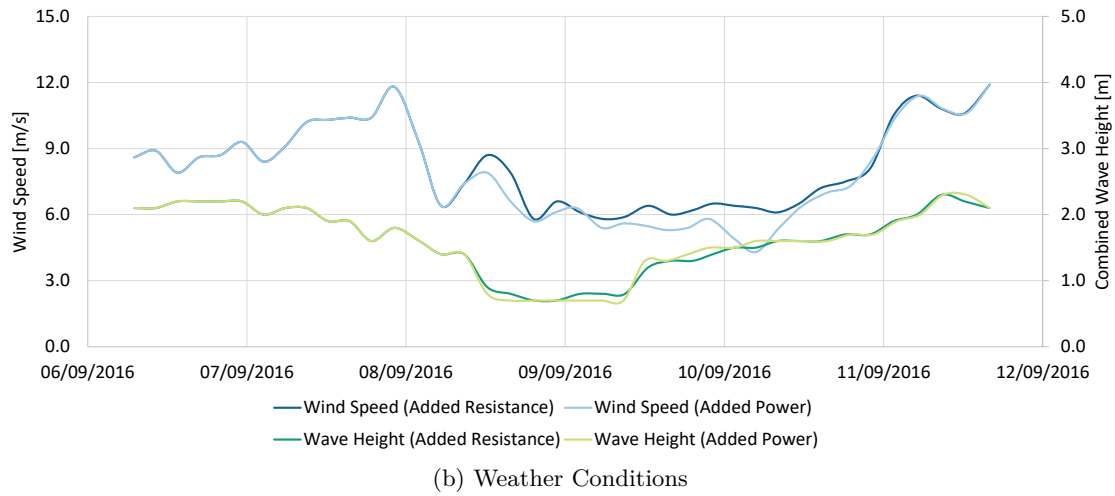
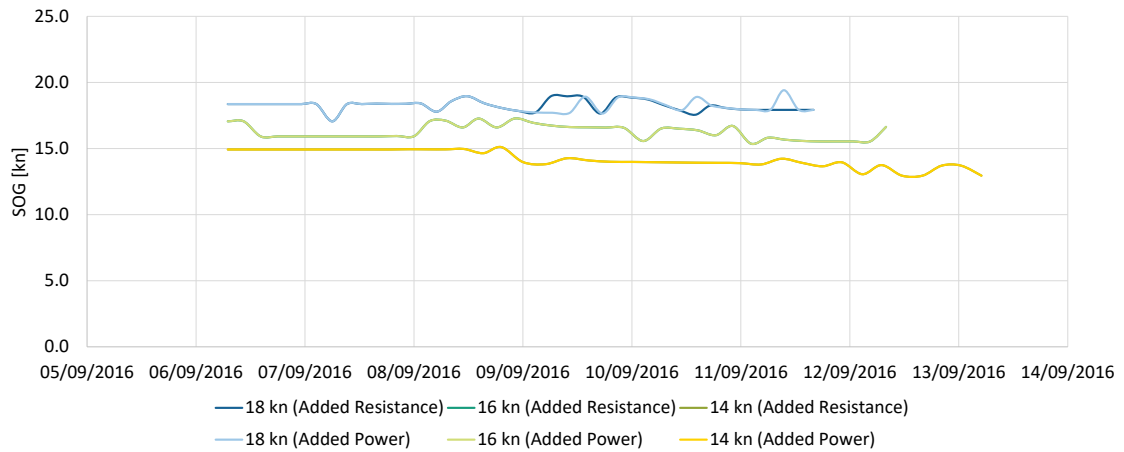
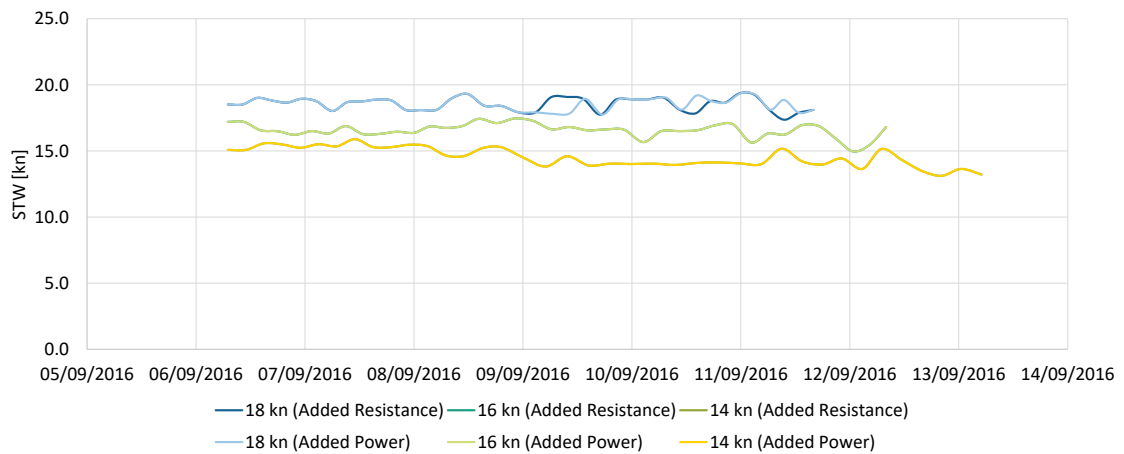


Figure A.4: Time Series of Optimization Results for Voyage 3

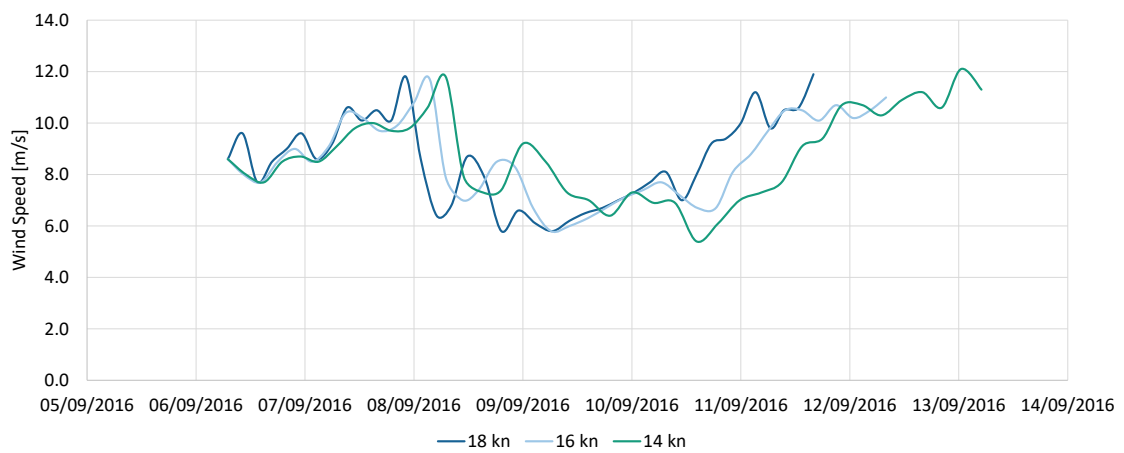
A ADDITIONAL ANALYSES



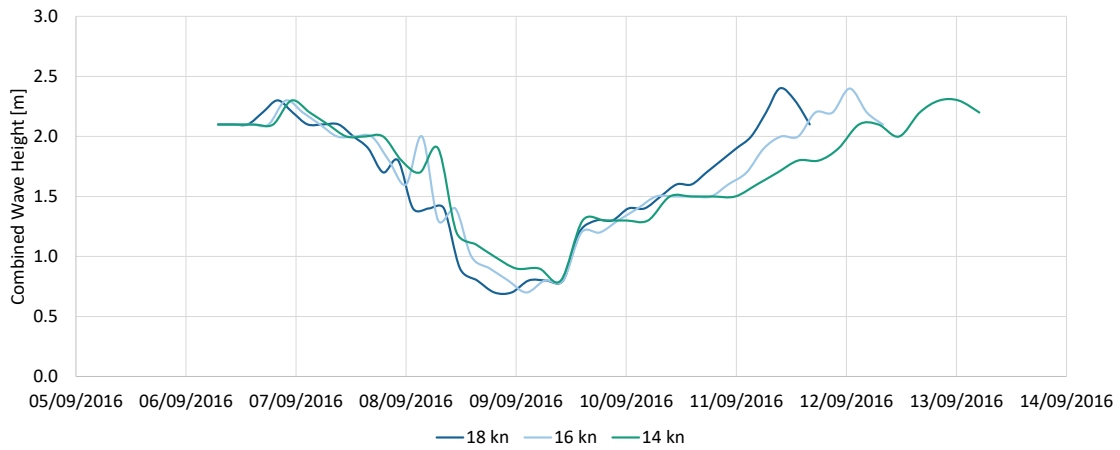
(a) Speed Over Ground



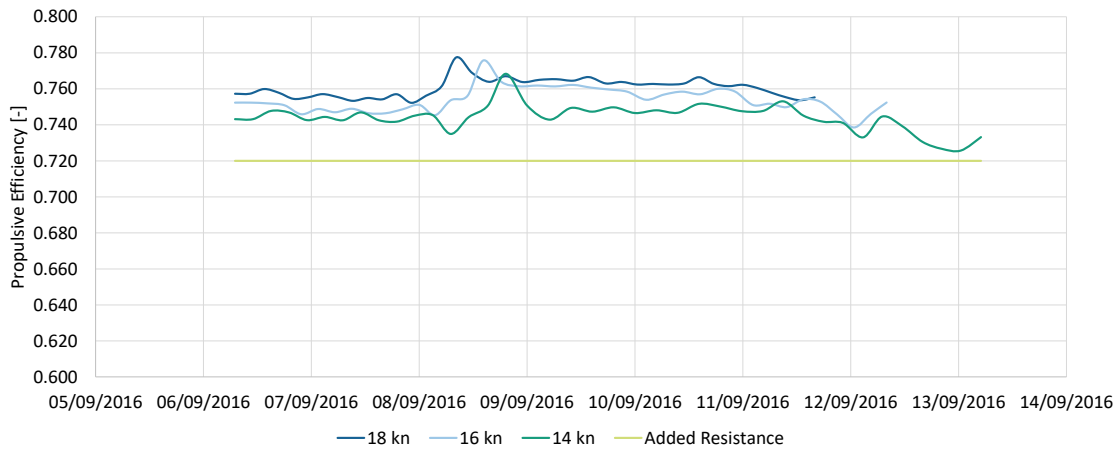
(b) Speed Through Water



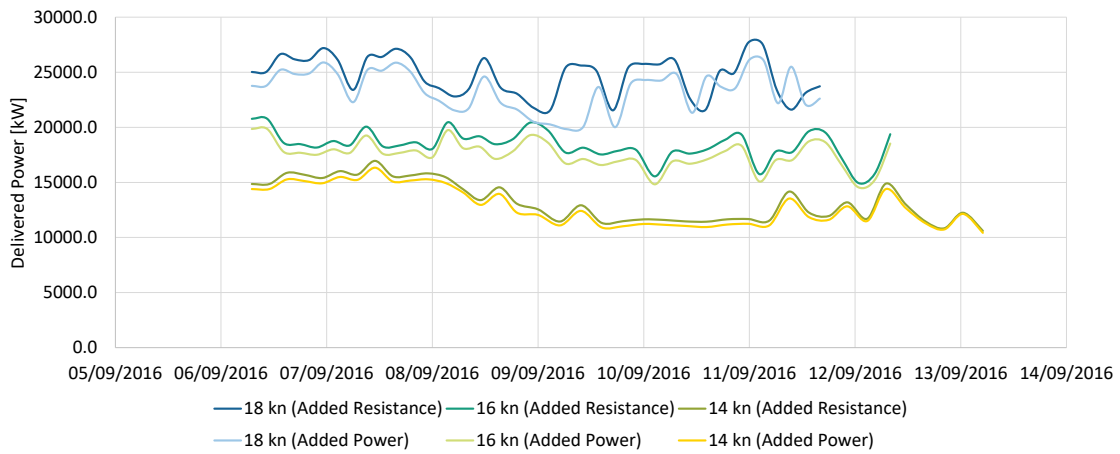
(c) Wind Conditions



(d) Wave Conditions



(e) Propulsive Efficiency



(f) Delivered Power

Figure A.5: Time Series of Results for Voyage 3 with Varying Arrival Times

Editor: Prof. Dr.-Ing. Carlos Jahn, Fraunhofer CML

In maritime shipping, weather routing systems are popular to reduce fuel consumption and emissions. One of the most comprehensive overviews of applied optimization approaches to date has been compiled as part of this thesis. To ensure applicability for various types of ships and to reduce data requirements, weather-dependent ship motions and fuel consumption are frequently considered in a simplified way. Since simplifications are often regarded as insufficiently accurate, the objective of this thesis is to analyze the impact of ship performance methods on weather routing. Therefore, a graph based ship weather routing system is developed in C++. It aims at minimum fuel consumption by route and/or speed optimization. When optimizing a voyage, either a rather simple ship performance method, referred to as added resistance method, or a more advanced, so called added power method can be selected. The latter includes a maneuvering model as well as propeller and engine characteristics. Calculation runs for various routes, arrival times and weather conditions are performed and selected results are compared to data collected on board of container ships.

